STUDIES ON MOLECULAR SENSORS FOR THE DETECTION OF ALKALI, ALKALINE EARTH AND TOXIC HEAVY METAL IONS

A Thesis

Submitted to the Bhavnagar University

For the degree of

DOCTOR OF PHILOSOPHY

in

CHEMISTRY

by

Mr. Vinod P. Boricha

Under the Guidance of

Dr. Parimal Paul

Analytical Science Division
Central Salt & Marine Chemicals Research Institute
Bhavnagar-364 002, Gujarat

March 2010

Dedicated to

My Wife Harsha, my son Keval and my Family

CANDIDATE'S STATEMENT

I hereby declare that the work incorporated in the present thesis is original and has not been submitted to any University/Institution for the award of a Diploma or a Degree. I further declare that the results presented in the thesis and the considerations made therein, contribute in general to the advancement of knowledge in Chemistry and in particular to the subject entitled **"*Studies on Molecular Sensors for the Detection of Alkali, Alkaline earth and Toxic Heavy Metal Ions*"**.

Signature of the candidate

Vinod P. Boricha

केन्द्रीय नमक व समुद्री रसायन अनुसंधान संस्थान
गीजुभाई बधेका मार्ग, भावनगर-३६४ ००२.
CENTRAL SALT & MARINE CHEMICALS RESEARCH INSTITUTE
Gijubhai Badheka Marg, Bhavnagar 364 002, Gujarat, India.
CSMCRI

Dr. Parimal Paul
Deputy Director
Head, Analytical Science Division
Email: ppaul@csmcri.org

Date: 30-03-2010

CERTIFICATE BY THE Ph. D. SUPERVISOR

This is to certify that the contents of this thesis entitled "***Studies on Molecular Sensors for the Detection of Alkali, Alkaline Earth and Toxic Heavy Metal Ions***" is the original research work of **Mr. Vinod P. Boricha**, carried out under my supervision in Analytical Science Division at Central Salt and Marine Chemicals Research Institute, Bhavnagar 364 002 (Gujarat), India.

Further, I hereby certify that the work has not been submitted either partly or fully to any other University or Institution for the award of any degree.

(Dr. Parimal Paul)

Signature of Ph.D. Supervisor

ACKNOWLEDGEMENT

I would like to take this opportunity to express my gratitude to my Ph. D. guide ***Dr. Parimal Paul*** for his splendid and valuable guidance, encouragement and support that he shared with me in the due course of my research period. His profound knowledge, enormous enthusiasm, and keen insights in the field of chemistry have, and will continue to be, a great source of inspiration for me. I am feeling privileged and indeed fortunate for being his student.

I wish to record my respectful regards to our exuberant Director, Central Salt and Marine Chemicals Research Institute ***Dr. P. K. Ghosh***, for giving me the opportunity to carry out my Ph. D. work, motivation and providing me the infrastructure facility.

I also would like to thank ***Prof. P. Natarajan,*** former-Director and ***Dr. S. D. Gomkale,*** former Acting Director of this institute for their profound encouragement and support.

I would like to express my extreme indebtedness to ***Dr. Mohan Bhadbhade and Dr. Amitava Das*** for their extreme support to start up my research work at CSMCRI. The experience of the work, which I have executed under their supervision, is extremely helpful to carry out my Ph. D. work.

I am thankful to ***Dr. P. S. Subramanian*** and ***Dr. E. Suresh*** for their fruitful discussion, constant guidance, suggestions and performing designed NMR experiments and single crystal x-ray diffraction analysis whenever I approached them for help. I express my sincere thanks to ***Mr. Vinod Agrawal*** for recording IR, ***Mr. Arunkumar Das*** for recording Mass spectra and ***Mr. Viral Vakani*** for CHN analysis.

I wish to express my special thanks to NMR group ***Hitesh Bhatt, Dr. Rajendra Singh Thakur, Hariom Gupta*** for their kind help and support especially during my thesis writing.

I would like to extend my gratitude towards ***Dr. R. V. Jasra***, former DC, Silicate and Catalysis Discipline, ***Dr. Amjad Husain, Dr. H. C. Bajaj***, ***Dr. N.H. Khan***, ***Dr. (Mrs.) R. I. Kureshy***, ***Dr. S. H. R. Abdi, Dr. B. Ganguli*** for their eloquent encouragement. I am also thankful to the scientists of silicates and catalysis division, ***Dr. H M Mody, Dr. S. Kannan, Dr. S. Muthusamy, Dr. R. S. Somani, Dr. S. D. Bhatt, Dr. R. S. Shukla, Dr. Jugnu Bhatt, Dr. Beena Tyagi, Dr. A. B. Boricha. Dr. Rajesh Tayade*** for their valuable suggestions and support.

I sincerely thank to all my friends and well-wishers ***Pragati Agnihotri***, ***Subrata Patra***, ***Sanjay Parihar, Yogendra Singh Chouhan, Pankaj Sanavada, Shreenidhi K. R., Shaju S. S., Ashish Chakraborthy, Debdeep Maity, Ravi Gunupuru, Darshak Trivedi***, ***Krishna Kumar D.***, ***Lakshminarayanan***, ***P. Mosae, Sandeep N., Amal Cherian, Kamal Bist, Neha Carpentor, M Suresh, Prasenjit Kar, Amilan Jose, Amrita Ghosh, Atindra Shukla, Paresh Dave, Beena Narayanan*** for their help and support.

I am also grateful to all the staff member of analytical science division especially ***Dr. Pragnya Bhatt, Dr. Anjani Bhatt, Chandrakanth C. K., Shobhit Singh Chauhan, Dr. Divesh Srivastava, Dr. Babulal, Rajesh Patidar, Harshad Brahmabhatt, Jayesh Choudhary, Shital Patel, Daksha Kuvadiya, Pradip Parmar, Mahesh Sanghani, Satyaveer Gotwal,*** for their wonderful company and help during my work.

My sincere thank is due to ***Chimanbhai Gohel*** who helped me in various ways to carry out my research work.

I am also thankful to ***Mr. Pramod Makwana*** for their constant helping in any computer related problem when I faced. I would also like to express gratitude to ***Popatbhai*** and ***Jitu Bhai*** for carrying out glass blowing work and ***Baraiyabhai*** for providing Xerox services efficiently, whenever I requested him.

All the staff members in ***Store & purchase***, ***Workshop, Library***, ***Administration, Planning cell, Account*** & ***Canteen*** and ***security staff*** are highly acknowledged for their cooperation and timely help.

I am also thankful to ***Mehulbhai Bhatt*** for his kind help and encouragement.

I am whole heartedly thankful to my friends ***Mahendra Kapure, Sanjay Makwana, Yuvrajsinh Gohil, Manish Dave, Mitul Mandaliya Hitesh Jogel*** for their help, moral support and light atmosphere during the stressed moment of my life.

I would like to show gratitude towards my wife ***Harsha,*** my son ***Keval***, ***Brother*** *and* ***Bhabhi***, my nephews ***Vishal*** and ***Hemang*** for being a source of inspiration for me. Their love and sacrifice motivated me to achieve this goal.

I would like to thanks all the Staff Members of CSMCRI who have helped me directly or indirectly during the tenure of my Ph. D.

Vinod P. Boricha

ABBREVIATIONS

PET	Photoinduced Charge Transfer
HOMO	Highest Occupied Molecular Orbital
LUMO	Lowest Unoccupied Molecular Orbital
PCT	Photoinduced Electron Transfer
Uv-vis	Ultra-violet visible
bpy	2,2'-bipyridine
phen	1,10-Phenanthroline
DPV	Differential Pulse Voltametry
SCE	**S**aturated Calomel Electrode
THF	Tetrahydrofuran
MHz	Mega Hertz
Hz	Hertz
LC-MS	Liquid chromatography Mass spectroscopy
IR	Infrared
Ph	Phenyl
Ar	Aromatic
Al –	Aliphatic
COSY	Co-relation spectroscopy
FT-NMR	Fourier Transformed Nuclear Magnetic Resonance
MLCT	Metal to Ligand Charge Transfer
CT	Charge Transfer
ppm	Parts per million
DMSO	Dimethyl sulfoxide

CHAPTER – I

Introduction

1.1 General introduction

The design and synthesis of functional molecules that could serve as molecular devices for sensing, switching and signaling selectively is an area of intense activity in current research.[1-4] Among various such functional molecules, the molecular sensors for detection of ions are of great interest because of their important role in many biological and environmental processes.[5-8] Among the various analytical methods that are available for the detection of cations, flame photometry, atomic absorption spectrometry, ion sensitive electrodes, electron microprobe analysis, neutron activation analysis, etc., are expensive, often require samples of large size and do not allow continuous monitoring. In contrast, the methods based on fluorescent sensors offer distinct advantages in terms of sensitivity, selectivity, response time, local observation (e.g. by fluorescence imaging spectroscopy), etc. Such molecular sensors can be constructed by the combination of an ionophore, designed for the binding of specific incoming ion, and a luminescent fragment whose photophysical properties perturbed during the recognition processes to produce a measurable output signal.[9-12]

1.2 Ionophores

To fabricate fluoroionophore, much attention needs to be given to design ionophores for selective binding of metal ions. It has been observed that the selectivity of ionophores with metal ion depends on several factors such as cavity dimension, shape and topology, substituent effects, conformational flexibility/rigidity and solvation effect.[13] Macrocyclic compounds are noted for their remarkable selectivity towards specific cations, making them excellent choices for the separation of desired ions from mixture of ions.[14] In the case of macrocyclic ionophores, the matching of size of the cavity of the ligands with the ionic diameter of cations is considered as a critically important factor that controls the selectivity towards different ions [15]. However, it has also been reported that flexible macrocycles such as the large poly ethers (27-33 ring size) discriminate principally among smaller cations (plateau selectivity) while retaining their affinity towards larger cations.[16] Non-covalent intermolecular interactions of non-macrocyclic compounds have also been used to generate supramolecules that have selective metal ion recognition property.[17] Examples of a few common type of ionophores are summarized in Figure 1.1.

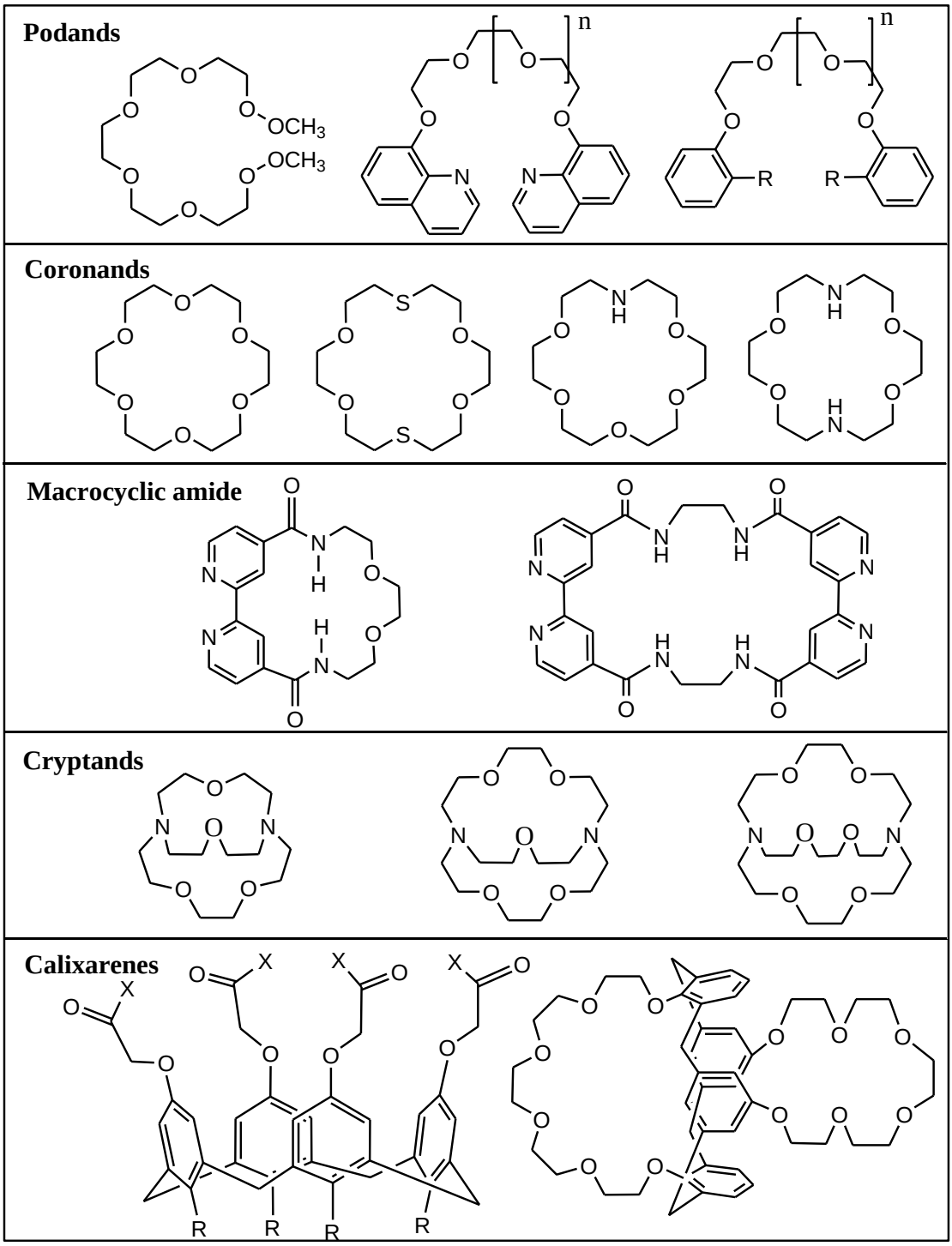

Figure 1.1 examples of ionophores for cations

1.3 Fluorophores

Fluorescent molecules, whose photophysical properties are well documented and can act as signal transducer that converts the information into an optical signal can be used to construct fluoroionophores. Fluorophore is the signaling species, the photophysical characteristics of which changes when the analytes interact with the

ionophore moiety. Fluorescent aromatic compounds such as pyrene, dye molecules, anthracene-based compounds etc. are mainly used as fluorophore.[18] However, in some cases polypyridyl-based luminescent metal complexes of Re(I), Ru(II) and Os(II) and cryptan-based lanthanides(III) complexes have also been used as fluorophore,[19] however the latter is of special interest because of some advantages over organic molecules. Besides changes in luminescence like organic molecules, they also exhibit measurable changes in electrogenerated chemiluminesence and redox property in the event of ion recognition process.[20-22] Structural drawing of some of the commonly used fluorophores are shown below (Figure 1.2).

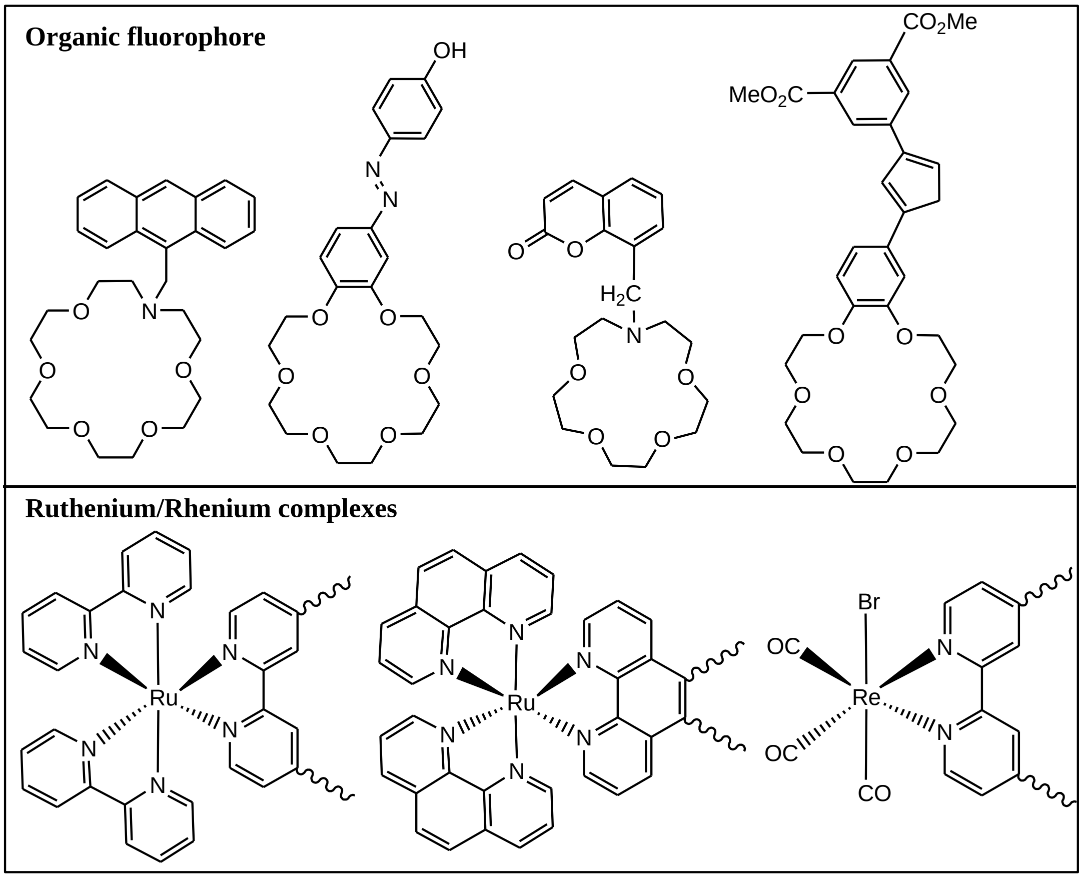

Figure 1.2 Examples of fluorophores (organic and metal complexes)

1.4 Design of fluoroionophores for the detection of cation

A fluoroionophore can be constructed by covalent linking of a fluorophore with an ionophore directly or through a spacer. A typical designing and function of a fluoroionophore is shown as a schematic diagram in the Figure 1.3. After cation binding, photophysical characteristics of the fluoroionophore changes due to the perturbation of photoinduced processes such as electron/energy transfer, which make

changes in quantum yield, emission lifetime and emission maxima.[23] The effectiveness of the photophysical changes, however depends on the efficiency with which metal-induced electronic communication takes place from metal bound ionophore to the fluorophore. The spacer is, therefore, plays crucial role to make efficient communication, a fully conjugated system is expected to be more effective for this purpose.[24-25]

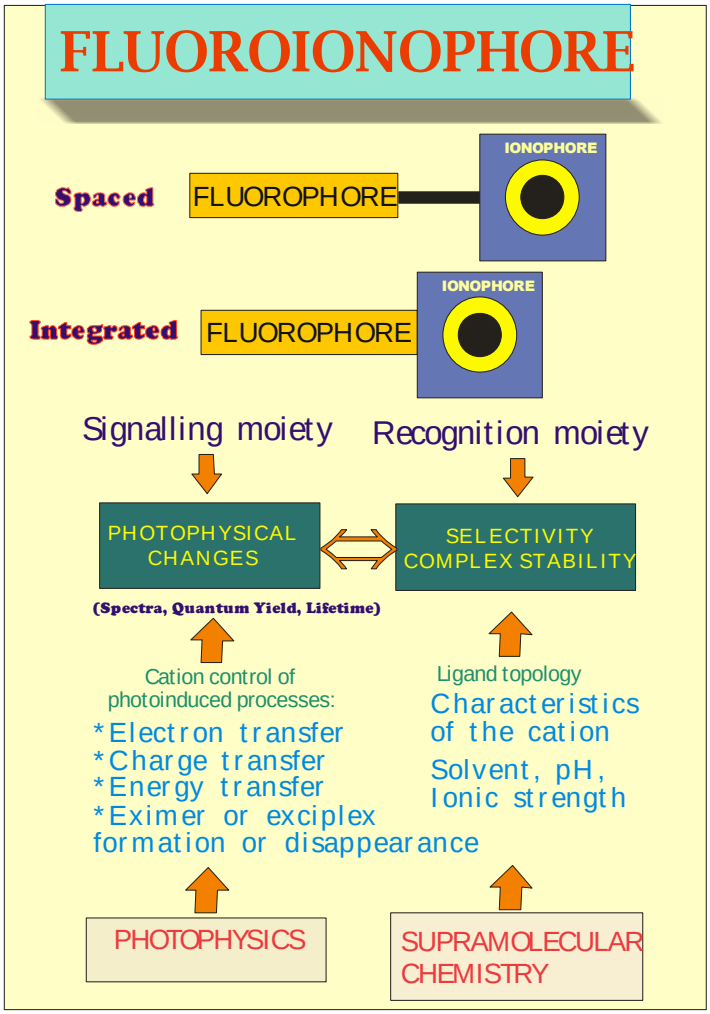

Figure 1.3 Main aspects of fluorescent molecular sensors for cation recognition

1.5 Photoinduced electron transfer (PET)

Fluoroionophore, which exhibits photoinduced electron transfer, generally consists of the combination of three components, fluorophore-spacer-receptor, as shown in the Figure 1.3.[26] In absence of any analyte (off state), excitation of the fluorophore component of the sensor promotes an electron transfer from the receptors

to the fluorophore. The thermodyanamic condition to happen this is that the excited state energy of the fluorophore needs to be sufficient to provide both the reduction potential of the fluorophore and the oxidation potential of the receptor. In the presence of metal ion (on state), excitation of the fluorophore results in fluorescence/enhancement of fluorescence intensity only because the photoinduced electron transfer (PET) process is arrested by the cation bound ionophore. These processes, expressed in terms of molecular orbital energy diagram, are shown in Figure 1.4.[27] The energy of the HOMO of the free receptor lies between those of the HOMO and LUMO of the excited fluorophore and then electron transfer from the HOMO of the receptor to the hole in the HOMO of the fluorophore takes place. This process does not occur in presence of analyte bound to the receptor causing enhancement of emission intensity. The PET also provides a mechanism for nonradiative deactivation of the excited state (Figure 1.4), leading to a decrease in emission intensity or "quenching" of the fluorescence.[28]

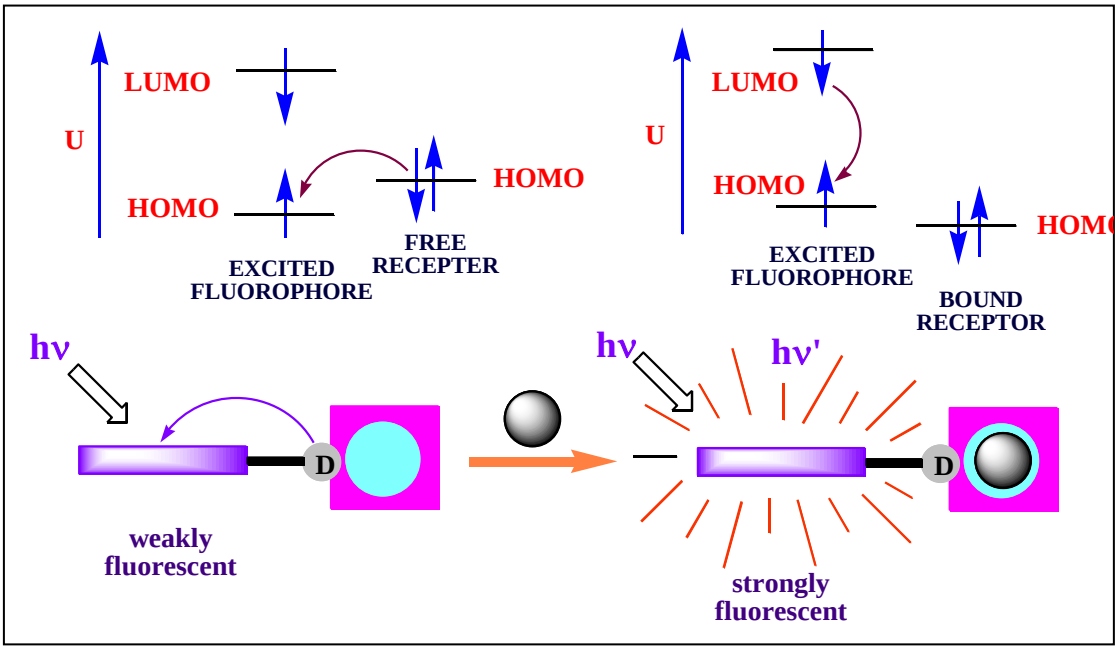

Figure 1.4 Principle of cation recognition by fluorescent PET sensors.

1.6 Photoinduced charge transfer (PCT)

Electronic excitation necessarily involves some degree of charge transfer, but in fluorophores containing both, electron withdrawing and electron-donating substituents, this charge transfer may occur over long distances and be associated with major dipole moment changes, making the process particularly sensitive to the microenvironment of the

fluorophore. This process becomes more sensitive upon excitation as the dipole moment in the excited state is larger than that in ground state.[29] Thus, cations or anions in close interaction with the donor or the acceptor moiety change the photophysical properties of the fluorophore. When the cation interacts with the donor group within the fluorophore, the electron-donating character of the donor group is reduced and consequently the excited state is more destabilized resulting in a blue shift of the absorption and emission spectra. In contrast, metal ion binding to the acceptor group enhances its electron-withdrawing character, making the excited state more stable than the ground state, which results in red-shift of the absorption and emission spectra. A pictorial view of the phenomenon in terms of the energy change is shown in the Figure 1.5.[30]

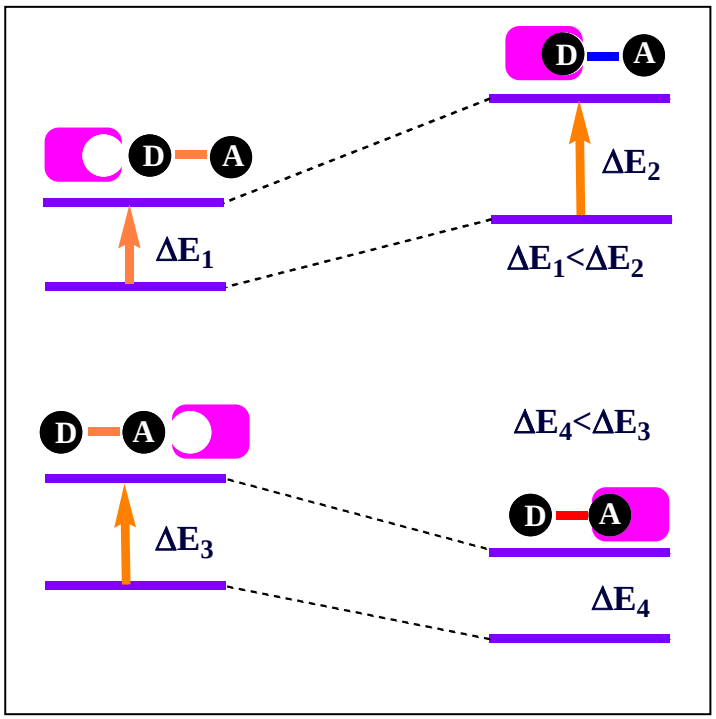

Figure 1.5 Photoinduced charge transfer system.

1.7 Important metal ions for detection

In general, selective detection and possible extraction/removal of any metal from a mixture of ions is very important because of the recovery of value added products for various applications and also environmental point of view. Heavy metals have found industrial, agricultural and military uses for several centuries of time.[31-33] As a result they are now widely dispersed in a range of different forms, and at present there are serious environmental problems, particularly with Pb^{2+}, Hg^{2+} and Cd^{2+}. The separation and recovery of precious metal is also a strong demand. They play

important role in high technology and the national economy, but the contents of these elements in the earth's crust or any other natural sources such as sea water are very low.[34-35] Therefore, it is desire to develop highly sensitive sensor/extractant for the detection of these metal ions.

Alkali and alkaline earth metal ions are of great importance because of their role in various biological and clinical processes.[36-38] Among these ions, potassium (potash) has gained special interest because of its use as fertilizer and our country used to import the entire of its requirement because no economically viable method for recovery of potassium from its natural source is available. Sodium and potassium salts are found on earth either in solution, in the oceans, or in under-ground deposits that are the residue of ancient seas. Seawater also contains significant amount of magnesium and calcium together with some other trace metal ions. Bittern (mother liquor obtained after the recovery of common salt from seawater) contains mainly Na^+, K^+, Mg^{2+} and Ca^{2+} and it is one of the largest natural sources of potassium. Therefore, selective extraction of these ions, especially potassium, from this mixture is one of the most challenging areas of research.

1.8 Literature on fluoroionophores as sensor for cation

As mentioned in the section **1.4** fluoroionophore consists of three units, *viz*, a fluorophore as signaling unit, an ionophore which binds cation, and a spacer which connect the two units. In the literature, large number of different type of fluoroionophores, which developed for various purposes, is available. Within the scope of the present work, the following discussion is restricted to certain type of fluoroionophores, which have been developed for some important cations and anions and in which metal complex based units or some typical commonly used organic molecules have been used as fluorophores; and crown ethers, calixarene or similar type of a few other macrocyclic units (relevant to the present work) have been used as ionophores.

1.8.1. Ruthenium-polypyridine complexes as fluorophore

The appearance of the ruthenium(II) polypyridine complexes has triggered an extensive growth in photochemistry and photophysics in the past few decades, largely

because of their highly versatile luminescent and photoredox properties. The Ru(II) ion in these complexes is a good reductant as well as oxidant and both the reduced and oxidized forms are quite stable towards reactions. Their powerful photosensitization capacity for energy transfer and electron transfer processes made these coordination compounds primary candidates for studies in photoluminescence, photoelectrochemistry and chemi- and electroluminescence. The metal-to-ligand charge transfer (MLCT) band in these complexes is basically used to study photoinduced processes.

The research group of P. D. Beer has used Ru(II)-bipyridine system extensively as fluorophore for the development of luminescent sensors. For the recognition of alkali and alkaline earth metal ions, various type of azacrown ethers as ionophore **[1]** – **[3]** have been extensively used incorporating Ru(II)-bipyridine as fluorophore.[39-41] The interaction of these sensor molecules with different metal ions have been mostly studied by fluorescence and absorption spectroscopy using Ru(II)-bipyridine as signaling unit. Most of the cases they exhibited selectivity towards K^+, however and in few cases they also exhibit selectivity towards Rb^+, Cs^+ and lanthanide cations [42,59] Interestingly, when receptors containing CONH group has been incorporated, then interaction with halide anions through hydrogen bonding interaction, CO-N-H---anion is noted.[43]

Fluoroionophore containing crown ether moiety directly fused with bipyridine/1,10-phenanthroline unit, which coordinated to Ru(II) ion **[4]-[6]**, have been reported.[44-49] These sensor molecules exhibited strong interaction with the metal ions Ba^{2+}, Hg^{2+} and Zn^{2+}. Diaza crown ethers, which act as bridging unit between photoactive metal chromophores [**7**], have also been reported as receptors for Ba^{2+} ion.[50] Ru(II)-polypyridine based complexes containing azacrown as ionophore [**8**]-[**9**] has recently been reported as quadruple-channel sensor for selective and quantitative analysis of Pb^{2+}, Cu^{2+} and Hg^{2+}.[51-52] Due to ion recognition, changes in UV-VIS-NIR, luminescence and electrochemiluminescence (ECL) spectra **[10]** occurred for selective metal ions.[53-54] A series of fluorescence sensors using aryl incorporated azacrown based ionophores **[11]** have synthesized and their selectivity towards Pb^{2+} and Na^+ have been reported. [55]

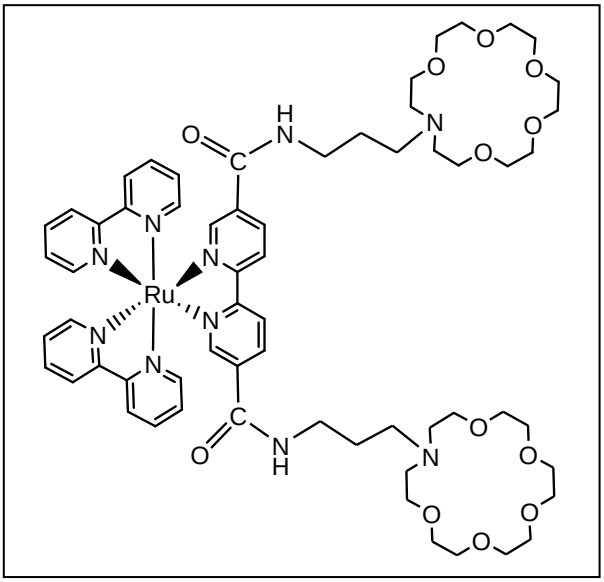

[1]

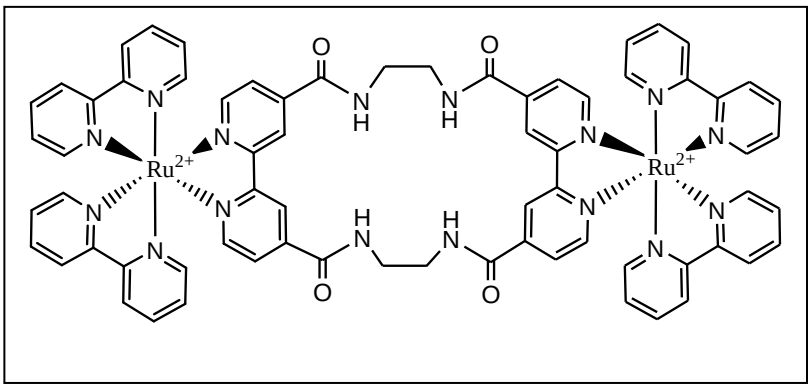

[2]

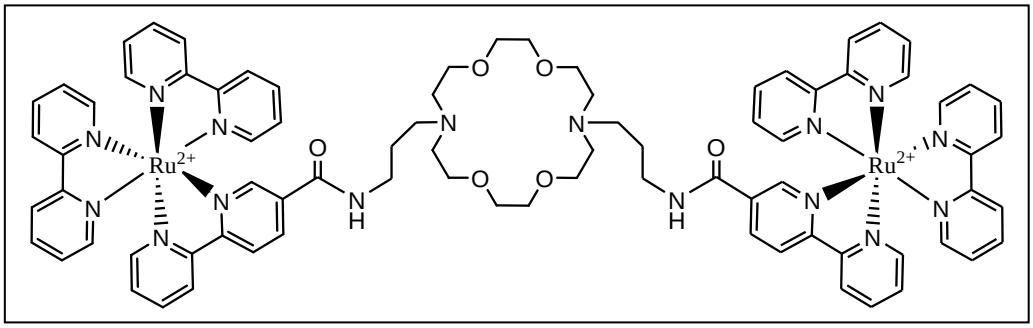

[3]

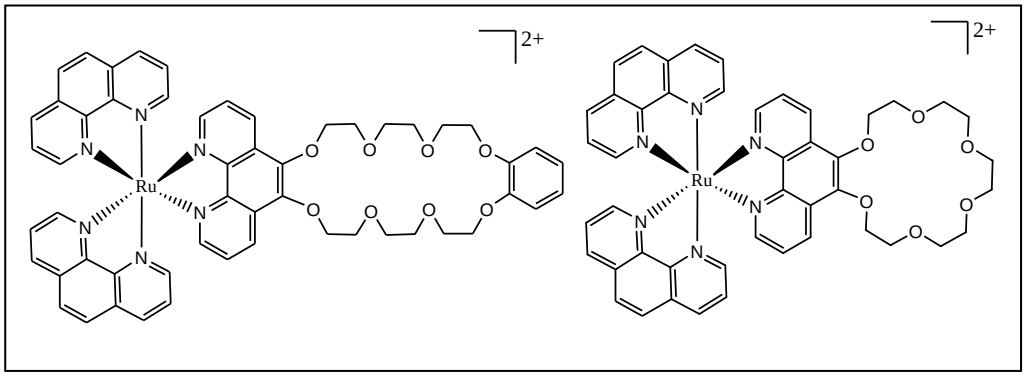

[4]

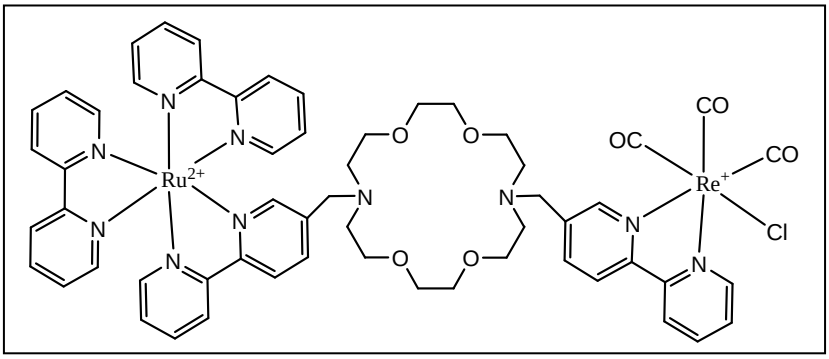

[5]

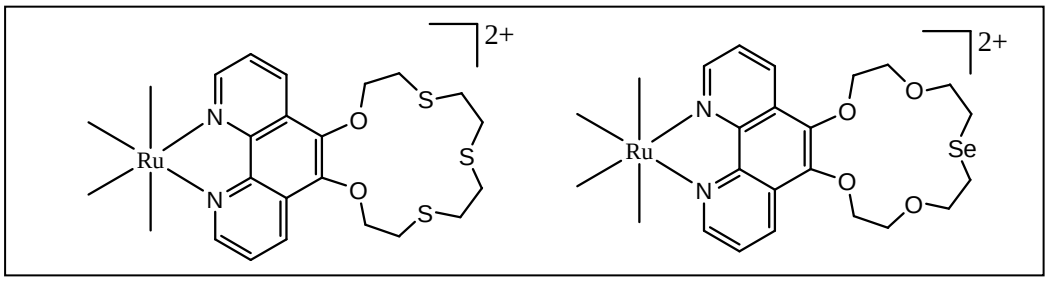

[6]

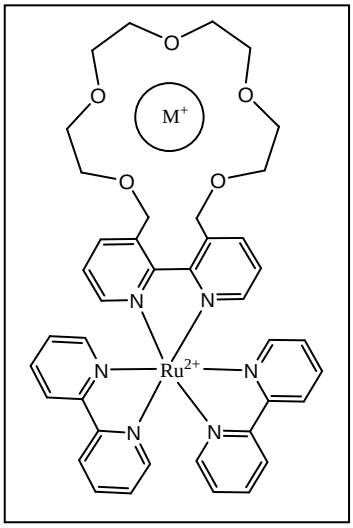

[7]

M. Schmittel, *et al* have reported Rutheinum complexes with azacrown ethers attached to the 4,7-positions of the phenanthroline **[8],** which shows fluorescence enhancement upon binding with Ba^{2+} ion.[56] V. W. Yam *et al* have reported ruthenium polypyridyl aza crown ether complexes **[9]** selective for Na^{+} ion.[51]

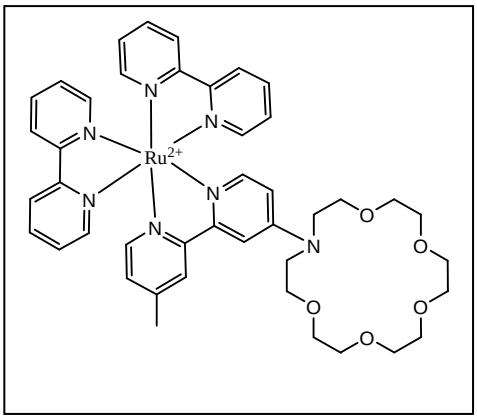

[8]

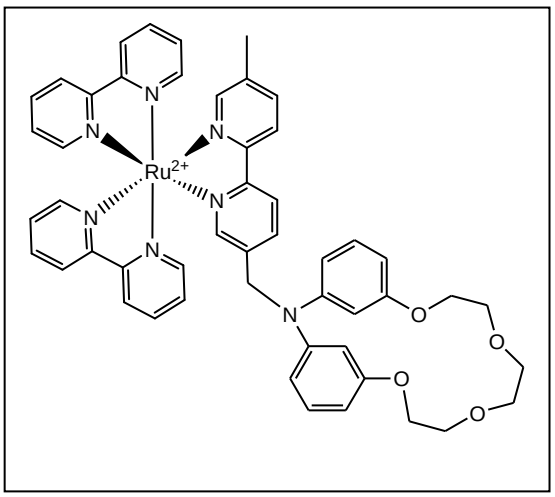

[9]

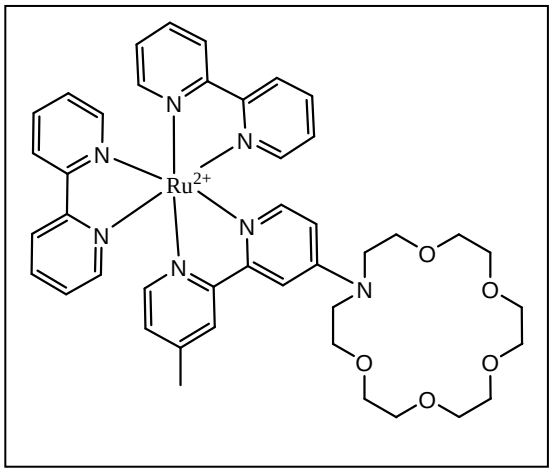

[10]

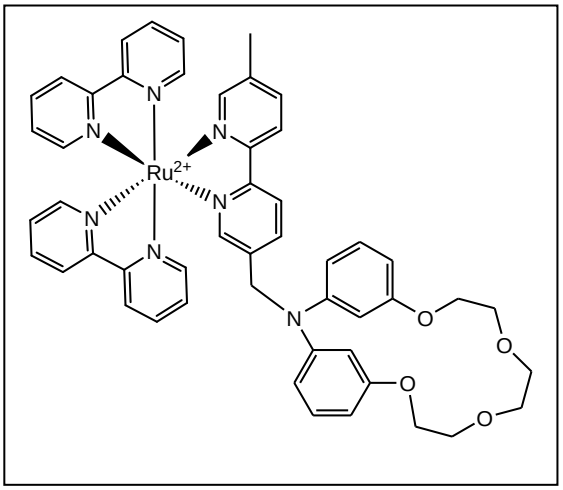

[11]

Instead of crown ethers, calixarene derivative has also been widely used as ionophore to develop fluorescence sensors. There are many examples, where photoactive organic molecules have been used as fluorophore.[16] Examples of calixarene based fluorescence sensors using Ru(II)-polypyridine moiety as signaling unit is limited. R. Grigg, *et al* has reported a sensor molecule where the Ru(II)-bipyridine unit is connected to the lower rim of the calixarene moiety through a spacer **[12]**.[57] The research group of Beer *et al* has reported fluoroionophores incorporating calixarene derivatives as ionophore for alkali and alkaline earth metal ions and in this case also recognition of ion-pair is noted.[58-59] Structural drawing of a few of these ionophores are shown below **[13]-[14].**

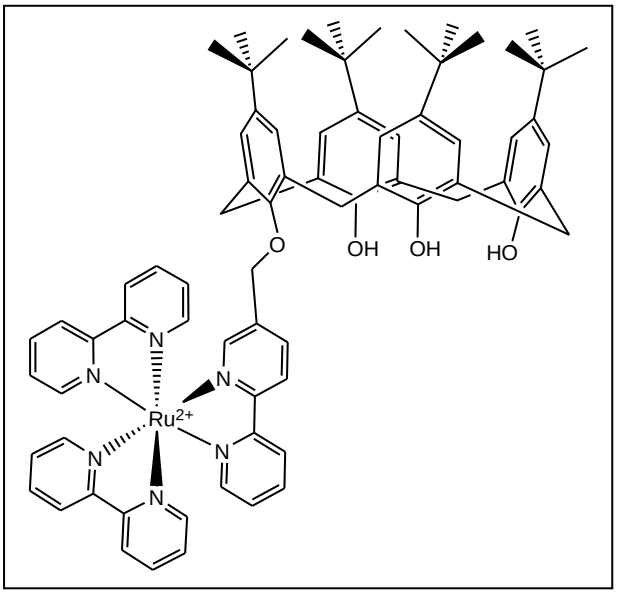

[12]

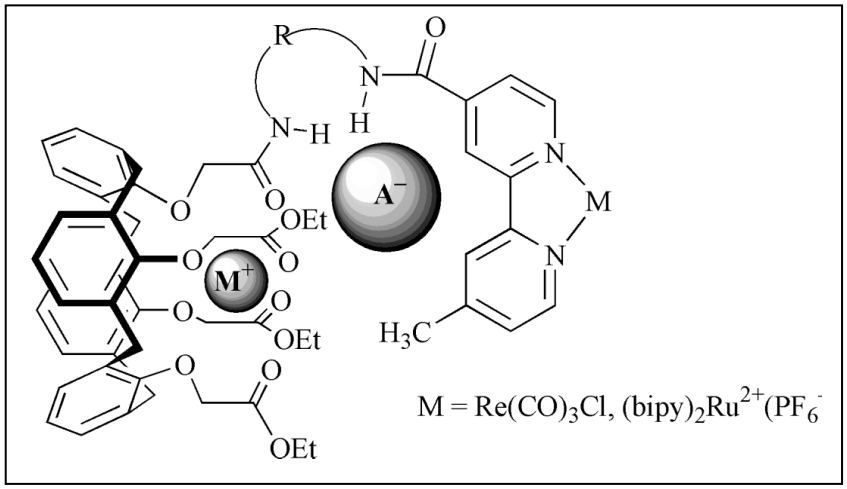
R
N
H
O
N–H
A⁻
M
N
O
OEt
M⁺
H3C
M = Re(CO)3Cl, (bipy)2Ru2+(PF6-

[13]

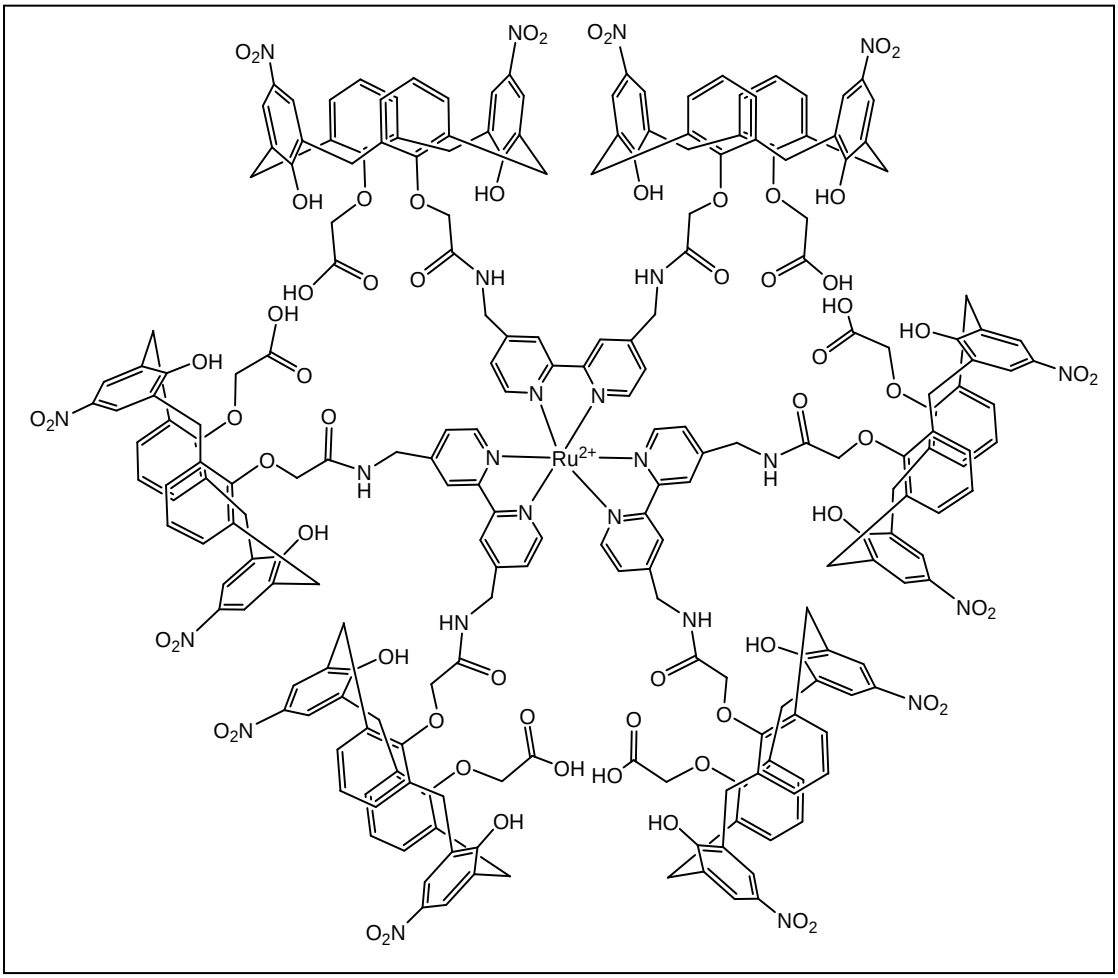
O2N
NO2
OH
HO
O
NH
HN
N
Ru2+

[14]

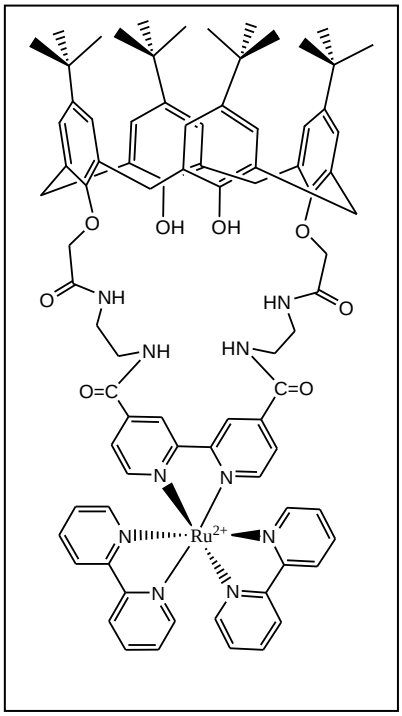

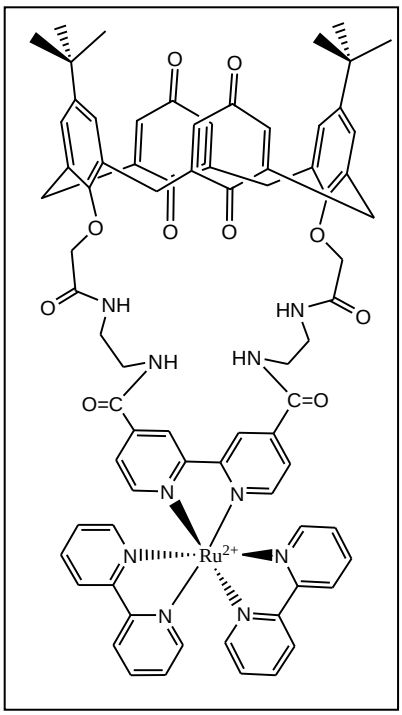

[15] **[16]**

Macrocyclic compounds with ubiquitous amide CO-NH groups, which has been incorporated into macrocyclic and calixarene structural frameworks **[15]-[17]** to produce novel receptors capable of the electrochemical and spectral recognition of anions have also been reported.[60-61]

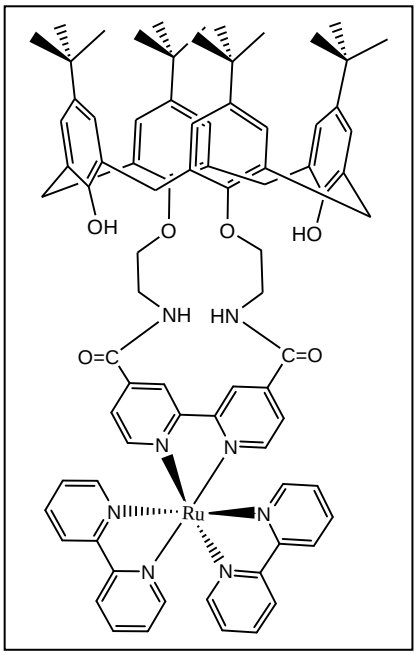

[17]

1.8.2 Rhenium complexes as fluoroionophore

Significant amount of work has been reported with Re(I)-bipyridine moiety as fluorophore. In general, the reaction of $Re(CO)_5X$ (X = Cl, Br) with the ionophore containing bipyridine unit results in the formation of $Re(CO)_3(bpy)X$ unit, which acts as fluorophore. Like Ru(II) based fluoroionophores, both crown ethers and calixarene derivatives have been used to prepare fluorescent receptors. Using benzocrown as ionophore and amide containing moiety as spacer **[18]-[21]** fluorescent receptors have been developed, which interact with both cations and anions.[62, 63] The anion binding site is formed by the NH of the amide moiety and 3,3'-protons of the bipyridine, while the cation site is composed of either a benzo-18-crown-6 group or two benzo-15-crown-5 moieties. [64]

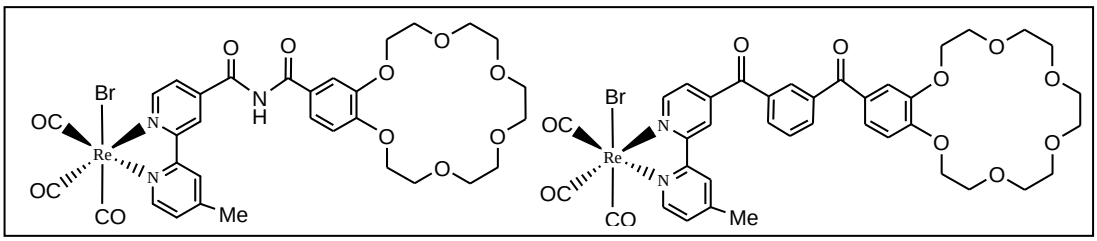

[18]

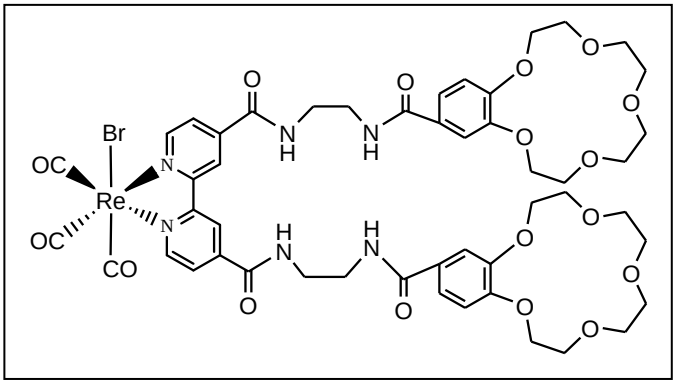

[19]

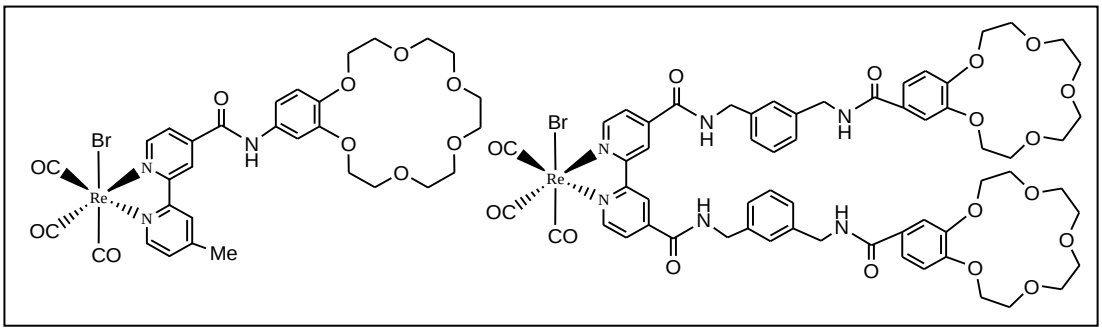

[20]

Complex containing azacrown ether, which connected to Re(I) via alkynyl pyridine **[21]-[22]**, has also been reported recently as light controlled ion switch for Ba^{2+}.[65-67]

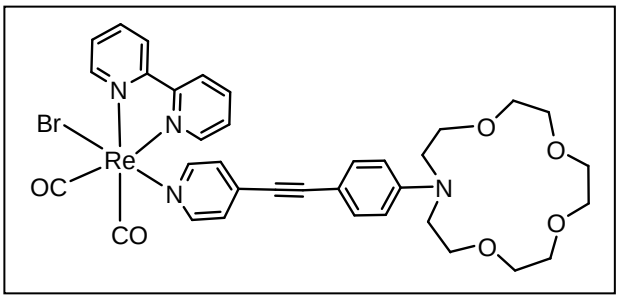

[21]

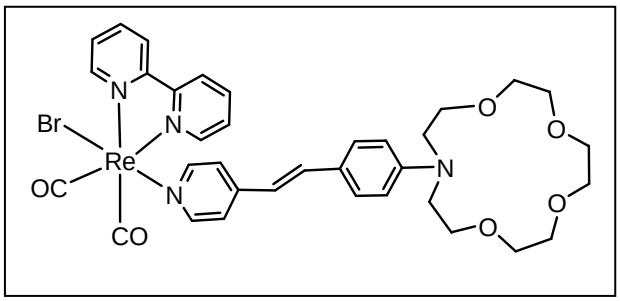

[22]

Y. Shen, *et al* reported the Pb^{2+} selective rhenium complex **[23]** with 1, 10-phenathroline containing aza crown ether.[68]

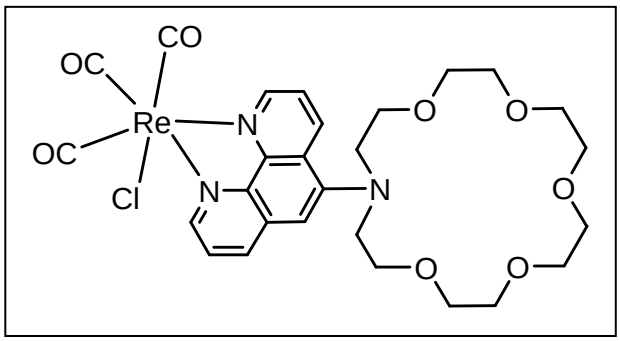

[23]

Using calixarene as ionophore, J. B. Cooper, *et al* has reported a number of interesting new heteroditopic bis(calix[4]arene) rhenium(I) bipyridyl receptor molecule **[24]**, which binds a variety of anions at the upper rim and alkali metal cations at the lower rim.[69]

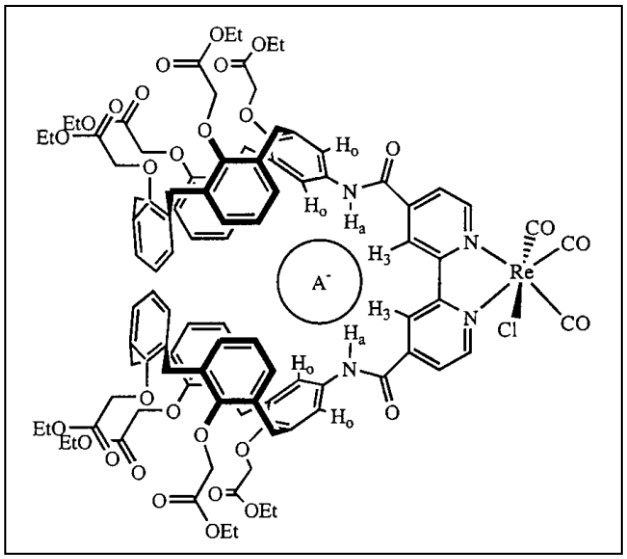

[24]

1.8.3 Fluorescent sensors with fluorophore other than metal complex

There are large numbers of fluorescent sensors, where the photoactive moiety, other than metal complex, has been used. Since in the present study, mainly crown ethers have been used as ionophore, therefore in the following section some examples with commonly used photoactive organic moiety as fluorophore and crown/azacrown ethers as ionophores have been described.

A. P. de Silva *et al* has reported PET sensor **[25]** with monoaza-18-crown-6 and guanidinium receptor units, which exhibited selectivity with amino acid zwitterions.[70] H. Nishida, et al synthesized fluorescent Li^+, $^+$ K^+ and Ca^2 selective crown ether reagents **[26]** from mono and diaza-18-crown-6. [71]

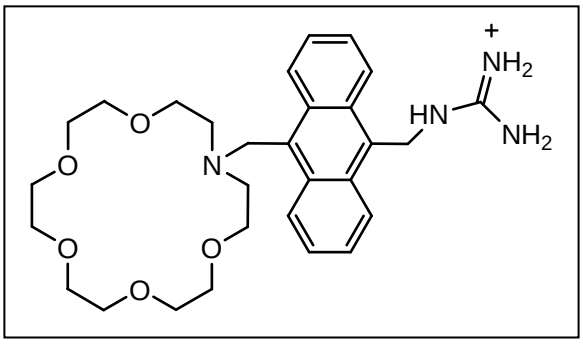

[25]

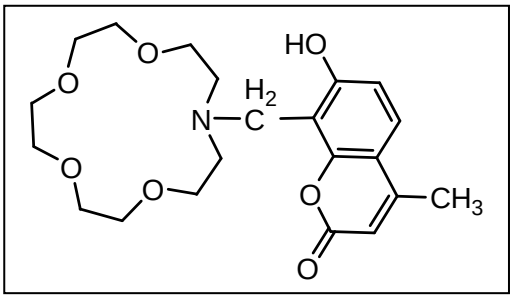

[26]

Chromogenic azacrown ethers **[27],** which exhibited selectivity towards Ba^{2+} and Ag^{+} ions has been reported by M. V. Alfimov, et al[72]

T. Hayashita *et al* synthesized bisbenzo-15-crown-5 azochromophore **[28]** which exhibits Uv-vis spectral response for K^{+} ion.[73] Na^{+} and K^{+} selective fluorescent sensor of benzocrown ether **[29]** has also reported in the literature.[74]

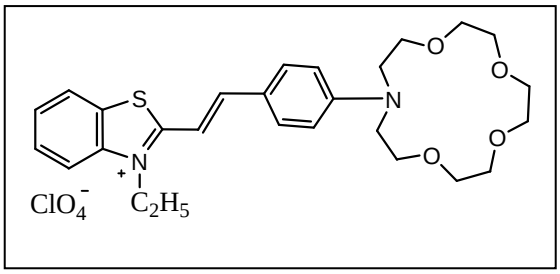

[27]

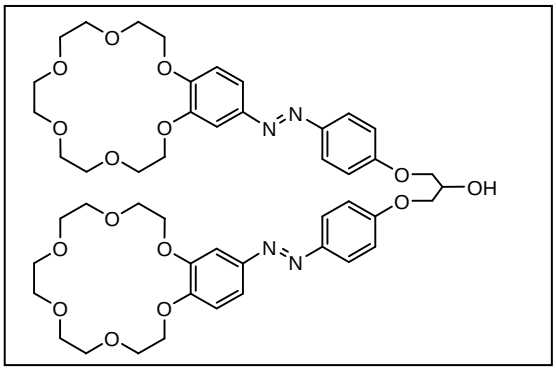

[28]

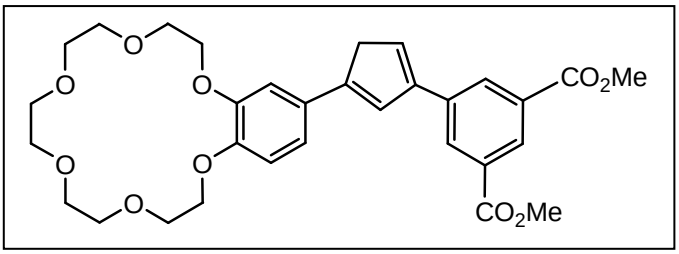

[29]

Ai-Jun Tong *et al* have synthesized a number of fluorescence sensors incorporating benzocrown ether **[30]** for selective sensing and extraction of alkali metal ions[75].

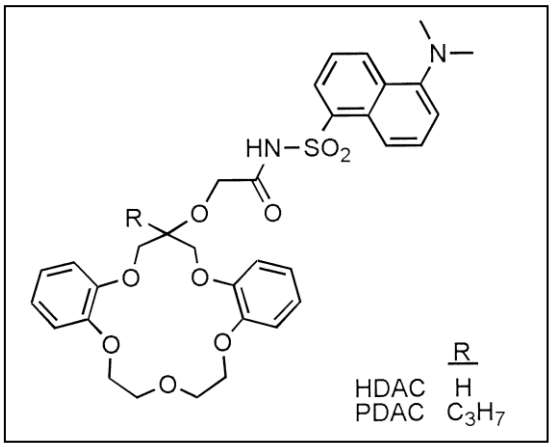

[30]

With the objective for selective binding with heavy metal ions, a number of molecular sensors have been developed by introducing N and S atoms in place of O**,** a few of them are shown below **[31]-[32].**[76 -79] Marin Regueiro-Figueroa *et al* have reported a number of sensors **[33]**, their complexation property with Pb^{2+} and Cd^{2+} and also studied the ring size effect on complexation**]**.[80] Y. H. Kim *et al* has also reported benzothiazolyl functionalized ionophore **[34]** based on a calix[4]arene-crown-5 ether which exhibited excellent selectivity towards Ca^{2+} ion.[81]

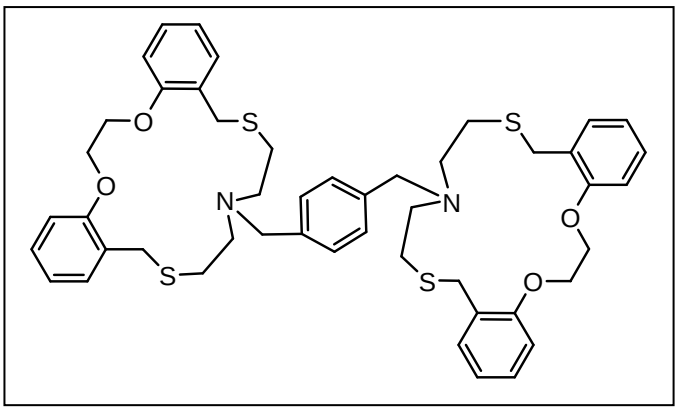

[31]

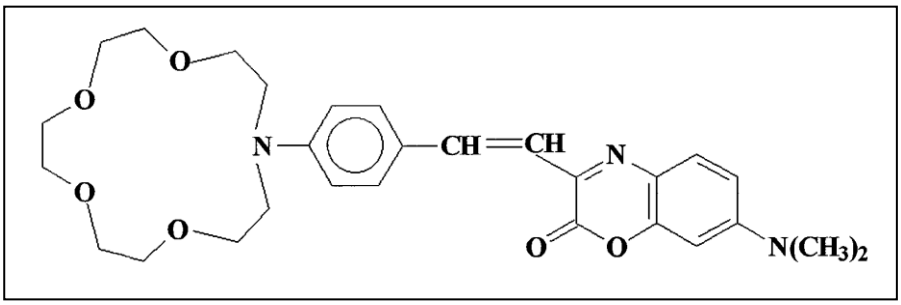

[32]

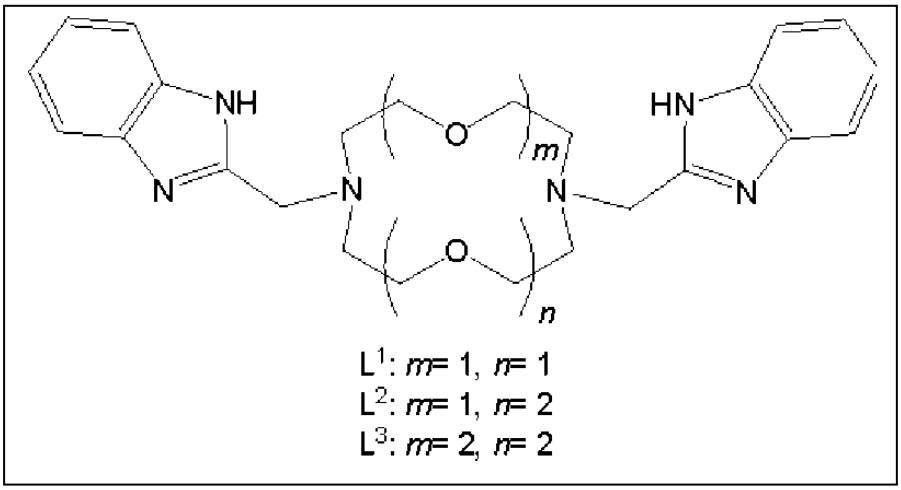

[33]

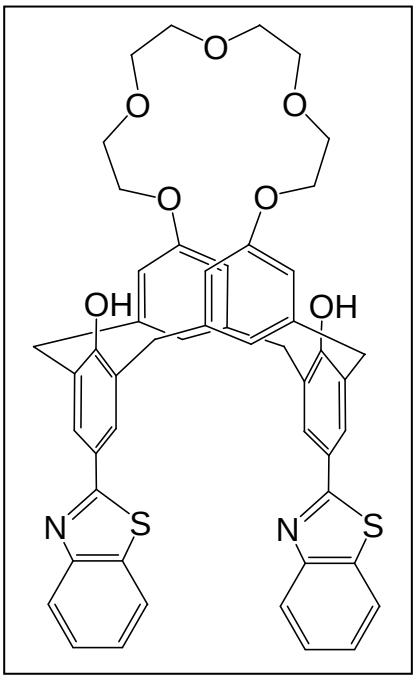

[34]

1.9 Objectives and scope of present work

Fluorescence spectroscopy is the most powerful research tool for the detection of ions at the molecular level. This method has some distinct advantages over many other existing analytical methods. Some analytical methods are commercially available, however extensive efforts are going on to develop fluorescent probe for alkali, alkaline earth and toxic heavy metal ions. Alkali and alkaline earth metal ions are involved in many biological processes such as transmission of nerve impulses, muscle contraction, regulation of cell activity and high blood pressure. Therefore detection of these metal ions for clinical purpose is important. In addition to this, detection of these metal ions in the samples (water) collected from different sources is also important to evaluate its ionic constituents, especially in analytical point of view. It is also know that mercury, lead and cadmium are highly toxic for organisms, and therefore, detection of these metal ions is the environment is very important. The present thesis work entitled "Studies on molecular sensors for the detection of alkali, alkaline earth and toxic heavy metal ions" reports the synthesis, characterization of various fluoroionophores comprising of Ru(II)/Re(I)-polypyridine based unit as fluorophore and macrocyclic ligand as ionophore for detection of alkali, alkaline earth and toxic heavy metal ions.

1.10 Outline of the thesis work

The present thesis is distributed in five chapters which describes the synthesis and characterization of various fluoroionophores comprising of Ru(II)/Re(I)-polypyridine based unit as fluorophore and macrocyclic ligand as ionophore. The macrocyclic unit is connected to the metal bound bipyridine or 1,10-phenathroline unit through various small spacer. The ion binding properties of these fluoroionophores have been investigated with a large number of cations and also with some selected anions. The ion recognition process monitored by luminescence, ^{1}H NMR, UV-Vis spectral changes and also by electrochemical study. Binding constant and stoichiometry of the complexes formed have also been determined.

Chapter 2 describes synthesis and characterization of series of fluoroionophores. Three new ligands incorporating aza-crown/benzocrown as ionophores (**L^1 – L^3**) and 2,2'-bipyridine/1,10-phenanthroline are coordinating units have been synthesized. Analytical and spectroscopic methods have been used to characterization of these complexes.

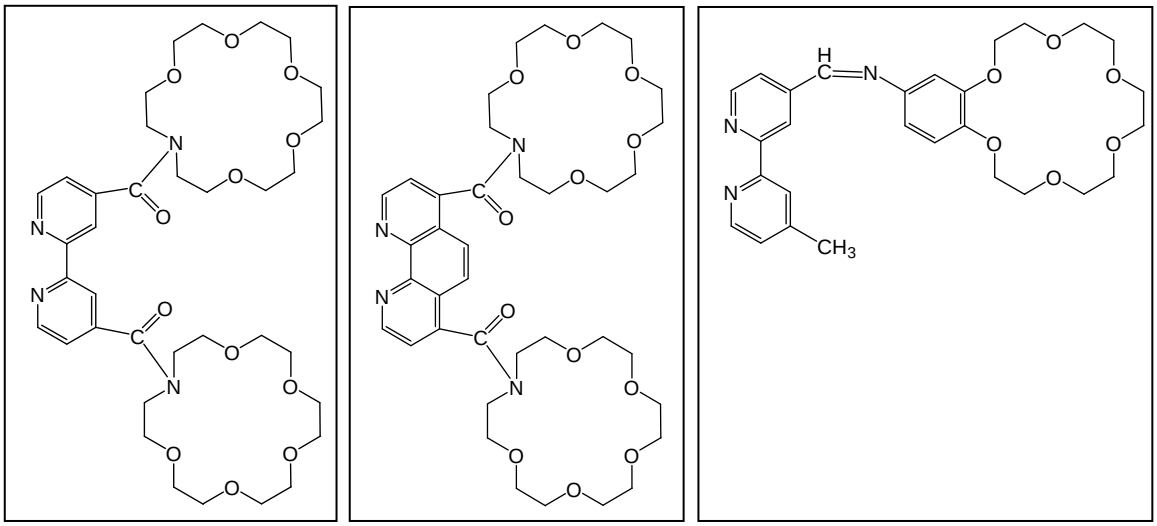

L^1 **L^2** **L^3**

Chapter 3 deals with the ion recognition study of the new complexes described in chapter 2. Cation binding property have been investigated with a series of cations Na^+, K^+, Rb^+, Mg^{2+}, Ca^{2+}, Zn^{2+}, Cd^{2+}, Hg^{2+}, Pb^{2+} and Cu^{2+}. The recognition event monitored by ^{1}H NMR, luminescence, oxidation potential of metal ion and UV/Vis absorption studies. Among large number of cations, a few exhibit strong complexation as indicated by emission and NMR spectral changes. Binding constants of strongly interacting metal ions have been calculated using titration data.

Chapter 4 describes synthesis and characterization of three ligands containing ester and aza macrocycles moiety as ionophore and 1,10-phenathroline unit as coordinating units (**L^4 – L^6**). Corresponding fluoroionophores of these ligands have been synthesized by their reaction with *cis*-$Ru(bpy)_2Cl_2$. These new complexes have been characterized and their luminescence and electrochemical properties have been studied. Luminescence titrations of all the fluoroionophores with selected ions have

been carried out and from titration data, binding constants (K_s) and stoichiometry of the complexes have been calculated.

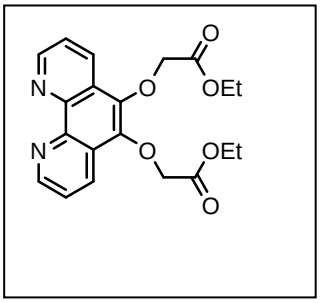

L[4]

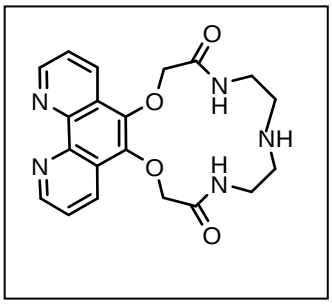

L[5]

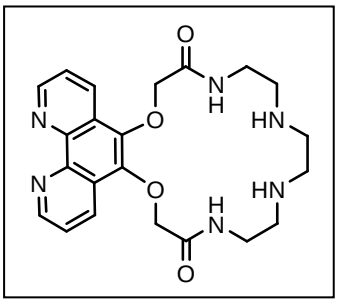

L[6]

Chapter 5 describes synthesis and characterization of new ionophore containing N, S, O-donor atoms in the macrocyclic ring (**L[7]** – **L[9]**). Corresponding fluoroionophores of these ligands have been synthesized using Ru(II) and Re(I) bipyridine based fluorophore and their ion binding property have been evaluated with a large number of metal ions.

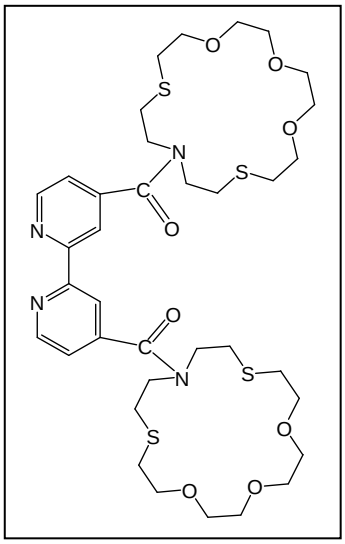

L[7]

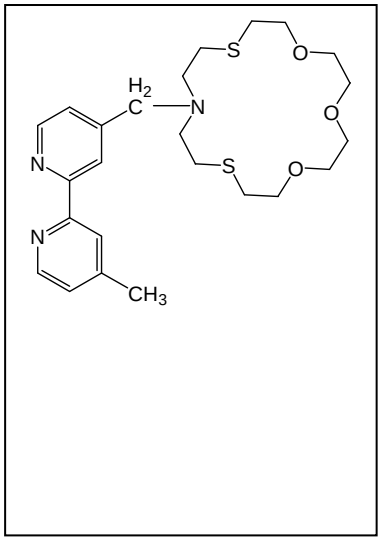

L[8]

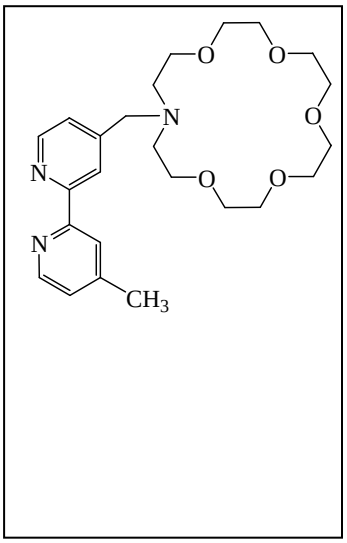

L[9]

1.11 References

1. R. A. Bissell, A. P. de Silva, H. Q. N. Gunaratne, P. L. M. Lynch, G. E. M. Maguireand K. R. A. S. Sandanayake, *Chem. Soc. Rev*. **1992**, *21*, 187.

2. R. Martinez-Manez and F. Sancenon, *Chem. Rev*. **2003**, *103*, 4419.

3. J. Y. Kwon, Y. J. Jang, Y. J. Lee, K. M. Kim, M. S. Seo, W. Nam and J. Yoon, *J. Am. Chem. Soc*. **2005**, *127*, 10107.

4. J. F. Callan, A. P. de Silva and D. C. Magri, *Tetrahedron* **2005**, *61*, 8551.

5. A. W. Czarnik, *Fluorescent Chemosensors of Ion and Molecule Recognition: Ed., ACS Sump. Ser. 538; American Chemical Society: Washington DC*, **1993**.

6. J. R. Lakowicz, *Probe Design and Chemical Sensing: Topics in Fluorescence Spectroscopy: Ed., Plenum Press: New York*, **1994,** Vol. *4*.

7. B. Valeur and I. Leray, *Coord. Chem. Rev*. **2000**, *205*, 3.

8. D. C. Magri, G. J. Brown, G. D. McClean and A. P. de Silva, *J. Am. Chem. Soc*. **2006**, *128*, 4950.

9. A. P. de Silva, D. B. Fox, A. J. M. Huxley and T. S. Moody, *Coord. Chem. Rev*. **2000**, *205*, 41.

10. C. W. Rogers and M. O. Wolf, *Coord. Chem. Rev*. **2002**, *233*, 341.

11. K. Rurack and U. Resch-Genger, *Chem. Soc. Rev.* **2002**, *37*, 116.

12. J. L. Bricks, A. Kovalchuk, C. Trieflinger, M. Nofz, M. Buschel, A. I. Tolmachev, J. Daub and K. Rurack, *J. Am. Chem. Soc*. **2005**, *127*, 13522.

13. Y. A. Zolotov (ed.), *Macrocyclic compounds in analytical chemistry*, wiley, New York, **1997**.

14. L. F. Lindoy, *The chemistry of Macrocyclic ligand Complexes*, Cambridge University Press, **1989**.

15. B. P. Hay and R. D. Hancock, *Coord. Chem. Rev.*, **2001**, *212*, 61.

16. J. S. Kim and D. T. Quang, *Chem. Rev*. **2007**, *107*, 3780.

17. A. Kumar, S.-S. Sun and A. J. Lees, *Coord. Chem. Rev.*, **2008**, *252*, 922.
18. C. Lodeiro and F. Pina, Coord. Chem. Rev., **2009**, *253*, 1353.
19. A. P. de Silva, H. Q. N. Gunaratne, G. Allen, J. M. Huxley, C. P. McCoy, J. T. Rademacher and T. E. Rice, *Chem. Rev.* **1997,** *97*, 1515.
20. P. D. Beer, P. A. Gale and G. Z. Chen, *Coord. Chem. Rev.*, , **1999**, *185-186*, 3.
21. V. Balzani, A. Juris, M. Venturi, S. Campagna and S. Serroni, *Chem. Rev.*, **1996**, *96*, 759.
22. P. D. Beer and E. J. Hayes, *Coord. Chem. Rev*, **2003**, *240*, 167.
23. O. Horvath and K. L. Stevenson, *Charge Transfer Photochemistry of Coordination Compounds*, VCH Publishers, New York City, **1993**, 231.
24. R. Badugu, *J. Fluorescence*, **2005**, *15*, 71.
25. T. Hirao, *Coord. Chem. Rev*, **2002**, *226*, 81.
26. R. Bergonzi, L. Fabbrizzi, M. Lichelli and C. Mangano, *Coord. Chem. Rev.*, **1998** *170*, 31.
27. L. Fabbrizzi, M. Licchelli, P. Pallavicini, L. Parodi and A. Taglietti, *Transition Metals in Supramolecular Chemistry*; John Wiley & Sons Ltd.: New York, **1999**, 93.
28. L. Fabbrizzi, M. Lichelli, P. Pallavicini, D. Sacchi and A. Taglietti, *Analyst*, **1996** *121*, 1763.
29. H.-G. Lohr and F. Vogtle, *Acc. Chem. Res.*, **1985**, *18*, 65.
30. E. U. Akkaya, M. E. Huston and A. W. Czarnik, *J. Am. Chem. Soc.* **1990**, *112*, 3590.
31. S. Manahan, *Toxicological Chemistry*, Lewis Publishers, Inc. **1992**.
32. T. E. Clevenger, *Water, Air and Soil Pollution*, **1990**, *50*, 241.
33. *Heavy Metals Release in Soils*, Edited by H. Magdi, Selim and Donald L. sparks, **2001**.
34. *Chemistry of Precious Metals*, Springer-Verlag, **1997.**
35. C. F. Bell, *Principles and Applications of Metal Chelation*, Clarendon Press, Oxford, **1977**.
36. *Extraction of Metals from Soils and Waters*, D. Max Roundhill, **2001**.

37. N. V. Sidgwick, *The Chemical Elements and Their Compounds*, Oxford University Press, London, **1950**, Vol. *1*.

38. C. S. G. Phillips and R. J. P. Williams, *Inorganic Chemistry*, Clarendon Press, Oxford, **1966**, Vol. *2*.

39. P. D. Beer, S. W. Dent and N. C. Fletcher, *Polyhedron*, **1996**, *15*, 2983.

40. L. H. Uppadine, F. R. Keene and Paul D. Beer, *J. Chem. Soc., Dalton Trans.* **2001**, 2188.

41. M. S. Vickers, K. S. Martindale and P. D. Beer, *J. Mater. Chem.*, **2005**, *15*, 2784.

42. P. R. A. Webber, P. D. Beer, G. Z.Chen, V. Felix and M. G. B. Drew, *J. Am. Chem. Soc.*, **2003**, *125*, 5774.

43. P. D. Beer, F. Szemes, V. Balzani, C. M. Sala, M. G. B. Drew, S. W. Dent and M. Maestri, *J. Am. Chem. Soc.*, **1997**, *119*, 11864.

44. M. –J. Li, Z. Chen, N. Zhu, V. W. Yam and Y. Zu, *Inorg. Chem.*, **2008**, *47*, 1218.

45. M. –J. Li, B. W. Chu, N. Zhu and V. W. Yam, *Inorg. Chem.*, **2007**, *46*, 720.

46. T. Lazarides, T. A. Miller, J. C. Jeffery, T. K. Ronson, H. Adams and M. D. Ward, *J. Chem. Soc., Dalton Trans.* **2005**, 528.

47. M. Chiba, K. Ogawa, K. Tsuge, M. Abe, H. –B. Kim, Y.Sasaki, and N. Kitamura, *Chem. Lett*., **2001**, 692.

48. R.Y. Lai, M. Chiba, N. Kitamura and A.J. Bard, **Anal. Chem.2002**, *74*, 551.

49. M. Chiba, H. –B. Kim and N. Kitamura, *Anal. Sci.*, **2002**, *18*, 461.

50. S. Encinas, K. L. Bushell, S. M. Couchman, J. C. Jeffery, M. D. Ward, L. Flamigni and F. Barigelletti, *J. Chem. Soc., Dalton Trans.* **2000**, 1783.

51. V. W. Yam and V. W. Lee, *J. Chem. Soc., Dalton Trans.* **1997**, 3005.

52. M. Schmittel, H. W. Lin, E. Thiel, A. J. Meixner and H. Ammon, *J. Chem. Soc., Dalton Trans.* **2006**, 4020.

53. M. Schmittel and H. W. Lin, *Angew. Chem., Int. Ed.*, **2006**, *45*, 1.

54. B. D. Muegge and M. M. Richter, ***Anal. Chem.***, **2002**, *74*, 547.

55. L. J. Charbonniere, R. F. Ziessel, C. A. Sams and A. Harriman, *Inorg. Chem.*, **2003,** *42*, 3466**.**

56. M. Schmittel, H. Lin, *J. Mater. Chem.*, **2008**, *18*, 333.

57. R. Grigg, J. M. Holmes, S. K. Jones and W. D. J. A. Norbert, *J. Chem. Soc., Chem. Commun.*, **1994**, 185.

58. J. B. Cooper, M. G. B. Drew and P. D. Beer, *J. Chem. Soc., Dalton Trans.* **2001**, 392.

59. P. D. Beer, F. Szemes, P. Passaniti and M. Maestri, *Inorg. Chem.*, **2004**, *43*, 3965.

60. F. Szemes, D. Hesek, Z. Chen, S. W. Dent, M. G. B. Drew, A. J. Goulden, A. R. Graydon, A. Grieve, R. J. Mortimer, T. Wear, J. S. Weightman, and Paul D. Beer, *Inorg. Chem.*, **1996,** *35*, 5868**.**

61. P. D. Beer, V. Timoshenko, M. Maestri, P. Passaniti and V. Balzani, *Chem. Comm.*, **1999**, 1755.

62. J. E. Redman, P. D. Beer, S. W. Dent and M. G. B. Drew, *Chem. Commun*., **1998**, 231.

63. P. D. Beer and S. W. Dent, *Chem. Commun.*, **1998**, 825.

64. L. H. Uppadine, J. E. Redman, S. W. Dent, M. G. B. Drew and P. D. Beer, *Inorg. Chem.*, **2001,** *40*, 2860**.**

65. J. D. Lewis and J. N. Moore, *Chem. Commun*., **2003**, 2858.

66. J. D. Lewis and J. N. Moore, *J. Chem. Soc., Dalton Trans.* **2004**, 1376.

67. J. D. Lewis, R. N. Perutz and J. N. Moore, *Chem. Commun.*, **2000**, 1865.

68. Y. Shen and B. P. Sullivan, *Inorg. Chem.*, **1995**, *34*, 6236.

69. J. B. Cooper, M. G. B. Drew and P. D. Beer, *J. Chem. Soc., Dalton Trans.* **2000**, 2721.

70. A. P. de Silva, H. Q. N. Gunaratne, C. McVeigh, G. M. Maguire, P. R. S. Maxwell and E. O'Hanlon, *Chem. Commun.*, **1996**, 2191.

71. H. Nishida, Y. Katayama, H. Katsuki, H. Nakamura, M. Takagi and K. Ueno, *Chem. Lett*., **1982**, 1853.

72. M. V. Alfimov, A. V. Churakov, Y. V. Fedorov, O. A. Fedorova, S. P. Gromov, R. E. Hester, J. A. K. Howard, L. G. Kuz'mina, I. K. Lendnev and J. N. Moore, *J. Chem. Soc., Perkin Trans. 2*, **1997**, 2249.

73. T. Hayashita, A. Murakami and N. Teramae, *Chem. Lett.*, **2004**, *33*, 568.

74. E. Cielen, A. Tahri, K. V. Heyen, G. J. Hoornaert, F. C. De Schryver and N. Boens, *J. Chem. Soc., Perkin Trans.2*, **1998**, 1573.

75. A. J. Tong, Y. S. Song, L. D. Li, T. Hayashita, N. Tetamae, C. Park and R. A. Bartsh, *Analytica Chimica Acta*, **2000**, *420*,57.

76. J. D. Chartres, A. M. Groth, L. F. Lindoy, M. P. Lowe and G. V. Meehan, *J. Chem. Soc., Perkin Trans.1*, **2000**, 3444.

77. R. S. Addleman, J. Bennet, S. H. Tweedy, S. Elshani and C. M. Wai, *Talanta*, **1998**, *46*, 573.

78. K. Ikeda and S. Abe, *Anal. Chim. Acta*, **1998**, *363*, 165.

79. Y. Jin, I. Yoon, J. Seo, J. E. Lee, S. T. Moon, J. Kim, S. W. Han, K. M. Park, L. F. Lindoy and S. S. Lee, *Dalton Trans.*, **2005**, 788.

80. M. Regueiro-Figueroa, D. Esteban-Gomez, C. Platas-Iglesias, A. deBlas and T. Rodriguez-Blas, *Eur. J. Inorg. Chem*., **2007**, 2198.

81. Y. H. Kim, N. R. Cha and S. K. Chang, *Tetrahedron Letters*, **2002**, *43*, 3883.

CHAPTER – II

Synthesis, Characterization, Electrochemical Studies of Ruthenium(II) and Rhenium(I) Bipyridine Crown Ether Receptor Molecules

2.1 Introduction

The design and synthesis of fluorescent molecular sensors for detection of ions are of great interest because of their important role in many biological and environmental processes.[1-8] Such molecular sensors can be constructed by the combination of an ionophore, designed for the binding of specific incoming ion, and a luminescent fragment whose photophysical properties perturbed during the recognition processes to produce a measurable output signal.[9-13] For the recognition of alkali, alkaline earth and heavy metal ions, photoactive units attached with crown ether or its derivatives which serves as receptors are generally used.[14-18] Both organic photoactive molecules and ruthenium(II)/rhenium(I)-polypyridine based photoactive metal complexes have been used as fluorophore, however the latter is of special interest because of some advantages over organic molecules. Besides changes in luminescence like organic molecules, they also exhibit measurable changes in electrogenerated chemiluminesence and redox property in the event of ion recognition process.[14-23] The spacers, which make connection between the fluorophore and ionophore, also play important role to make electronic communication between the two units. As ionophore, macrocyclic compounds, which are noted for their remarkable selectivity towards specific cations, have been extensively used for cation recognition study. In this regard, crown ethers are excellent choices as complexing agents for alkali and alkaline earth metal ions.[16-21,23]

Considerable amount of work in this area has been reported in the literature, where fluoroionophores comprising of Ru(II)/Re(I)-polypyridine based fluorophore and crown ether based ionophores have been used.[16,17,20,22] Fluoroionophore containing crown ether moiety directly fused with bipyridine/1,10-phenanthroline unit have also been reported.[24-27] Ru(II)-polypyridine based complexes containing azacrown as ionophore has recently been reported as quadruple-channel sensor for selective and quantitative analysis of Pb^{2+}, Cu^{2+} and Hg^{2+}.[28,29]

In the present study, with the aim to prepare fluoroionophores for cation recognition, three new ligands have been synthesized incorporating aza/benzocrown ethers as ionophore and bipyridine/phenanthroline unit as coordinating moiety. The fluoroionophores have been synthesized by the reaction of *cis*-$[Ru(bpy)_2Cl_2]$/*cis*-$[Ru(phen)_2Cl_2]$ and respective ligands and isolated with PF_6^- counter ion. The

macrocyclic unit (ionophore) is connected to the metal bound bipyridine or 1,10-phenanthroline unit through amide (>C=O) or imino (-CH=N-) moiety. All of these complexes have been characterized on the basis of analytical and spectroscopic studies. Absorption, luminescence and electrochemical properties of these receptors have been studied.

2.2 Experimental Section

2.2.1 Materials

The complexes *cis*-$[Ru(bpy)_2Cl_2]\cdot 2H_2O$ and *cis*-$[Ru(phen)_2Cl_2]\cdot 2H_2O$ were prepared following the literature procedure.[30,31] Hydrated ruthenium trichloride was purchased from Arora Matthey. All other starting materials and reagents used in this study were purchased from Aldrich and S. D. Fine Chemicals. All solvents were analytical grade and purified by standard procedure before use.[32]

2.2.2 Physical measurements

Elemental analyses (C, H and N) were performed on a model 2400 Perkin-Elmer elemental analyzer. NMR spectra were recorded on a model DPX 200 and Avance II 500 MHz Bruker FT-NMR instruments. Infrared spectra were recorded on a Perkin Elmer Spectrum GX FT-IR system. Mass spectra were recorded on a Q-Tof micro^{TM} LC-MS instrument. The UV-Vis spectra were recorded on a CARY 500 scan Varian spectrophotometer. Luminescence spectra were recorded on a Perkin-Elmer LS-50B spectrofluorimeter. Quantum yields were measured in optically diluted solution following the literature procedure using $[Ru(bpy)_3]^{2+}$ ($\phi = 0.062$) as reference emitter.[30] Electrochemical measurements were made using CHI 660A electrochemical workstation equipment. Cyclic and DPV studies were carried in a three electrode cell consisting of a glassy-carbon working electrode, a platinum-wire auxiliary electrode and an SCE reference electrode. Solutions of the complexes in purified acetonitrile containing 0.1 M tetrabutylammonium tetrafluoroborate as supporting electrolyte were deaerated by bubbling nitrogen for 15 minutes prior to

each experiment. Cyclic voltammogram of $[Ru(bpy)_3]^{2+}$ was recorded first for calibration of the instrument. Single crystal structures were determined using Bruker SMART 1000 (CCD) diffractometer.

2.2.3 Synthesis of Ligands

L^1: A mixture of 2,2'-bipyridine-4,4'-dicarboxilic acid (0.244 g, 1 mmol), which was prepared following a published procedure,[33] and thionyl chloride (10 mL) was refluxed under nitrogen atmosphere at 80^0C for 20 h. Excess thionyl chloride was then removed by rotary evaporation and the yellowish solid mass thus obtained was directly used in the next step. In the second step, 1-aza-18-crown-6 (0.50 g, 1.90 mmol) was dissolved in dry THF (50 mL) and triethylamine (2 mL) was added into this solution. Then THF solution (10 mL) of the acid chloride, obtained in the previous step, was added dropwise into the reaction mixture over a period of 0.5 h and the solution was stirred at room temperature for 24 h. the product, which separated during stirring, was isolated by filtration and the solid mass was dissolved in dichoromethane (50 mL) and extracted with water (50 mL, 3 times) to remove triethylamine hydrochoride salt. The organic layer was dried with anhydrous sodium sulphate and the solvent was evaporated to dryness. The crude product was purified by column chromatography using silica gel (100-200 mesh) as packing material and dichloromethane with 5% methanol as eluent. Yield: 0.40 g (54 %). ^{1}H NMR (200 MHz, $CDCl_3$): δ = 8.73 (d, J = 4.4 Hz, 2 H, 6-H and 6′-H of bpy), 8.48 (s, 2 H, 3-H and 3′-H of bpy′), 7.40 (d, J = 4.4 Hz, 2 H, 5-H and 5′-H of bpy), 3.83 (s br, 8 H, -CH_2N of crown ether), 3.67-3.58 (m, 40 H, -CH_2O of crown ether) ppm. LC-MS: *m/z* = 773.63 (31%, calcd. for [$\mathbf{L^1}$ + K^+]: 773.47), 757.57 (94%, calcd. for [$\mathbf{L^1}$ + Na^+]: 757.36), 735.68 (18%, calcd. for [$\mathbf{L^1}$ + H^+]: 735.38). IR (KBr pellets): ν = 1619 cm^{-1} (C = O). $C_{36}H_{54}N_4O_{12}$ (734.37): calcd. C 58.85, H 7.35, N 7.63; found C 58.42, H 7.39, N 7.51.

L^2: This compound was synthesized following the similar method as described for L^1. The required intermediates 1,10-phenanthroline-4,7-dicarboxaldehyde and 1,10-phenanthroline-4,7-dicarboxilic acid were synthesized following the published procedures.[33] Corresponding acid chloride and thereby the ligand $\mathbf{L^2}$ were synthesized

following the method mentioned above for $\mathbf{L^1}$. Yield: 0.15 g (53 %) (with respect to dicarboxylic acid derivative). ^{1}H NMR (200 MHz, $CDCl_3$): δ = 9.23 (d, *J* = 4.4 Hz, 2 H, 2-H and 9-H of phen), 7.87 (s, 2 H, 5-H and 6-H of phen), 7.62 (d, *J* = 4.4 Hz, 2 H, 3-H and 8-H of phen), 4.00-3.93 (m, 8 H, -CH_2N of crown ether), 3.76-3.42 (m, 40 H, -CH_2O of crown ether). LC-MS: *m/z* = 781.45 (100%, calcd. for [$\mathbf{L^2}$ + Na^+]: 781.84), 759.49 (44%, calcd. for [$\mathbf{L^2}$ + H^+]: 759.86). IR (KBr pellets): ν = 1617 cm^{-1} (C = O). $C_{38}H_{54}N_4O_{12}$ (758.85): calcd. C 60.14, H 7.17, N 7.38; found C 59.82, H 7.30, N 7.31.

$\mathbf{L^3}$: A mixture of 4′-methyl-2,2′-bipyridine-4-carbaldehyde (0.20 g, 1.01 mmol), which was prepared following published procedure and 4′-aminobenzo-18-crown-6 (0.33 g, 1.0 mmol) was refluxed in ethanol (20 mL) for 8 h. After refluxing, the dark red solution was kept at room temperature for overnight during which brown coloured microcrystalline compound was separated. The compound was isolated by filtration, washed with diethyl ether and dried. Yield: 0.425 g (83 %). ^{1}H NMR (200 MHz, $CDCl_3$): δ = 8.78 (d, *J* = 5.2 Hz, 1 H, 6-H or 6′-H of bpy), 8.75 (s, 1 H, *CH*=N), 8.58 (s, 1 H, 3-H or 3′-H of bpy), 8.57 (d, *J* = 5.2 Hz, 1 H, 6′-H or 6-H of bpy), 8.28 (s, 1 H, 3′-H or 3-H of bpy), 7.85 (d, *J* = 4.8 Hz, 1 H, 5-H or 5′-H of bpy), 7.17 (d, *J* = 4.8 Hz, 1 H, 5′-H or 5-H of bpy), 6.92 (m, 3 H, phenyl), 4.20 (m, 4 H, -CH_2O crown ether), 3.96 (m, 4 H, -CH_2O crown ether), 3.77-3.70 (m, 12 H, -CH_2O crown ether), 2.47 (s, 3 H, CH_3). LC-MS: *m/z* = 530.70 (16%, calcd. for [$\mathbf{L^3}$ + Na^+]: 530.57), 508.74 (11%, calcd. for [$\mathbf{L^3}$ + H^+]: 508.59). IR (KBr pellets): ν = 1594 cm^{-1} (C=N). $C_{28}H_{33}N_3O_6$ (507.58): calcd. for C 66.26, H 6.55, N 8.28; found C 66.10, H 6.84, N 8.24.

2.2.4 Synthesis of Complexes

General Procedure for the synthesis of $[Ru(bpy)_2(L^1)][PF_6]_2.2H_2O$ (1), $[Ru(bpy)_2(L^2)][PF_6]_2.2H_2O$ (2), $[Ru(phen)_2(L^2)]$ $[PF_6]_2.2H_2O$ (3) and $[Ru(bpy)_2(L^3)]$ $[PF_6]_2.2H_2O$ (4): A mixture of *cis*-$Ru(bpy)_2Cl_2{\cdot}2H_2O$/*cis*-$Ru(phen)_2Cl_2{\cdot}2H_2O$ (0.2 mmol) and appropriate ligand $\mathbf{L^1}$/$\mathbf{L^2}$/$\mathbf{L^3}$ (0.2 mmol) in ethanol-water (1:1, 50 mL) was refluxed for 12 h. The volume of the reaction mixture was reduced to ca 20 ml by rotary evaporation, filtered and to the filtrate an aqueous

solution of NH_4PF_6 (0.20 g, 1.3 mmol) was added. The precipitate was filtered off and washed with water and diethyl ether. The compound was purified by column chromatography packed with neutral alumina, with acetonitrile-toluene (3:2) as eluent. The solvent of the desired fraction was removed by rotary evaporation and the compound was washed with diethyl ether and vacuum dried. Yield: 0.2 g (72 %) for **1**, 0.19 g (66%) for **2**, 0.14 g (53 %) for **3** and 0.12 g (54 %) for **4**.

Characterization Data (complex 1): ^{1}H NMR (500 MHz, CD_3CN): δ = 8.58 (s, 2 H, 3-H and 3′-H of bpy of $\mathbf{L^1}$), 8.51 (d, J = 8.0 Hz, 4 H, 6-H and 6′-H of bpy), 8.06-8.10 (overlapped triplets, 4 H, 5-H and 5′-H of bpy), 7.80 (d, J = 5.5 Hz, 2 H, 3-H and 3′-H of bpy), 7.76 (d, J = 5.5 Hz, 2 H, 6-H and 6′-H of bpy of $\mathbf{L^1}$), 7.71 (d, J = 5.5 Hz, 2 H, 3-H and 3′-H of bpy), 7.44 (d, J = 5.5 Hz, 2 H, 5-H and 5′-H of bpy of $\mathbf{L^1}$), 7.40-7.45 (overlapped triplets, 4 H, 4-H and 4′-H of bpy), 3.43-3.72 (m, 48 H, -CH_2O of crown ether). LC-MS: *m/z* = 1461.69 (31%, calcd. for [**1** + Na^+]: 1461.33), 1293.62 (94%, calcd. for [**1** – PF_6^-]$^+$: 1293.24), 1147.62 (18%, calcd. for [**1** – H^+ – $2PF_6^-$]$^+$: 1147.27). IR (KBr pellets): ν = 1634 cm^{-1} (C = O), 840 cm^{-1} (PF_6^-). UV-Vis (CH_3CN): λ = 454 nm (ε, 1.28 x 10^4 $M^{-1}cm^{-1}$), 288 nm (ε, 6.31 x 10^4 $M^{-1}cm^{-1}$). $C_{56}H_{74}F_{12}N_8O_{14}P_2Ru$ (1474.23): calcd. for C 45.62, H 5.02, N 7.60; found: C 45.49, H 4.84, N 7.43.

Complex 2: ^{1}H NMR (500 MHz, CD_3CN): δ = 8.68 (d, J = 8.0 Hz, 2 H, 6-H and 6′-H of bpy), 8.61 (s, 2 H, 5-H and 6-H of phen of $\mathbf{L^2}$), 8.56 (d, J = 8.0 Hz, 2 H, 6-H and 6′-H of bpy), 8.28 (d, J = 5.5 Hz, 2 H, 3-H and 3′-H of bpy), 8.23-8.28 (overlapped triplets, 4 H, 5-H and 5′-H of bpy), 7.88 (d, J = 5.5 Hz, 2 H, 3-H and 3′-H of bpy), 7.83 (dd, J_1 = 8.0 Hz, J_2 = 5.5 Hz, 2 H, 4-H and 4′-H of bpy), 7.70 (d, J = 6.0 Hz, 2 H, 2-H and 9-H of phen of $\mathbf{L^2}$), 7.57 (dd, J_1 = 8.0 Hz, J_2 = 5.5 Hz, 2 H, 4-H and 4′-H of bpy), 7.33 (dd, J_1 = 6.0 Hz, J_2 = 1.5 Hz, 2 H, 3-H and 8-H of phen of $\mathbf{L^2}$), 3.35-3.70 (m, 48 H, -CH_2O of crown ether). LC-MS: *m/z* = 1341.92 (38%, calcd. for [**2** – H^+ – PF_6^- + Na^+]$^+$: 1341.25). IR (KBr pellets): ν = 1632 cm^{-1} (C = O), 840 cm^{-1} (PF_6^-). UV-Vis (CH_3CN): λ = 445 nm (ε, 1.62x10^4 $M^{-1}cm^{-1}$), 262 nm (ε, 7.66 x 10^4 $M^{-1}cm^{-1}$). $C_{58}H_{74}F_{12}N_8O_{14}P_2Ru$ (1498.25): calcd. for C 46.50, H 5.00, N, 7.48; found C 46.28, H 5.14, N 7.3.

Complex 3: ^{1}H NMR (200 MHz, CD_3CN): δ = 8.63 (d, *J* = 5.0 Hz, 2 H, 2-H and 9-H of phen), 8.59 (d, *J* = 5.0 Hz, 2 H, 2-H and 9-H of phen), 8.25 (s, 4 H, 5-H and 6-H of phen), 8.13 (s, 2 H, 5-H and 6-H of phen of **L^2**), 7.99-8.08 (m, 6 H, 4-H and 7-H of phen; and 2-H and 9-H of phen of **L^2**), 7.60-7.71 (m, 6 H, 3-H and 8-H of phen including **L^2)**, 3.47-3.84 (m, 48 H, -*CH*$_2$O of crown ether). LC-MS: *m/z* = 1532.09 (5 %, calcd. for [**3** + Na^+]$^+$: 1533.25), 1364.74 (30 %, calcd. for [**3** – PF_6]$^+$: 1365.30). IR (KBr pellets): ν = 1633 cm^{-1} (C = O), 841 cm^{-1} (PF_6^-). UV-Vis (CH_3CN): λ = 435 nm (ε, 1.54 x 10^4 $M^{-1}cm^{-1}$), 263 nm (ε, 8.22 x 10^4 $M^{-1}cm^{-1}$). $C_{62}H_{74}F_{12}N_8O_{14}P_2Ru$ (1546.29): calcd. for C 48.15, H 4.82, N 7.24; found C 47.86, H 4.96, N 7.10.

Complex 4: ^{1}H NMR (200 MHz, CD_3CN): δ = 8.91 (s, 1 H, -C*H*=N), 8.74 (s, 1 H, benzocrown-ArH), 8.50 (d, *J* = 8.0 Hz, 4 H, 6-H and 6′-H of bpy), 8.06 (t, *J* = 8.0 Hz, 4 H, 5-H and 5′-H of bpy), 7.81 (m, 2 H, 6-H and 6′-H of bpy of **L^3**) 7.73 (d, *J* = 5.6 Hz, 4 H, 3-H and 3′-H of bpy), 7.56 (d, *J* = 6.0 Hz, 1 H, 5-H or 5′-H of bpy of **L^3**), 7.37-7.44 (m, 4 H, 4-H and 4′-H of bpy), 7.27 (d, *J* = 6.0 Hz, 1 H, 5′-H or 5-H of bpy of **L^3**), 7.02-7.06 (m, 3 H, Ar-H of benzocrown), 4.20 (m, 4 H, -*CH*$_2$O of crown ether), 3.78 (m, 4 H, -*CH*$_2$O of crown ether), 3.56-3.60 (m, 12 H, -*CH*$_2$O of crown ether), 2.57 (s, 3 H, *CH*$_3$). LC-MS: *m/z* = 1234.29 (4 %, calcd. for [**4** + Na^+]: 1233.93), 1066.29 (100 %, calcd. for [**4** – PF_6]$^+$: 1065.98), 920.31 (10 %, calcd. for [**4** – H^+ – 2PF_6^-]$^+$: 920.02). IR (KBr pellets): ν = 1621 cm^{-1} (C=N), 842 cm^{-1} (PF_6^-). UV-Vis (CH_3CN): λ = 465 nm (ε, 1.92 x 10^4 $M^{-1}cm^{-1}$), 288 nm (ε, 5.92 x 10^4 $M^{-1}cm^{-1}$) . $C_{48}H_{53}F_{12}N_7O_8P_2Ru$ (1246.97): calcd. for C 46.23, H 4.28, N 7.86; found C 45.92, H 4.32, N 7.78.

General Procedure for the synthesis of [Re(L^1)(CO)$_3$Cl].THF (5) and [Re(L^3)(CO)$_3$Cl].THF (6): A mixture of $[Re(CO)_5Cl]$ (0.10 g, 0.275 mmol) and appropriate ligand **L^1/L^3** (0.275 mmol) was refluxed in dry THF (30 mL) under nitrogen atmosphere for 15 h. The solution was then allowed to cool to room temperature and the solvent was removed by rotary evaporation. The residue thus obtained was dissolved in dichloromethane (10 mL) and was added dropwise into n-hexane (50 mL) with stirring. The precipitate thus obtained was isolated by filtration

and purified by column chromatography packed with neutral alumina using acetonitrile-toluene (1:1) as eluent. The solvent from the desired fraction was removed by evaporation. Yield: 0.13 g (47 %) for **5** and 0.1 g (40 %) for **6**.

Characterization Data (complex 5): ^{1}H NMR (200 MHz, $CDCl_3$): δ = 9.03 (d, *J* = 5.6 Hz, 2 H, 6-H and 6′ of bpy), 8.50 (s, 2 H, 3-H and 3′-H of bpy), 7.64 (d, *J* = 5.6, 2 H, 5-H and 5′-H of bpy), 3.75 (s, 8 H, -CH_2N of crown ether), 3.52-3.62 (m, 40 H, -CH_2O of crown ether and -CH_2O of THF), 1.92 (m, 4 H, -CH_2 of THF). LC-MS: *m/z* = 1063.52 (100 %, calcd. for [**5** + Na^+]: 1063.51). IR (KBr pellets): ν_{CO} = 2021 (A_1), 1900 and 1894 (E) cm^{-1}. UV-Vis (CH_3CN): λ = 385 nm (ε, 4.13 x 10^3 $M^{-1}cm^{-1}$), 297 nm (ε, 1.77 x 10^3 $M^{-1}cm^{-1}$). $C_{43}H_{62}ClN_4O_{16}Re$ (1112.63): calcd. for C 46.42, H 5.62, N 5.04; found C 46.19, H 5.98, N 4.97.

Complex 6: ^{1}H NMR (200 MHz, $CDCl_3$): 9.07 (d, *J* = 5.6 Hz, 1 H, 6-H or 6′-H of bpy), 8.87 (d, *J* = 5.6 Hz, 1 H, 6′-H or 6-H of bpy), 8.66 (s, 1 H, 3-H or 3′-H of bpy), 8.34 (s, 1 H, 3′-H or 3-H of bpy), 8.16 (s, 1 H, -*CH*=N), 7.84 (dd, J_1 = 5.8 Hz, J_2 = 1.4 Hz, 1 H, 5-H or 5′-H of bpy), 7.47 (d, *J* = 5.8 Hz, 1 H, 5′-H or 5-H of bpy), 7.38 (s, 1 H, benzocrown-Ph-H), 7.21-7.25 (m, 2 H, benzocrown-Ph-H), 4.33 (m, 4 H, -CH_2O of crown ether), 3.84 (m, 4 H, -CH_2O of crown ether), 3.55-3.70 (m, 16 H, -CH_2O of crown ether and –CH_2O of THF), 2.54 (s, 3 H, CH_3), 1.94 (m, 4 H, -CH_2 of THF). LC-MS: *m/z* = 907.7 (50%, calcd. for [**6** + Na^+]: 908.36). IR (KBr pellets): ν_{CO} = 2018 (A_1), 1910 and 1889 (E) cm^{-1}. UV-Vis (CH_3CN): λ = 342 nm (ε, 1.37 x 10^4 $M^{-1}cm^{-1}$), 292 nm (ε, 2.04 x 10^4 $M^{-1}cm^{-1}$). $C_{35}H_{41}ClN_3O_{10}Re$ (885.37): calcd. for C 47.48, H 4.68, N 4.75; found C 47.13, H 4.84, N 4.35.

2.2.5 X-ray Crystallography

The crystallographic data and details of data collection are given in Table 1. Crystal of suitable size was selected from the mother liquor is mounted on the tip of a glass fiber and cemented using epoxy resin. Intensity data for the crystal was collected using MoK_α (λ = 0.71073Å) radiation on a Bruker SMART APEX diffractometer equipped with CCD area detector at 100K. The data integration and reduction were processed with SAINT software. [34] An empirical absorption correction

was applied to the collected reflections with SADABS using XPREP.[34,35] The structures were solved by direct methods using SHELXTL and was refined on F^2 by the full-matrix least-squares technique using the SHELXL-97 program package.[36,37] Graphics for packing diagram was generated using PLATON.[38] All non-hydrogen atoms were refined anisotropically till convergence is reached. Hydrogen atoms attached to the ligand moieties are either located from the difference Fourier map or sterochemically fixed.

2.3 Results and Discussion

2.3.1 Synthesis of Ligands L^1-L^3

The route followed for the synthesis of **L^1** is shown in Scheme 1; similar procedure has also been used for the synthesis of **L^2** with the exception that 4,7-dimethyl-1,10-phenanthroline has been used instead of 4,4'-dimethylbipyridine as starting material. **L^3** was prepared by the reaction of 4′-methyl-2,2′-bipyridine-4-carbaldehyde with 4′-aminobenzo-18-crown-6, the former aldehyde was synthesized following the published procedure.[39]

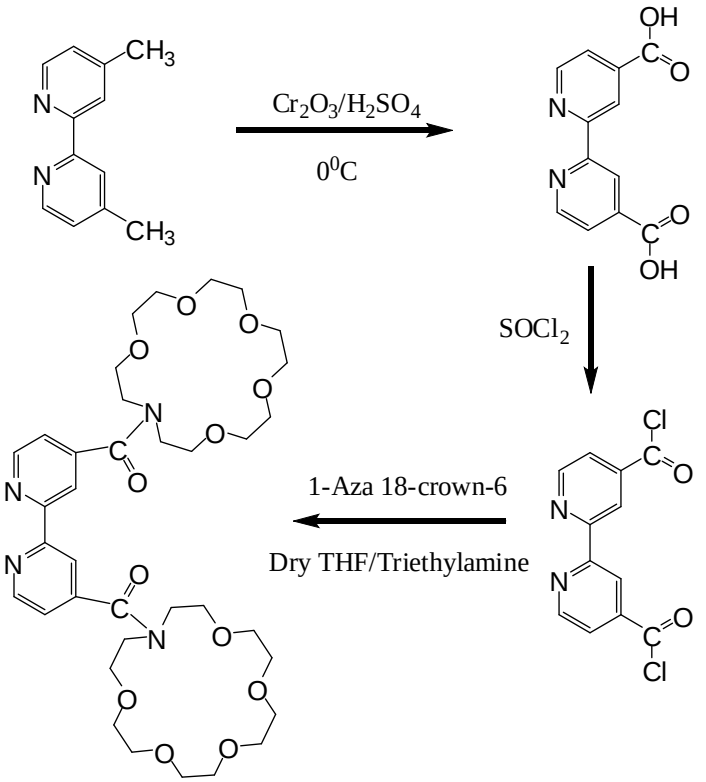

L^1

Scheme 1. Route followed for the synthesis of **L^1**

Table 1 Crystal, data collection and refinement details for **L^1**

Formula	$C_{36}H_{54}N_4O_{12}$
Molecular weight	734.83
Crstal colour	Yellow
Crstal size (mm^3)	0.23x 0.16 x 0.06
T/K	293
Crystal system	Monoclinic
Space group	$P2_1/n$
a/Å)	10.5750(7)
b/Å	10.4136(7)
c/Å	16.8608(11)
α/°	90
β/°	107.1990(10)
γ/°	90
Z	2
V/$Å^3$	1773.7(2)
ρ/g cm^{-3}	1.376
Absorption coefficient/mm^{-1}	0.103
F(000)	788
Reflections collected	10193
Independent reflections	4079 [R(int) = 0.0171]
Number of parameters	343
GOF on F^2	1.240
*R*1, *wR*2 (I>2σ(I)	0.0552 / 0.1230
*wR*1, *wR*2 (all data)	0.0566 / 0.1238

Microanalytical (C, H and N), mass spectrometric, IR and ^{1}H NMR spectral data of all these ligands are given in the Experimental Section. ^{1}H NMR spectra of **L^1,** **L^2** and **L^3** are shown in Figures 2.1-2.3, respectively. Microanalytical and mass spectrometric data are in agreement with the calculated values. It may be noted that *e/m* values of all these compounds correspond to Na^+/K^+ adduct (ligand + Na^+/K^+), which is a well known phenomenon when LC-MS is used for the measurement of mass.[40,41] In the ^{1}H NMR spectra, the aromatic region of **L^1** and **L^2** exhibit two doublets and a singlet, which are expected from symmetrically substituted bipyridine/1,10-phenanthroline unit. The high field doublet (δ = 8.73 for **L^1** and δ = 9.23 for **L^2)** are assigned to 6-H and 6′-H of the bpy of **L^1** and 2-H and 9-H of phen of the **L^2** (usual nomenclature of the protons for 2,2'-bipyridine and 1,10-phenanthroline are used). The low field doublets at δ = 7.40 for **L^1** and at δ = 7.62 for **L^2** are due to 5-H and 5′-H of bpy of **L^1** and 3-H and 8-H of phen of **L^2**, respectively. The singlets at δ = 8.48 (**L^1**) and δ = 7.87 (**L^2**) are due to 3-H and 3′-H of bpy, and 5-H and 6-H of phen, respectively. The protons attached to crown moieties appear as multiplets in the region δ = 3.5 to 4.0. The NMR data are consistent to the proposed structures shown in Scheme 1 (**L^1**) and Figure 2.4 **(L^2**). In case of **L^3,** four doublets and two singlets, as expected for the unsymmetrically 4,4′-substituted 2,2'-bipyridine unit (Figure 2.5) are appeared in the range δ = 8.78 – 7.17 (detail assignment of peaks is given in the Experimental Section). Protons for the benzocrown unit appeared as multiplets at δ = 6.92 (phenyl), 4.20, 3.96 and 3.77-3.70 (crown ether). The methyl group attached to bpy moiety appeared as singlet at δ = 2.47. Molecular structure of **L^1** is established by single crystal X-ray study.

2.3.2 Crystal Structure of L^1

The molecular structure of **L^1** is determined by single crystal X-ray study. It crystallizes in monoclinic space group $P2_1/n$ and possesses a center of symmetry at the midpoint of the C1-C1a bond of the bipyridine moiety bridging the azacrowns on either side. The ORTEP view of the L^1 is shown in Figure 2.6. For the 2,2'-bipyridine moiety, the two pyridine rings are planar but the nitrogen atoms are in opposite sides. The symmetrically disposed carbonyl oxygen O1 from either side of the 2,2'-b

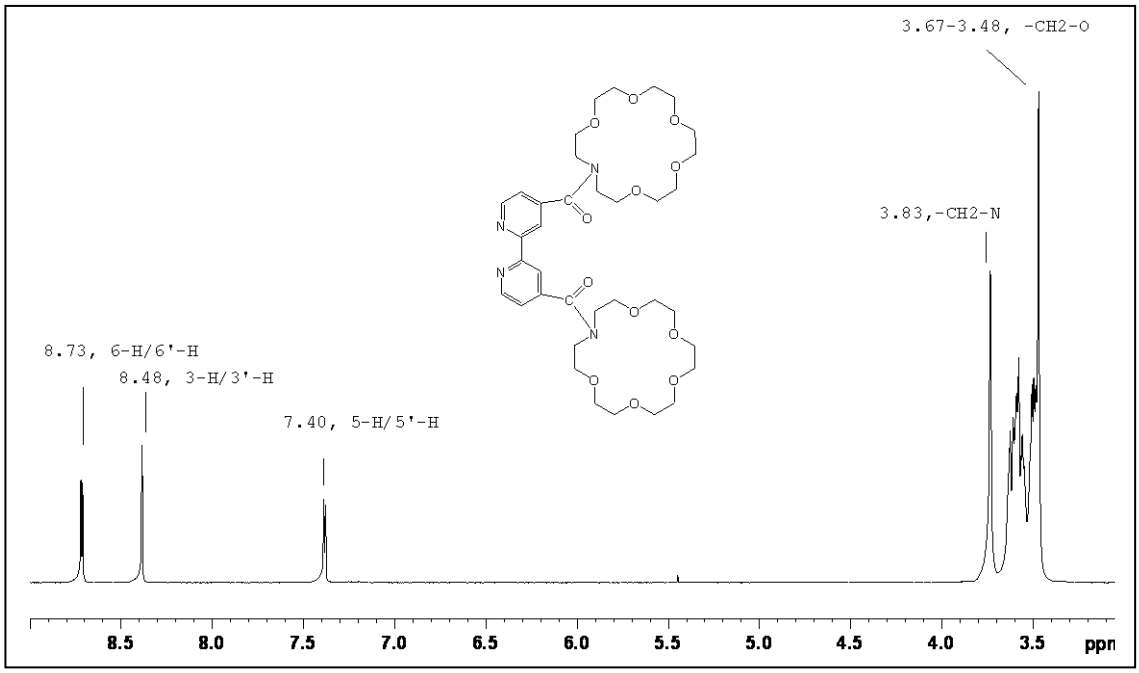

Figure 2.1 ^{1}H NMR spectra of L^{1}

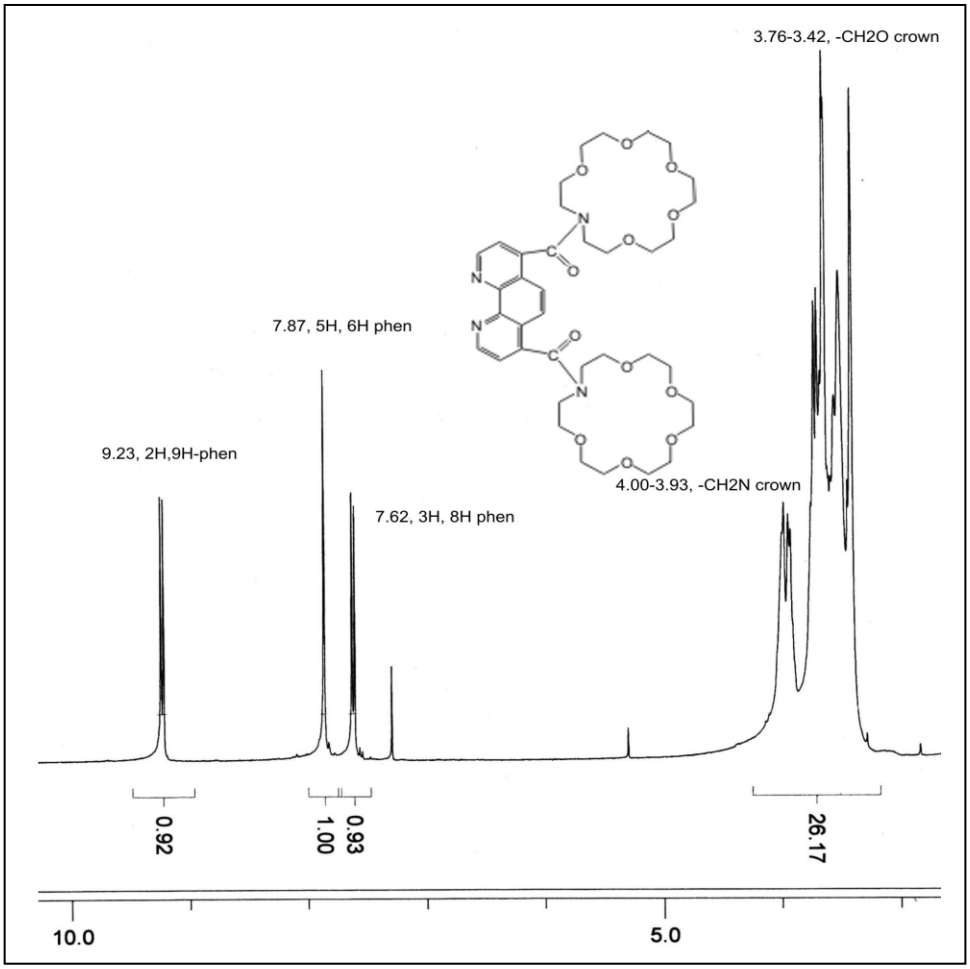

Figure 2.2 ^{1}H NMR spectra of L^{2}

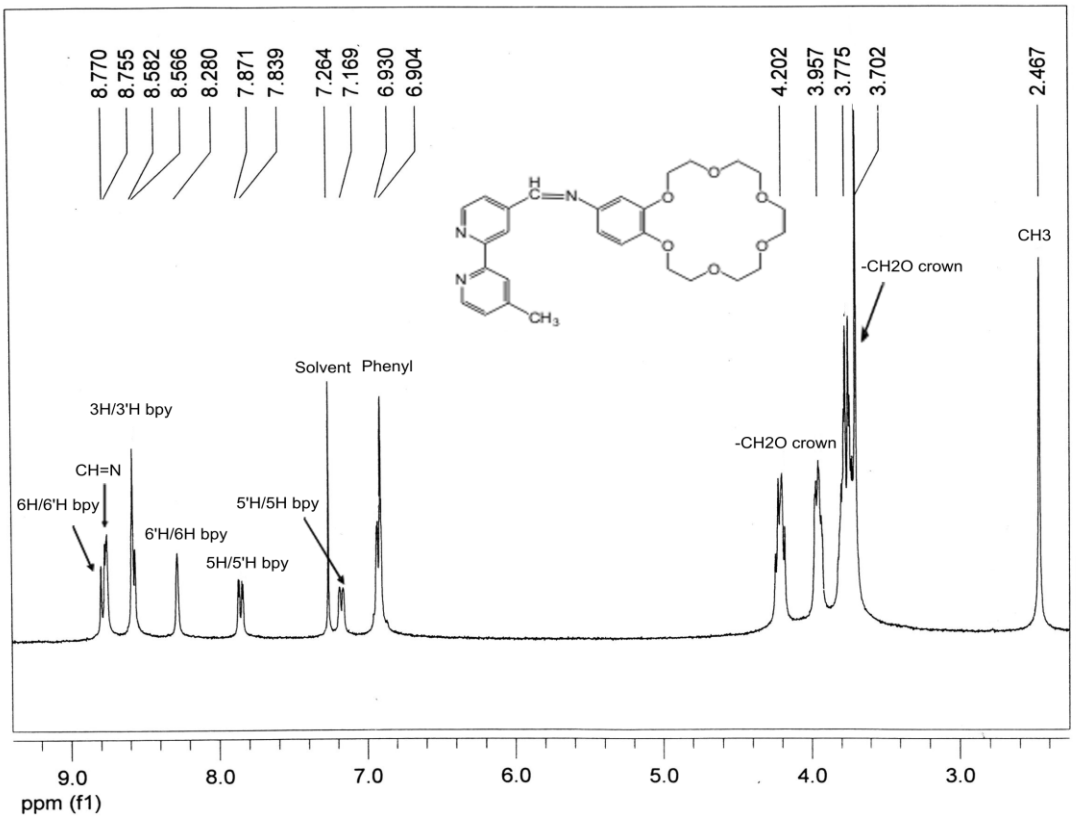

Figure 2.3 ^{1}H NMR spectra of L^{3}

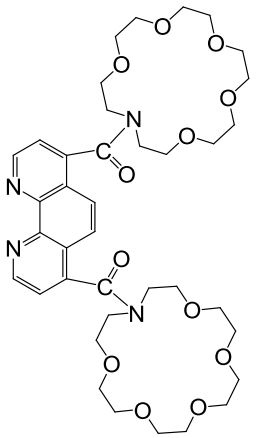

L^{2}

Figure 2.4 Structural drawing of **L^{2}**

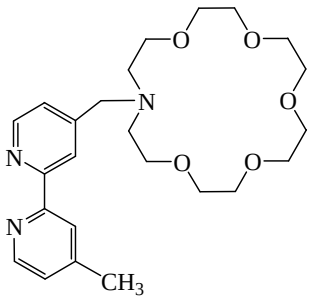

Figure 2.5 Structural drawing of **L^{3}**

bipyridine moiety is involved in two intermolecular C-H…O interaction with phenyl hydrogen H4 and methylene hydrogen H112 generating a layered net work structure (Figure 2.7).Several strong intermolecular C-H…O interactions involving methylene

hydrogen atoms from C17 and C18 with oxygen atoms O4, O2 and O3 of the crown moieties also exist. Details of this pertinent hydrogen bonding interaction with symmetry code are given in Table 2.

Table 2. Hydrogen bonding parameters for $\mathbf{L^1}$ with symmetry code

D-H···A	***d*(H···A), Å**	***d*(D···A), Å**	**<DHA deg**
C(4)-H(4)...O(1)[1]	H(4)...O(1)= 2.54(2)	C(4)...O(1) = 3.309(2)	C(4)-H(4)...O(1)= 140.2(17)
C(11)-H(112)…O(1)[2]	H(112)...O(1)= 2.52(2)	C(11)...O(1) =3.466(2)	C(11)-H(112)...O(1))= 166.4(19)
C(17)-H(172)…O(4)[3]	H(172)...O(4)= 2.48(2)	C(17)...O(4)= 3.477(2)	C(17)-H(172)…O(4)= 164.9(16)
C(18)-H(182)…O(2)[3]	H(182)...O(2) = 2.43(2)	C(18)...O(2)= 3.152(2)	C(18)-H(182)…O(2)= 129.2(16)
C(18)-H(182)...O(3)[3]	H(182)...O(3)= 2.37(2)	C(18)...O(3)= 3.221(2)	C(18)-H(182)...O(3)= 142.3(17)
1. 1-x,1-y,-z 2. x,1+y,z 3. x, y, z			

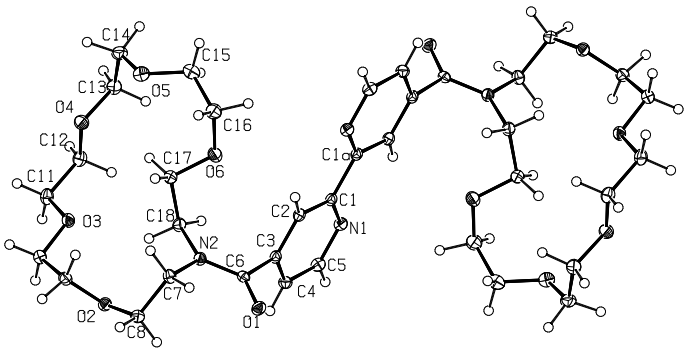

Figure 2.6 ORTEP diagram of the ligand $\mathbf{L^1}$ with atom numbering scheme (50% probability factor for the thermal ellipsoids).

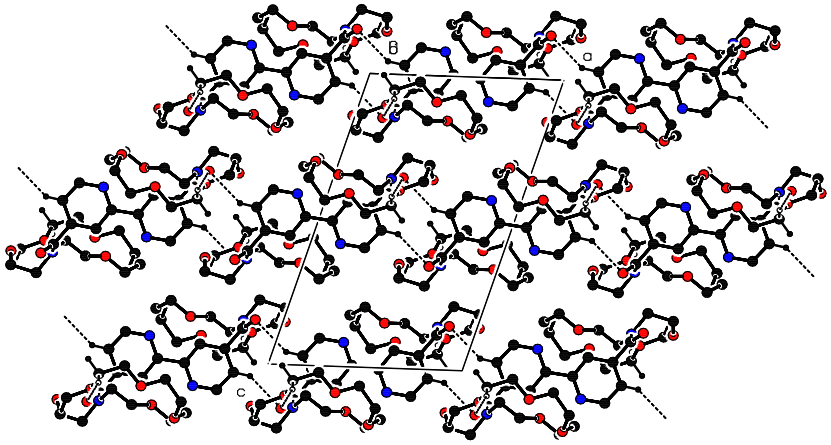

Figure 2.7 Packing diagram of $\mathbf{L^1}$ viewed down b-axis with the intermolecular C-H…O interaction depicting the layered arrangement.

2.3.3 Synthesis of Complexes 1-6

The Ru(II) complexes (**1-4**) were synthesized by the reaction of *cis*-$[Ru(bpy)_2Cl_2]$/*cis*-$[Ru(phen)_2Cl_2]$ and $\mathbf{L^1}$/$\mathbf{L^2}$/$\mathbf{L^3}$ in refluxing ethanol-water, isolated with PF_6^- counter ion and purified by column chromatography as described in the Experimental Section. All of these complexes gave satisfactory C, H and N analysis. Mass spectrometry data are in excellent agreement with the calculated values. Mass spectra of complexes **1-4** are shown in Figures 2.8-2.11. It may be noted that like ligands, the complexes also exhibit *e/m* values correspond to the Na^+ adduct with PF_6^-. The ^{1}H NMR spectra of complexes **1-4** were recorded in CD_3CN and the data with assignment of peaks are given in the Experimental Section. ^{1}H NMR spectra of complexes **1-3** are shown in Figures 2.12-2.14. The assignment has been made with the aid of COSY spectra recorded in the same solvent. The COSY spectrum of **1** is shown in Figure 2.15. On the basis of the information from COSY spectra, detail of peak assignment for complex **1** is described below. The most deshielded singlet at δ = 8.58 is due to 3-H and 3′-H of the bpy moiety of $\mathbf{L^1}$. The doublet at δ = 8.51 (4 H, J = 8.0 Hz) is due to 6-H and 6′-H of the two bpy ligands. The overlapped triplets in the range δ = 8.06-8.10 (4 H) are due to 5-H and 5′-H of the bpy ligand. The doublets at δ = 7.80 (2 H, J = 5.5 Hz) and δ = 7.71 (2 H, J = 5.5 Hz) are due to 3-H and 3′-H of the bpy units. The other doublets at δ = 7.76 (2 H, J = 5.5 Hz) and δ = 7.44 (2 H, J = 5.5 Hz) are due to 6-H, 6′-H and 5-H, 5′-H of the bpy of L^1, respectively. The overlapped triplets in the range δ = 7.40-7.45 (4 H) are due to 4-H and 4′-H of the bpy ligand. The signals due to crown moiety appear as multiplets in the region δ = 3.43-3.72. For **2**-4, detail NMR data with assignment of peaks are given in the Experimental Section and no further discussion on assignment is made in this section.

The Re(I) complexes (**5** and **6**) were synthesized by the reaction of $[Re(CO)_5Cl]$ and L^1/L^3 in refluxing dry THF and the crude product was purified by column chromatography. Microanalytical (C, H and N) and mass spectral data are in consistent with the composition of the complexes. Mass spectrum of complex **5** and ^{1}H NMR spectra of **5** and **6** are shown in Figure 2.16-2.18. ^{1}H NMR spectra of **5** exhibits two doublets at δ = 9.03 and 7.64 and a singlet at δ = 8.50 for aromatic protons, the spectral pattern is similar to that of $\mathbf{L^1}$, however slight up field shift of the doublets is noted, which is due to coordination of the bpy moiety to metal ion. In the

aliphatic region, the –NCH_2 and -OCH_2 protons of the azacrown moiety appeared at δ = 3.75 and δ = 3.52-3.62, respectively. For complex **6**, the ^{1}H NMR spectral pattern is similar to that of $\mathbf{L}^3$ with slight changes in chemical shifts, detail assignment of peaks are given in the Experimental Section. The IR spectra of these complexes exhibit three strong bands at 2021, 1900 and 1894 cm^{-1} for **5** and 2018, 1910 and 1889 cm^{-1} for **6.** These CO-stretching frequencies are within the range normally found for the typical '*fac*-Re(CO)$_3$' moiety with C_{3v} symmetry (A_1 and E for high and two low energy bands, respectively).[42-44] The CO frequencies therefore, suggest facial arrangement of the carbonyl groups in this complexes. On the basis of all these analytical and spectroscopic data the assigned molecular structures of **1**-**6** are shown in Figures 2.19-2.24.

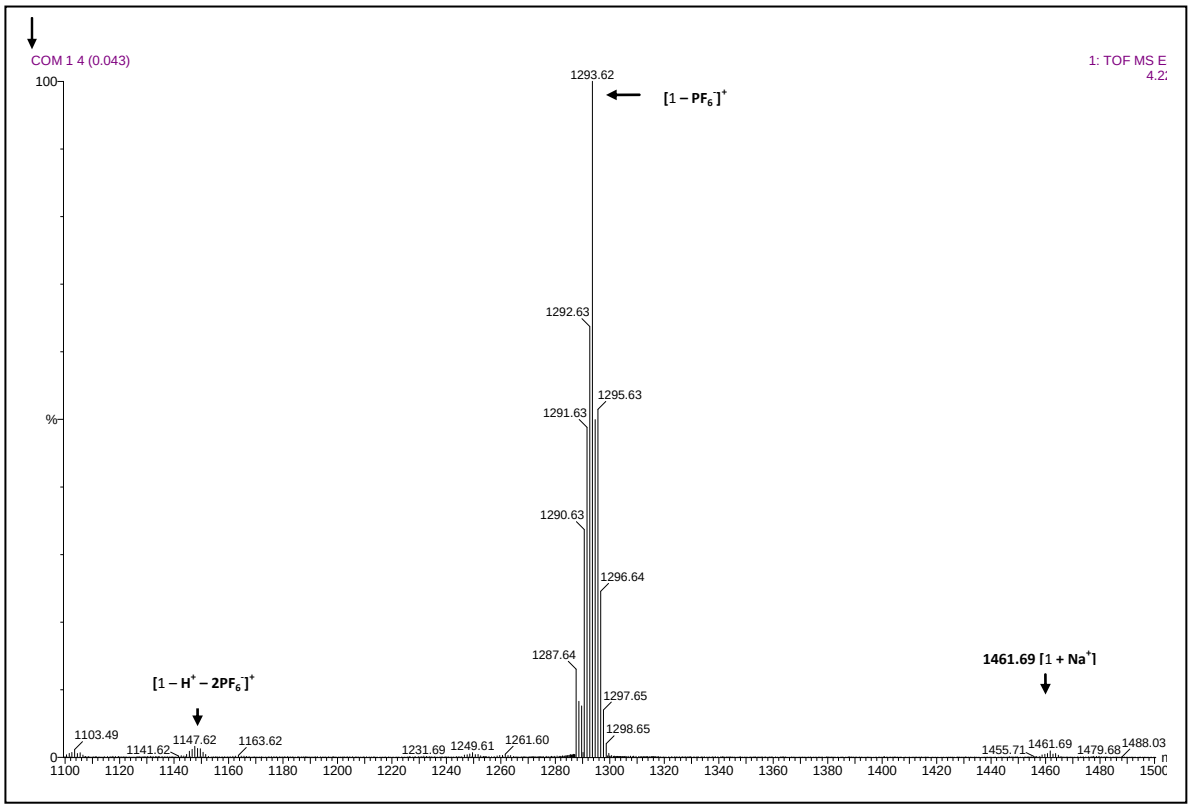

Figure 2.8 Mass spectra of complex **1**.

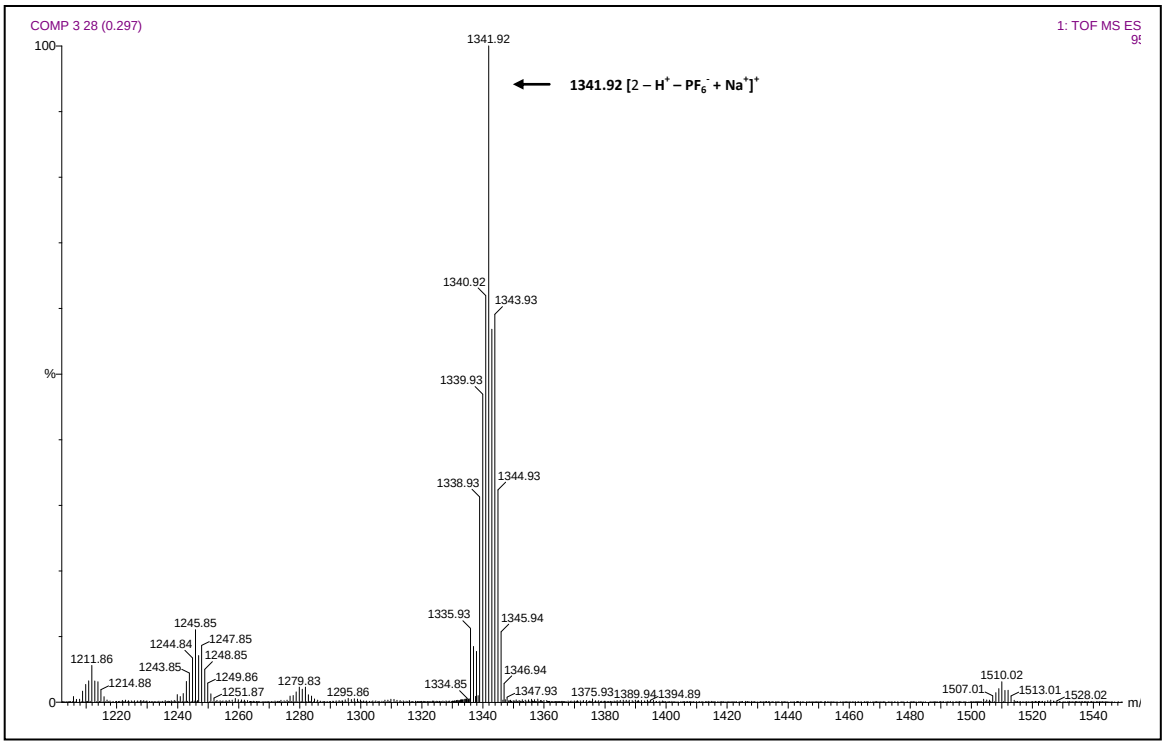

Figure 2.9 Mass spectra of complex **2**

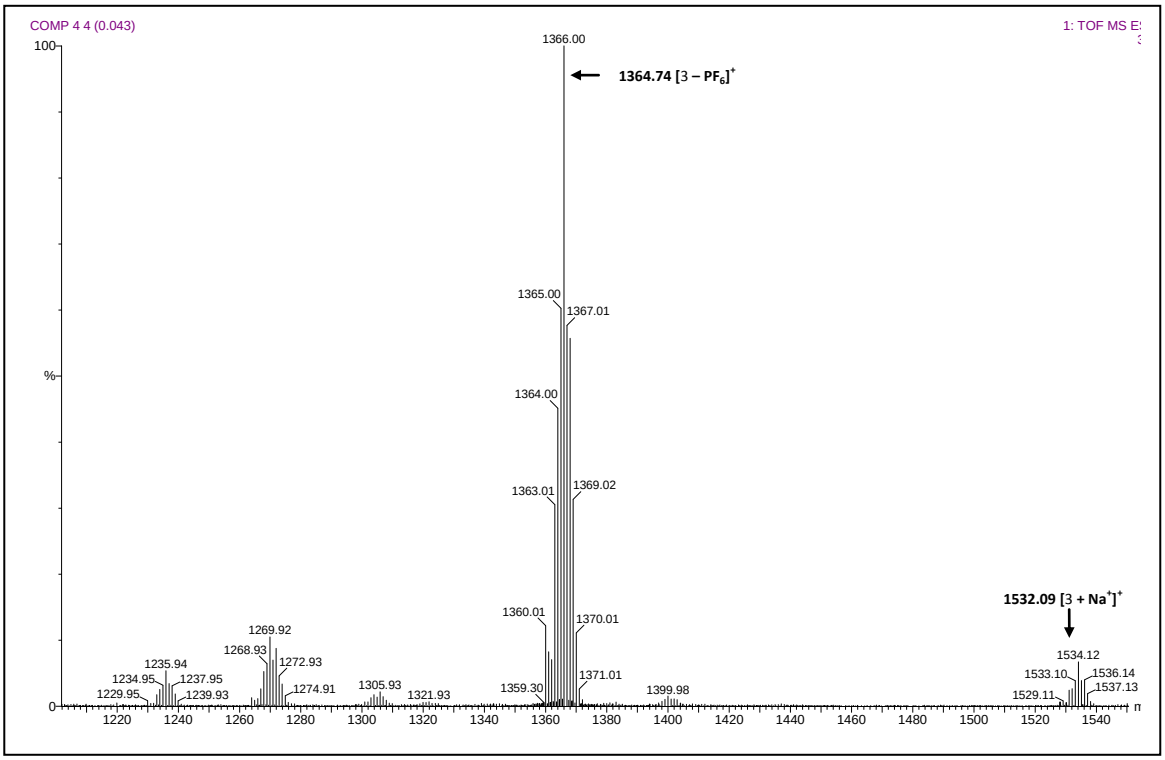

Figure 2.10 Mass spectra of complex **3**

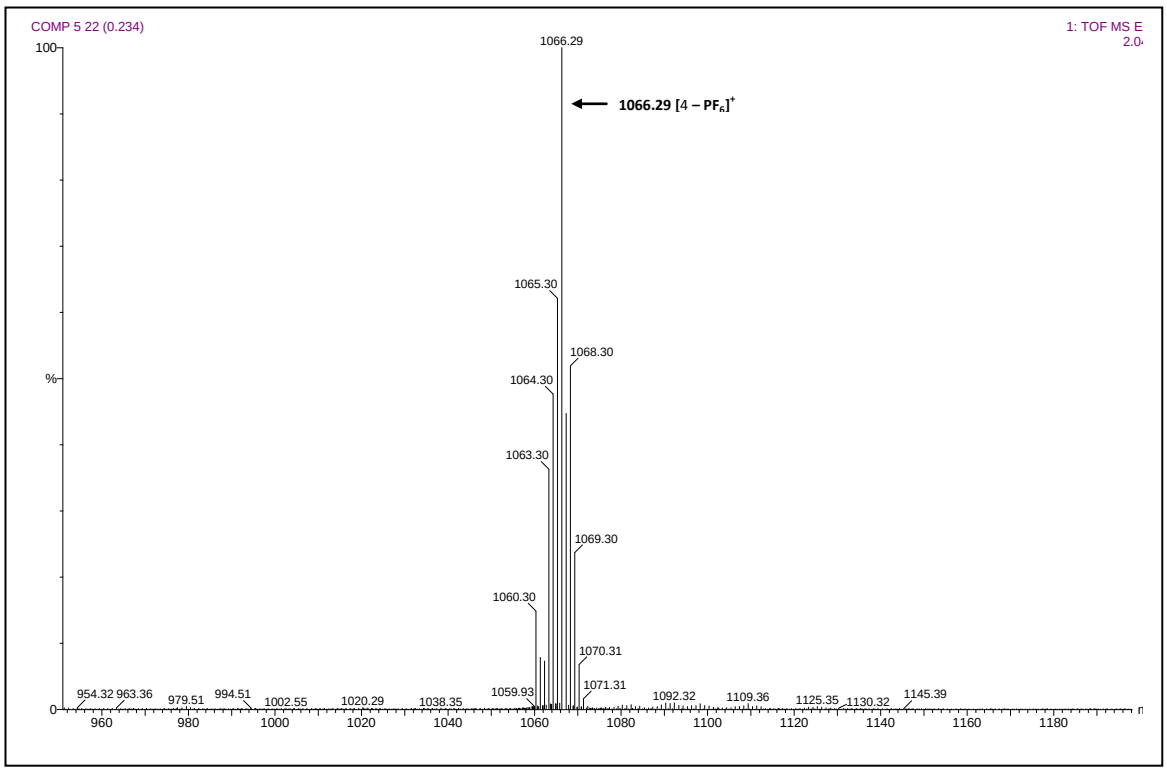

Figure 2.11 Mass spectra of complex **4**

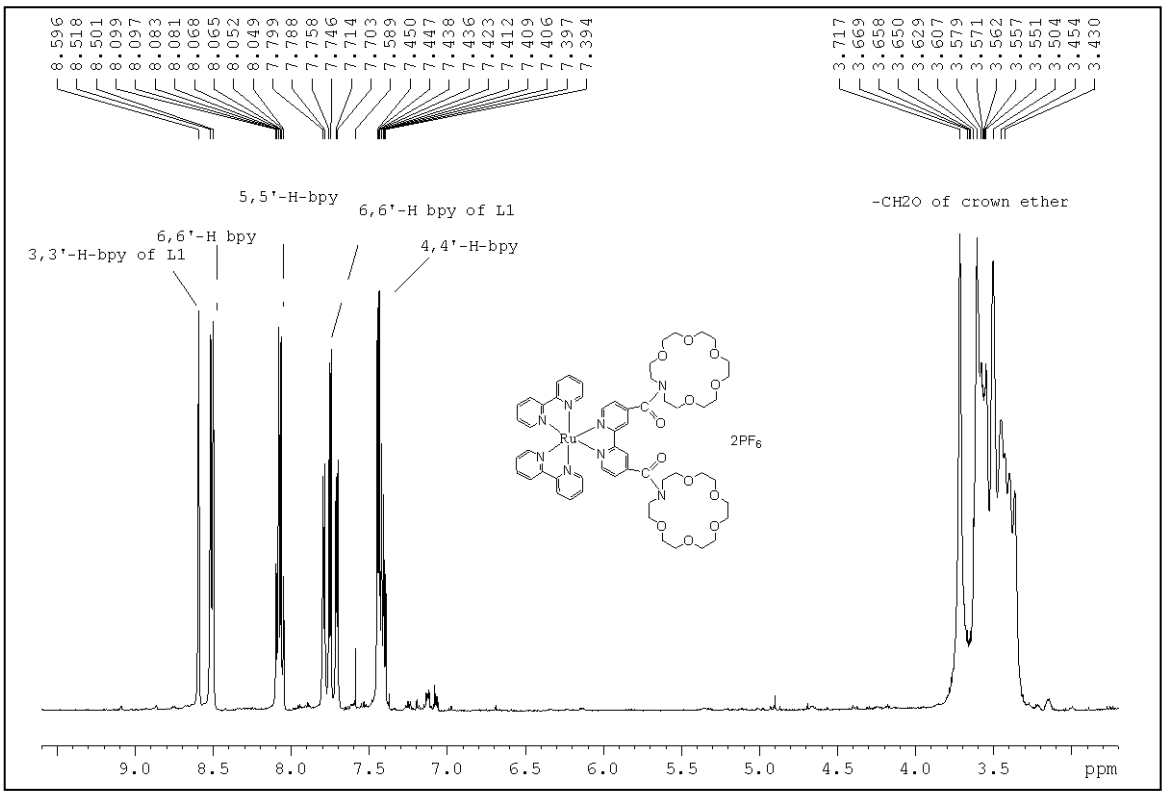

Figure 2.12 ^{1}H NMR spectra of **1**

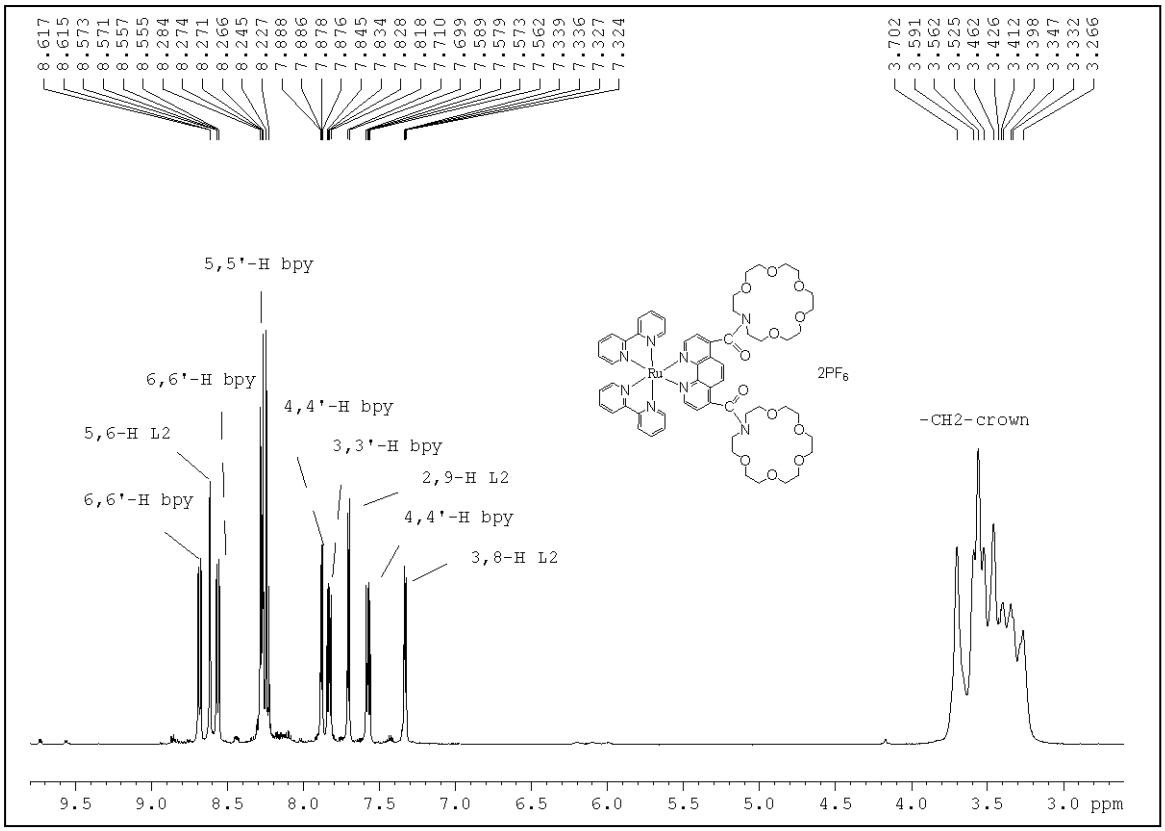

Figure 2.13 ^{1}H NMR spectra of **2**

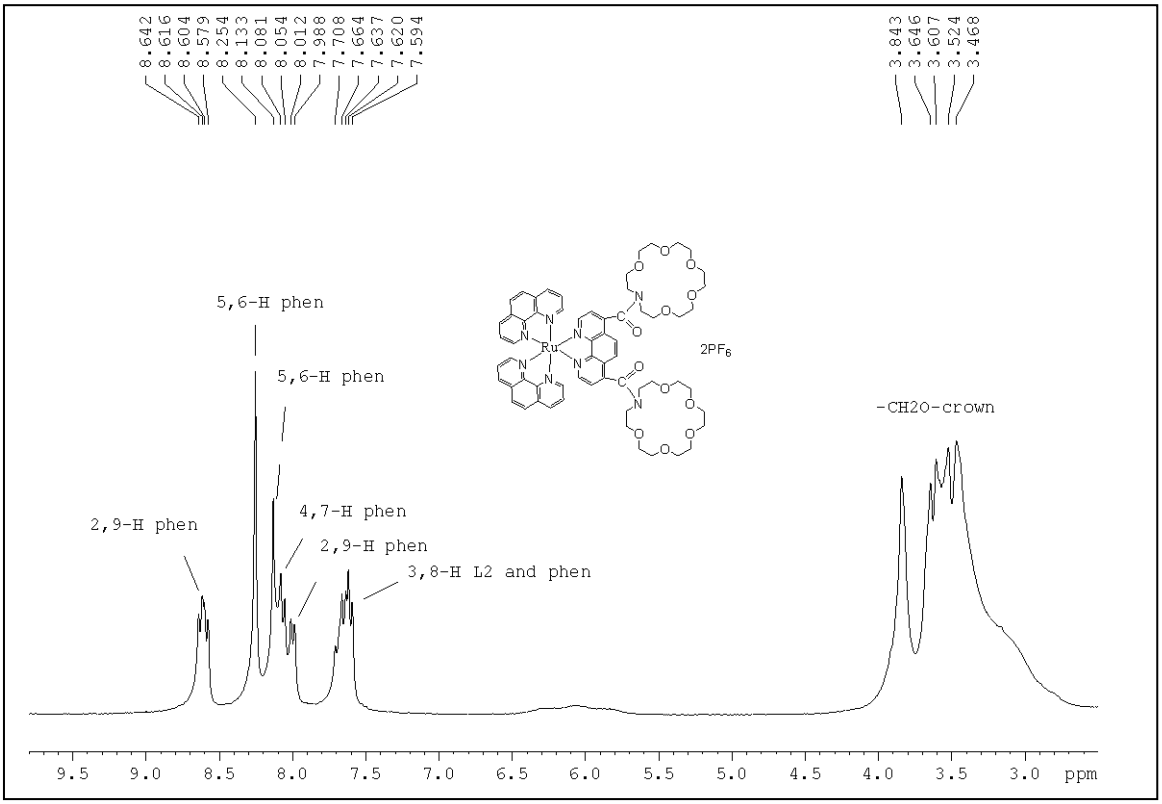

Figure 2.14 ^{1}H NMR spectra of **3**

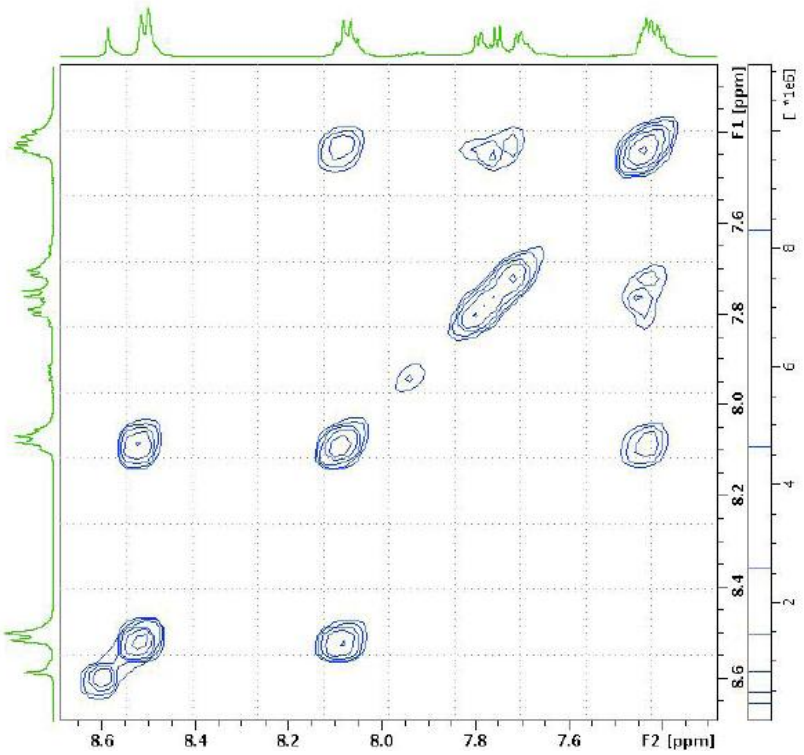

Figure 2.15 2D [COSY] ^{1}H NMR spectra of the aromatic region of **1**

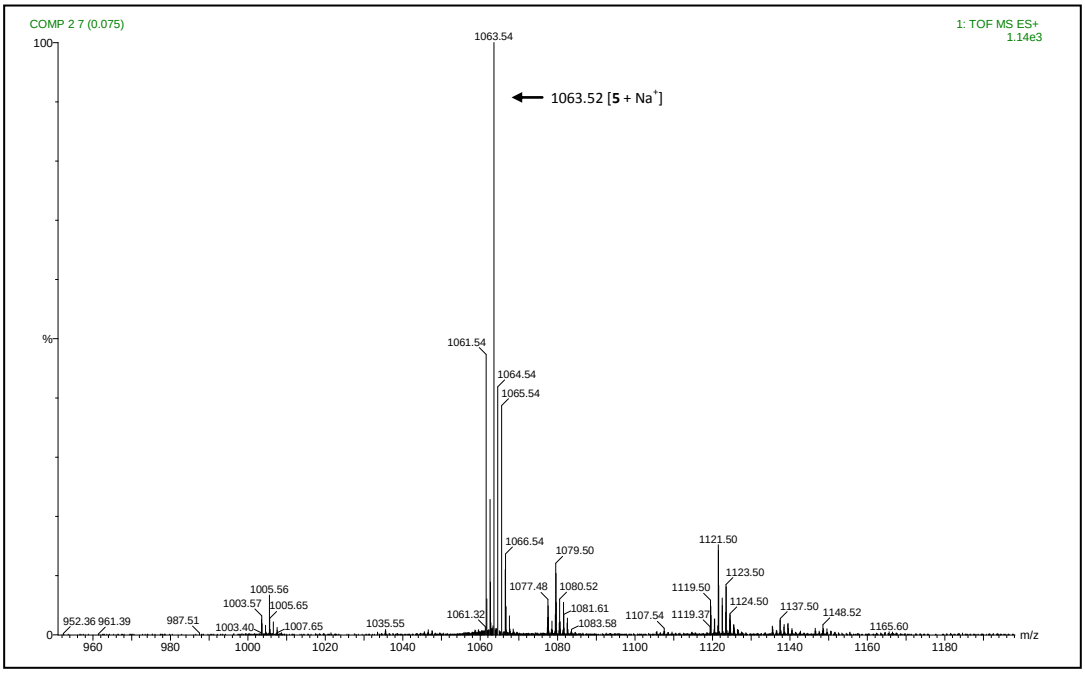

Figure 2.16 Mass spectra of complex **5**

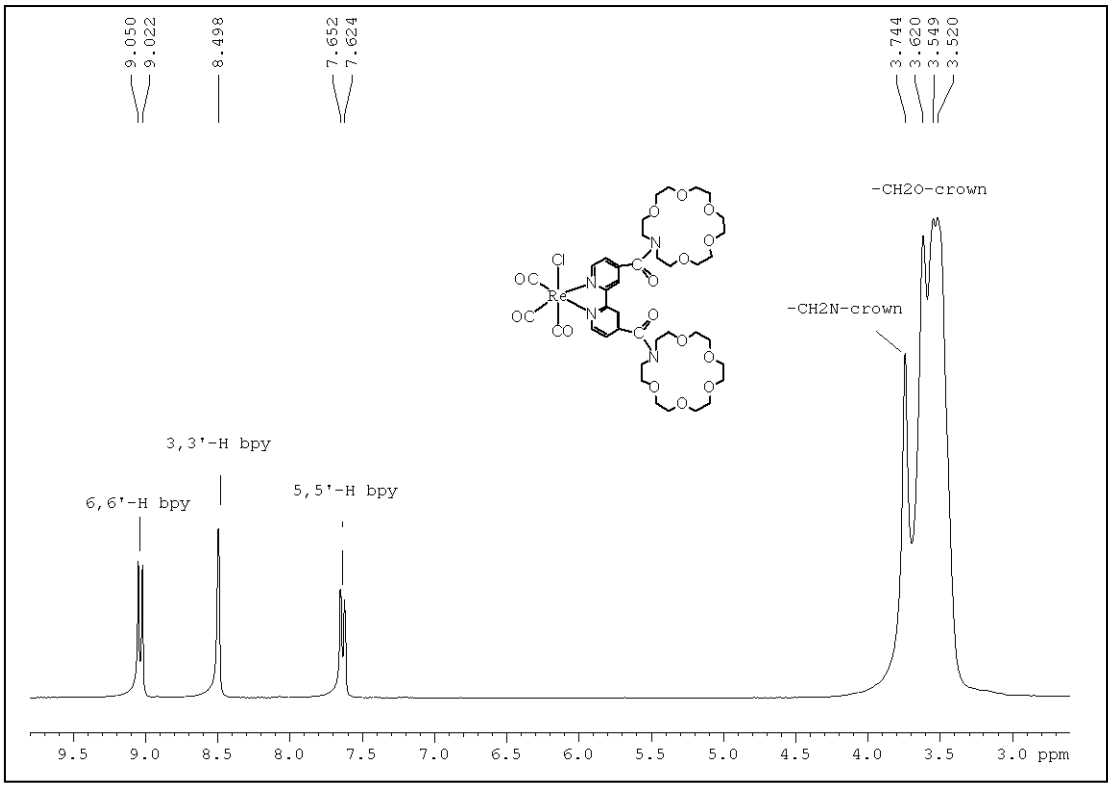

Figure 2.17 ^{1}H NMR spectra of **5**

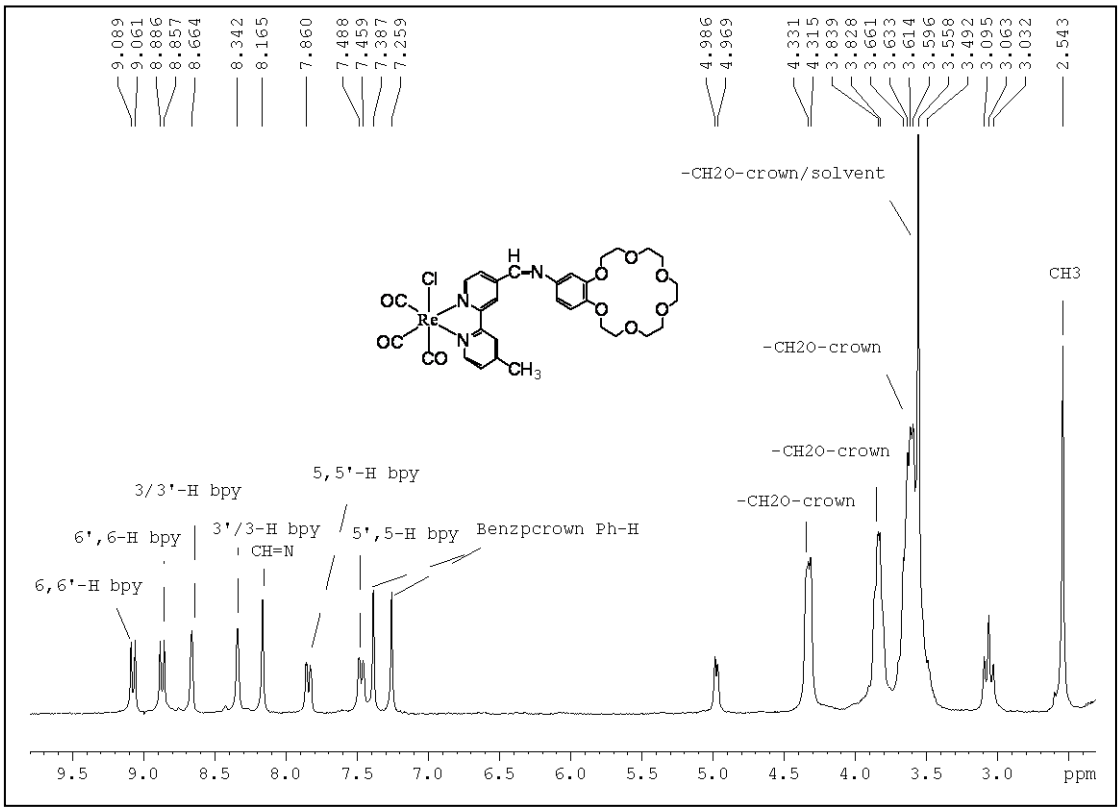

Figure 2.18 ^{1}H NMR spectra of **6**

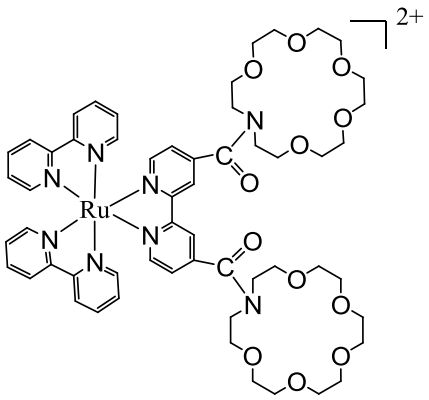

Figure 19 Structure of complex **1**

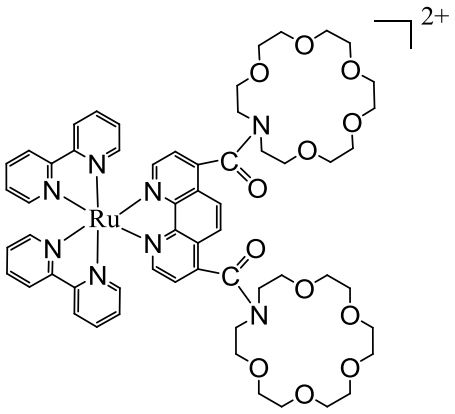

Figure 20 Structure of complex **2**

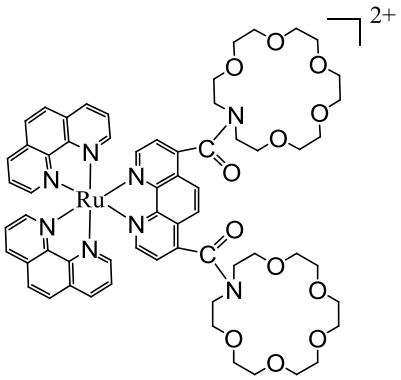

Figure 21 Structure of complex **3**

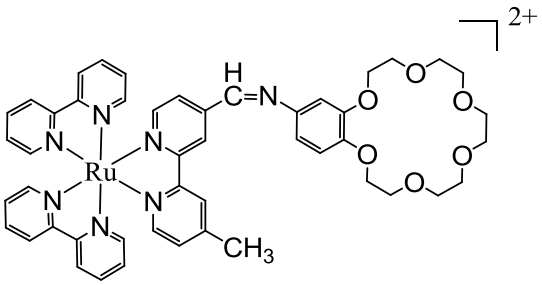

Figure 22 Structure of complex **4**

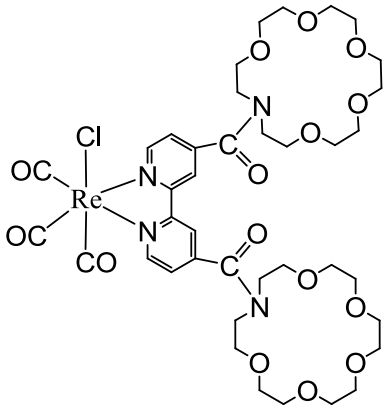

Figure 23 Structure of complex **5**

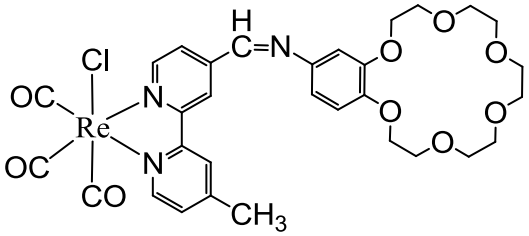

Figure 24 Structure of complex **6**

2.3.4 Absorption and Luminescence

The absorption and luminescence spectra of all complexes were recorded in acetonitrile and the data are given in the Experimental Section. Absorption and emission spectra of **1** and **5**, as a representative of this series of complexes, are shown in the Figures 2.25-2.28. The low energy band in the region 435-465 nm for Ru(II) and 385 and 342 nm for Re(I) are due to metal-to-ligand (bpy/phen) charge-transfer (MLCT) transitions ($d\pi \rightarrow \pi^*$).[45,46] The high-energy bands, which appeared around 290 and 245 nm are ligand-centered charge transfer (CT) due to $\pi \rightarrow \pi^*$ transitions.[45,46] The steady-state emission spectra (λ_{em}) and quantum yield (ϕ) of all complexes were recorded in acetonitrile at room temperature and the data are given in Table 2. All of the Ru(II) complexes exhibit a strong ^{3}MLCT emission band in the region 617-633 nm, whereas Re(I) complexes show weak emission at 630 and 603 nm for **5** and **6**, respectively.

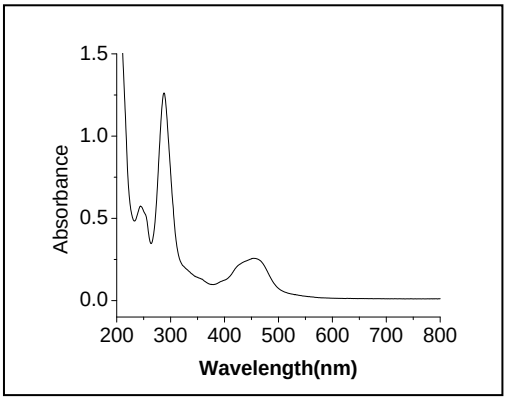

Figure 2.25 Absorption spectra of **1**

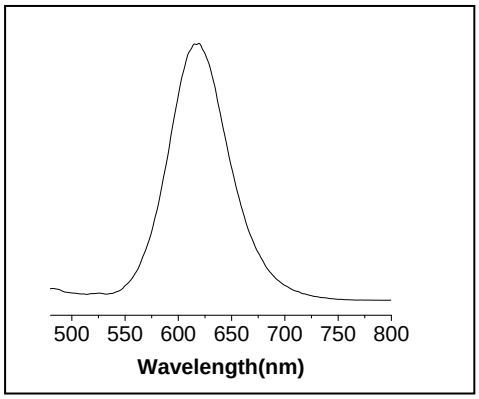

Figure 2.26 Emission spectra of **1**

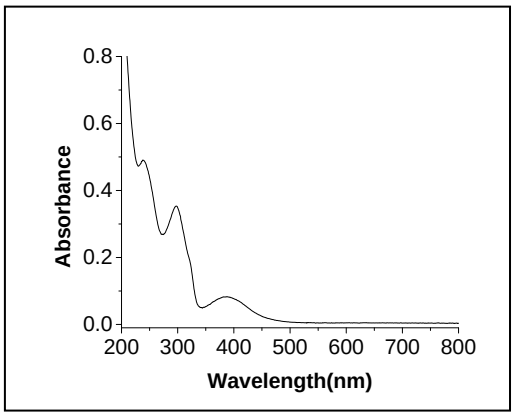

Figure 2.27 Absorption spectra of **5**

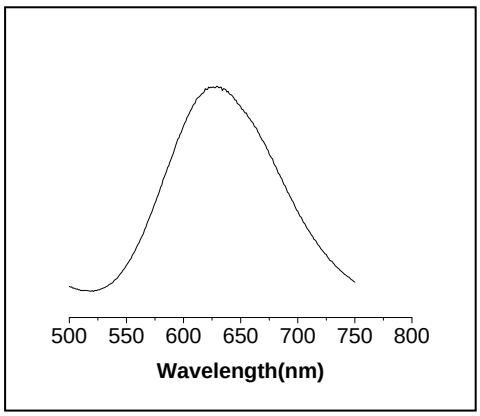

Figure 2.28 Emission spectra of **5**

Table 2. Emission maxima and quantum yield for the complexes 1-6.

Complex	λ_{em}	Quantum yield (ϕ)
1	633	0.0555
2	627	0.0628
3	617	0.0578
4	624	0.0086
5	630	0.0030
6	603	0.0149

2.3.5 Electrochemistry

Cyclic voltammograms of all complexes were recorded in acetonitrile and the results are listed in Table 3. Cyclic voltammograms of complexes **1**, **2**, **3** and **5** are shown in Figures 2.29 – 2.32. All the Ru(II) complexes exhibit a reversible redox couple in the potential range 1.43 to 1.55 V, which are due to Ru(II)→Ru(III) oxidation.[16,26,45,46] They also show three ligand based redox couples in the potential range -1.03 to -1.72 V, which are assigned to sequential one electron reduction of three bpy/phen moieties (bpy/phen→bpy/phen$^{\cdot -}$) coordinated to metal ion.[16,26,45,46] For Re(I) complexes, a quasireversible metal based oxidation wave (Re(I)→Re(II)) appear at 1.53 and 1.57 V for **5** and **6**, respectively.[47] The ligand (bpy) based single electron reduction for both the complexes occur at -1.05 and -1.28 V, for **5** and **6**, respectively.

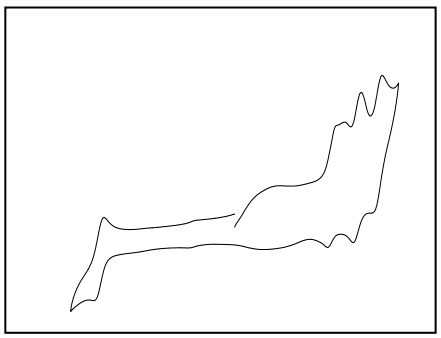

Figure 2.29 Cyclic voltammogram of complex **1**

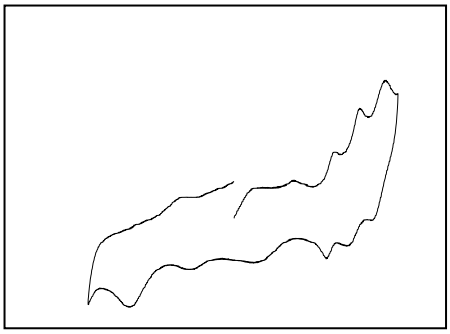

Figure 2.30 Cyclic voltammogram of complex **2**

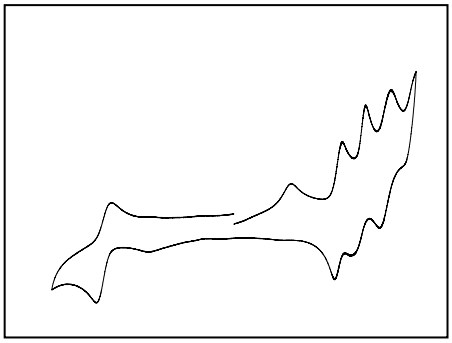

Figure 2.31 Cyclic voltammogram of complex **3**

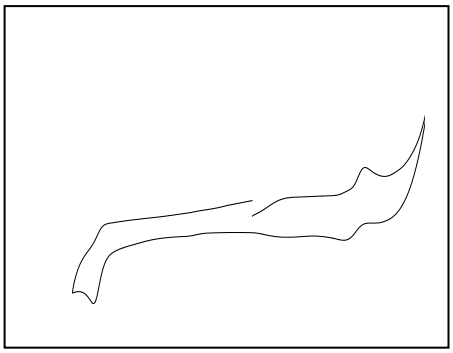

Figure 2.32 Cyclic voltammogram of complex **5**

Table 3. Electrochemical data of complexes **1**-**6** in acetonitrile

Complex	$E_{1/2}^{ox}$/V (ΔE_p, mV)	$E_{1/2}^{red1}$/V (ΔE_p, mV)	$E_{1/2}^{red2}$/V (ΔE_p, mV)	$E_{1/2}^{red3}$/V (ΔE_p, mV)
1	1.55 (170)	-1.06 (120)	-1.34 (140)	-1.60 (155)
2	1.55 (170)	-1.03 (110)	-1.29 (200)	-1.60 (172)
3	1.43 (170)	-1.14 (78)	-1.38 (146)	-1.66 (135)
4	1.52 (127)	-1.21 (110)	-1.44 (110)	-1.72 (200)
5	1.53 (85)	-1.05 (90)	--	--
6	1.57 (140)	-1.28 (180)	--	--

2.4 Conclusions

With the aim to prepare a series of fluoroionophores, three new ligands have been synthesized incorporating aza/benzocrown ethers as ionophore and bipyridine/phenanthroline unit as coordinating moiety. The molecular receptors have been synthesized by the reaction of ruthenium(II)/rhenium(I) bipyridine moiety with the newly synthesized ligands. Thus new fluoroionophores have been obtained, in which the crown ether moiety as ionophore is connected to the 4,4'-positions of the bipyridine/phenanthroline unit through >C=O and –HC=N- spacer. All these complexes have been characterized on the basis of analytical and spectroscopic data. The absorption spectra of these complexes exhibit low energy band in the region 435-465 nm for Ru(II) and 385 and 342 nm for Re(I), which are due to metal-to-ligand (bpy/phen) charge-transfer (MLCT) transitions ($d\pi \rightarrow \pi^*$). The high-energy bands, which appeared around 290 and 245 nm are ligand-centered charge transfer (CT) due to $\pi \rightarrow \pi^*$ transitions. All of the Ru(II) complexes exhibit a strong ^{3}MLCT emission band in the region 617-633 nm, whereas Re(I) complexes show weak emission at 630 and 603 nm. All the Ru(II) complexes exhibit a reversible redox couple (Ru(II)→Ru(III)) in the potential range 1.43 to 1.55 V and also show three ligand based redox couples in the potential range -1.03 to -1.72 V. Re(I) complexes exhibit a

quasireversible metal based oxidation wave (Re(I)→Re(II)) at 1.53 and 1.57 V and a ligand (bpy) based single electron reduction at -1.05 and -1.28 V. All of these fluoroionophores were subjected to interact with various metal ions to ascertain their ion recognition property. This work has been done and presented in the next chapter.

2.5 References

1. R. A. Bissell, A. P. de Silva, H. Q. N. Gunaratne, P. L. M. Lynch, G. E. M. Maguire and K. R. A. S. Sandanayake, *Chem. Soc. Rev.* **1992**, *21*, 187.

2. L. Fabbrizzi and A. Poggi, *Chem. Soc. Rev.* **1995**, *14*, 197.

3. A. P. de Silva, H. Q. N. Gunaratne, T. Gunnlaugsson, J. M. Huxley, C. P. Mchoy, J. D. Rademacher and T. E. Rice, *Chem. Rev.* **1997**, *97*, 1515.

4. R. Martinez-Manez and F. Sancenon, *Chem. Rev.* **2003**, *103*, 4419.

5. W. T. Wasan, *Fluorescent and Luminescent Probes for Biological Activity: Ed., Academic Press: San Diego*, **1993**.

6. J. R. Lakowicz, *Probe Design and Chemical Sensing: Topics in Fluorescence Spectroscopy: Ed., Plenum Press: New York*, **1994,** Vol. *4*.

7. B. Valeur and I. Leray, *Coord. Chem. Rev*. **2000**, *3*, 205.

8. D. C. Magri, G. J. Brown, G. D. McClean and A. P. de Silva, *J. Am. Chem. Soc*. **2006**, *128*, 4950.

9. P. D. Beer, P. A. Gale and G. Z. Chen, *Coord. Chem. Rev.* **1999**, *186*, 3.

10. A. P. de Silva, D. B. Fox, A. J. M. Huxley and T. S. Moody, *Coord. Chem. Rev.* **2000**, *41*, 205.

11. P. D. Beer and P. A. Gale, *Angew. Chem., Int. Ed*. **2001**, *40*, 486.

12. C. W. Rogers and M. O. Wolf, *Coord. Chem. Rev.* **2002**, *341*, 233.

13. J. L. Bricks, A. Kovalchuk, C. Trieflinger, M. Nofz, M. Buschel, A. I. Tolmachev, J. Daub and K. Rurack, *J. Am. Chem. Soc*. **2005**, *127*, 13522.

14. C. T. Chen and W. P. Huang, *J. Am. Chem. Soc*. **2002**, *124*, 6247.

15. S. J. M. Koskela, T. M. Fyles and T. D. James, *J. Chem. Soc. Chem. Commun.* **2005**, 945.

16. P. D. Beer, S. W. Dent and N. C. Fletcher, *Polyhedron*, **1996**, *15*, 2983.

17. J. E. Redman, P. D. Beer, S. w. Dent and M. G. B. Drew, *J. Chem. Soc. Chem. Commun.* **1998**, 231.

18. B. D. Muegge and M. M. Richter, *Anal. Chem.* **2002**, *74*, 547.

19. P. D. Beer, F. Szemes, V. Balzani, C. M. Sala, M. G. B. Drew, S. W. Dent and M. Maestri, *J. Am. Chem. Soc*. **1997**, *119*, 11864.

20. P. D. Beer and S. W. Dent *J. Chem. Soc. Chem. Commun.* **1998**, 825.

21. J. D. Lewis, R. N. Perutz and J. N. Moore, *J. Chem. Soc. Chem. Commun.* **2000**, 1865.

22. L. H. Uppadine, J. E. Redman, S. W. Dent, M. G. B. Drew and P. D. Beer, *Inorg. Chem.* **2001**, *40*, 2860.

23. L. J. Charbonniere, R. F. Ziessel, C. A. Sams and A. Harriman, *Inorg. Chem.* **2003**, *42*, 3466.

24. M. Chiba, H. B. Kim and N. Kitamura, *Anal. Sci.* **2002**, *18*, 461.

25. T. Lazarides, T. A. Miller, J. C. Jeffery, T. K. Ronson and H. Adams, *J. Chem. Soc. Dalton Trans.* **2005**, 528.

26. M.-J. Li, B. W.-K. Chu, N. Zhu and V. W.-W. Yam, *Inorg. Chem.* **2007**, *46*, 720.

27. M.-J. Li, Z. Chen, N. Zhu and V. W.-W. Yam, Y. Zu., *Inorg. Chem.* **2008**, *47*, 1218.

28. M. Schmittel, H. W. Lin, E. Thiel, A. J. Meixner and H. Ammon, *J. Chem. Soc. Dalton Trans.* **2006**, 4020.

29. M. Schmittel and H. W. Lin, *Angew. Chem., Int. Ed*. **2006**, *45*,1.

30. R. F. Beeston, W. S. Aldridge, J. A. Treadway, M. C. Fitzgerald, B. A. DeGraff and S. E. Stitzel, *Inorg. Chem*. **1998**, *37*, 4368.

31. B. P. Sullivan, D. J. Salmon and T. J. Meyer, *Inorg. Chem.* **1978**, *17*, 3334.

32. D. D. Perrin, W. L. F. Armarego and D. R. Perrin, *Purification of Laboratory Chemicals*, 2nd Ed, **1980**.

33. N. Garelli and P. Vierling, *J. Org. Chem*. **1992**, *57*, 3046.

34. G. M. Sheldrick, *SAINT and XPREP, 5.1 Ed., Siemens Industrial Automation Inc*., Madison, WI, **1995**.

35. SADABS, *empirical absorption Correction Program*; University of Göttingen: Göttingen, Germany, **1997**.

36. G. M. Sheldrick, *SHELXTL Reference Manual: Version 5.1*; Bruker AXS: Madison, WI, **1997**.

37. G.M. Sheldrick, *SHELXL-97: Program for Crystal Structure Refinement*, University of Göttingen, Göttingen, Germany, **1997**.

38. A. L. Spek, *PLATON-97*, University of Utrecht: Utrecht, The Netherlands, **1997**.

39. B. P. Sullivan, D. J. Salmon and T. J. Meyer, *Inorg. Chem.* **1978**, *17*, 3335.

40. P. Agnihotri, E. Suresh, P. Paul and P. K. Ghosh, *Eur. J. Inorg. Chem*. **2006**, 3369.

41. S. Patra, E. Suresh and P. Paul, *Polyhedron* **2007**, *26*, 4971.

42. S. R. Banerjee, A.Nagasawa and J. Zubieta, *Inorg. Chim. Acta.* **2002**, *340*, 155.

43. U. Abram, S. Abram, R. Schibli, R. Alberto and J. R. Dilworth, *Polyhedron*, **1998**, *17*, 1303.

44. L. Salassa, C. Garino, A. Albertino, G. Volpi, C. Nervi, R. Gobetto and K. I. Hardcastle, *Organometallics* **2008**, *27*, 1427.

45. A. K. Bilakhiya, B. Tyagi, P. Paul and P. Natarajan, *Inorg. Chem*. **2002**, *41*, 3830.

46. J. Bolger, A. Gourdon, E. Ishow and J.-P. Launay, *Inorg. Chem.* **1996**, *35*, 2937.

47. L. A. Worl, R. Duessing, P. Chen, L. D. Ciana and T. J. Meyer, *J. Chem. Soc. Dalton Trans.* **1991**, 849.

CHAPTER – III

Ion-binding Study of Ruthenium(II) and Rhenium(I) Bipyridine Crown Ether Receptor Molecules

3.1 Introduction

Selective recognition of metal ion by molecular sensor is an area of intense activity in current research.[1-5] Among various such sensing systems, the fluorescent molecular sensor for detection of ion is of great interest because of its high sensitivity and selectivity.[6-11] As described in the previous section (chapter - II), with the aim to develop such molecular systems a series of fluoroionophores comprising of Ru(II)/Re(I)-polypyridine based unit as fluorophor and azacrown/benzocrown as ionophore have been synthesized. In these complexes, the macrocyclic unit (ionophore) is connected to the metal bound bipyridine or 1,10-phenanthroline unit through the amide (>C=O) or imino (-CH=N-) moiety as spacer. The structures of these complexes are shown below.

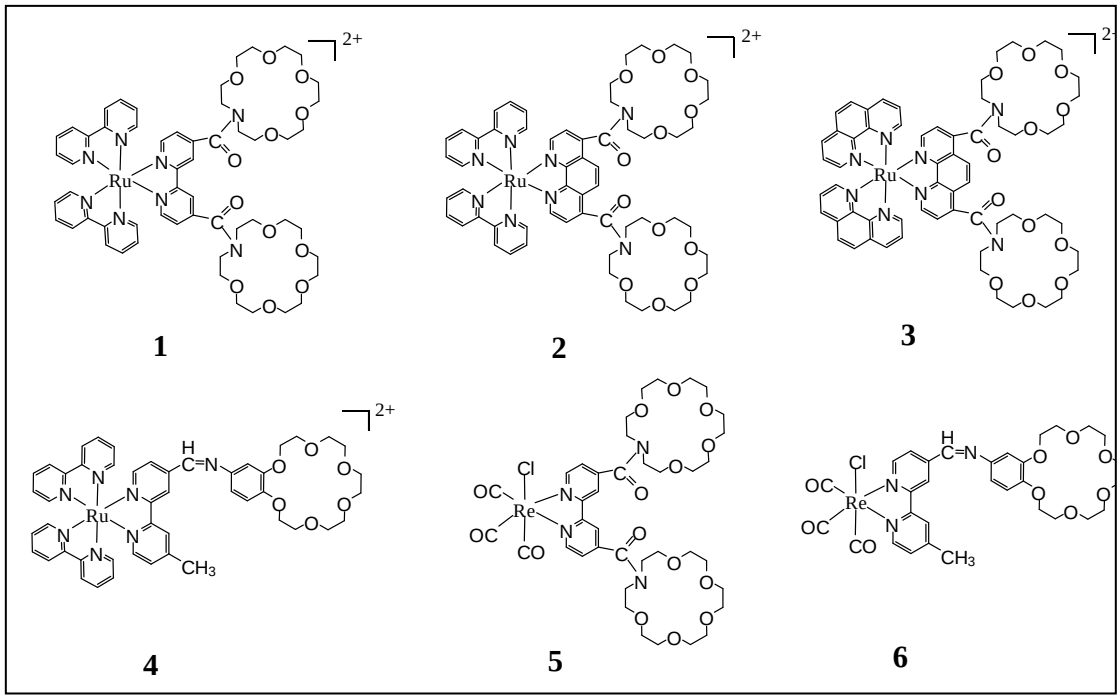

The complexes **1-4,** exhibit strong fluorescence but the emission for Re(I) complexes (**5** and **6**) are rather weak. To investigate their ion recognition property, all of these complexes are treated with a large number of cations (Na^+, K^+, Rb^+, Mg^{2+}, Ca^{2+}, Zn^{2+}, Cd^{2+}, Hg^{2+}, Pb^{2+} and Cu^{2+}) and the ion recognition process is monitored by luminescence, ^{1}H NMR and UV-Vis spectral changes and also by electrochemical study. Binding constants and stoichiometry of the complexes formed by the strongly interacting metal ions have been determined and all the data are analyzed in light of ion recognition property and intramolecular energy transfer.

3.2 Experimental Section

3.2.1 Materials

The complexes described in the chapter – II are used for the present study. Perchlorate salts of the metal ions were purchased from Arora Matthey. All other reagents used in this study were purchased from Aldrich and S. D. Fine Chemicals. All solvents were analytical grade and purified by standard procedure before use.[12]

3.2.2 Physical measurements

NMR spectra were recorded on a model DPX 200 and Avance II 500 MHz Bruker FT-NMR instruments. Mass spectra were recorded on a Q-Tof micro^{TM} LC-MS instrument. The UV-Vis spectra were recorded on a CARY 500 scan Varian spectrophotometer. Luminescence spectra were recorded on a Perkin-Elmer LS-50B spectrofluorimeter. Electrochemical measurements were made using CHI 660A electrochemical workstation equipment. Cyclic and DPV studies were carried in a three electrode cell consisting of a glassy-carbon working electrode, a platinum-wire auxiliary electrode and an SCE reference electrode. Solutions of the complexes in purified acetonitrile containing 0.1 M tetrabutylammonium tetrafluoroborate as supporting electrolyte were deaerated by bubbling nitrogen for 15 minutes prior to each experiment.

3.2.3 Ion-Binding Study

Stock solutions of the complexes (4×10^{-5} M) and that of perchlorate salts (4×10^{-3} M) of various cations were prepared in freshly purified acetonitrile. Then 5 mL stock solution of the complex and 5 mL stock solution of each metal salts were taken in a 10 mL volumetric flask, so that the effective concentration of the complex is 2×10^{-5} M and that of the metal ions are 2×10^{-3} M (100 fold excess). The luminescence spectra of the resulting solutions were recorded with excitation at the absorption maxima (λ_{max}) of the MLCT band, which is 454, 445, 435, 465 nm for **1-4,**

respectively and 385 nm for **5**. For emission titration study, the same stock solutions of the complexes were used and the metal perchlorate solutions of desired concentration were prepared by proper dilution of the concentrated standard solution (4×10^{-2} M). Then 5 mL of each solution were mixed in a 10 mL volumetric flask and the luminescence spectra of the resulting solutions were recorded. Binding constant and stoichiometry of complex formation were calculated following the literature procedure, described in the Results and Discussion section. The same solutions were also used to study UV-Vis spectral change. For NMR study, 5 mg of the complex was dissolved in 0.5 mL of [D_3]acetonitrile and ^{1}H NMR spectra of the solution was recorded. Then solid perchlorate salt of the metal ion (50 equiv) was added into the solution and the spectra of the resultant solutions were recorded after 30 min. Electrochemical study was also carried out in dry acetonitrile, DPV of the complexes in the region 1.2 to 1.8 V for metal oxidation was recorded first and then solid metal salt (Na^+, K^+ and Pb^{2+}, 50 equiv) was added into the solution and the DPV of the same region has been recorded.

3.3 Results and Discussion

The binding of a number of metal ions such as Na^+, K^+, Rb^+, Mg^{2+}, Ca^{2+}, Zn^{2+}, Cd^{2+}, Hg^{2+}, Pb^{2+} and Cu^{2+} with the ionophores **1-6** have been investigated. The host-guest interactions were monitored by luminescence, ^{1}H NMR and UV-Vis spectral changes and also by electrochemical study on oxidation potential of metal ion.

3.3.1 Luminescence Study

Photoluminescence of all the six ionophores (**1-6**) in presence of various metal ions in acetonitrile have been investigated. For complexes **1-3**, the characteristic luminescence from ^{3}MLCT state was found to decrease in intensity in presence of certain metal ions. The emission intensities were quenched by 75-85 % (with 100 equiv) with the addition of Pb^{2+} and 90-97% in presence of Cu^{2+} (with 500 equiv) for all three complexes. The emission maxima for all three complexes underwent red shift by 13 nm with the addition of Pb^{2+}, however no shift of the emission maxima is observed with Cu^{2+}. The addition of Na^+ and Hg^{2+} (~500 equiv) resulted in the

reduction of 25-40 % of emission intensities for **1**-**3** with small red shift (4-5 nm) of the emission maxima. Among other metal ions studied, Cd^{2+} exhibits some quenching but others did not show significant change in emission intensities. Luminescence spectra of **1** in acetonitrile in the presence of various metal ions are shown in Figure 3.1. Changes in luminescence intensities with the addition of increasing concentrations of Pb^{2+}, Hg^{2+}, Cu^{2+} and Na^{+} for the complexes **1**-**3** are shown in Figures 3.2 – 3.13. Interestingly, for complex **4**, instead of quenching, enhancement of emission intensities by 140 and 124 % are observed by the addition of Cu^{2+} and Hg^{2+} (with 100 equiv), respectively; and also substantial red shift (47 nm) of the emission maxima (λ_{em}) for both metal ions are noted. With the addition of Na^{+}, the enhancement of emission intensity is about 20 %, however with Pb^{2+}, some enhancement of intensity was observed initially but it started decreasing subsequently and no further detail studies on it has been made. The enhancements of luminescence intensity with the addition of increasing concentration of Cu^{2+} and Hg^{2+} for **4** are shown in Figures 3.14 and 3.15, respectively. The Re(I) complex of $\mathbf{L^1}$ (**5**), which shows weak emission in acetonitrile (ϕ = 0.003), gave rise to 17 and 20 times enhancement of the emission intensities with hypsochromic shift of λ_{em} by 57 and 55 nm by the addition of Cd^{2+} and Hg^{2+}, respectively (Figure 3.16). The change in luminescence intensity with the addition of increasing concentration of Cd^{2+} and Hg^{2+} for **5** is illustrated in Figures 3.17 and 3.18. The other metal ions did not induce significant change in emission intensity. Complex **6** did not show significant change in emission spectra with the addition of same metal ions.

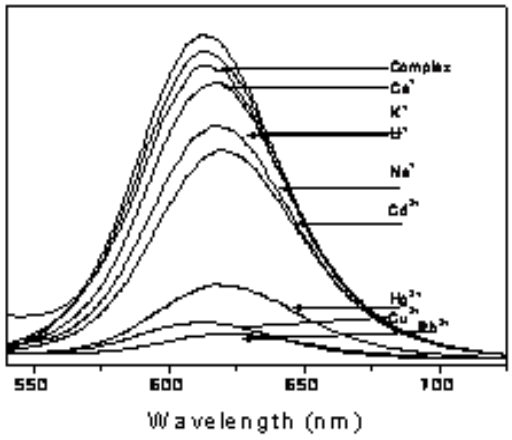

Figure 3.1 Luminescence spectra of **1** in presence of various metal ions.

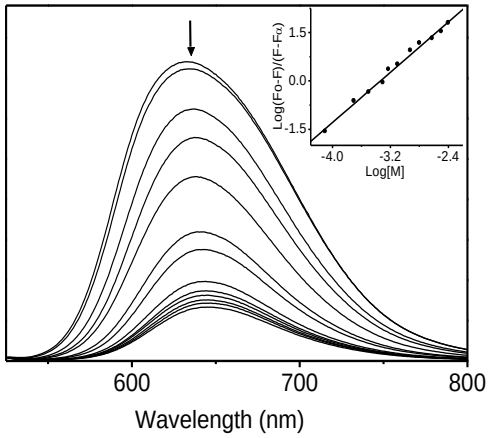

Figure 3.2 Emission spectral changes of **1** (1 x 10^{-5} M) upon addition of increasing concentration of $Pb(ClO_4)_2$. Excitation wavelength: 452 nm. Inset: linear regression fit (double-logarithmic plot) of the titration data as a function of concentration of metal ion.

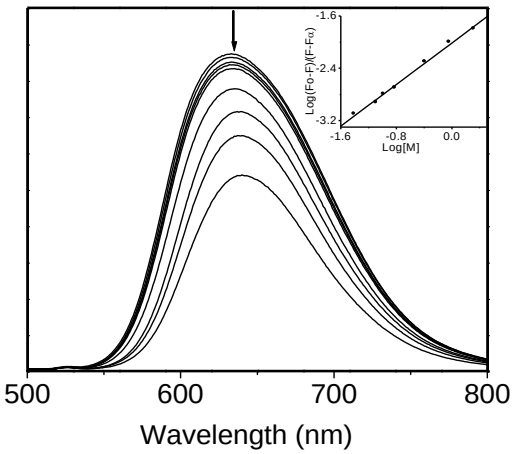

Figure 3.3 Emission spectral changes of **1** (1 x 10^{-5} M) upon addition of increasing concentration of $Hg(ClO_4)_2$. Excitation wavelength: 452 nm. Inset: linear regression fit (double-logarithmic plot) of the titration data as a function of concentration of metal ion.

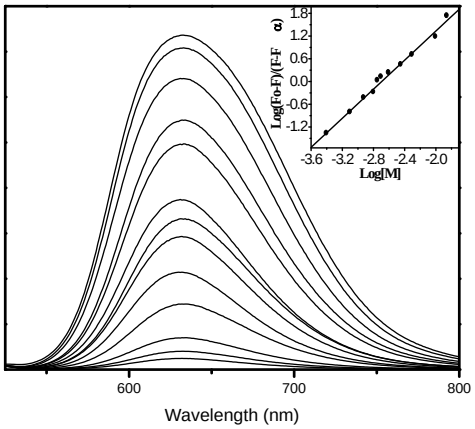

Figure 3.4 Emission spectral changes of **1** (1 x 10^{-5} M) upon addition of increasing concentration of $Cu(ClO_4)_2$. Excitation wavelength: 452 nm. Inset: linear regression fit (double-logarithmic plot) of the titration data as a function of concentration of metal ion.

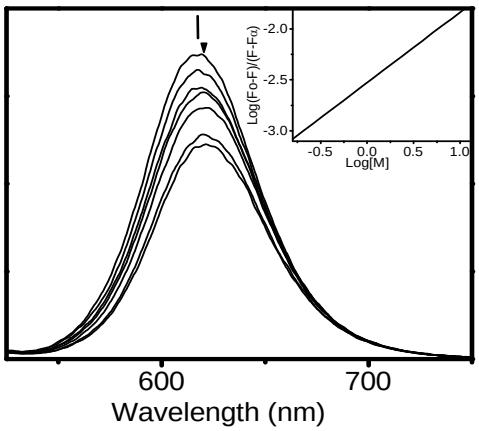

Figure 3.5 Emission spectral changes of **1** (1 x 10^{-5} M) upon addition of increasing concentration of $NaClO_4$. Excitation wavelength: 452 nm. Inset: linear regression fit (double-logarithmic plot) of the titration data as a function of concentration of metal ion.

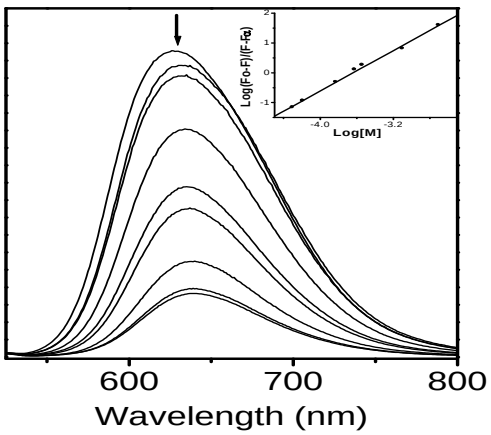

Figure 3.6 Emission spectral changes of **2** (1 x 10^{-5} M) upon addition of increasing concentration of $Pb(ClO_4)_2$. Excitation wavelength: 452 nm. Inset: linear regression fit (double-logarithmic plot) of the titration data as a function of concentration of metal ion.

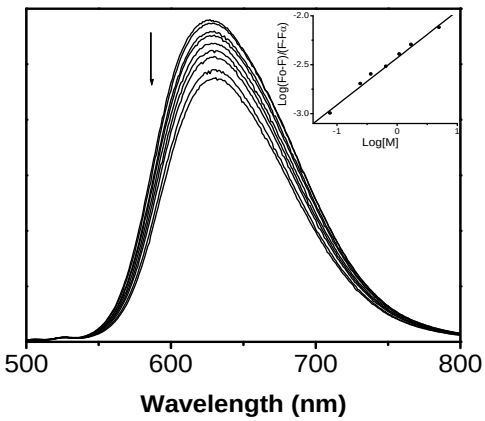

Figure 3.7 Emission spectral changes of **2** (1 x 10^{-5} M) upon addition of increasing concentration of $Hg(ClO_4)_2$. Excitation wavelength: 452 nm. Inset: linear regression fit (double-logarithmic plot) of the titration data as a function of concentration of metal ion.

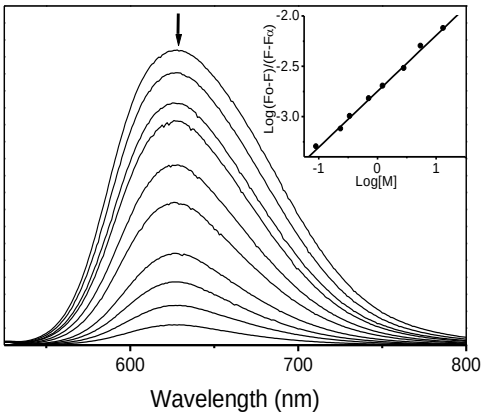

Figure 3.8 Emission spectral changes of **2** (1 x 10^{-5} M) upon addition of increasing concentration of $Cu(ClO_4)_2$. Excitation wavelength: 452 nm. Inset: linear regression fit (double-logarithmic plot) of the titration data as a function of concentration of metal ion.

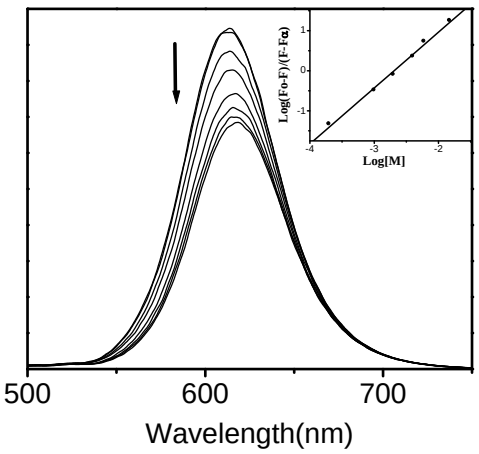

Figure 3.9 Emission spectral changes of **2** (1 x 10^{-5} M) upon addition of increasing concentration of $NaClO_4$. Excitation wavelength: 452 nm. Inset: linear regression fit (double-logarithmic plot) of the titration data as a function of concentration of metal ion.

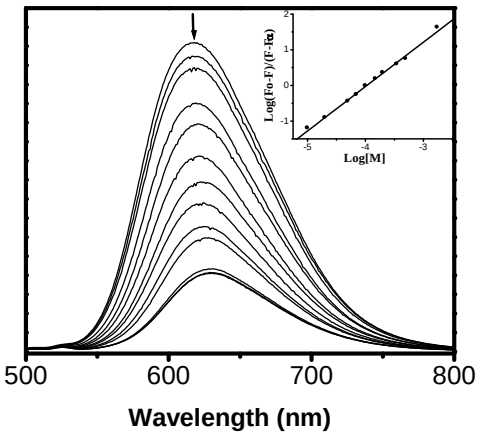

Figure 3.10 Emission spectral changes of **3** (1 x 10^{-5} M) upon addition of increasing concentration of $Pb(ClO_4)_2$. Excitation wavelength: 452 nm. Inset: linear regression fit (double-logarithmic plot) of the titration data as a function of concentration of metal ion.

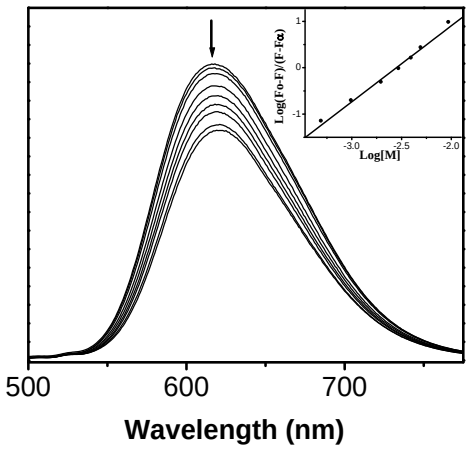

Figure 3.11 Emission spectral changes of **3** (1 x 10^{-5} M) upon addition of increasing concentration of $Hg(ClO_4)_2$. Excitation wavelength: 452 nm. Inset: linear regression fit (double-logarithmic plot) of the titration data as a function of concentration of metal ion.

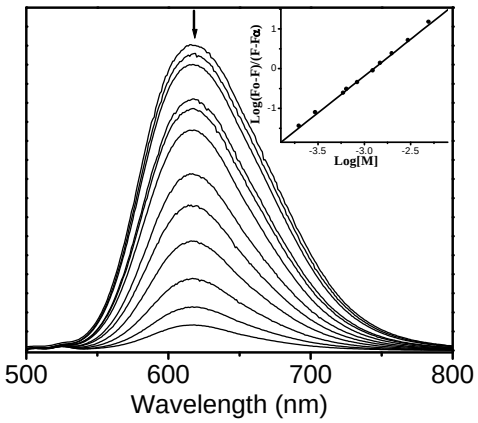

Figure 3.12 Emission spectral changes of **3** (1 x 10^{-5} M) upon addition of increasing concentration of $Cu(ClO_4)_2$. Excitation wavelength: 452 nm. Inset: linear regression fit (double-logarithmic plot) of the titration data as a function of concentration of metal ion.

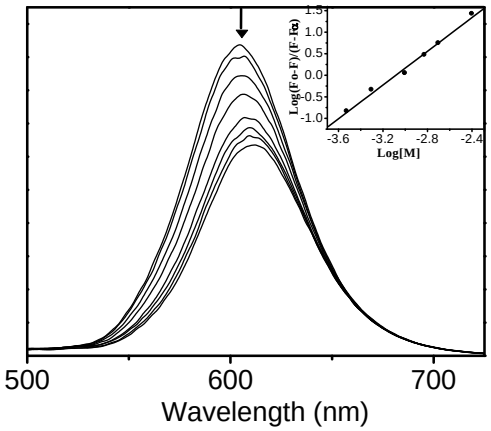

Figure 3.13 Emission spectral changes of **3** (1 x 10^{-5} M) upon addition of increasing concentration of $NaClO_4$. Excitation wavelength: 452 nm. Inset: linear regression fit (double-logarithmic plot) of the titration data as a function of concentration of metal ion.

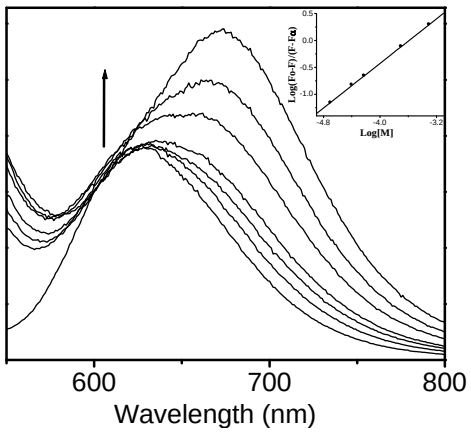

Figure 3.14 Emission spectral changes of **4** (1 x 10^{-5} M) upon addition of increasing concentration of $Cu(ClO_4)_2$. Excitation wavelength: 452 nm. Inset: linear regression fit (double-logarithmic plot) of the titration data as a function of concentration of metal ion.

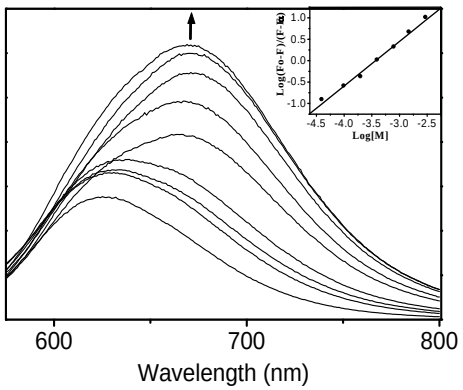

Figure 3.15 Emission spectral changes of **4** (1 x 10^{-5} M) upon addition of increasing concentration of $Hg(ClO_4)_2$. Excitation wavelength: 452 nm. Inset: linear regression fit (double-logarithmic plot) of the titration data as a function of concentration of metal ion.

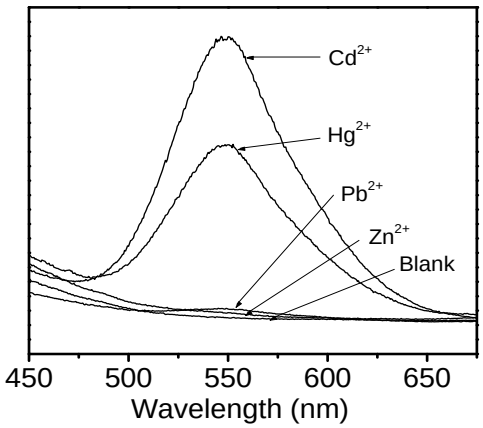

Figure 3.16 Luminescence spectra of **5** in presence of various metal ions.

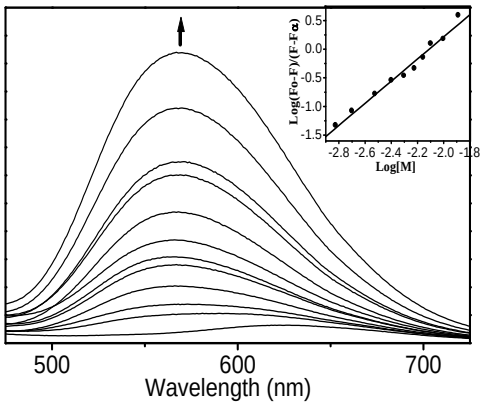

Figure 3.17 Emission spectral changes of **5** (1 x 10^{-5} M) upon addition of increasing concentration of $Cd(ClO_4)_2$. Excitation wavelength: 390 nm. Inset: linear regression fit (double-logarithmic plot) of the titration data as a function of concentration of metal ion.

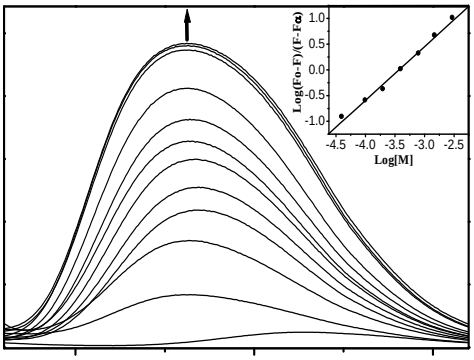

Figure 3.18 Emission spectral changes of **5** (1 x 10^{-5} M) upon addition of increasing concentration of $Hg(ClO_4)_2$. Excitation wavelength: 390 nm. Inset: linear regression fit (double-logarithmic plot) of the titration data as a function of concentration of metal ion.

Binding constants of strongly interacting metal ions for **1-5** were calculated using emission titration data following literature procedure.[13-15] According to this procedure, the fluorescence intensity (F) scales with the metal ion concentration ([M]) through $(F_0 - F)/(F - F_\infty) = ([M]/K_{diss})^n$. The binding constant ($K_s$) is obtained by plotting $\log[(F_0 - F)/(F - F_\infty)]$ versus log[M], where F_0 and F_∞ are the relative fluorescence intensities of the complex without addition of guest metal ion and with maximum concentration of metal ion (when no further change in emission intensity takes place), respectively. The slope of the plot obtained from experimental data gives the value of n, number of metal ion bound to each complex, whereas the value of log[M] at $\log[(F_0 - F)/(F - F_\infty)] = 0$ gives the value of $\log(K_{diss})$, the reciprocal of which is the binding constant (K_s). The plots $\log[(F_0 - F)/(F - F_\infty)]$ versus log[M] are shown as insets of the Figures 3.2–3.15, 3.17 and 3.18. The titration data showed nice linear fit ($R^2 = 0.99$) with the above equation. The binding constants and values of 'n' of all complexes are summarized in Table 1. The values of 'n' for **1-3** and **5** with all metal ions studied are in the range 1.85 – 2.09, which suggest 1:2 complex formation, which means both the crown cavities are occupied by the guest metal ions. For complex **4,** the 'n' values of 0.99 and 1.04 indicate 1:1 complex formation.

Table 1 Luminescence data, binding constant (K_s) and stoichiometry of complex formation for the ionophores

Complex	λ_{em}	Quantum yield (ϕ)	Metal ion	Binding constant (K_s) x 10^{-2} M^{-1}	Value of n*
1	633	0.0555	Pb^{2+}	21.80	1.95
			Hg^{2+}	1.99	1.86
			Cu^{2+}	4.95	1.92
			Na^{+}	7.12	2.03
2	627	0.0628	Pb^{2+}	49.15	1.98
			Hg^{2+}	2.69	2.09
			Cu^{2+}	5.90	1.96
			Na^{+}	9.95	1.91
3	617	0.0578	Pb^{2+}	99.72	1.90
			Hg^{2+}	4.19	1.88
			Cu^{2+}	8.81	2.03
			Na^{+}	12.12	1.96
4	624	0.0086	Hg^{2+}	26.63	1.04
			Cu^{2+}	45.99	0.99
5	630	0.0030	Hg^{2+}	34.88	1.85
			Cd^{2+}	1.28	1.93
6	603	0.0149	--	--	--

* Complex: guest metal ion ratio

Analysis of the data (Table 1) show that for complexes **1**-**3**, the binding constants (K_s) follow the order Pb^{2+} > Na^{+} > Cu^{2+} > Hg^{2+}; complex **4** also follows similar order, Cu^{2+} > Hg^{2+} (K_s for Na^{+} was not calculated because of small changes in emission intensity). For **5**, binding constant with Hg^{2+} is significantly higher compared to that with Cd^{2+}. Complexing ability of the macrocyclic ionophores such as crown ether with various metal ions depends on the size of the macrocyclic cavity and ionic diameter of the metal ion (size matching), conformation of the macrocyles and type of donor atoms. Diameter of the 18-crown-6, which used in this study, is in the range 2.6-3.2 Å and it matches very well with the ionic diameter of K^{+} (2.66 Å)

and expected to form stable complex with these ionophores.[16,17] However, both fluorescence and NMR studies (discussed below) suggest poor complexing ability of theses ionophores with K^+. The ionic diameter of the metal ions, which formed stable complexes, are Pb^{2+} = 2.34, Na^+ = 1.96, Hg^{2+} = 1.86, Cu^{2+} = 1.84 and Cd^{2+} = 1.84 Å, which are less compared to that of K^+ (2.66 Å).[17] ^{1}H NMR study of the ligand $\mathbf{L^1}$ in presence of K^+ indicates that it forms complex with K^+ (discussed below). The result therefore, suggests that the crown rings in the complexes are not planar, it twisted and the effective cavity size of the crown moiety available for incoming metal ions is less that that observed for planar conformation and no metal ions with ionic diameter higher or equal to K^+ will form stable complexes with these ionophores. Non-planarity of the crown moiety in complexes might be due to steric hindrance and intra-/intermolecular interactions.

The emission quantum yield (ϕ, ~0.06) and complexation property of **1-3** with guest metal ions are similar, the significant emission quenching of these ionophores in presence of the above mentioned metal ions is probably related to orientation of the complexed crown moiety with respect to the attached bpy/phen unit. The crown moieties attached to bpy/phen are flexible and these units together with amide >C=O are involved in intra- and intermolecular hydrogen bonding interactions and after complexation of crown units, these interactions is expected to change or break to minimize steric hindrance. This effect certainly changes orientation and conformation of the complexed crown moieties as indicated by NMR and electrochemical studies (discussed below), this change of orientation with respect to the coordination sphere of Ru(II) probably promotes non-radiative decay process.[18-20] The enhancement of emission intensity observed in **4** and **5** is probably due to blocking of the intramolecular electron-transfer quenching process because of coordination of metal ion into the crown cavity reduce the ability of the donor atoms of the crown moiety to quench emissive ^{3}MLCT state by photoinduced electron transfer.[21-24] It may be noted that **4** contains one crown moiety ($\mathbf{L^3}$) and **5** is the Re(I) complex containing CO and Cl, instead of bpy as ligand, therefore steric crowding and intra-/intermolecular interactions of these two complexes are expected to be different from that of **1-3**. Enhancement and quenching of emission intensity of the same/similar complexes in presence of different ions are well documented.[18-20,22,24]

3.3.2 ^{1}H NMR Study

The ^{1}H NMR spectra of selected complexes were recorded in presence of various metal ions. Typical spectra of **1** and that in presence of Na^+, K^+ and Pb^{2+} are shown in Figure 3.19. It may be noted that the spectra recorded in presence of Na^+ and Pb^{2+} exhibit significant changes in both aliphatic and aromatic regions compared to **1,** however the spectrum recorded in presence of K^+ did not show significant change, except slight upfield shifts of the signals due to the protons attached to crown moiety and signals of 4,4′-H of two bpy. Upon addition of Na^+ and Pb^{2+}, the signals of the crown moiety have deshielded with significant change in splitting pattern indicating complex formation of crown moiety with guest metal ion. This complexation resulted in changes in the chemical environment of the coordination sphere, which in turn affected chemical shift of some of the protons associated with the bipyridine ligand (Figure 3.19). For complexes **2** and **3,** similar changes in ^{1}H NMR spectra in presence of Na^+ and Pb^{2+} were observed in both aliphatic and aromatic regions (Figure 3.20 for **2)**. It may be noted that the splitting pattern and change in chemical shifts of the signals due to crown moiety are significantly different for Na^+ and Pb^{2+} (Figures 3.19 and 3.20) for a particular receptor molecule. This difference is due to different ionic size and charge of the metal ions (diameter, Na^+ = 1.96 Å, Pb^{2+} = 2.34 Å), coordination of these metal ions into the same crown cavity resulted in different chemical environment for the $–CH_2$- protons of the crown moiety. For Re(I) complexes, similar ^{1}H NMR spectral change in the aliphatic region is observed in presence of Na^+ and Pb^{2+}. Like Ru(II), Re(I) complexes also exhibit minor spectral changes in presence of K^+ though ionic diameter of K^+ matches very well the cavity size of the crown. For better understanding of it, the ^{1}H NMR spectral changes of $\mathbf{L^1}$ in presence of K^+ (20 quiv) is recorded, it shows significant change in the region for crown moiety (Figure 3.21), indicating stable complex formation. The observation, therefore, suggest that in the Ru(II)/Re(I) complexes the crown moiety is not in planar conformation and the effective cavity size is smaller than that of free crown moiety, consistent to the observation noted in fluorescence study.

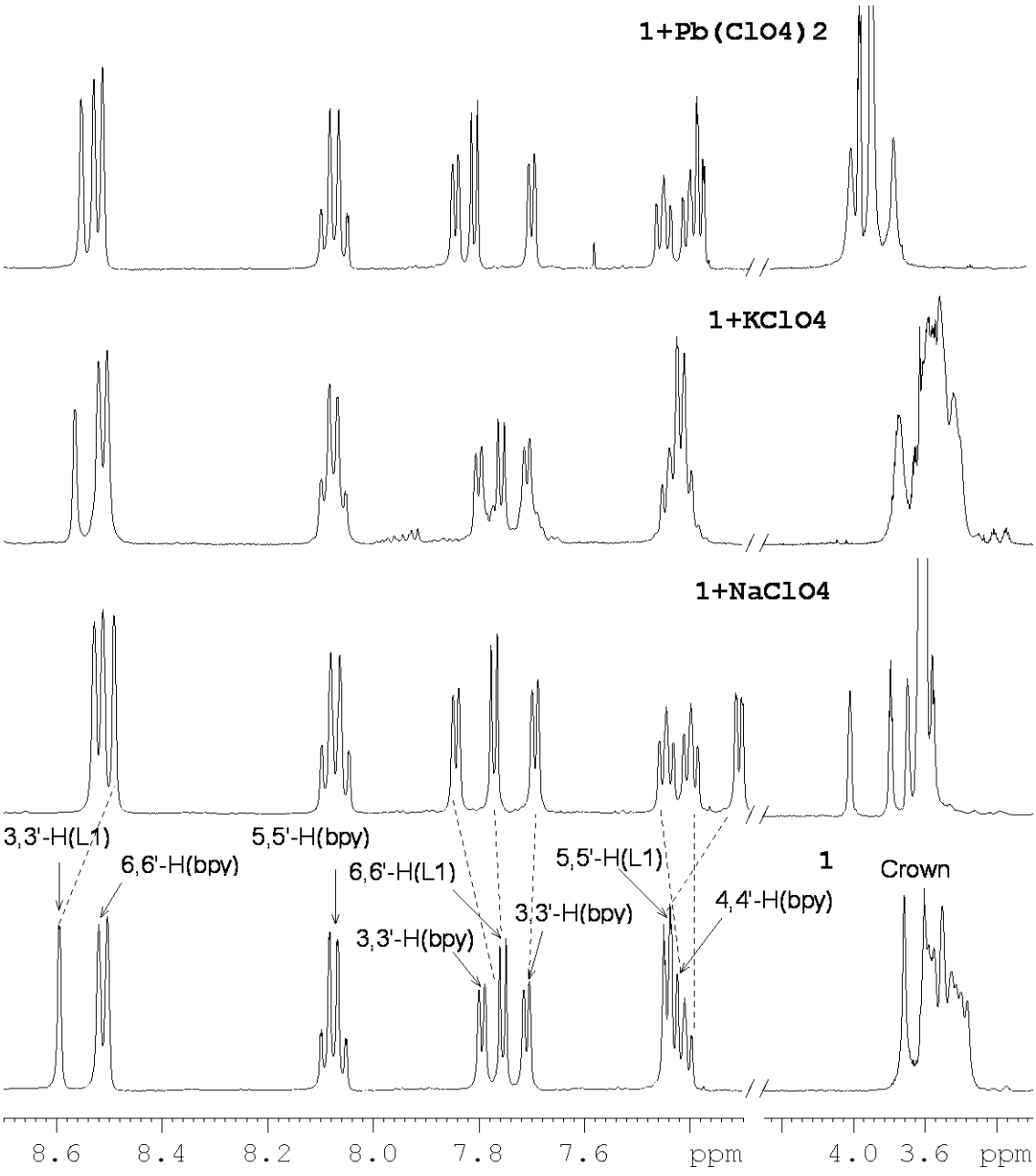

Figure 3.19. Selected portion of the ^{1}H NMR spectra of **1**, [**1**+$NaClO_4$], [**1**+$KClO_4$] and [**1**+ $Pb(ClO_4)_2$], recorded in CD_3CN at room temperature.

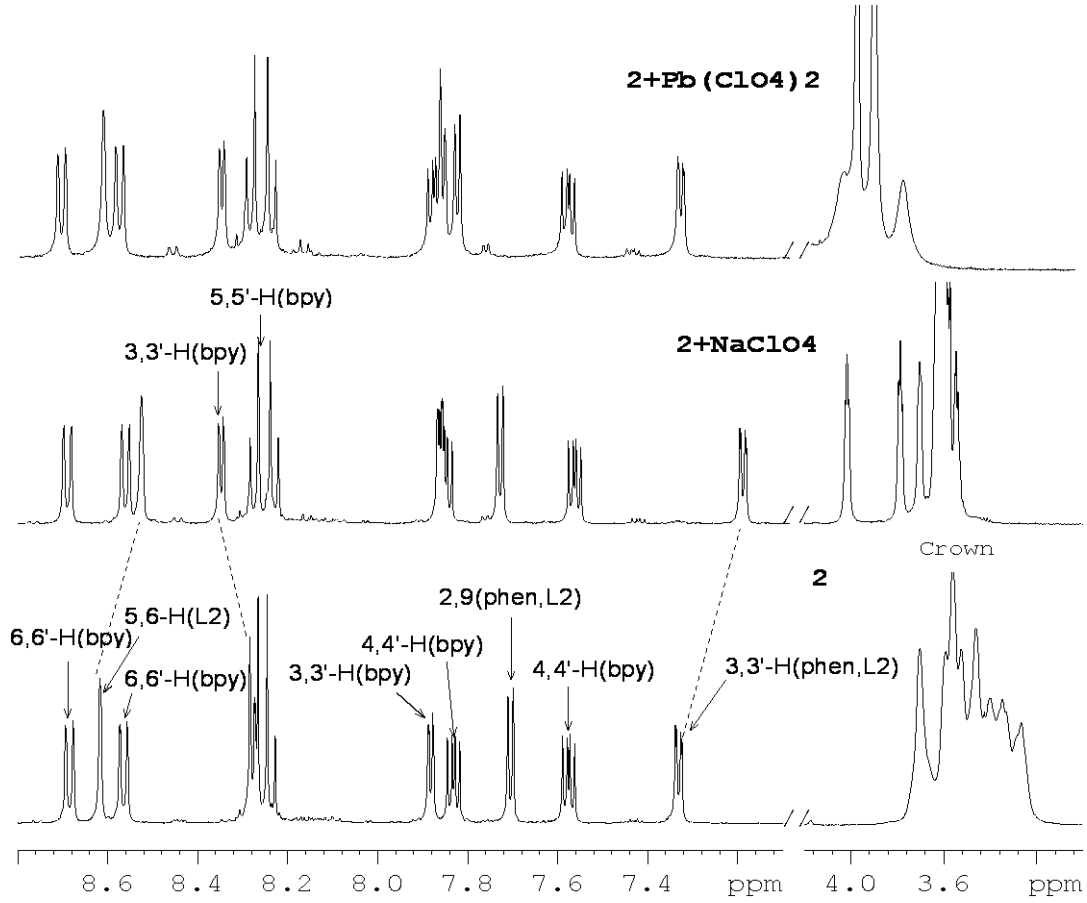

Figure 3.20. Selected portion of the ^{1}H NMR spectra of **2**, [**2**+$NaClO_4$] and [**2**+ $Pb(ClO_4)_2$], recorded in CD_3CN at room temperature.

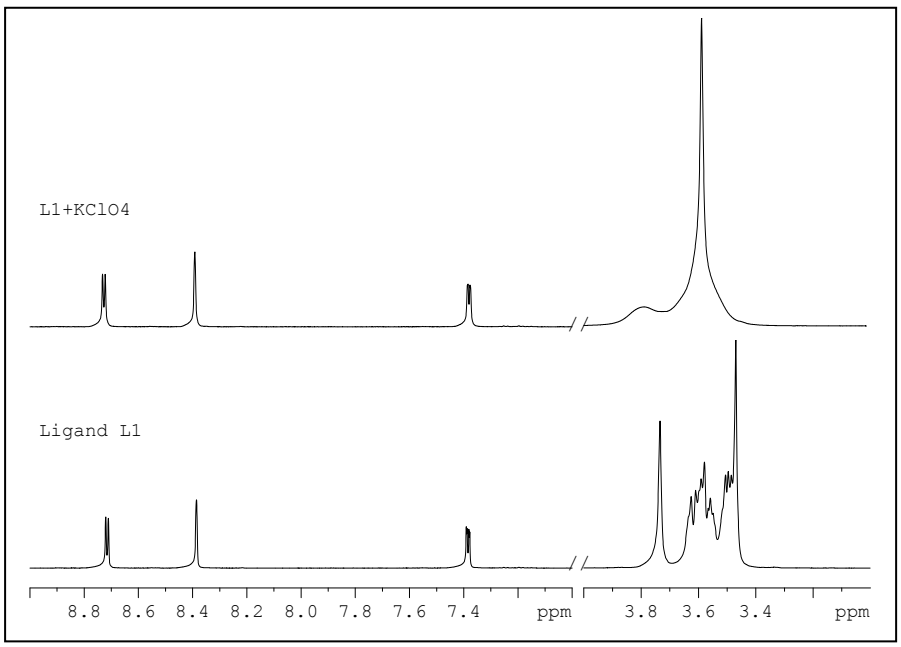

Figure 3.21. ^{1}H NMR spectra of $\mathbf{L^1}$ and [$\mathbf{L^1}$ + $KClO_4$] in acetonitrile

3.3.3 Electrochemical Study

Redox behaviour of Ru(II) in **1** - **3** in presence of Na^+, K^+ and Pb^{2+} have been investigated. Upon addition of these ions (50 equiv), the Ru(II)→Ru(III) oxidation potential of **1** shifted cathodically by 88 and 128 mV for Na^+ and Pb^{2+}, respectively, whereas with K^+ a little shift (<50 mV) is observed. Similar changes were also noted for **2** and **3**. However, **4** and Re(I) complexes (**5** and **6**) did not show significant changes in presence of these metal ions. The oxidation potential (DPV) of Ru(II) and the same in presence of K^+, Na^+ and Pb^{2+} (50 equiv) for **1** and **2** in acetonitrile are shown in Figures 3.22 - 3.23. Generally, upon complexation of crown moiety with metal ion anodic shift of the Ru(II)→Ru(III) oxidation wave is noted.[25,26] However, most of these cases the crown moiety is directly attached with bipyridine unit, in the cases where >C=O and -HN-C=O type of spacer has connected the crown and bipyridine units, the Ru(II) based oxidation potential did not show significant change.[27] It may be noted that the redox potential of the metal centres of complexes **1**-**3** are significantly high (1.55 to 1.65 V) compared to that found in other similar systems (1.01 to 1.07 V) containing azacrown connected to 5,5'- position of the bipyridine unit through >C=O and amide moiety.[27] This difference probably is related to strong H-bonding between >C=O and hydrogen atoms attached to the 3,3'-positions of the bipyridine unit and 5,6-positions of the 1,10-phenanthroline moiety. The >C=O moieties of complexes **1**-**3** are attached at the 4,4'-positions of the bpy/phen unit and at such a situation the oxygen atom of the >C=O unit is in a favorable position to make >C=O….H interaction with the hydrogen atoms at the 3,3'-position of the bipyridine unit making a five membered ring as shown in Figure 3.24. Strong electron withdrawing effect of the >C=O units through hydrogen atoms makes bipyrydine moiety more electron deficient, which resulted in anodic shift of the oxidation potential of the metal centre. On complexation, the orientation of the complexed crown moiety has changed, which resulted in loss of >C=O…H interaction, which in turn reduced electron withdrawing ability of the amide moiety causing cathodic shift of the oxidation potential of the metal ion. Evidence in support of this argument is noted in the NMR spectra. Upon complexation of $\mathbf{L^1}$ with the $Ru(bpy)_2$ unit, the chemical shift of the protons attached to 6,6'-positions of the bipyridine unit of $\mathbf{L^1}$ have substantially shielded (0.98 ppm), whereas the protons attached to 3,3'-positions are deshielded (0.12 ppm). Upon coordination through

nitrogen, shielding of adjacent protons (6,6') is expected but there is no obvious reason of deshielding of protons attached to 3,3'-positions other than its involvement in some kind of H-bonding interaction. Again, after complexation of the crown moiety with metal ion (Na^+/Pb^{2+}), the deshielding effect on these protons is lost and the protons at 3,3'-positions shifted to their original positions as found in the ligand (δ 8.48), whereas chemical shift of the protons at 6,6'-positions remain unchanged (Figures 3.19 and 3.20). This observation is consistent to that noted in the electrochemical study.

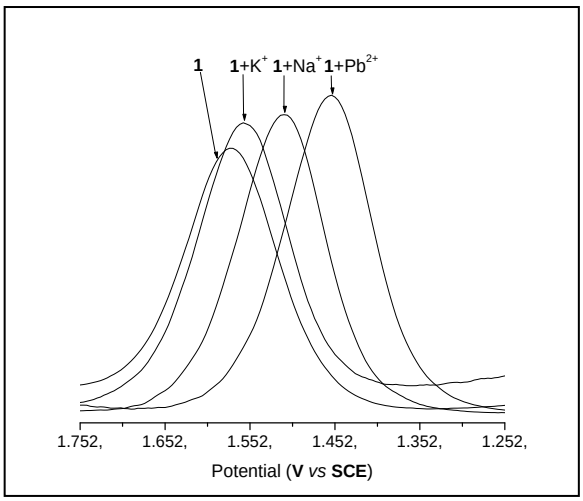

Figure 3.22 Oxidation potential (DPV) of the metal ion [Ru(II)] of **1** and the same in presence of K^+, Na^+ and Pb^{2+} (50 equiv) in acetonitrile

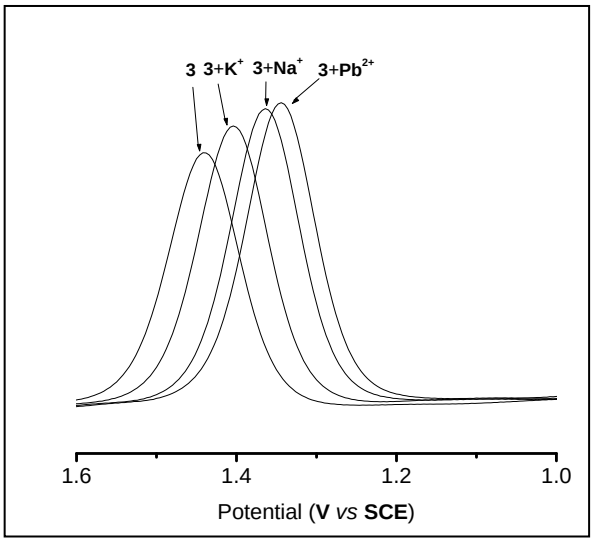

Figure 3.23 Oxidation potential (DPV) of the metal ion [Ru(II)] of **3** and the same in presence of K^+, Na^+ and Pb^{2+} (50 equiv) in acetonitrile

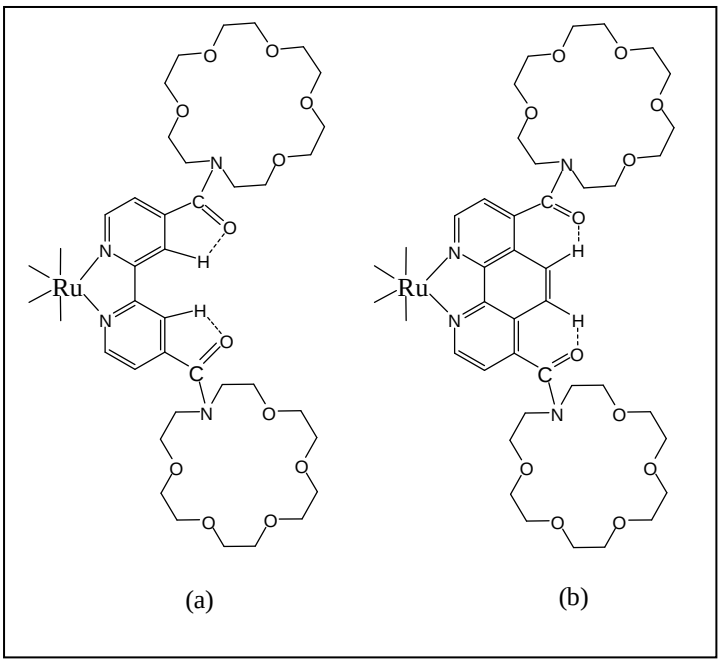

Figure 3.24 Partial drawing of complexes **1** and **2** showing H-bonding interactions between the oxygen atom of C=O and hydrogen atoms at 3,3'-positions of bpy and 5,6-positions of the phen moieties

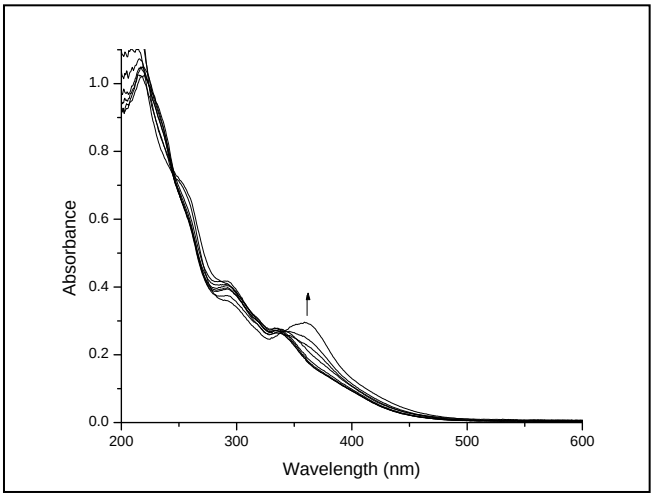

Figure 3.25. UV/Vis spectral change of **6** in acetonitrile with the addition of increasing concentration of $Na(ClO_4)$.

The UV/Vis spectra of the ionophores **1**-**6** have been recorded in acetonitrile with 100 fold excess of various metal ions and no significant change except complex **6** is noted. For complex **6**, spectral change with the addition of increasing concentration of Na^+ ion resulted in the shift of the ^{3}MLCT band from 342 to 360 nm with a slight increase in absorption intensity with an isosbestic point at 246 nm (Figure 3.25).

3.4 Conclusions

Cation binding property of a series of receptor molecules containing ruthenium(II)/ rhenium(I) bipyridine moiety as fluorophore and crown ether as ionophore have been investigated using a large number of cations with the aid of fluorescence, ^{1}H NMR, electrochemistry and UV-Vis spectral studies. The receptors **1**-**3** exhibit strong quenching of emission intensity in presence of Pb^{2+}, Cu^{2+}, Hg^{2+} and Na^+; whereas **4** and **5** show substantial increase of emission intensity in presence of Hg^{2+} and Cu^{2+}/Cd^{2+}. Coordination of the metal ion with the crown moiety blocked the intramolecular photoinduced reductive electron-transfer process resulting in enhancement of emission intensity. From fluorescence titration data, stoichiometry and binding constant of strongly interacting metal ions for **1**-**5** have been calculated. Complexes containing ligands $\mathbf{L^1}$ and $\mathbf{L^2}$ formed 1:2 complexes encapsulating metal ions in both the crown cavities and complexes of $\mathbf{L^3}$ form 1:1 complex**.** The decreasing order of binding constant for **1**-**5** is $Pb^{2+} > Na^+ > Cu^{2+} > Hg^{2+} > Cd^{2+}$, the size of the cation plays important role to form stable complexes. The effective size of the crown cavity in complexes is less compared to that of free crown ring, which does not allow K^+ to form stable complexes. The steric crowding and intramolecular interaction are probably responsible for twisting the crown moiety. Strong complex formation with Pb^{2+} and Na^+ has also been demonstrated by ^{1}H NMR study, which exhibit significant spectral change in presence of these metal ions. Electrochemical oxidation of Ru(II) in absence and in presence of metal ions also suggests strong interaction of the ionophores with Pb^{2+} and Na^+. The spacer >C=O apparently plays significant role in intramolecular interactions, which promoted electronic communication between fluorophore and ionophore as evident from electrochemical study and ^{1}H NMR spectral changes.

3.5 References

1. J. P. Desvergne, A. W. Czarnik, *Chemosensors of Ion and Molecule Recognition: NATO ASI Series Kluwer, Dordrecht*, **1997**.

2. Y. Zeng, J. Orbulescu, X. Ji, F. M. Andrepoulos, S. M. Pham, R. M. Leblanc, *J. Am. Chem. Soc*. **2003**, *125*, 2680.

3. J. Y. Kwon, Y. J. Jang, Y. J. Lee, K. M. Kim, M. S. Seo, W. Nam, J. Yoon, *J. Am. Chem. Soc*. **2005**, *127*, 10107.

4. S. Yoon, A. E. Albers, A. p. Wong, C. J. Chang, *J. Am. Chem. Soc*. **2005**, *127*, 16030;

5. J. S. Kim, D. T. Quang, *Chem. Rev*. **2007**, *107*, 3780.

6. A. W. Czarnik, *Fluorescent Chemosensors of Ion and Molecule Recognition: Ed., ACS Sump. Ser. 538; American Chemical Society: Washington DC*, **1993**.

7. D. C. Magri, G. J. Brown, G. D. McClean, A. P. de Silva, *J. Am. Chem. Soc*. **2006**, *128*, 4950.

8. A. P. de Silva, S. A. de Silva, *J. Chem. Soc. Chem. Commun.* **1986**, 1707.

9. K. Rurack, U. Resch-Genger, *Chem. Soc. Rev.* **2002**, *37*, 116.

10. V. W. W. Yam, C-C.Ko, B. W. K. Chu, N. Zhu, *J. Chem. Soc. Dalton Trans.* **2003**, 3914.

11. S. Banthia, A. Samanta, *J. Phys. Chem. B* **2006**, *110*, 6437.

12. D. D. Perrin, W. L. F. Armarego, D. R. Perrin, *Purification of Laboratory Chemicals*, 2nd Ed, **1980**.

13. A. C. Tedesco, D. M. Oliveira, Z. G. M. Lacava, R. B. Azevedo, E. C. D. Lima, P. C. Morais, *J. Magnetism Magnetic Mater*. **2004**, *272-276*, 2404.

14. S. S. Lehrer, G. D. Fashman, *Biochem. Biophys. Res. Commun.* **1966**, *2*, 133.

15. D. M. Chipman, V. Grisaro, N. Shanon, *J. Biol. Chem*. **1967**, *242*, 4388.

16. J. J. Christensen, D. J. Eatough, R. M. Izatt, *Chem. Rev*. **1974**, *74*, 351.

17. F. A. Cotton , G. Wilkinson, *Advanced Inorganic Chemistry A Comprehensive Text.* **1962**, 43.

18. P. D. Beer, S. W. Dent, T. J. Wear, *Dalton Trans.* **1996**, 2341;

19. L. H. Uppadine, J. E. Redman, S. W. Dent, M. G. B. Drew, P. D. Beer, *Inorg. Chem.* **2001**, *40*, 2860.

20. P. D. Beer, V. Timoshenko, M. Maestri, P. Passaniti, V. Balzani, *Chem. Commun*. **1999**, 1755.

21. P. D. Beer, S. W. Dent *J. Chem. Soc. Chem. Commun.* **1998**, 825.

22. M. Chiba, K. Ogawa, K. Tsuge, M. Abe, H. B. Kim, Y. Sasaki, N. Kitamura, *Chem. Lett*. **2001**, 692.

23. J. B. Cooper, M. G. B. Drew, P. D. Beer, *J. Chem. Soc. Dalton Trans.* **2001**, 392;

24. P. V. Bemhardt, E. G. Moore, *Aus. J. Chem.* **2003**, *56*, 239.

25. M. Schmittel, H. W. Lin, *Angew. Chem., Int. Ed*. **2006**, *45*,1.

26. M. Schmittel, H. W. Lin, E. Thiel, A. J. Meixner, H. Ammon, *J. Chem. Soc. Dalton Trans.* **2006**, 4020.

27. P. D. Beer, S. W. Dent, N. C. Fletcher, *Polyhedron*, **1996**, *15*, 2983.

CHAPTER – IV

Luminescent Metalloreceptors with Pendant Macrocyclic Ionophore: Synthesis, Characterization, Electrochemistry and Ion-binding Study

4.1 Introduction

Development of artificial receptors capable of detecting the presence of specific ions has received considerable interest in current research.[1-5] Among various anions, detection of fluoride and phosphates are gaining increasingly importance because of their involvement in many biological and environmental processes.[6-10] In the design of anion receptors, various noncovalent interactions, such as hydrogen-bonding, electrostatic, hydrophobicity are mainly considered.[2,6-14] For this purpose, both the open chain and macrocyclic units, which can effectively interact with the incoming ions, have been used as ionophore. Macrocyclic ionophores are commonly used for the detection of cations, however they have also been used for anion recognition because of their ability to associate with anions by hydrogen-bonding interaction.[2,7,9,11]

Incorporation of luminescent chromophores in designing of receptors has also gained considerable current attention.[6-18] The photophysical property of the luminescent unit is sensitive to interactions between host and guest, and therefore can be used as a tool to monitor the recognition event. This method of ion recognition is superior to other spectroscopic methods because of high sensitivity of luminescence detection. Fluorescent organic molecules have been widely used as fluorophore for the recognition of both cations and anions.[10,19-21] Binding of ions to the recognition sites leads to changes in certain properties of the receptors such as colour, luminescence, excited-state lifetime and that serves as indicators of ion-recognition. Rhenium(I) and ruthenium(II)-polypyridyl complexes are also highly luminescent and have been used as fluorophore in designing chemisensors for cations, anions and biological molecules.[2,3,6-9,11-13,22-26] For designing of anion receptors, incorporation of metal-complex based fluorophores offers some advantages over organic molecules. The positive charge on the metal ion makes enhanced electrostatic interaction with negatively charged species leading to strong host-guest interaction.

In this chapter, synthesis of a number of luminescent receptors and studies on their photophysical, electrochemical and ion recognition properties has been reported. Ionophores of two of these receptors are pendant macrocyclic units of different size covalently attached to 1,10-phenanthroline moiety, which is coordinated to the metal ion of the *cis*-$Ru(bpy)_2$ unit. In these macrocyclic units, amide and amine groups have

been incorporated so that anions can make strong interactions with the hydrogen atoms of these groups through hydrogen-bonding. The performance of these receptors have been examined with a large number of anions and cations, among which only F^- and $H_2PO_4^-$ have shown strong interactions with two of the receptors and Cu^{2+} exhibits strong complexation with one of the receptors. Binding constants have been determined and the results presented and discussed in light of ion-binding ability of the new receptors and perturbation of luminescence property due to complexation.

4.2 Experimental

4.2.1 Materials

Chemicals used in this study were purchased from Aldrich and S.D. Fine Chemicals. All metal perchlorate salts were purchased from Alfa Aesar (Johnson Matthey Company) and hydrated ruthenium trichloride was purchased from Arora Matthey. All organic solvents were analytical grade and were used as received for synthetic purpose. Solvents for spectral and electrochemical studies were freshly purified by standard procedures before use.[27] The starting compounds 1,10-phenanthroline-5,6-dione,[28] 5,6-dihydroxy-1,10-phenanthroline[28] and *cis*-$[Ru(bpy)_2Cl_2].2H_2O$[29] were synthesized following the literature procedures.

4.2.2 Physical measurements

Elemental analyses (C, H, and N) were performed on a model 2400 Perkin-Elmer elemental analyzer. Mass spectra were recorded on a Q-TOF Micro™ LC-MS instrument. IR spectra were recorded on a Perkin-Elmer spectrum GX FT-IR spectrophotometer as KBr pellets. NMR spectra were recorded on Avance II 500 Brucker FT-NMR instruments. The UV/vis spectra were recorded on a CARY 500 Scan UV-VIS-NIR spectrophotometer (Varian). Luminescence spectra were recorded on a model Fluorolog Horiba Jobin Yvon spectrofluorimeter at room temperature. Electrochemical measurements were made using CHI 660A electrochemical workstation equipment. Cyclic voltammetry and differential pulse voltammetry (DPV) studies were carried out in a three-electrode cell consisting of a platinum

working electrode, a platinum-wire auxiliary electrode, and an SCE reference electrode. Solutions of the complexes in purified acetonitrile containing 0.1M tetrabutylammonium tetrafluoroborate as supporting electrolyte were deaerated by bubbling nitrogen for 10 min prior to each experiment. Luminescence quantum yields were measured in optically diluted solution, using $[Ru(bpy)_3]^{2+}$ in oxygen-free acetonitrile (ϕ= 0.062) as reference emitter.[30,31]

Caution: Perchlorate salts of metal ions are potentially explosive. Therefore, they should be handled with great care.

4.2.3 Synthesis of ligands

4.2.3.1 Synthesis of L^1

This compound was prepared following a modified literature procedure.[7] To a solution of 5,6-dihydroxyphenanthroline (1.5 g, 7.0 mmol) in 50 mL dry acetonitrile were added potassium carbonate (3 g), ethyl bromoacetate (2.5 g, 16 mmol) and a catalytic amount of triethylbenzylammonium chloride (0.10 g). The mixture was allowed to reflux under nitrogen for 15 h with constant stirring. After completion of the reaction, the solid suspension was filtered while hot to remove suspended inorganic salts. The solvent of the filtrate was removed under reduced pressure and the residue was dissolved in toluene (70 mL) and filtered. The volume of the filtrate was then reduced to 25 mL and then diethyl ether (75 mL) was added slowly into it and kept for over night. The white product thus deposited was isolated by filtration and dried in vacuum. Yield 1.70 g (63 %). ^{1}H NMR (500 MHz, $CDCl_3$): δ = 1.29 (t, 6H, J = 7.0 Hz, OCH_2CH_3), 4.27 (q, 4 H, J = 7.0 Hz, OCH_2CH_3), 4.91 (s, 4H, OCH_2CO), 7.67 (dd, 2H, J_1 = 8.3, J_2 = 4.3, 3-H-phen), 8.76 (dd, 2H, J_1 = 8.3, J_2 = 1.8, 2-H-phen), 9.15 (dd, 2H, J_1 = 4.3, J_2 = 1.8, 4-H-phen) ppm. MS: *m*/*z* (%): 791.39 (100) [$2\mathbf{L^1} + Na^+$] (calcd. 791.25), 407.35 (85) [$\mathbf{L^1} + Na^+$] (calcd. 407.12), 385.33 (40) [$\mathbf{L^1} + H^+$] (calcd. 385.14). IR (KBr pellets): ν = 1751 cm^{-1} (C=O). $C_{20}H_{20}N_2O_6$ (384.13): calcd. for C 62.48, H 5.25, N 7.29; found C 62.35, H 5.06, N 7.18.

4.2.3.2 Synthesis of L^2

A solution of $\mathbf{L^1}$ (1.15 g, 3 mmol) and diethylenetriamine (0.36 g, 3.5 mmol) in dry ethanol–toluene (1:1, 60 ml) were refluxed for 48 h under nitrogen. The solution was then allowed to cool to room temperature, filtered and the solvent of the filtrate was removed under reduced pressure. After removal of the solvent the crude product was purified by column chromatography using neutral alumina as packing material and methanol–toluene (1:19) mixture as eluent. Removal of solvent from desired fraction gave white product. Yield 0.68 g (57 %). ^{1}H NMR (500 MHz, CD_3OD): δ = 2.86 (t, 4H, J = 5.25 Hz, CH_2NHCH_2, macrocycle), 3.52 (t, 4H, J = 5.25, $NHCH_2CH_2$, macrocycle), 4.79 (s, 4H, OCH_2CO, macrocycle), 7.78 (dd, 2H, J_1 = 8.5 Hz, J_2 = 4.5 Hz, 3-H-phen), 8.64 (dd, 2H, J_1 = 8.5 Hz, J_2 = 1.5, 2-H-phen), 9.05 (dd, 2H, J_1 = 4.25 Hz, J_2 = 1.75, 4-H-phen) ppm. MS: m/z (%): 829.25 (18) [$2\mathbf{L^2} + K^+$] (calcd. 829.28), 813.28 (70) [$2\mathbf{L^2} + Na^+$] (calcd. 813.31), 434.33 (23) [$\mathbf{L^2} + K^+$] (calcd. 434.12), 418.33 (60) [$\mathbf{L^2} + Na^+$] (calcd. 418.15), 396.34 (100) [$\mathbf{L^2} + H^+$] (calcd. 396.17). IR (KBr pellets): ν = 3424, 3275 (N-H), 1673 cm^{-1} (C=O). $C_{20}H_{21}N_5O_4$ (395.16): calcd. for C 60.73, H 5.35, N 17.71; found C 60.12, H 5.64, N 17.49.

4.2.3.3 Synthesis of L^3

The ligand $\mathbf{L^3}$ was prepared following the similar procedure as described above for $\mathbf{L^2}$, except the use of triethylenetetraamine instead of diethylenetriamine. Yield (52%). ^{1}H NMR (500 MHz, CD_3OD): δ = 2.75 (s, 4H, $NHCH_2CH_2NH$, macrocycle), 2.84 (t, 4H, J = 5.25 Hz, CH_2CH_2NH, macrocycle), 3.54 (t, 4H, J = 5.25 Hz, CH_2CH_2NH, macrocycle), 4.8 (s, 4H, OCH_2CO, macrocycle), 7.81 (dd, 2H, J_1 = 7.75 Hz, J_2 = 4.5 Hz, 3-H-phen), 8.67 (dd, 2H, J_1 = 8.25 Hz, J_2 = 1.75 Hz, 2-H-phen), 9.07 (dd, 2H, J_1 = 4.25 Hz, J_2 = 1.75 Hz, 4-H-phen) ppm. MS: m/z (%) 878.6 (35) [$2\mathbf{L^3} + H^+$] (calcd. 877.41) 462.50 (15) [$\mathbf{L^3} + Na^+$] (calcd. 462.20), 439.53 (100) [$\mathbf{L^3} + H^+$] (calcd. 439.21). IR (KBr pellets): ν = 3461, 3325, 3287 (N-H), 1655 cm^{-1} (C=O). $C_{22}H_{26}N_6O_4$ (438.20): calcd. for C 60.24, H 5.97, N 19.17; found C 59.90, H 5.62, N 18.94.

4.2.4 General procedure for the synthesis of $[Ru(bpy)_2(L^1)][PF_6]_2$ (1), $[Ru(bpy)_2(L^2)][PF_6]_2$ (2) and $[Ru(bpy)_2(L^3)][PF_6]^2$ (3)

A mixture of *cis*-$[Ru(bpy)_2Cl_2]\cdot 2H_2O$ (0.52 g, 1.0 mmol) and the appropriate ligand (**L**^{1}/**L**^{2}/**L**^{3}, 1.0 mmol) in ethanol-water (2:1, 60 mL) was refluxed for 12 h. The reaction mixture was then allowed to cool to room temperature; volume was reduced to *ca*. 20 mL by rotary evaporation, filtered and to the filtrate was added solid NH_4PF_6 (0.815 g, 5 mmol). The precipitate was filtered off and washed with water and diethyl ether. The complexes were purified by column chromatography using a column packed with deactivated (10% water) alumina and acetonitrile-toluene (2:1 for **1**, 9:1 for **2** and **3**) as eluent. The small first fraction was discarded; the large orange-red colored second fraction gave the desired complex. After removal of the solvent, the residue was redissolved in acetonitrile and was precipitated by vapor diffusion method using diethyl ether. In case of **1**, X-ray quality single crystals were obtained and for **2** and **3**, microcrystalline compounds were separated. Yield 0.675 g (67%) for **1**, 0.626 g (57%) for **2** and 0.58 g (50%) for **3.**

4.2.4.1 Data for 1

^{1}H NMR (500 MHz, CD_3CN): δ = 1.16 (t, 6H, *J* = 7.0 Hz, -OCH$_2$*CH$_3$*), 4.17 (q, 4H, *J* = 7.0 Hz, -O*CH$_2$*CH$_3$), 5.01 (s, 4H, -O*CH$_2$*CO), 7.26-7.22 (overlapped triplets, 2H, bpy), 7.46-7.43 (overlapped triplets, 2H, bpy), 7.53 (d, 2H, *J* = 5.5 Hz, bpy), 7.73 (dd, 2H, J_1 = 8.5, J_2 = 5.5, 3-H of phen, **L**^{1}), 7.83 (d, 2H, *J* = 6.0 Hz, bpy), 8.02-7.98 (m, 4H, bpy, 2-H of phen, **L**^{1}), 8.11-8.08 (dt, 2H, J_1 = 7.5 Hz, J_2 = 1.5 Hz, bpy), 8.49 (d, 2H, *J* = 8.0 Hz, bpy), 8.53 (d, 2H, *J* = 8.5 Hz, bpy), 8.91 (dd, 2H, J_1 = 8.5 Hz, J_2 = 1.0 Hz, 4-H of phen, **L**^{1}) ppm. MS: *m/z* (%) 943.46 (100) [**1** - PF_6^-]$^+$ (calcd. 943.14). IR (KBr pellets): ν = 1751 (C = O), 839 cm^{-1} (PF_6^-). UV/Vis (CH_3CN): λ (ε) = 451 (6.78 x 10^3), 286 (2.54 x 10^4 mol^{-1} cm^{-1}). $C_{40}H_{36}N_6O_6P_2F_{12}Ru$ (1088.10): calcd. for C 44.11, H 3.33, N 7.72; found C 43.81, H 3.16, N, 7.62.

4.2.4.2 Data for 2

^{1}H NMR (500 MHz, CD_3CN): δ = 3.00 (poorly resolved triplet, 4H, CH_2NHCH_2 of macrocycle, $\mathbf{L^2}$), 3.47 (t, 2H, J = 5.5 Hz, CH_2CH_2NH of the macrocycle, $\mathbf{L^2}$), 3.48 (t, 2H, J = 5.5 Hz, CH_2CH_2NH of the macrocycle, $\mathbf{L^2}$), 4.78 (s, 4H, OCH_2CO of the macrocycle, $\mathbf{L^2}$), 7.24-7.27 (overlapped triplet, 2H, bpy), 7.34 (br , 2H, -CO*NH*), 7.43-7.46 (overlapped triplet, 2H, bpy), 7.54 (d, 2H, J = 5.5 Hz, bpy), 7.72 (dd, 2H, J_1 = 8.5 Hz, J_2 = 5.0 Hz, 3-H of phen, $\mathbf{L^2}$), 7.83 (d, 2H, J = 5.5 Hz, bpy), 8.01 (t, 2H, J = 8.0 Hz, bpy), 8.05 (dd, 2H, J_1 = 5.5 Hz, J_2 = 1.0 Hz, 2-H of phen, $\mathbf{L^2}$), 8.10 (t, 2H, J = 8.0 Hz, bpy), 8.49 (d, 2H, J = 8.0 Hz, bpy), 8.53 (d, 2H, J = 8.5 Hz, bpy), 8.72 (dd, 2H, J_1 = 8.5 Hz, J_2 = 1.0 Hz, 4-H of phen, $\mathbf{L^2}$) ppm. MS: *m/z* (%) 953.86 (30) [**2** - PF_6^-]$^+$ (calcd. 954.16), 808.11 (20) [**2** - 2PF_6^- + H^+]$^+$ (calcd. 809.20). IR (KBr pellets): ν = 3640, 3407 (N-H), 1671 (C = O), 841 cm^{-1} (PF_6^-). UV/Vis (CH_3CN): λ (ε) = 450 (6.21 x 10^3), 285 (2.42 x 10^4 mol^{-1} cm^{-1}). $C_{40}H_{37}N_9O_4P_2F_{12}Ru$ (1099.13): calcd. for C 43.67, H 3.39, N 11.46; found C 43.27, H 3.50, N 11.24.

4.2.4.3 Data for 3

^{1}H NMR (500 MHz, CD_3CN): δ = 3.00 (s, 4H, $NHCH_2CH_2NH$ of the macrocycle, $\mathbf{L^3}$), 3.01 (t, 4H, J = 5.5 Hz, CH_2CH_2NH of the macrocycle, $\mathbf{L^3}$), 3.53 (t, 4H, J = 5.5 Hz, CH_2CH_2NH of the macrocycle, $\mathbf{L^3}$), 4.82 (s, 4H, OCH_2CO of the macrocycle, $\mathbf{L^3}$), 7.24-7.27 (overlapped triplet, 2H, bpy), 7.44-7.47 (overlapped triplet, 2H, bpy), 7.55 (d, 2H, J = 5.0 Hz, bpy), 7.70 (br , 2H, -CO*NH*), 7.73 (dd, 2H, J_1 = 8.5 Hz, J_2 = 5.0 Hz, 3-H of phen, $\mathbf{L^3}$), 7.84 (d, 2H, J = 5.5 Hz, bpy), 8.01 (t, 2H, J = 8.0 Hz, bpy), 8.05 (dd, 2H, J_1 = 5.5 Hz, J_2 = 1.0 Hz, 2-H of phen, $\mathbf{L^3}$), 8.10 (t, 2H, J = 8.0 Hz, bpy), 8.50 (d, 2H, J = 8.0 Hz, bpy), 8.53 (d, 2H, J = 8.0 Hz, bpy), 8.73 (dd, 2H, J_1 = 8.0 Hz, J_2 = 1.0 Hz, 4-H of phen, $\mathbf{L^3}$) ppm. MS: *m/z* (%) 996.82 (30) [**2** - PF_6^-]$^+$ (calcd. 997.20), 851.08 (40) [**2** - 2PF_6^- + H^+]$^+$ (calcd. 852.24). IR (KBr pellets): ν = 3645, 3409, 3239 (N-H), 1669 (C = O), 840 cm^{-1} (PF_6^-). UV/Vis (CH_3CN): λ (ε) = 452 (5.58 x 10^3), 285 (2.18 x 10^4 mol^{-1} cm^{-1}). $C_{42}H_{42}N_{10}O_4P_2F_{12}Ru$ (1142.17): calcd. for C 44.12, H 3.70, N 12.26; found C 43.78, H 3.54, N 12.03.

4.2.5 Crystal structure determination

The crystallographic data and details of data collection are given in Table 1. Crystal of suitable size was selected and then mounted on the tip of a glass fiber and cemented using epoxy resin. Intensity data of the crystal was collected using MoK_α (λ = 0.71073 Å) radiation on a Bruker SMART APEX diffractometer equipped with CCD area detector at 100K. The data integration and reduction were processed with SAINT software.[32] An empirical absorption correction was applied to the collected reflections with SADABS.[33] The structure was solved by direct methods using SHELXTL and were refined on F^2 by the full-matrix least-squares technique using the SHELXL-97 program package.[34,35] All non-hydrogen atoms were refined anisotropically till convergence is reached and hydrogen atoms attached to the ligand moiety is located from the difference Fourier map and refined isotropically.

4.2.6 Ion-binding property

4.2.6.1 Luminescence method

Stock solutions of the complexes **1-3** (2 x 10^{-5} M) and that of the tetrabutyl ammonium salts (2 x 10^{-3} M) of various anions (F^-, Cl^-, Br^-, I^-, $H_2PO_4^-$, ClO_4^-, NO_3^-, BF_4^-, CH_3COO^-, and HSO_4^-) were prepared in freshly purified acetonitrile. Then 2 mL stock solution of the complex and 2 mL stock solution of each anion salt were taken in a 5 mL volumetric flask, so that the effective concentration of the complex is 1 x 10^{-5} M and that of the anions are 1 x 10^{-3} M (100 fold). The luminescence spectra of the resulting solutions and that of the original complex (1 x 10^{-5} M) were recorded with excitation at the absorption maxima (λ_{max}) of the MLCT band, which is 451, 450 and 452 nm for **1-3,** respectively. The spectra of the anion containing reaction mixtures were compared with that of the original solution to ascertain the interactions of the anions with the ionophore. Similar experiments were also carried out with perchlorate salts of various cations (Na^+, K^+, Mg^{2+}, Ca^{2+}, Zn^{2+}, Ba^{2+}, Sr^{2+} Cd^{2+}, Hg^{2+}, Pb^{2+} and Cu^{2+}) to ascertain the interactions of the metal ions with the ionophore. The UV/Vis spectra of all the solutions containing anions and cations (100 equiv) were also recorded and the same were compared to that of the original solutions to examine the changes.

Table 1. Summary of crystallographic data for complex **1**

Identification code	Compound **1**
Chemical formula	$C_{40}H_{36}F_{12}N_6O_6P_2Ru_1$
Formula weight	1087.76
Crystal colour	Wine red
Crystal size (mm^3)	0.38x 0.28 x 0.21
Temperature (K)	100
Crystal system	Monoclinic
Space group	$P2_1/n$
a(Å)	16.5335(11)
b(Å)	14.0125(9)
c(Å)	18.0203(13)
α(°)	90
β(°)	90.288(2)
γ (°)	90
Z	4
V($Å^3$)	4174.8(5)
Density (Mg/m^3)	1.731
Absorption coefficient (mm^{-1})	0.563
F(000)	2192
Reflections collected	20679
Independent reflections	7356 [R(int) = 0.0635]
Number of parameters	259
S (Goodness of Fit) on F^2	1.135
Final R1 , wR2 (I>2σ(I)	0.0753/ 0.1591
Weighted R1, wR2(all data)	0.1018/ 0.1710

Anions and cations, which exhibited substantial changes in emission intensity, were considered for emission titration to evaluate association constant. For emission titration study, the same stock solutions of the complexes (**2** and **3**) were used and the solution of tetrabutyl ammonium salts of the selected anions (F^- and $H_2PO_4^-$) and the perchlorate salt of the cation (Cu^{2+} for **3**) of desired concentration ($0.4 \times 10^{-5} - 2 \times 10^{-3}$ M) were prepared by proper dilution of the stock solution. Then 2 mL of each solution were mixed in a 5 mL volumetric flask to prepare reaction mixture with 0.2 to 100 molar equivalent of the concentration of metal ion with respect to the concentration of complexes and the luminescence spectra of the resulting solutions were recorded. Binding constants were calculated following the literature procedure as described below in the Results and Discussion Section.[36,37]

4.2.6.2 NMR method

To investigate the interaction of anions with fluoroionophore, ^{1}H NMR spectroscopic study was carried out. These complexes are highly soluble in acetonitrile, however after addition of anions, all the new products formed are not highly soluble in acetonitrile, particularly in the case of $H_2PO_4^-$. Because of this solubility problem, different solvents were chosen for ^{1}H NMR study with various anions. ^{1}H NMR spectra of the solutions containing 2 mg of complex, dissolved in 0.5 mL of solvent (CD_3CN/DMSO-d_6/CD_3OD), were recorded. The solutions of anions were then added with increasing concentration to make it 1.5 molar equivalent of the concentration of complex and the corresponding ^{1}H NMR spectra were recorded. The spectra in presence and in absence of anions were compared to assess the interactions between anions and the ionophores.

4.2.7 Synthesis of dihydrogenphosphate complexes

About 50 mg of the complex (**1** and **2**) was dissolved in 10 mL of acetonitrile and tetrabutyl ammonium phosphate monobasic (5 M equiv) was added slowly into the solution with stirring. The reaction was continued for 1 h at room temperature during which reddish brown precipitate was separated. The compound was isolated by filtration, washed 3 times with acetonitrile and dried in vacuum. ^{1}H NMR, Mass and IR spectra of these compounds were recorded for characterization of the products.

4.3 Results and discussion

4.3.1 Ligands (L^1-L^3)

The route followed for the synthesis of **L^1- L^3** is shown in Scheme 1. The ligand **L^1** was synthesized following a modified published procedure.[7] Ligands **L^2** and **L^3** were synthesized from **L^1** by the reaction with diethylenetriamine and triethylenetetraamine, respectively in refluxing ethanol–toluene and were purified by column chromatography. Elemental analysis (C, H and N), ^{1}H NMR and mass spectrometric data, and selected IR bands are given in the Experimental Section. Mass and ^{1}H NMR spectra of **L^1- L^3** are displayed in the Figures 4.1 – 4.6. C, H and N analysis and mass data are in excellent agreement with the calculated values. It may be noted that *e/m* values of all these compounds correspond to the $Na^+/K^+/H^+$ adduct, which is a well known phenomenon when LC-MS is used for the measurement of mass.[26,37-39] The aromatic region of the ^{1}H NMR spectra of **L^1-L^3** exhibit three doublets of doublets in the ranges δ = 7.67 – 7.81, 8.64 – 8.76 and 9.05 – 9.15, which are assigned to 3-H, 2-H and 4-H, respectively of the 1,10-phenanthroline units (usual numbering scheme of phen is used). In the aliphatic region, **L^1** exhibits three signals at δ = 1.29(t), 4.27(q) and 4.91(s), which are due to *CH_3*, *CH_2* and O*CH_2* groups, respectively of the ester units. The macrocyclic unit of **L^2** exhibits three signals at δ = 2.86(t), 3.52(t) and 4.79(s), which are assigned to *b*-*CH_2*, *a*-*CH_2* and O*CH_2* protons (Scheme 1 for numbering of protons), respectively. The macrocyclic unit of **L^3** exhibits four signals at δ = 2.75(s), 2.84(t), 3.54(t) and 4.80(s), which are due to *c*-*CH_2*, *b*-*CH_2*, *a*-*CH_2* and O*CH_2* protons, respectively. For NH protons of **L^2** and **L^3**, no ^{1}H NMR signal was observed in CD_3OD. The IR spectra, however exhibit sharp bands at 3424 and 3275 cm^{-1} for **L^2** and at 3461, 3325 and 3287 cm^{-1} for **L^3,** which are assigned to N-H protons of the macrocyclic units of the ligands.[30] The IR spectra of **L^1 – L^3** also exhibit *v*(C=O) at 1751, 1673 and 1655 cm^{-1}, respectively. On the basis of these data, the proposed structures of the ligands are shown in Scheme 1.

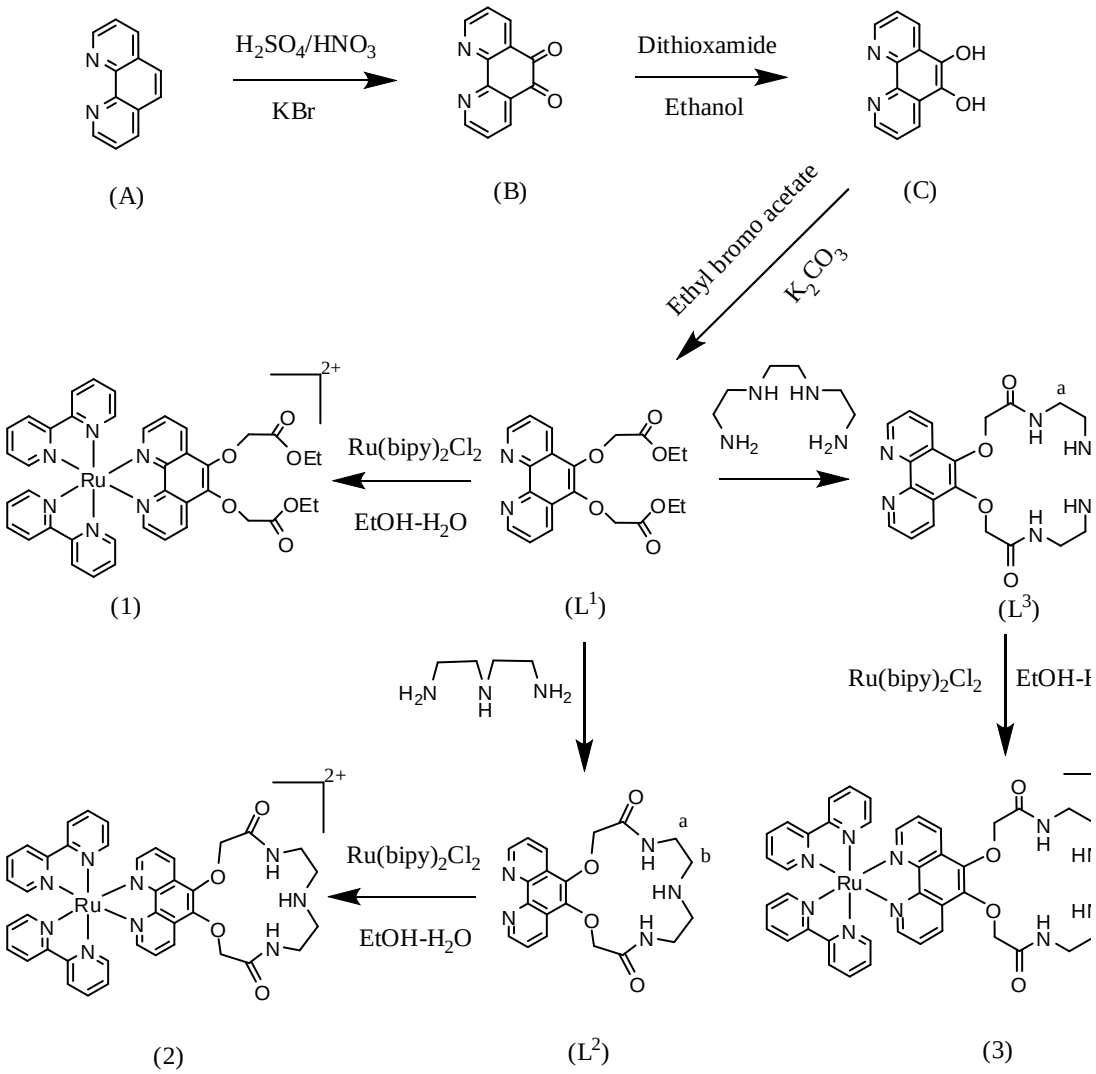

Scheme 1. Synthetic route for the ligands (**L^1-L^3**) and complexes (**1-3**).

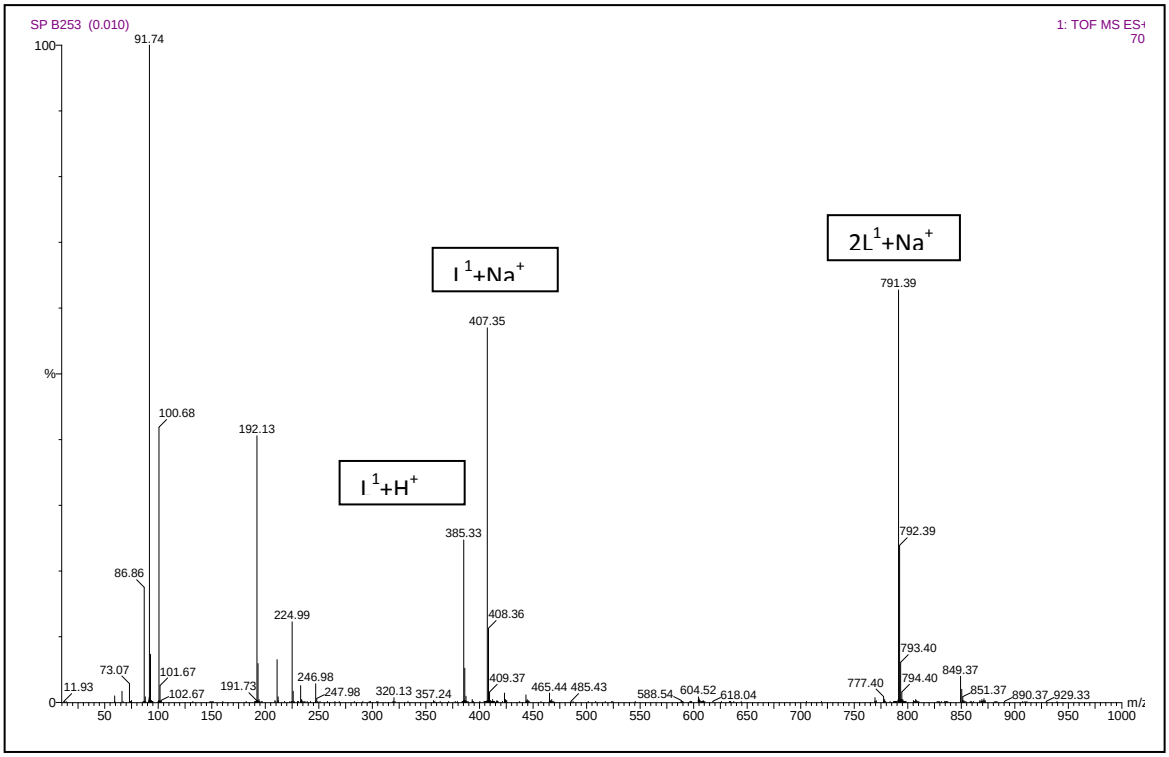

Figure 4.1 Mass spectra of L^1

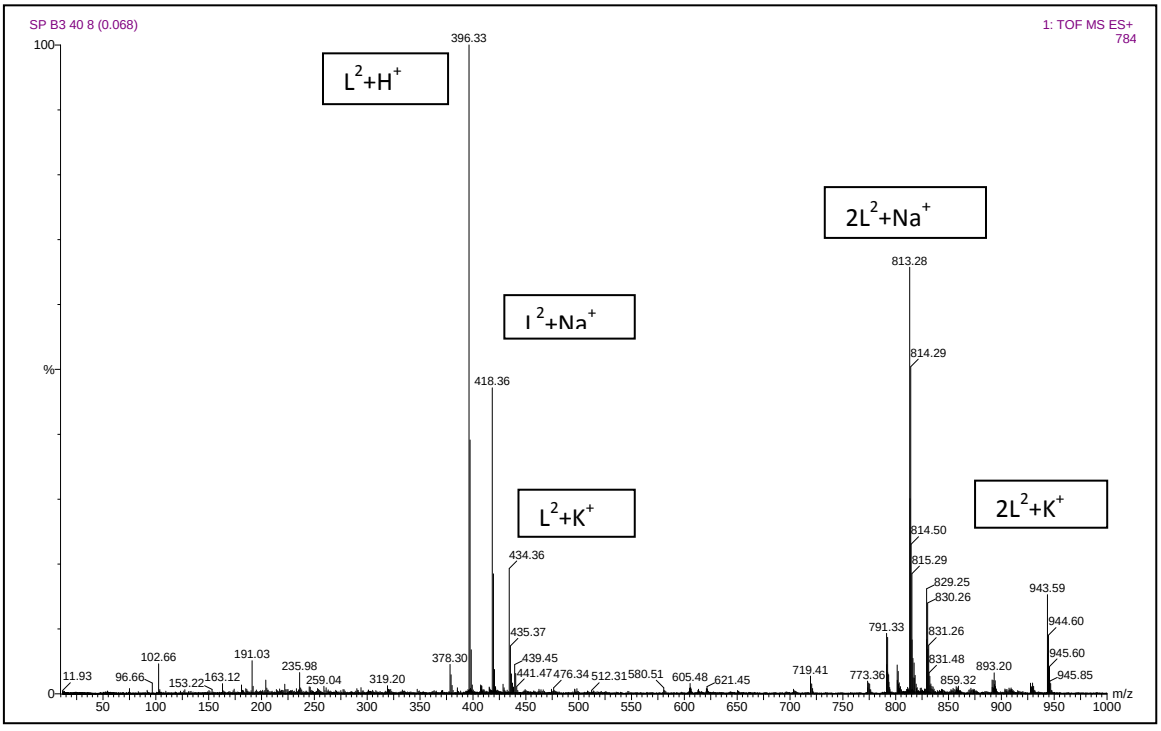

Figure 4.2 Mass spectra of L^2

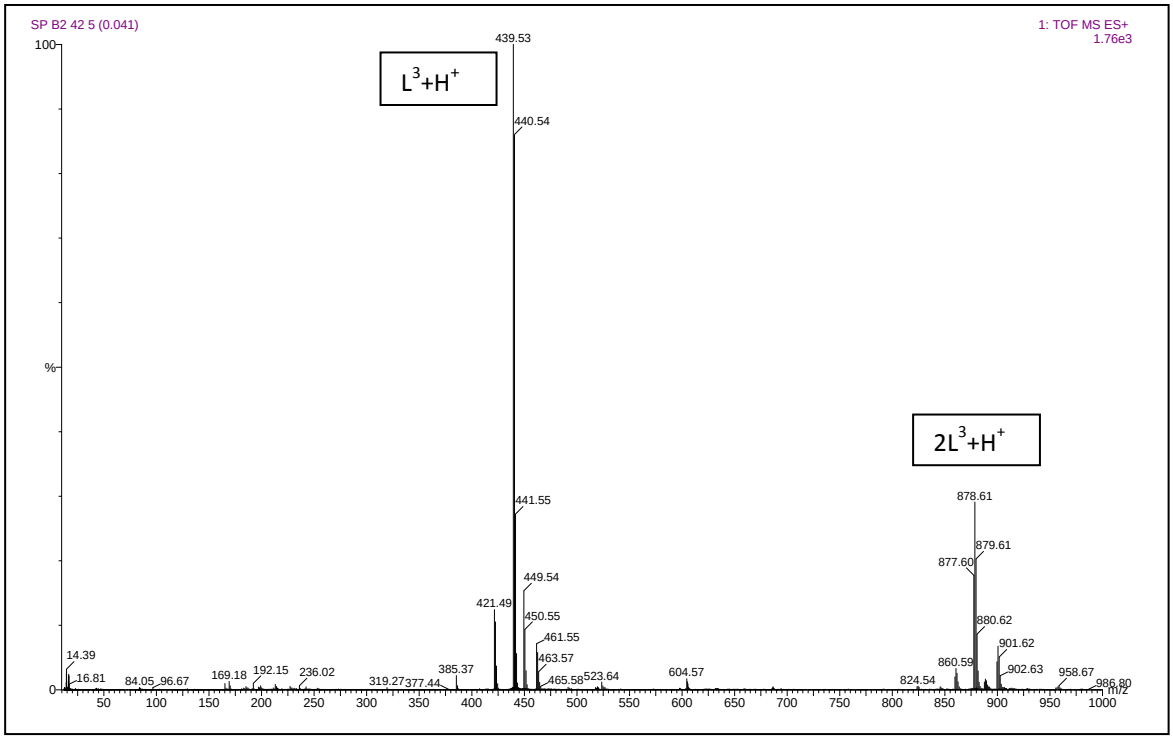

Figure 4.3 Mass spectra of L^3

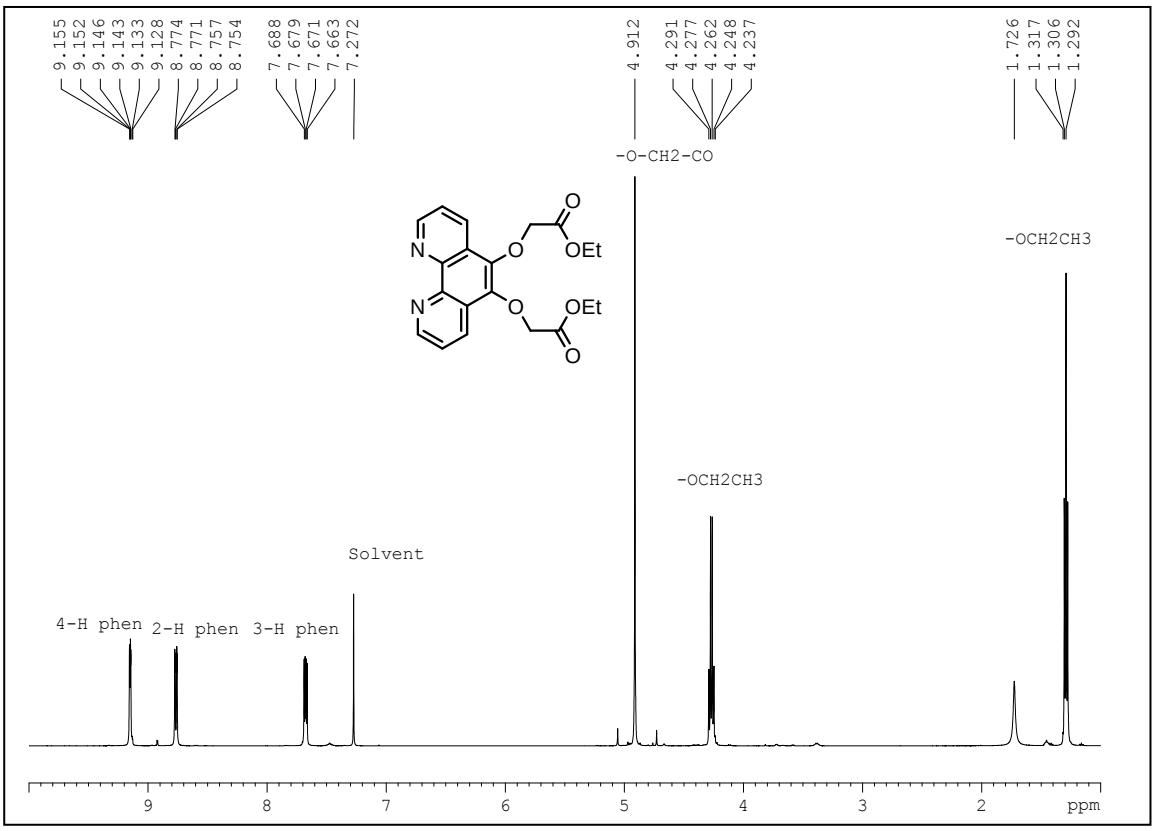

Figure 4.4 ^{1}H NMR spectra of L^1

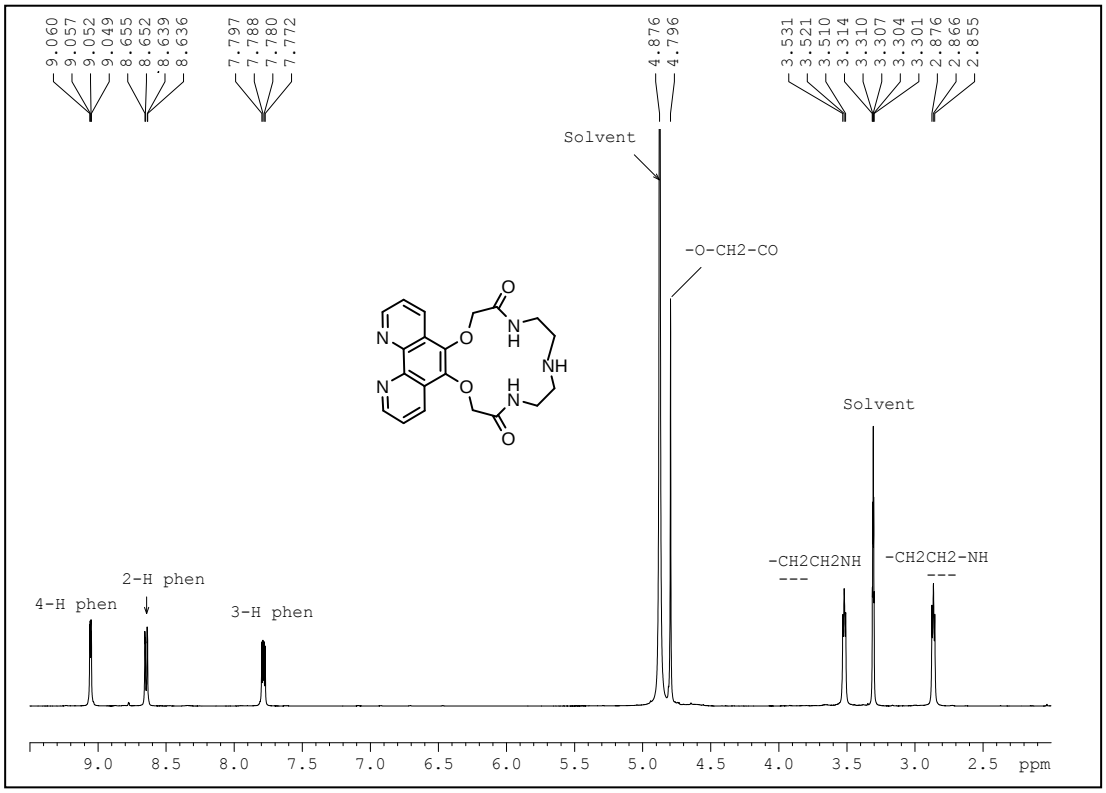

Figure 4.5 ^{1}H NMR spectra of L^{2}

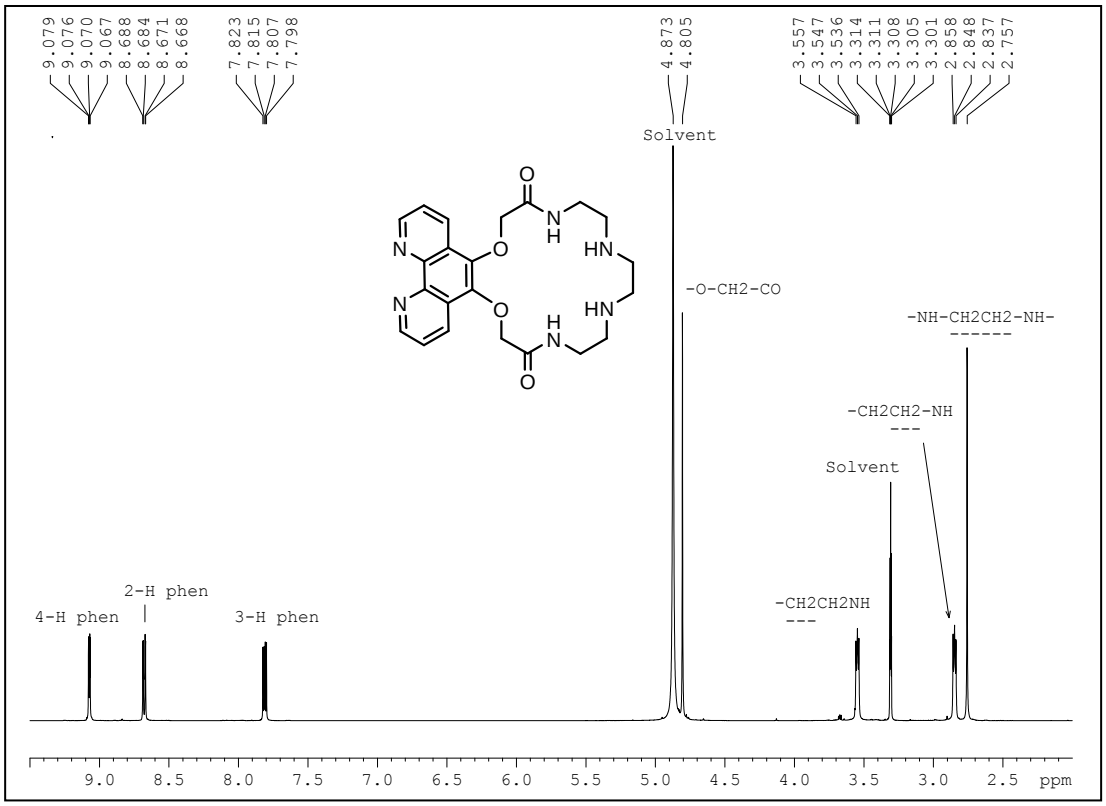

Figure 4.6 ^{1}H NMR spectra of L^{3}

4.3.2 Complexes (1-3)

The Ru(II) complexes were synthesized by the reaction of *cis*-$[Ru(bpy)_2Cl_2].2H_2O$ and $\mathbf{L^1/L^2/L^3}$ in refluxing ethanol-water, isolated with PF_6^- counter anion and purified by column chromatography. All of these complexes gave satisfactory C, H and N analysis. Mass spectrometry data are in excellent agreement with the calculated values. The ^{1}H NMR spectra of complexes **1-3** were recorded in CD_3CN and the data with assignment of peaks are given in the experimental section. Mass and ^{1}H NMR spectra for the complexes **1** – **3** are shown in Figures 4.7 – 4.12. For the complexes, the signals of the two bipyridine units attached to Ru(II) appeared in the aromatic region along with the signals due to phen moiety of the ligands ($\mathbf{L^1}$-$\mathbf{L^3}$). The protons of the macrocyclic units (**2** and **3**) and for ester groups (**1**) of the complexes appeared in the aliphatic region and the chemical shifts (δ) are close to that found in ligands (maximum shift 0.2 ppm). A broad signal for CO*NH* of **2** and **3** is observed at δ = 7.35 and 7.00, respectively in CD_3CN. When the spectra were recorded in DMSO-d_6 the same signals appeared at δ = 8.16 and 8.40, respectively. However, no signal for the NH of CH_2*NH*CH_2 moieties for both **1** and **2** were observed in CD_3CN and DMSO-d_6. One of the possibilities is that this signal is overlapped with signals from solvents. Evidence in support of this argument is noted for **2** when fluoride anion is added into the acetonitrile solution of the complex, a broad signal corresponds to 1H appeared at δ = 3.55, which is attributed to NH. The interaction of the NH proton with F^- resulted in low-field shift of this signal, which made it visible. Similar experiment with **3**, exhibits two broad signals at δ = 3.48 and 3.62, which are due to two NH protons of the macrocyclic unit. The IR spectra exhibit sharp bands for NH at 3660 and 3407 cm^{-1} for **2** and 3645, 3409 and 3239 cm^{-1} for **3**. On the basis of these data, the proposed structures of **1** – **3** are shown in Scheme 1.

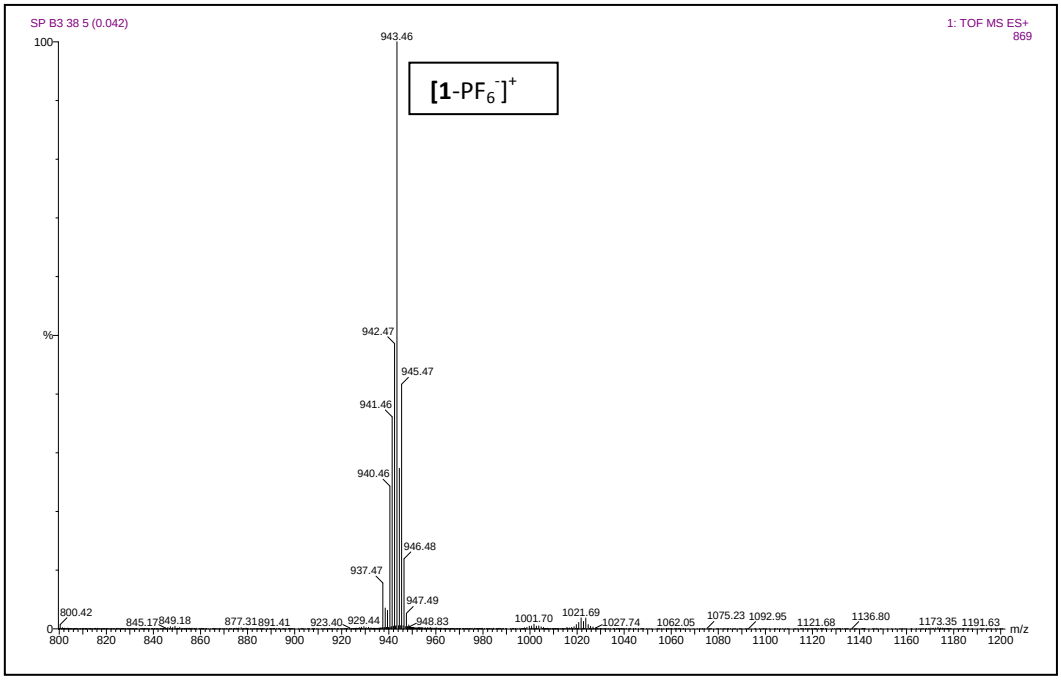

Figure 4.7. Mass spectra of **1**

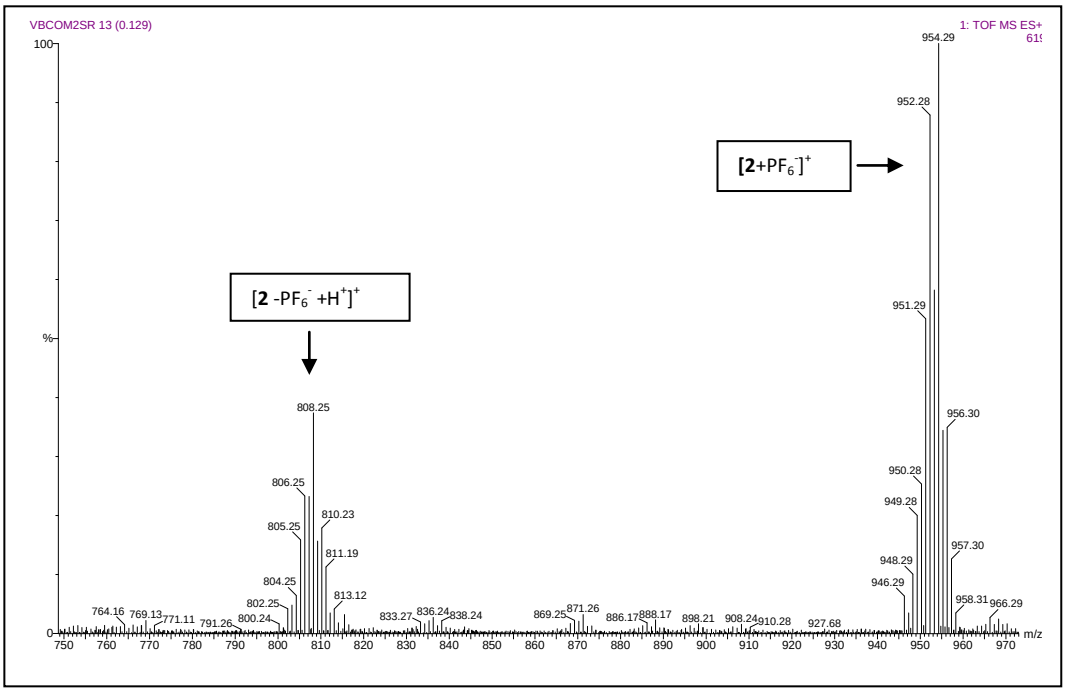

Figure 4.8. Mass spectra of **2**

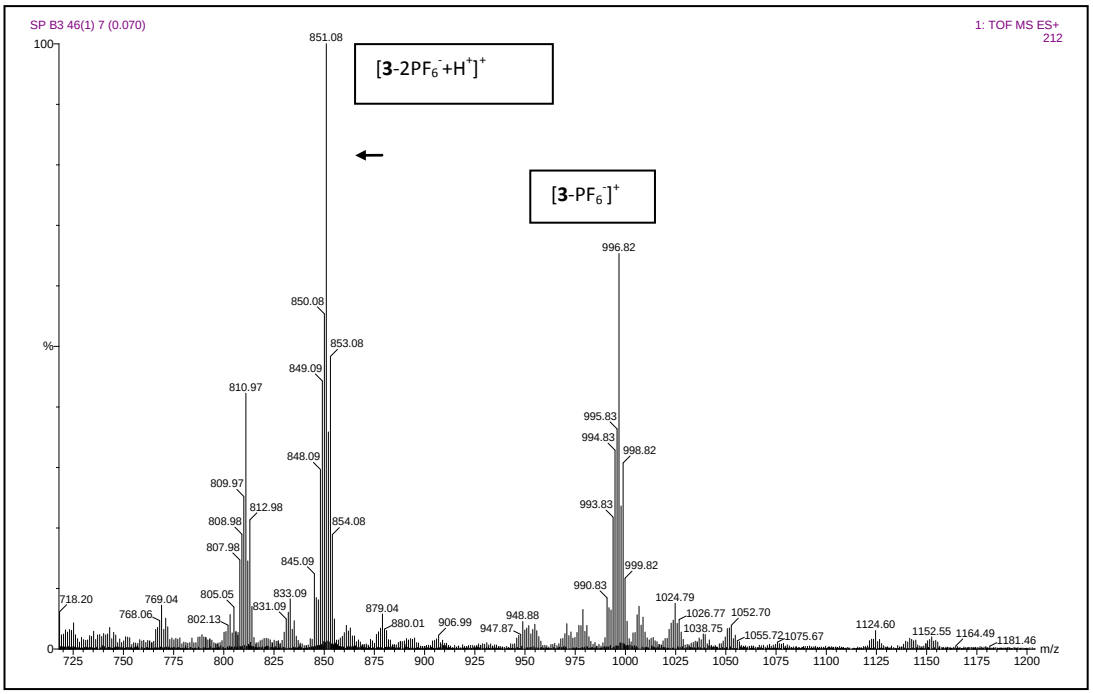

Figure 4.9. Mass spectra of **3**

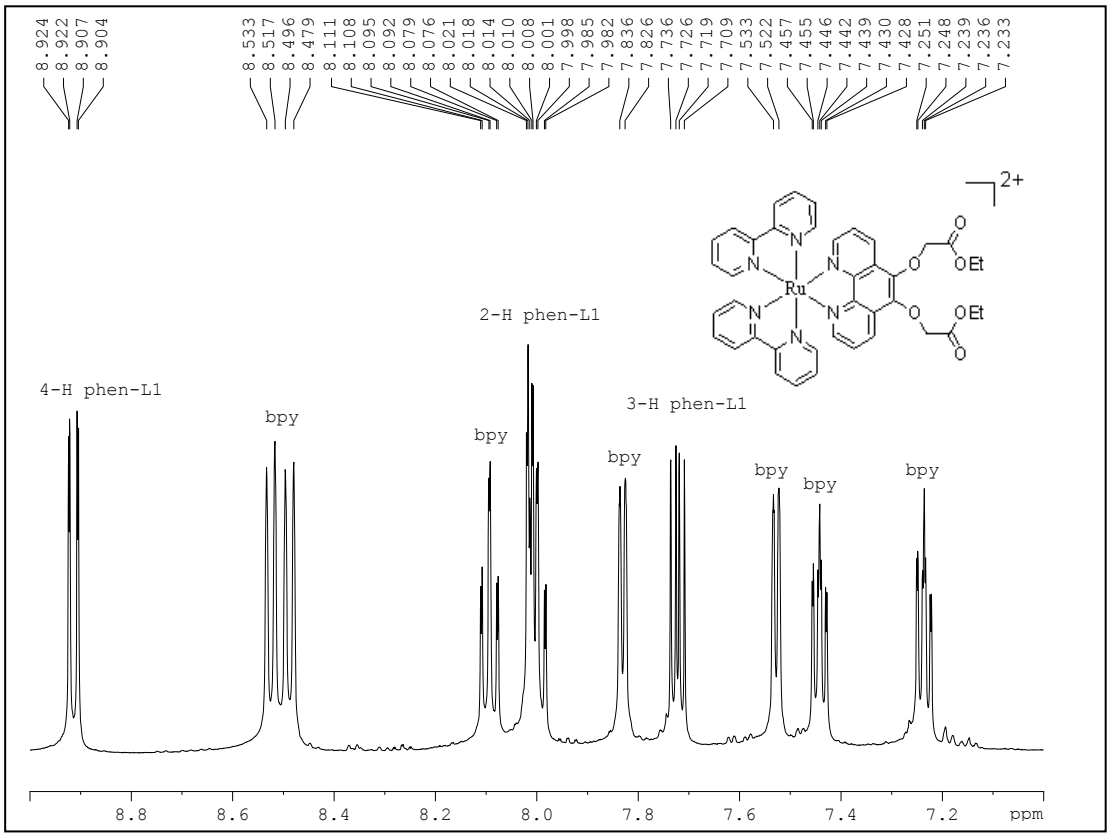

Figure 4.10a ^{1}H NMR spectra of Complex **1**(aromatic region)

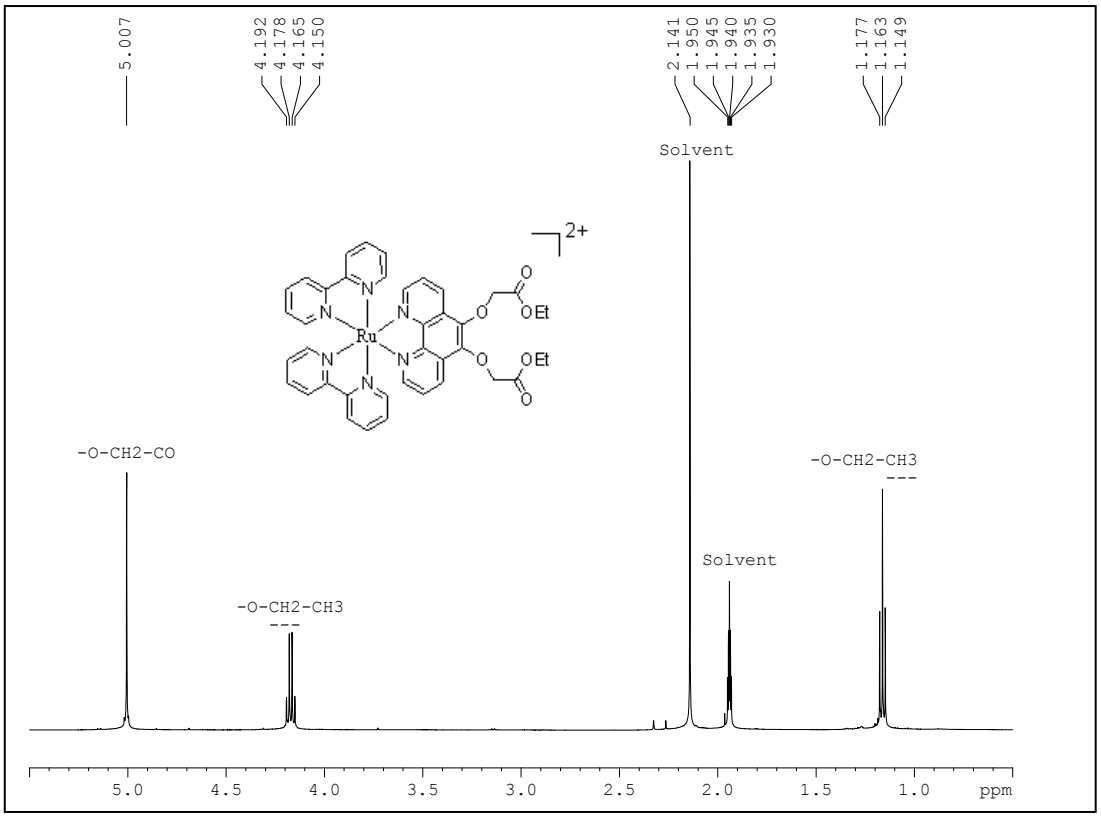

Figure 4.10b ^{1}H NMR spectra of Complex **1**(aliphatic region)

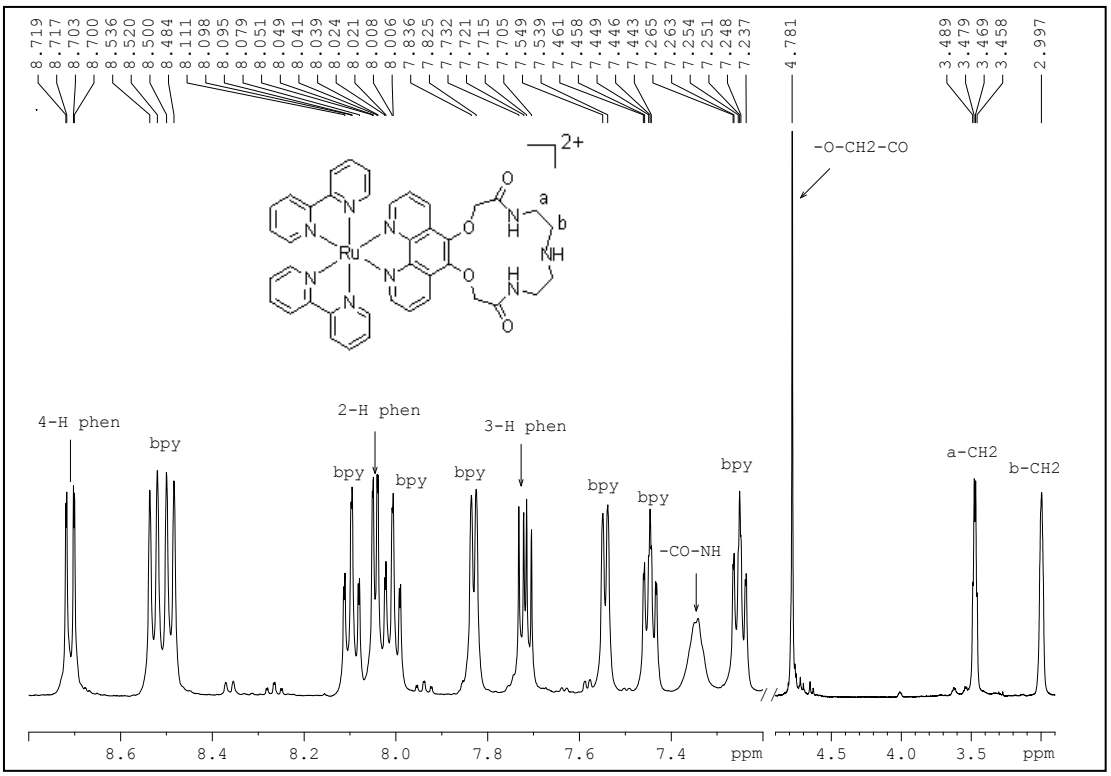

Figure 4.11 ^{1}H NMR spectra of Complex **2**

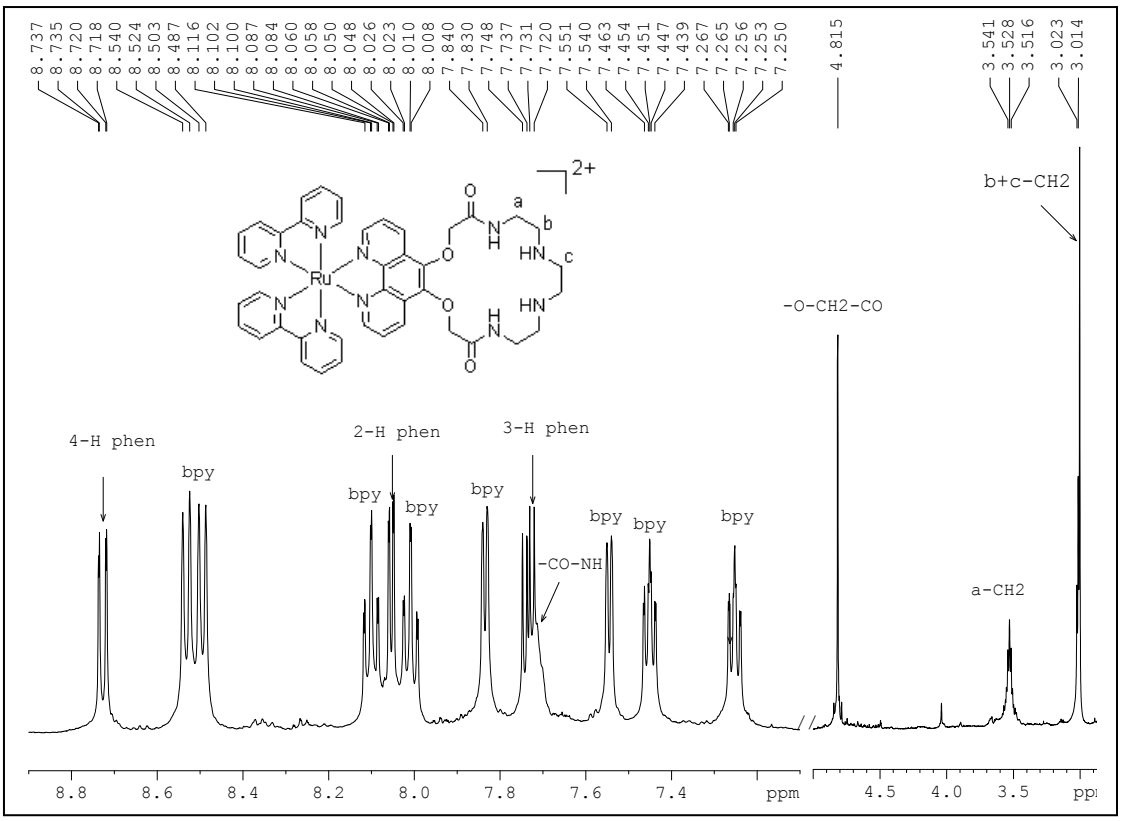

Figure 4.12 ^{1}H NMR spectra of Complex **3**

4.3.3 Description of structure (1)

ORTEP diagram depicting the cationic part of the complex **1** along with atom numbering scheme is depicted in Figure 4.13. The mixed ligand Ru(II) complex crystallizes in monoclinic space group $P2_1/n$ with PF_6^- counter anions. The metal center possesses a distorted octahedral geometry in which the square base is constituted by one nitrogen atom each from the two 2,2'-bipyridine ligands (N1 and N3) and two nitrogen atoms from the 1,10-phenanthroline moiety (N5 and N6). The apical coordination is provided by the bipyridine nitrogen atoms N2 and N4 and the Ru-N distances of Ru(1)-N(4) = 2.057(5)Å and Ru(1)-N(2) = 2.059(5)Å with *trans* angle N(4)-Ru(1)-N(2) = 173.7(2)° are well within the range of the reported values.[40,41] Selected bond lengths and angles involving the coordination sphere are given in Table 2.

An analysis of the packing diagram revealed that the cationic part of screw related Ru(II) complex is oriented in zigzag fashion along b-axis with inter- and

intramolecular C-H…O and C-H…N interactions. The PF_6^- anions are positioned in the clefts generated between the adjacent zigzag layers making intra- and intermolecular C-H…F interactions with the coordinated ligands. The packing diagram along with H-bonding interactions viewed down a-axis is shown in Figure 4.14 and details of all the hydrogen bonding parameters with symmetry codes are given in the Table 3.

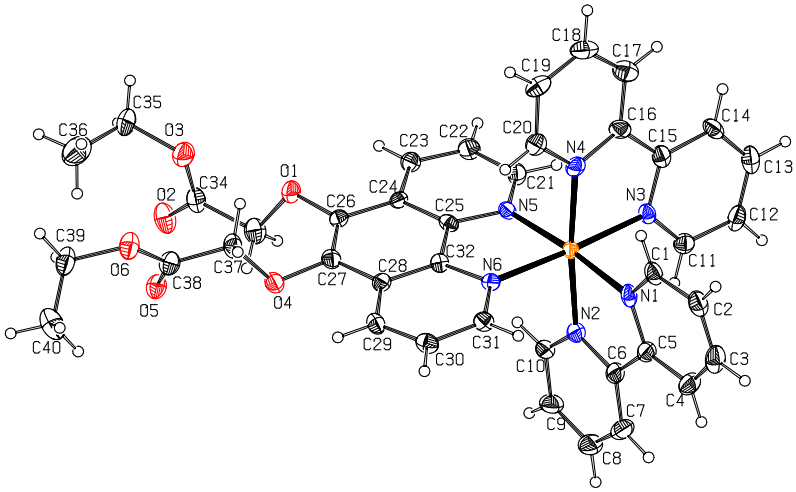

Figure 4.13 ORTEP diagram depicting the cationic part of the complex **1** along with atom numbering scheme.

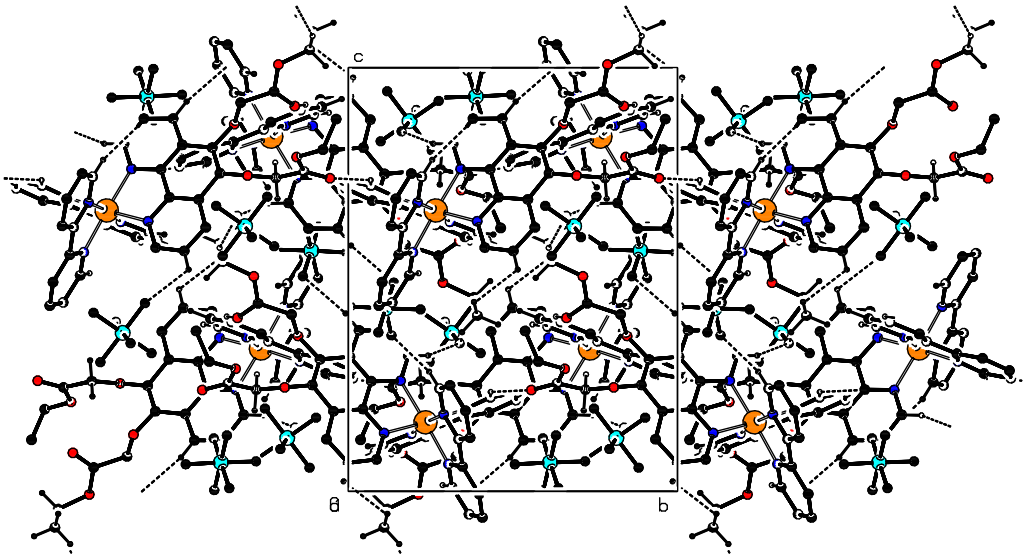

Figure 4.14 Packing diagram of **1** along with H-bonding interactions viewed down a-axis.

Table 2. Selected bond distances (Å) and angles (°) for complex 1

Ru(1)-N(1)	2.067(5)	Ru(1)-N(2)	2.059(5)
Ru(1)-N(3)	2.061(5)	Ru(1)-N(4)	2.057(5)
Ru(1)-N(5)	2.070(5)	Ru(1)-N(6)	2.078(5)
N(4)-Ru(1)-N(2)	173.7(2)	N(4)-Ru(1)-N(3)	78.4(2)
N(2)-Ru(1)-N(3)	95.9(2)	N(4)-Ru(1)-N(1)	98.0(2)
N(2)-Ru(1)-N(1)	78.8(2)	N(3)-Ru(1)-N(1)	86.77(19)
N(4)-Ru(1)-N(5)	85.56(19)	N(2)-Ru(1)-N(5)	98.0(2)
N(3)-Ru(1)-N(5)	97.41(19)	N(1)-Ru(1)-N(5)	174.99(19)
N(4)-Ru(1)-N(6)	100.0(2)	N(2)-Ru(1)-N(6)	85.76(19)
N(2)-Ru(1)-N(6)	85.76(19)	N(3)-Ru(1)-N(6)	176.67(19)
N(1)-Ru(1)-N(6)	96.38(19)	N(5)-Ru(1)-N(6)	79.49(19)

Table 3. Hydrogen bonding interaction in the metal complex

D-H···A	***d*(H···A) (Å)**	***d*(D···A) (Å)**	**< D-H-A (°)**
C(1)-H(1)...O(2)[1]	H(1)...O(2)= 2.42	C(1)...O(2) = 3.135(8)	C(1)-H(1)...O(2)= 134
C(8)-H(8)...O(5)[2]	H(8)...O(5)= 2.30	C(8)...O(5) =3.145(8)	C(8)-H(8)...O(5))= 150
C(9)-H(9)...F(4)[3]	H(9)...F(4)= 2.47	C(9)...F(4)= 3.155(9)	C(9)-H(9)...F(4)= 130
C(10)-H(10)...F(5)[3]	H(10)...F(5) = 2.52	C(10)...F(5)= 3.155(8)	C(10)-H(10)...F(5)= 126
C(11)-H(11)...N(2)[3]	H(11)...N(2)= 2.62	C(11)...N(2)= 3.182(9)	C(11)-H(11)...N(2)= 119
C(20)-H(20)...F(12)[2]	H(20)...F(12) =2.29	C(20)...F(12) = 3.057(12)	C(20)-H(20)...F(12)= 139
C(22)-H(22)...F(4)[4]	H(22)...F(4)= 2.55	C(22)...F(4)= 3.134(8)	C(22)-H(22)...F(4)= 122
C(29)-H(29)...F(11)[5]	H(29)...F(11)= 2.46	C(29)...F(11) = 3.380(10)	C(29)-H(29)...F(11)= 168
C(31)-H(31)...F(3)[2]	H(31)...F(3)= 2.35	C(31)...F(3)= 3.185(7)	C(31)-H(31)...F(3)= 150
C(33)-H(33A)...O(4)[3]	H(33A)...O(4)= 2.40	C(33)...O(4)= 3.027(9)	C(33)-H(33A)..O(4)= 122
C(33)-(H33A)...O(5)[3]	(H33A)...O(5)= 2.55	C(33)...O(5)= 3.208(9)	C(33)-(H33A)...O(5)= 125
C(33)-H(33B)...F(6)[3]	H(33B)...F(6) = 2.53	C(33)....F(6) = 3.366(8)	C(33)-H(33B)...F(6) = 144
C(39)-H(39B)...F(3)[5]	H(39B)...F(3)= 2.50	C(39)...F(3)= 3.404(9)	C(39)-H(39B)...F(3)= 155
1. x,-1+y, z 2.3/2-x,-1/2+y,3/2-z 3. x, y, z 4. 2-x,1-y,1-z 5.1/2+x,3/2-y,1/2+z			

4.3.4 Absorption and luminescence

Absorption spectra of **1-3** were recorded in acetonitrile and the data are given in the Experimental Section. The low energy band observed in the region 450-452 nm is assigned to metal-to-ligand (bpy) charge-transfer (MLCT) transitions ($d\pi \rightarrow \pi^*$).[26,30] The high-energy band around 286 nm is ligand-centered charge transfer (CT) due to $\pi \rightarrow \pi^*$ transitions. The luminescence spectra were also recorded in acetonitrile with excitation at the absorption maxima (λ_{max}) of the MLCT bands, which are 451, 450 and 452, nm for **1**-**3**, respectively and the band observed at 604 (**1** and **2**) and 603 nm (**3)** is attributed to ^{3}MLCT emission.[6,30,42] Absorption and luminescence spectra of **3** are shown in Figures 4.15 and 4.16, respectively. Luminescence quantum yields (ϕ) were also measured in acetonitrile and the data for emission maxima (λ_{max}) and quantum yield are given in Table 4. The luminescence quantum yields for **1**-**3** are 0.0625, 0.0612 and 0.0593, respectively, which are close to the value for $[Ru(bpy)_3]^{2+}$ (ϕ = 0.062) in acetonitrile.

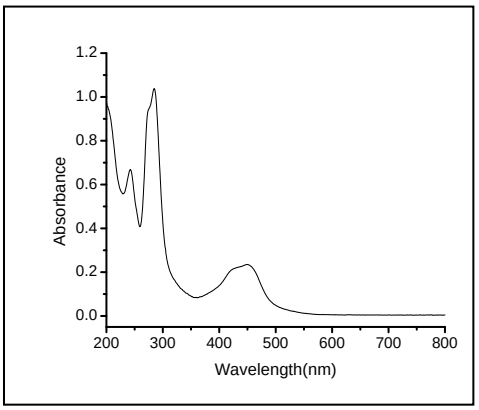

Figure 4.15 Absorption spectra of **3**

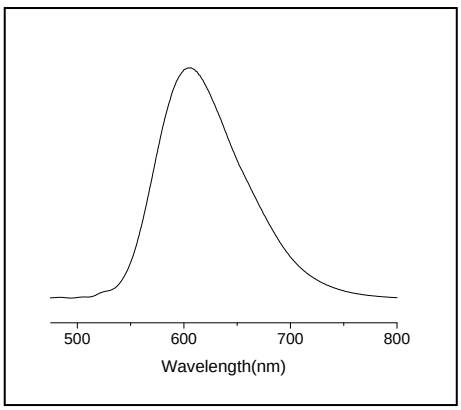

Figure 4.16 Luminescence spectra of **3**

Table 4. Emission maxima, quantum yield and binding constant (K_s) for **2** and **3**.

Complex	λ_{em}	Quantum yield (ϕ)	In presence of guest ions		
			Ion	λ_{em} [a]	Binding constant (K_s) M^{-1}
2	604	0.0612	F^-	610	$1.40x10^3$
			$H_2PO_4^-$	615	$3.39x10^4$
3	603	0.0593	F^-	605	$2.85x10^2$
			$H_2PO_4^-$	612	$4.48x10^4$
			Cu^{2+}	606	$2.01x10^3$

[a] Emission maxima (λ_{em}) of the spectra recorded in presence of maximum concentration of metal ion for luminescence titration.

4.3.5 Electrochemistry

Cyclic voltammograms (CV) of all complexes were recorded in acetonitrile, the voltammograms of **1-3** are displayed in Figures 4.17 – 4.19 and the data are summarized in Table 5. All of these complexes exhibit a metal-based oxidation in the potential range 1.46 to 1.48 V, which are attributed to Ru(II) $\rightarrow$ Ru(III) oxidation.[30,42,43] The oxidation potential of the metal ion in **1-3** is slightly higher compared to that generally observed in $[Ru(bpy)_3]^{2+}$. All of these complexes also exhibit three ligand-based redox couples in the potential range -1.15 to -1.70 V (Table 5), which are assigned to sequential one-electron reduction of the two bipyridine and a phenanthroline ligands coordinated to the metal ion.[30,42,43]

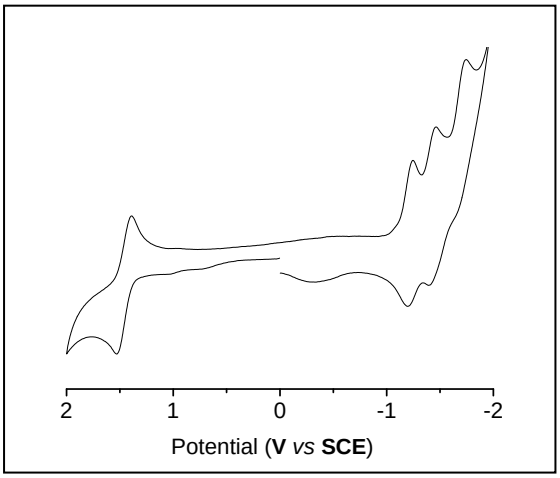

Figure 4.17. Cyclic voltammogram of **1** recorded in acetonitrile.

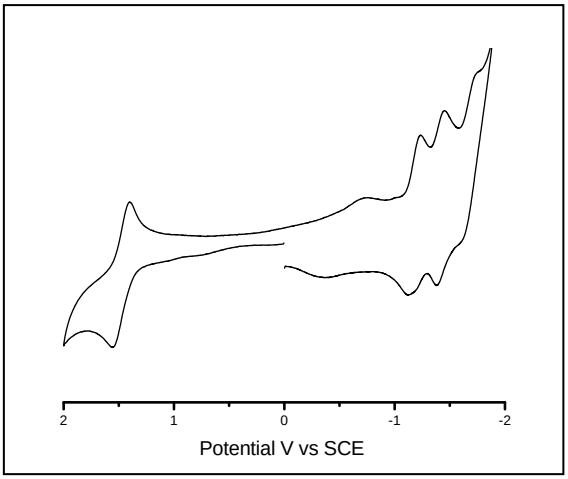

Figure 4.18. Cyclic voltammogram of **2** recorded in acetonitrile.

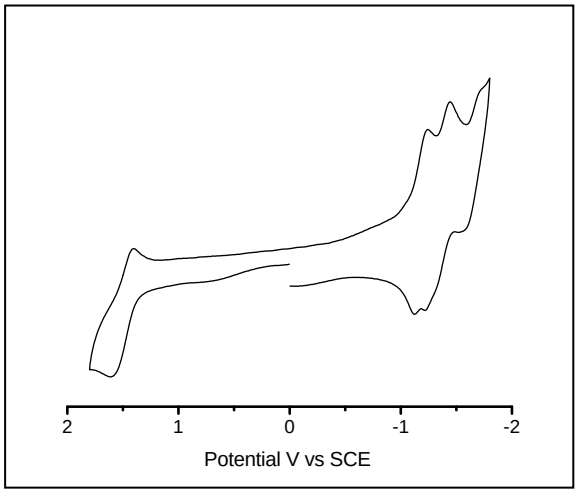

Figure 4.19. Cyclic voltammogram of **3** recorded in acetonitrile.

Table 5. Electrochemical data of complexes **1-3** in acetonitrile.

Complex	$E_{1/2}^{ox}$/V (ΔE_p, mV)	$E_{1/2}^{red1}$/V (ΔE_p, mV)	$E_{1/2}^{red2}$/V (ΔE_p, mV)	$E_{1/2}^{red3}$/V (ΔE_p, mV)
1	1.46 (129)	-1.22 (44)	-1.43 (66)	-1.70 (88)
2	1.48 (158)	-1.18 (110)	-1.42 (65)	-1.68 (99)
3	1.48 (136)	-1.15 (109)	-1.36 (119)	-1.67 (123)

4.3.6 Ion-binding property

Ion-binding property of **1-3** have been investigated with a series of anions (F^-, Cl^-, Br^-, I^-, $H_2PO_4^-$, ClO_4^- , NO_3^-, BF_4^-, CH_3COO^-, and HSO_4^-) and cations (Na^+, K^+,

Mg^{2+}, Ca^{2+}, Zn^{2+}, Ba^{2+}, Sr^{2+}, Cd^{2+}, Hg^{2+}, Pb^{2+} and Cu^{2+}), and the host-guest interactions monitored by luminescence and ^1H NMR spectral changes.

4.3.6.1 Luminescence study

The luminescence spectra of **1-3** were recorded in acetonitrile at room temperature. The same spectra were recorded again in presence of various anions and cations (100 fold excess). For complex **1**, upon addition of both cations and anions no significant change in emission spectra was observed (Figures 4.20 and 4.21). For **2**, no change for cations was observed but substantial quenching of emission intensity (76%) was noted upon addition of F^- ion (Figures 4.22 and 4.23). Interestingly, the same compound exhibited significant enhancement in emission intensity (50%) when the spectra was recorded in presence of $H_2PO_4^-$ anion, other anions did not show any significant change in the emission spectra (Figure 4.23). In the case of **3**, 93% quenching in emission intensity was noted for Cu^{2+}, whereas other metal ions did not show any significant change (Figure 4.24). For anions, only $H_2PO_4^-$ and F^- exhibited 66% and 32% quenching, respectively (Figure 4.25). These observations suggest that **2** and **3** form strong complexes with $H_2PO_4^-$ and F^- and only **3** forms complex with Cu^{2+}.

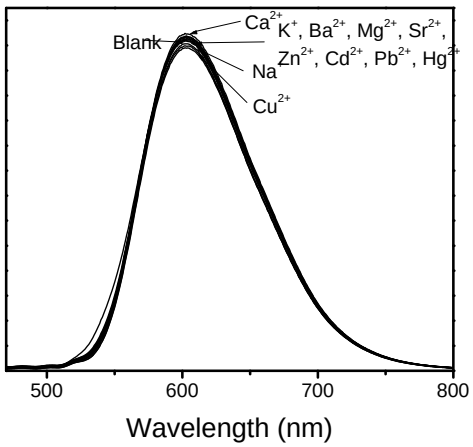

Figure 4.20 Luminescence spectra of **1** in acetonitrile in presence of various cations (100 equiv).

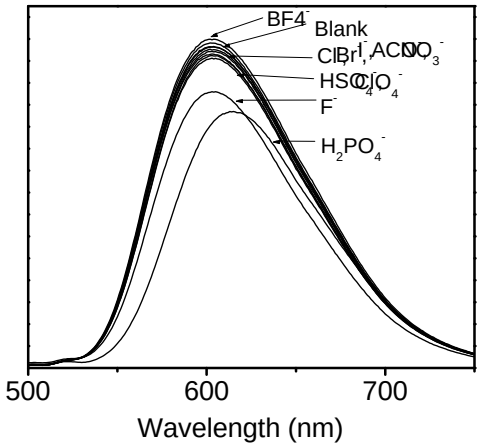

Figure 4.21 Luminescence spectra of **1** in acetonitrile in presence of various anions (100 equiv).

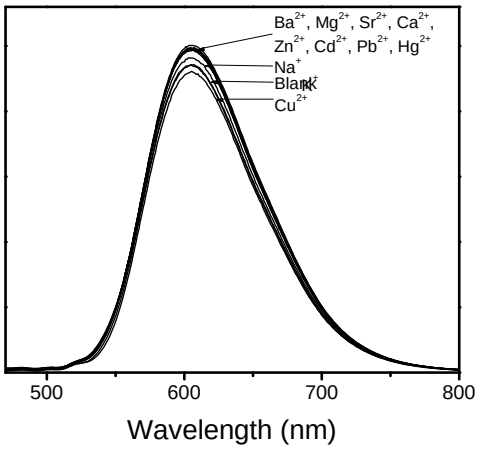

Figure 4.22 Luminescence spectra of **2** in acetonitrile in presence of various cations (100 equiv).

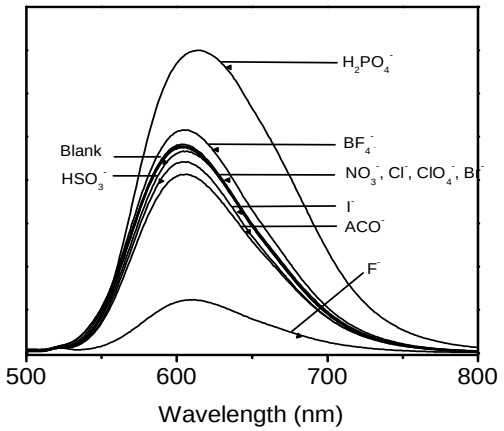

Figure 4.23 Luminescence spectra of **2** in acetonitrile in presence of various anions (100 equiv).

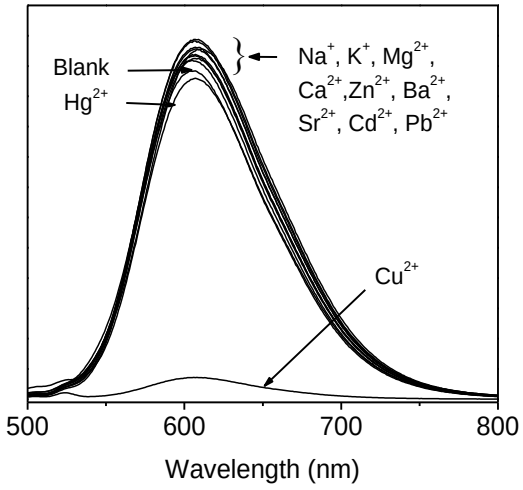

Figure 4.24 Luminescence spectra of **3** in acetonitrile in presence of various cations (100 equiv).

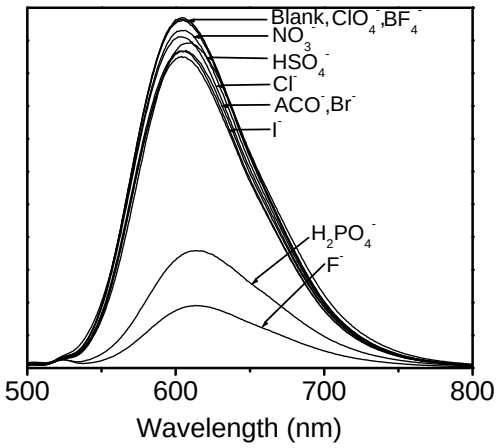

Figure 4.25 Luminescence spectra of **3** in acetonitrile in presence of various anions (100 equiv).

4.3.6.2 NMR study

The ^{1}H NMR spectra of **2** and **3** were recorded with the addition of increasing concentration of F^- and $H_2PO_4^-$ anions. In case of phosphate, precipitate was formed in the NMR tube for both the complexes even before addition of one equivalent of anion in acetonitrile. Therefore with $H_2PO_4^-$ anion, NMR study was carried out in DMSO-d_6, in which no precipitate was observed up to 1.5 fold excess addition of anion. For F^-, NMR study was conducted in CD_3CN. The ^{1}H NMR spectral change upon addition of F^- and $H_2PO_4^-$ for **2** and **3** are shown in Figures 4.26 – 4.29. In the Figure 4.26, it may be noted that the signal for the proton of CO*NH* has shifted substantially (3.3 ppm) towards low-field region. In the aliphatic region, the CH_2*NH* proton, which was not observed as a distinct peak in the spectrum of **2,** was visible upon addition of F^- and it slightly moved towards down-field region (δ = 3.49 to δ 3.57) with increasing the concentration of the anion. The signals for *CH*$_2$ protons, adjacent to the NH groups (*a*-CH_2 and *b*-CH_2, scheme 1 for nomenclature), were shielded slightly ($\Delta\delta$ = 0.24 ppm for *a*-CH_2 and 0.15 ppm for *b*-CH_2). For **3,** similar observation with F^- anion is noted, however the extent of low-field shift of the CO*NH*

signal is slightly less (2.10 ppm) compared to that found for **2.** The upfield shift of the *CH₂* protons, however close to that found for **2**, Δδ = 0.18, 0.30 and 0.34 ppm for *a*-CH_2, *b*-CH_2 and *c*-CH_2, respectively. These observations suggest that the F^- anion is encapsulated in the macrocyclic cavity making strong N-H…F interactions with the CO*NH* protons (Figure 4.30). The strong interaction with F^- leads to the amide N-H protons more acidic causing substantial lowfield shift of this signal. On the other hand, the presence of negatively charged ion in the macrocyclic cavity probably causes slight shielding of all *CH₂* protons at the vicinity of the anion. In the case of $H_2PO_4^-$ anion in DMSO-*d₆*, the CO*NH* protons of compounds **2** and **3** were deshielded by 0.40 and 0.77 ppm, respectively and the *CH₂* protons, adjacent to NH groups, shielded by 0.13 to 0.15 ppm for both the compounds. This data is similar to that found for F^- and it suggests complexation of both **2** and **3** with $H_2PO_4^-$.

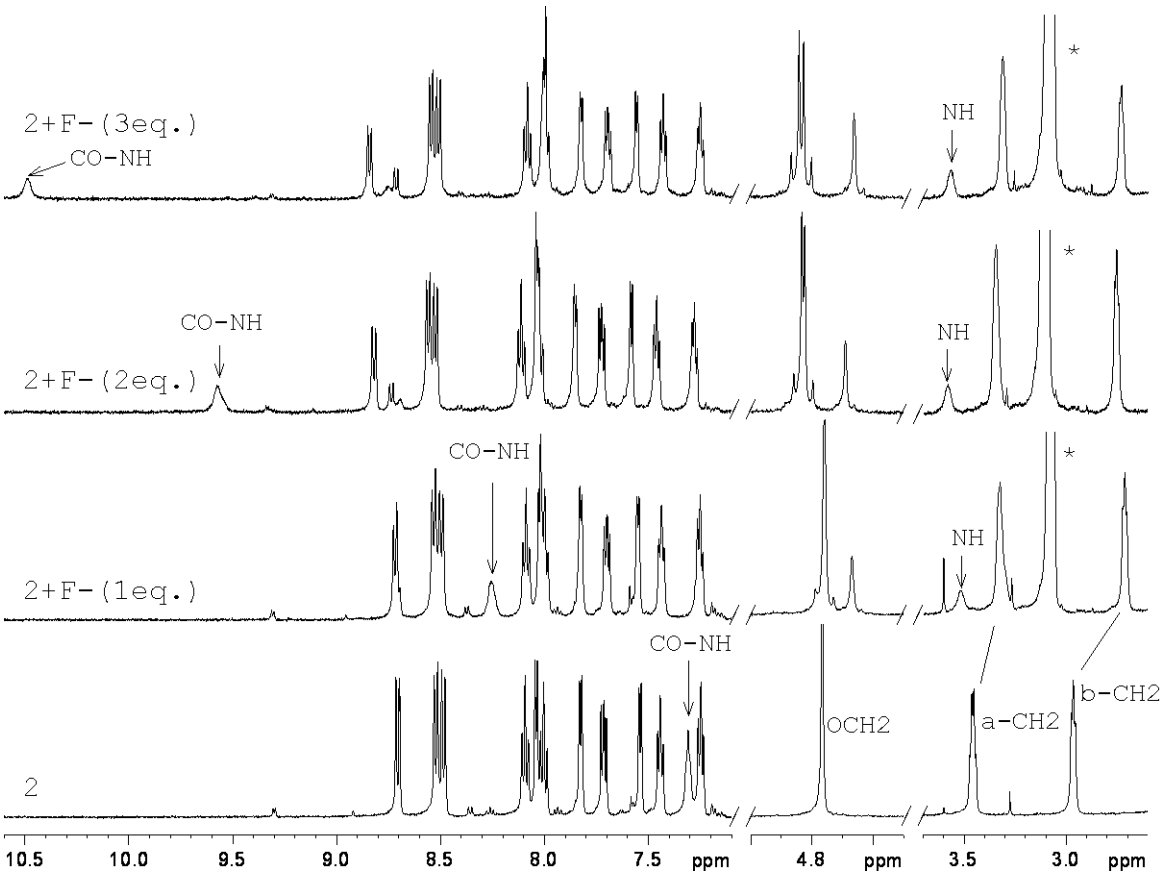

Figure 4.26 Selected portion of the ^1H NMR spectra of **2** recorded in CD_3CN with the addition of increasing concentration of F^-. The signal with * mark is due to the CH_2 protons of the tetrabutyl ammonium cation.

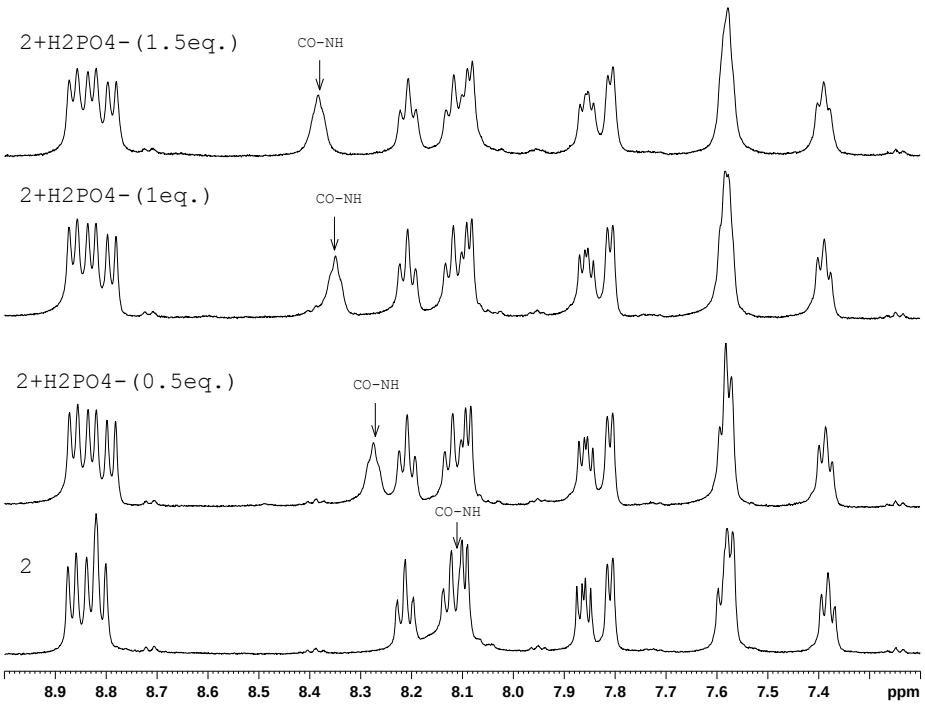

Figure 4.27 Selected portion of the ^{1}H NMR spectra of **2** recorded in DMSO-d_6 with the addition of increasing concentration of $H_2PO_4^-$.

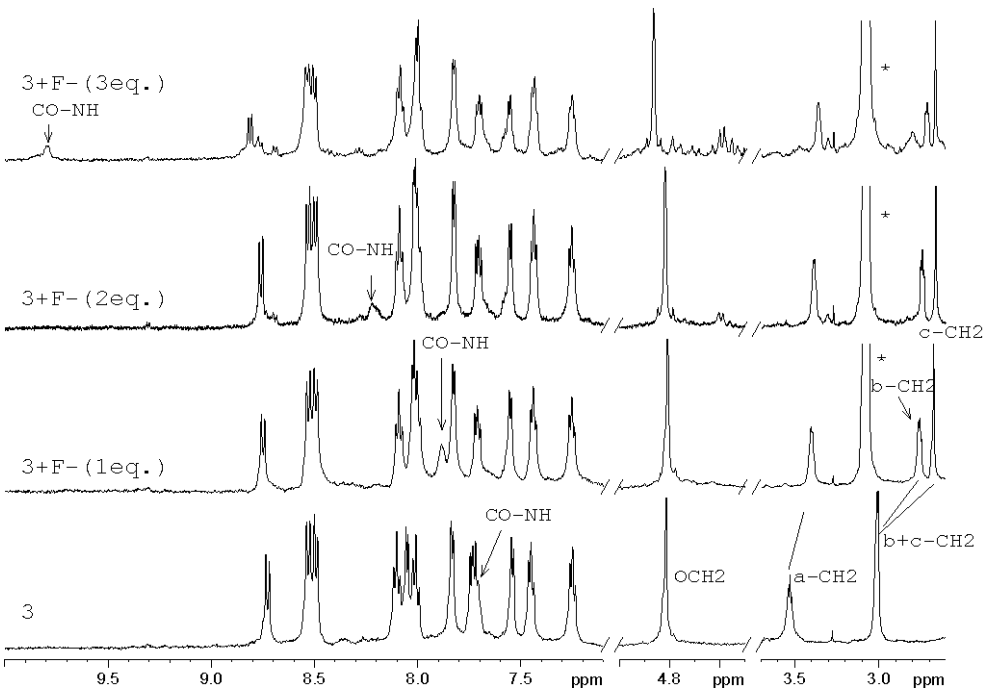

Figure 4.28 Selected portion of the ^{1}H NMR spectra of **3** recorded in CD_3CN with the addition of increasing concentration of F^-. The signal with * mark is due to the CH_2 protons of the tetrabutyl ammonium cation.

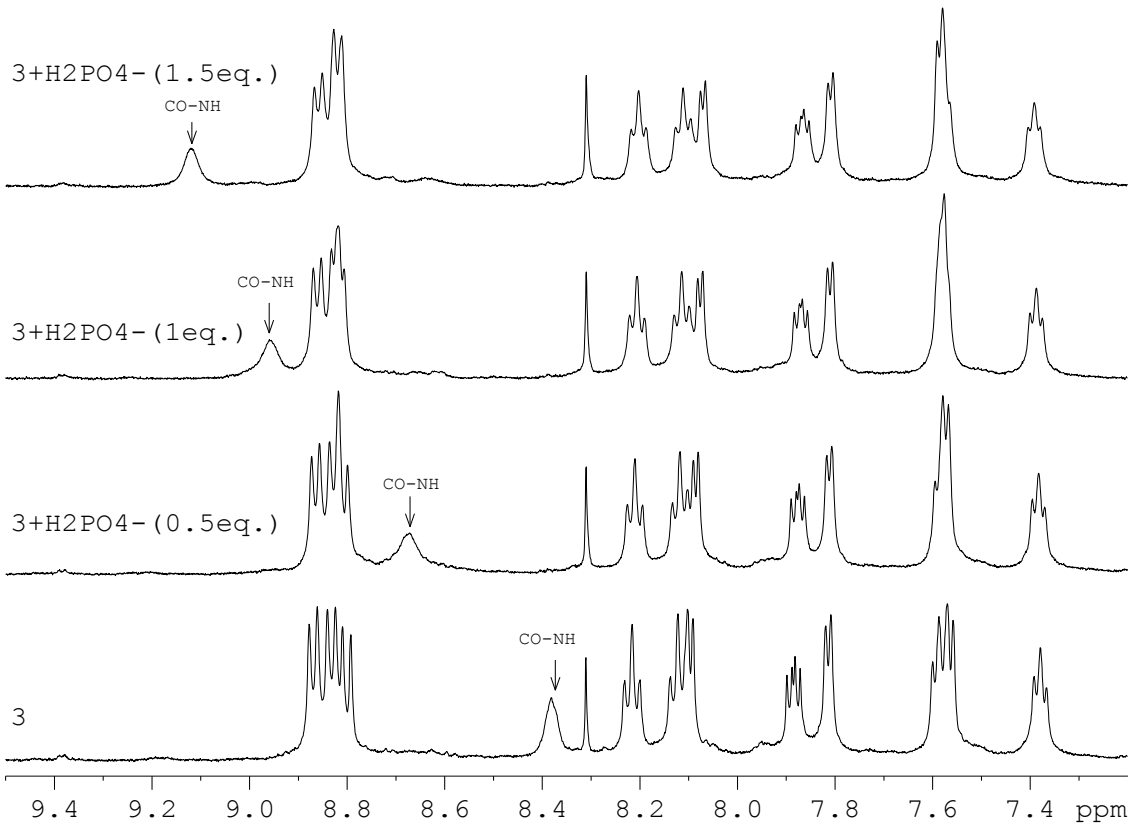

Figure 4.29 Selected portion of the ^{1}H NMR spectra of **3** recorded in DMSO-d_6 with the addition of increasing concentration of $H_2PO_4^-$.

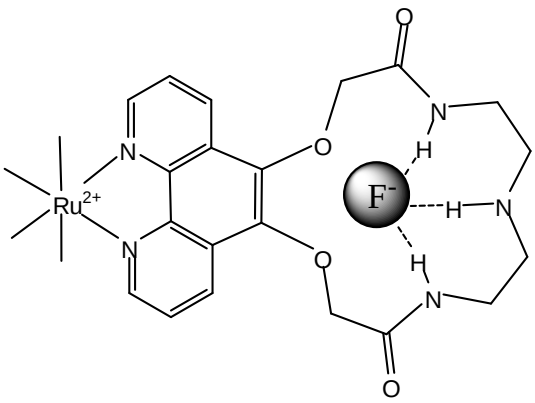

Figure 4.30 Structure of the F^- bound macrocyclic unit of **2** showing the N-H…F interaction.

The complexes **2** and **3** contain amine groups, therefore addition of a proton source into the system may results protonation of the amine groups, which certainly affects the ion binding affinity of the ionophore. For F^- in acetonitrile media, the question of protonation does not arise as there is no source of protons. However, for diprotic anion $H_2PO_4^-$, there is a possibility of protonation of the amine groups of the macrocyclic unit. We examined this possibility by ^1H NMR study. It is known that the proton chemical shifts most affected upon protonation of an amino group are those of the proton nuclei attached to the carbon atoms placed in α-position with respect to it.[44] It is also known that upon protonation of the amine group the signals for CH_2 protons, α-position to amine, shift downfield.[44] For both the complexes, upon addition of $H_2PO_4^-$ all the CH_2 protons, adjacent to amine, exhibited upfield shift by about 0.15 ppm, which is similar to that observed for F^- (upfield shifts by 0.15 to 0.34 ppm) and it has no proton source. This observation clearly suggests that the amine groups are not protonated upon addition of $H_2PO_4^-$. However, to confirm it further, the ^1H NMR spectra of **2** and **3** are recorded under similar experimental conditions with addition of increasing amount of HNO_3 as proton source. As a result of this addition, the CH_2 protons exhibited downfield shift by 0.19 to 0.58 ppm, indicating protonation of the amine groups in presence of strong acid. The relevant portions of the ^1H NMR spectra showing the changes in chemical shifts of the CH_2 protons for both the complexes upon addition of increasing amount of $H_2PO_4^-$ and HNO_3 are shown in Figures 4.31 and 4.32. It may be noted that upon addition of acid, the CH_2 signals shifted downfield upto the addition of a certain amount of HNO_3 and after that their positions remain same upto the maximum amount of acid added (~10 fold excess). The observation, therefore confirmed that amine groups are not protonated upon addition of $H_2PO_4^-$ under the experimental conditions used. Complexes of $H_2PO_4^-$ adducts of both **2** and **3** were isolated in solid state for further characterization.

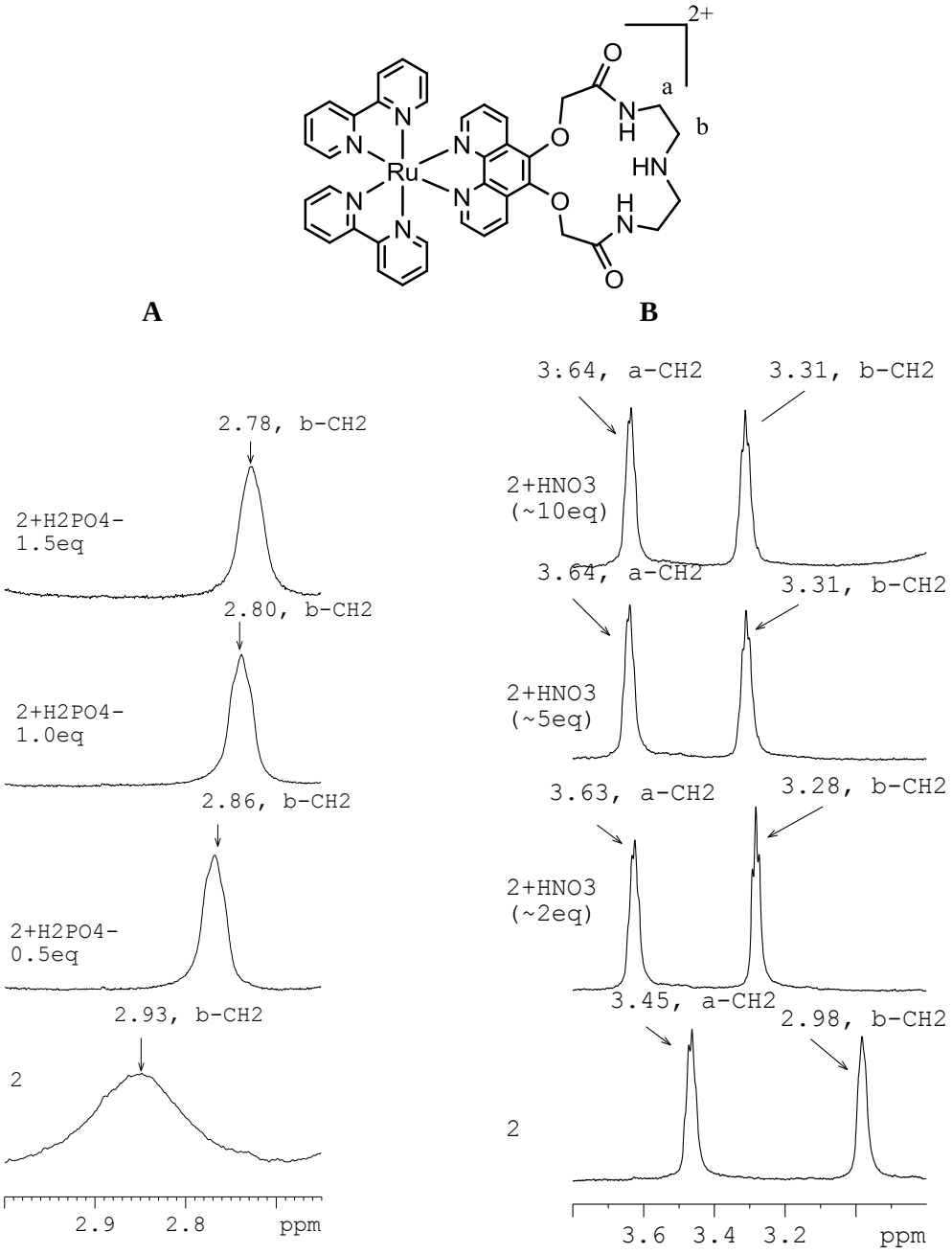

Figure 4.31 Relevant portion of the ^{1}H NMR spectra of **2** recorded with the addition of increasing amount of $H_2PO_4^-$ in DMSO-d_6 (A) and HNO_3 in CD_3CN (B). For $H_2PO_4^-$ the chemical shifts of the CH_2 protons move upfield whereas for HNO_3 they move downfield.

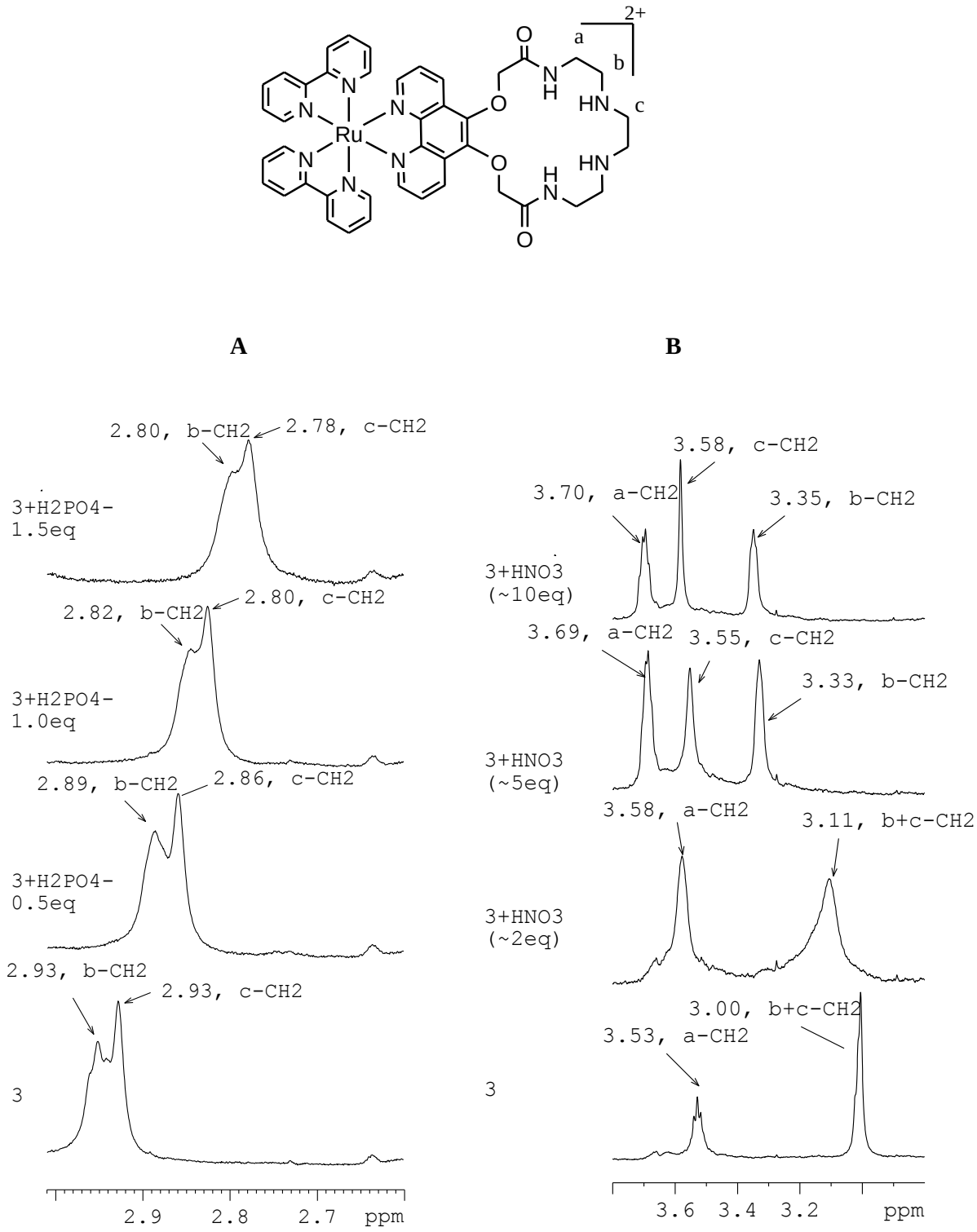

Figure 4.32 Relevant portion of the ^{1}H NMR spectra of **3** recorded with the addition of increasing amount of $H_2PO_4^-$ in DMSO-d_6 (A) and HNO_3 in CD_3CN (B). For $H_2PO_4^-$ the chemical shifts of the CH_2 protons move upfield whereas for HNO_3 they move downfield.

4.3.7 Isolated dihydrogenphosphate complexes

The $H_2PO_4^-$ complexes of **1** and **2** were prepared and ^1H NMR, ^{31}P NMR, mass and IR spectra of these complexes were recorded. The ^1H NMR spectra in DMSO-d_6 resembles with the final spectra recorded upon addition of $H_2PO_4^-$, indicating that the isolated compounds are similar to that observed in solution after addition of maximum amount of anion. The ^{31}P NMR spectra of the tetrabutyl ammonium phosphate ($H_2PO_4^-$) and its complexes, [**2**+ $H_2PO_4^-$] and [**3**+ $H_2PO_4^-$], are shown in Figure 4.33. It may be noted that the ^{31}P signals for [**2**+ $H_2PO_4^-$] and [**3**+ $H_2PO_4^-$] are broaden and deshielded compared to that of free $H_2PO_4^-$, indicating interaction of the anion with the ionophores. The data also suggest that there is only one type of ionophore bound $H_2PO_4^-$ anion and no free $H_2PO_4^-$ presents in the isolated complexes. The relevant portion of the mass spectra of [**2**+ $H_2PO_4^-$] is shown in Figure 4.34, in which the peaks (*e/m*) at 954.12 and 906.19 are in excellent agreement with the calculated values of 954.16 and 906.17 for [**2**-PF_6^-]$^+$ and [**2**–2PF_6^- + $H_2PO_4^-$]$^+$, respectively. Compound [**3**+ $H_2PO_4^-$] also exhibits two peaks at 996.35 and 948.44, which corresponds to [**3**- PF_6^-]$^+$ and [**3**–2PF_6^- + $H_2PO_4^-$]$^+$, respectively. The mass data, therefore suggest 1:1 complex formation between the ionophore and $H_2PO_4^-$ anion. The IR spectra of the isolated $H_2PO_4^-$ and F^- adducts of **2** and **3** were recorded and the 4000 - 3000 cm^{-1} region of the spectra for **2** is shown in the Figure 4.35. The sharp bands for N-H at 3639 and 3408 cm^{-1} for **2** are not observed in the $H_2PO_4^-$ and F^- bound complexes, instead a broad band centering around 3425 cm^{-1} is observed. The strong interaction of the hydrogen atoms of N-H with F^- and $H_2PO_4^-$ (through oxygen atoms) makes N-H bond weaker, which resulted in shifting of this band to lower frequency, which is also consistent to the NMR observation. On the basis of all these data the proposed structures of the macrocyclic units of **2** and **3,** showing N-H….F and N-H…O interactions, are illustrated in Figures 4.30 and 4.36, respectively.

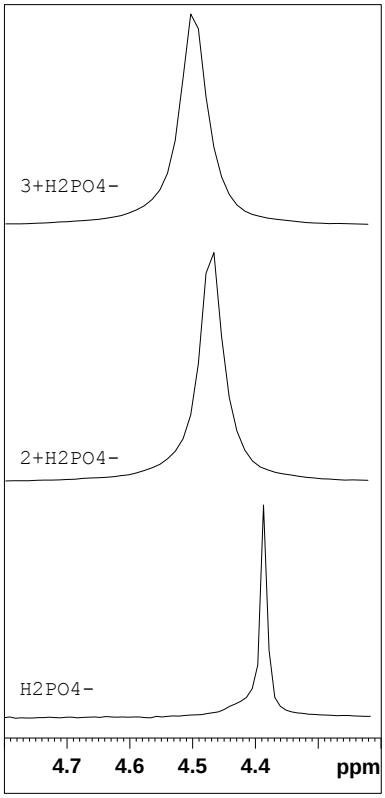

Figure 4.33 ^{31}P NMR spectra of $H_2PO_4^-$ and its complexes with **2** and **3** recorded in acetonitrile.

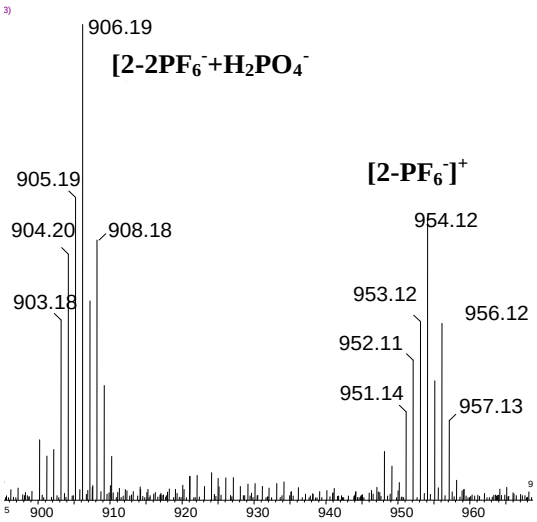

Figure 4.34 Relevant portion of the mass spectra of the isolated $H_2PO_4^-$ complex of **2**.

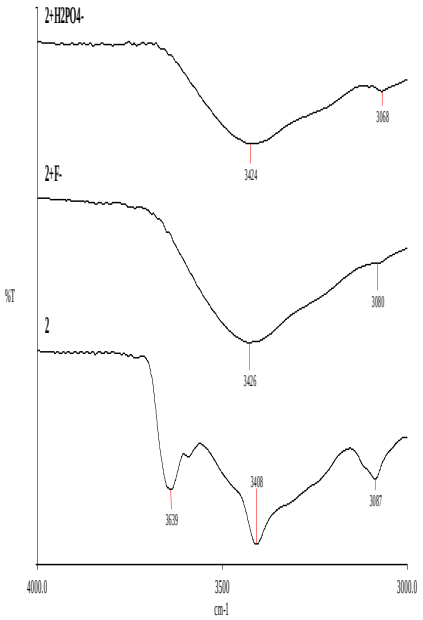

Figure 4.35 Selected portion of the IR spectra (4000 - 3000 cm^{-1} region) of **2** and its isolated complexes of $H_2PO_4^-$ and F^-

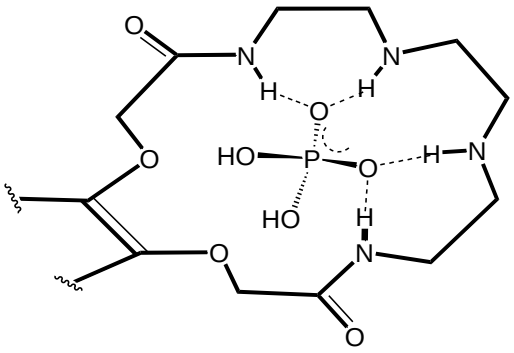

Figure 4.36 Structure of the $H_2PO_4^-$ complexed macrocyclic unit of **3** showing the N-H…O interaction.

4.3.8 Binding constant

Binding constants of the ions for **2** and **3** were calculated using emission titration data following literature procedure.[36,37] The titration experiments were carried out following the method described in the experimental section and the changes in emission intensities for **2** with F^- and $H_2PO_4^-$ and for **3** with F^-, $H_2PO_4^-$ and Cu^{2+} are

shown in Figures 4.37 – 4.41. It is clear from NMR study that the amine groups are not protonated upon addition of $H_2PO_4^-$, therefore this method is suitable for the determination of binding constants for these systems. According to this procedure, the fluorescence intensity (F) scales with the metal ion concentration ([M]) through $(F_0 - F)/(F - F_\infty) = ([M]/K_{diss})^n$. The binding constant ($K_s$) is obtained by plotting $\log[(F_0 - F)/(F - F_\infty)]$ versus log[M], where F_0 and F_∞ are the relative fluorescence intensities of the complex without addition of guest metal ion and with maximum concentration of metal ion (when no further change in emission intensity takes place), respectively. The value of log[M] at $\log[(F_0 - F)/(F - F_\infty)] = 0$ gives the value of $\log(K_{diss})$, the reciprocal of which is the binding constant (K_s). The plots $\log[(F_0 - F)/(F - F_\infty)]$ versus log[M] are shown as insets of the Figures 4.37 – 4.41. The titration data showed a nice linear fit ($R = 0.99$) with the above equation. The binding constants are summarized in Table 4. Analysis of the data show that (i) the binding constants (K_s) of $H_2PO_4^-$ for both the compounds are significantly higher compared to that of F^-, (ii) F^- binds strongly with **2** compared to that of **3** and (iii) $H_2PO_4^-$ binds strongly with **3** compared to that of **2**. The stronger binding ability of $H_2PO_4^-$ is probably due to its bidentate chelating nature, two of the oxygen atoms with the delocalized negative charge interact simultaneously to the hydrogen atoms of two N-H groups and form stable complex by chelating effect (Figure 4.36). The stronger binding of F^- with **2** compared to that of **3** is attributed to the cavity size of the macrocyclic units, the F^- ion being smaller in size fits appropriately in the smaller macrocyclic cavity of **2** making strong complex. On the other hand, $H_2PO_4^-$ needs large cavity size, in this regard cavity size of **3** is probably appropriate for $H_2PO_4^-$ to form strong complex.

These ionophores are basically designed for anions, however their performance towards a series of cations have also been evaluated. The donor sites of **2** and **3** are not favourable for alkali and alkaline earth metal ions, and from the series of cations studied, only Cu^{2+} showed strong complex formation with **3** (Figure 4.41). The metal center (Ru^{2+}) of the receptor molecule possesses two positive charges and therefore, it is difficult for the guest metal ion to make strong interaction with the adjacent ionophore because of the electrostatic repulsion. The cavity size and donor atoms of the ionophore also play important role for complexation. In the ionophore moiety, the two oxygen atoms attached to 1,10-phenanthroline ligand are poor donor because of electron delocalization in the attached aromatic ring. The macrocyclic unit of **2** with

three NH donor atoms may not be suitable for complexation with metal ions but the larger cavity size of **3** with four NH donors is found to be suitable for the Cu^{2+}. The binding constant for Cu^{2+} determined from emission titration data is 2.01 x 10^2 M^{-1}, a moderate value, which probably a balance between the strong coordination with four NH donors and electrostatic repulsion between positively charged cations.

Fluoride has the high affinity towards N-H proton, makes strong N-H…F interaction and in presence of excess F^- deprotonation of NH may also takes place causing substantial quenching in emission intensity.[9] With $H_2PO_4^-$ anion, significant enhancement (50%) in emission intensity was observed for **2,** this observation is similar to that noted for a $Ru(bpy)_3$ based metalloreceptor in presence of phosphate anion.[6] It may be due to structural rigidity developed by phosphate anion because of its complexation with the ionophore. Structural rigidity inhibits vibrational and rotational relaxation modes of nonradiative decay causing increase in emission intensity.[6,45] In the case of small F^-, the cavity size of both the macrocycles are sufficiently large to accommodate the anions without imposing any structural rigidity. However, in the case of $H_2PO_4^-$, the cavity size of the macrocyclic unit of **3** may be enough to fit but the cavity size of **2** is certainly not enough to accommodate the $H_2PO_4^-$ anion in the cavity. The phosphate anion possesses tetrahedral geometry and the complexation with macrocyclic unit might have imposed structural rigidity in the molecule causing enhancement in emission intensity.

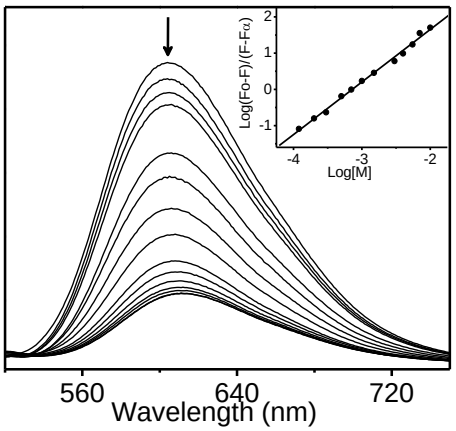

Figure 4.37 Emission spectral changes of **2** (1 x 10^{-5} M) upon addition of increasing concentration of F^-. Excitation wavelength: 450 nm. Inset: linear regression fit (double-logarithmic plot) of the titration data as a function of concentration of metal ion.

Figure 4.38 Emission spectral changes of **2** (1 x 10^{-5} M) upon addition of increasing concentration of $H_2PO_4^-$. Excitation wavelength: 450 nm. Inset: linear regression fit (double-logarithmic plot) of the titration data as a function of concentration of metal ion.

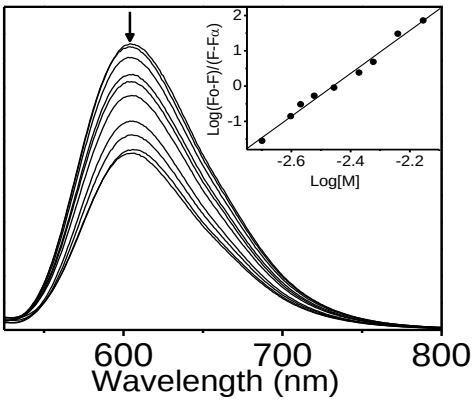

Figure 4.39 Emission spectral changes of **3** (1 x 10^{-5} M) upon addition of increasing concentration of F^-. Excitation wavelength: 452 nm. Inset: linear regression fit (double-logarithmic plot) of the titration data as a function of concentration of metal ion.

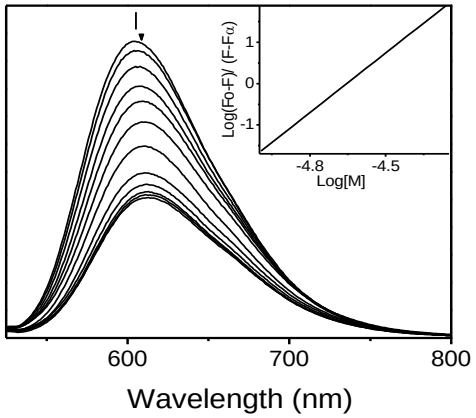

Figure 4.40 Emission spectral changes of **3** (1 x 10^{-5} M) upon addition of increasing concentration of $H_2PO_4^-$. Excitation wavelength: 452 nm. Inset: linear regression fit (double-logarithmic plot) of the titration data as a function of concentration of metal ion.

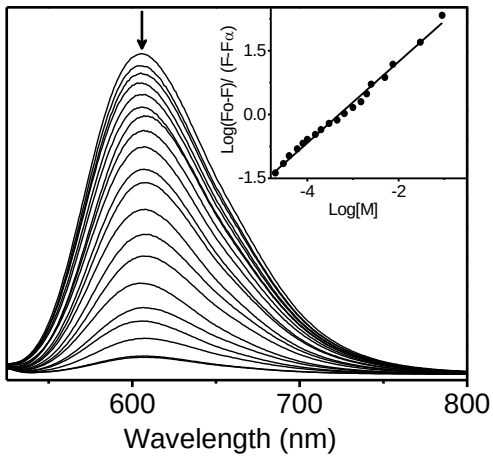

Figure 4.41 Emission spectral changes of **3** (1 x 10^{-5} M) upon addition of increasing concentration of $Cu(ClO_4)_2$. Excitation wavelength: 452 nm. Inset: linear regression fit (double-logarithmic plot) of the titration data as a function of concentration of metal ion.

4.4 Conclusions

Fluoroionophores incorporating macrocyclic unit as ionophore and $Ru(bpy)_3$ moiety as fluorophore have been synthesized and their ion binding property with a large number of cations and anions have been investigated. The ion-recognition property has been monitored by luminescence and ^1H NMR spectral change, which suggest that F^- and $H_2PO_4^-$ form strong complexes with the receptors **2** and **3**, and Cu^{2+} forms strong complex only with **3**. Binding constants (K_s) for these ions have been calculated using luminescence titration data and the values are in the range 2.85 x 10^2 to 4.48 x 10^4 M^{-1}. An analysis of the data reveal that K_s of $H_2PO_4^-$ > K_s of F^- for both the receptors, F^- binds strongly with **2** compared to that of **3** and $H_2PO_4^-$ binds strongly with **3** compared to that of **2**. The stronger binding ability of $H_2PO_4^-$ is attributed to its bidentate chelating effect, two of the oxygen atoms can interact simultaneously to the hydrogen atoms of the two N-H groups to form stable complex. The stronger binding of F^- with **2** is due to smaller cavity size of the ionophore, which fits nicely with the F^- ion making N-H….F interaction. The larger cavity size of **3** makes it suitable to form strong complex with $H_2PO_4^-$ encapsulating the anion in the cavity. The ^1H NMR study demonstrated the formation of complexes with F^- and $H_2PO_4^-$ anions through N-H…F and N-H...O interaction, respectively. The $H_2PO_4^-$ bound complexes of **2** and **3** have been isolated and the ^1H NMR, ^{31}P NMR, mass and IR spectroscopy confirmed 1:1 complex formation through H-bonding interaction. The strong N-H…F and N-H…O interactions causes substantial quenching in luminescence intensity. The enhancement in emission intensity observed for **2** with $H_2PO_4^-$, is attributed to structural rigidity due to complex formation with smaller macrocyclic unit.

4.5 References

1. A.P. de Silva, H.Q.N. Gunaratne, T.Gunnlaugsson, J.M. Huxley, C.P. Mchoy, J.D. Rademacher, T.E. Rice, Chem. Rev. 97 (1997) 1515.

2. P.D. Beer, P.A. Gale, Angew. Chem. Int. Ed. 40 (2001) 486.

3. P.D. Beer, E.J. Hayes, Coord. Chem. Rev. 240 (2003) 167.

4. J. Yoon, S.K. Kim, N.J. Singh, K.S. Kim, Chem. Soc. Rev. 35 (2006) 355.

5. J.S. Kim, D.T. Quang, Chem. Rev. 107 (2007) 3780.

6. S. Watanabe, O. Onogawa, Y. Komatsu, K. Yoshida, J. Am. Chem. Soc. 120 (1998) 229.

7. T. Lazarides, T.A. Miller, J.C. Jeffery, T.K. Ronson, H. Adams, M.D. Ward, Dalton Trans. (2005) 528.

8. Z. Lin, S. Ou, C. Duan, B. Zhang, Z. Bai, Chem. Commun. (2006) 624.

9. Y. Cui, H. Mo, J. Chen, Y. Niu, Y. Zhong, K. Zheng, B. Ye, Inorg. Chem. 46 (2007) 6427.

10. E. Kim, H.J. Kim, D.R. Bae, S.J. Lee, E.J. Cho, M.R. Seo, J.S. Kim, J.H. Jung, New J. Chem. 32 (2008) 1003.

11. P.D. Beer, A. Szemes, V. Balzani, C.M. Sala, M.G.B. Drew, S.W. Dent, M. Maestri, J. Am. Chem. Soc. 119 (1997) 11864.

12. T. Lin, C. Chen, Y. Wen, S. Sun, Inorg. Chem. 46 (2007) 9201.

13. D. Pelleteret, N.C. Fletcher, A.P. Doherty, Inorg. Chem. 46 (2007) 4386.

14. S.J. Dickson, M.J. Paterson, C.E. Willians, K.M. Anderson, J.W. Steed, Chem. Eur. J. 14 (2008) 7296.

15. A.W. Czarnik, Fluorescent Chemosensors of Ion and Molecule Recognition: Ed., ACS Sump. Ser. 538; American Chemical Society: Washington DC, (1993).

16. J.R. Lakowicz, Probe Design and Chemical Sensing: Topics in Fluorescence Spectroscopy: Ed., Plenum Press: New York, 4, (1994**)**.

17. A.P. de Silva, D.B. Fox, A.J.M. Huxley, T.S. Moody, Coord. Chem. Rev. 41 (2000) 205.

18. P.R.A. Webber, A. Cowley, M.G.B. Drew, P.D. Beer, Chem. Eur. J. 9 (2003) 2439.

19. F. Bolletta, A. Garelli, M. Montalti, L. Prodi, S. Romano, N. Zaccheroni, L. Canovese, G. Chessa, C. Santo, F. Visentin, Inorg. Chim. Acta 357 (2004) 4078.

20. S.H. Lee, H.J. Kim, Y.O. Lee, J. Vicens, J.S. Kim, Tetrahedron Lett. 43 (2006) 4373.

21. S.E. Plush, S.F. Lincoln, K.P. Wainwright, Inorg. Chim. Acta 362 (2009) 3097.

22. V.W.-W. Yam, A.S.-F. Kai, Inorg. Chim. Acta 300-302 (2000) 82.

23. B.D. Muegge, M.M. Richter, Anal. Chem. 74 (2002) 547.

24. M. Schmittel, H. Lin, Angew. Chem. Int. Ed. 46 (2007) 893.

25. X. Shang, J. Li, H. Lin, P. Jiang, Z. Cai, H. Lin, Dalton Trans. (2009) 2096.

26. V. P. Boricha, S. Patra, Y. S. Chouhan, P. Sanavada, E. Suresh, P. Paul, Eur. J. Inorg. Chem. (2009) 1256.

27. D.D. Perrin, W.L.F. Armarego, D.R. Perrin, Purification of Laboratory Chemicals, 2nd Ed, Pergamon, Press, Oxford, (1980).

28. W. Paw, R. Eisenberg, Inorg. Chem. 36 (1997) 2287.

29. B.P. Sullivan, D.J. Salmon, T.J. Meyer, Inorg. Chem. 17 (1978) 3334.

30. A.K. Bilakhiya, B. Tyagi, P. Paul, P. Natarajan, Inorg. Chem. 41 (2002) 3830.

31. R.F. Beeston, W.S. Aldridge, J.A. Treadway, M.C. Fitzgerald, B.A. DeGraff, S.E. Stitzel, Inorg. Chem. 37 (1998) 4368.

32. G.M. Sheldrick, SAINT 5.1 ed.; Siemens Industrial Automation Inc.: Madison, WI, (1995).

33. SADABS, Empirical Absorption Correction Program; University of Göttingen: Göttingen, Germany (1997).

34. G.M. Sheldrick, SHELXTL Reference Manual: Version 5.1; Bruker AXS: Madison, WI (1997).

35. G.M. Sheldrick, SHELXL-97: Program for Crystal Structure Refinement; University of Göttingen: Göttingen, Germany (1997).

36. A.C. Tedesco, D.M. Oliveria, Z.J.M. Lacava, R.B. Azevedo, E.C.D. Lima, P.C. Morais, J. Magn. Magn. Mater. 272-276 (2004) 2404.

37. S. Patra, P. Paul, Dalton Trans. (2009) DOI:10.1039/b905695e.

38. P. Agnihotri, E. Suresh, P. Paul, P. K. Ghosh, Eur. J. Inorg. Chem. (2006) 3369.

39. S. Patra, E. Suresh, P. Paul, Polyhedron 26 (2007) 4971.

40. V. Rajendiran, M. Murali, E. Suresh, S. Sinha, K. Somasundaram, M. Palaniandavar, Dalton Trans. (2008) 148.

41. V. Rajendiran, M. Murali, E. Suresh, M. Palaniandavar, V. S. Periasamy, M.A. Akbarsha, Dalton Trans. (2008) 2157.

42. M.-J. Li, B.W.-K. Chu, N. Zhu, V.W.-W. Yam, Inorg. Chem. 46 (2007) 720.

43. P. Paul, B. Tyagi, A.K. Bilakhiya, P. Dastidar and E. Suresh, Inorg. Chem. 39 (2000) 14.

44. L. Rodriguez, J. C. Lima, A. J. Parola, F. Pina, R. Meitz, R. Aucejo, E. Garcia-Espana, J. M. Llinares, C. Soriano, J. Alarcon, Inorg. Chem. 47 (2008) 6173.

45. P. D. Beer, Chem. Commun. (1996) 686.

CHAPTER – V

Synthesis, Characterization and Ion-binding Property of Fluoroionophores Containing Ru(II) and Re(I) Bipyridine Unit and Appended Crown having NS_2O_3 Donors

5.1 Introduction

The removal of toxic metal ions from hazardous waste is becoming one of the high priority research areas in present scenario.[1-4] A number of heavy metals that are toxic either by their interaction with enzymes or their tendency to form bond strongly with thiol (-SH) groups on protein.[5-7] The inorganic salt of these heavy metals form strong bond with protein and other biologically important compounds. This feature is significant because –SH groups are common components of active sites of many enzymes. It is therefore, important to develop extractants, which can selectively interact with these heavy metals. In the literature it has been reported that the chelating agents, which contain two or more hetero atoms show more flexibility towards the selectivity of these metal ions.[8-11] This finding encourage us to change the donor atoms of the macrocyclic moiety of fluoroionophores.

This chapter illustrates the synthesis and characterization of four luminescent receptors containing Ru(II)/Re(I)-polypyridine unit as fluorophore and macrocyclic unit with NS_2O_4 donor atoms as ionophore. For comparison, azacrown ether having NO_5 donor atoms has also been incorporated in one compound. All of these compounds have been characterized on the basis of analytical and spectroscopic methods. Ion-binding property of these molecules has been ascertained with a series of sixteen metal ions and with a dozen of anions. The recognition event is monitored by fluorescence, Uv-vis and NMR spectral changes. These compounds exhibited high selectivity towards a few cations and anions, the binding constant with the strongly interacting ions have been evaluated mainly by fluorescence titration. The ^{1}H NMR spectral change with some selective anions provided information about binding site of the anions with the ionophores. The selectivity and electron/energy transfer involved in the recognition process is presented in details.

5.2. Experimental section

5.2.1 Reagents and materials

Most of the chemicals used in this study has also been used earlier and has been mentioned in the earlier Chapters. Some new chemicals such as bis(2-chloroethyl)amine hydrochloride, ditertiarybutyl dicarbonate(BOC_2O), potassium

thioacetate, tetra ethylene glycol, cesium carbonate, trifluoro acetic acid, used in this study were purchased from Aldrich and S. D. fine chemicals. All metal perchlorate salts were purchased from Alfa Aesar (Johnson Matthey Company) as mentioned earlier. All organic solvents were analytical grade and were used as received for synthetic purpose. Solvents for spectral studies were freshly purified by standard procedures[12]. *Cis*-$[Ru(bpy)_2Cl_2]\cdot 2H_2O$[13], 2,2'-bipyridine-4,4'-dicarboxilic acid[14] and 4-(bromomethyl)-4'-methyl-2, 2'-bipyridine[15] were prepared according to the literature procedures.

5.2.2 Physical measurement

All physical measurements were carried out using the instruments mentioned in the earlier chapters.

Caution: Perchlorate salts of metal ions are potentially explosive. Therefore, they should be handled with great care.

5.2.3 Synthesis of the intermediate compounds (1-8)

Synthesis of N- tert-butoxy carbonyl-bis(2-chloroethyl)amine [1]

The intermediate compound **1** was synthesized by a modified published procedure.[16] In a typical experiment bis(2-chloroethyl)amine hydrochloride (7.2 g, 40.3 mmol) was added to a cold solution of sodium hydroxide (6.5 g, 162.0 mmol) dissolved in 100 mL of water. Then di-tertiarybutyl dicarbonate (BOC_2O) (10.0 g, 45.8 mmol) was added carefully over a period of 1 h and the reaction mixture was stirred overnight at room temperature. The product thus formed was then extracted with ethyl acetate (3 x 50 mL), dried over anhydrous $NaSO_4$ and the solvent of the reaction mixture was removed by rotary evaporation, which gave the product N-Boc-bis (2-chloro ethyl) amine as a pale yellow oil, yield: 8.9 g (91 %). ^{1}H NMR (500 MHz, $CDCl_3$): δ = 1.47 (s, 9H, $C(CH_3)_3$), 3.59-3.6 (m, 8H, CH_2CH_2Cl).

Synthesis of N-tert-butoxy carbonyl bis(2-thiocacetoxyethyl)amine [2]

This intermediate compound was also synthesized following a modified literature procedure.[17] To a stirred solution of **1** (8.95 g, 37 mmol) in DMF excess potassium thioacetate (9.1 g, 79.7 mmol) was added. The reaction mixture was then maintained at room temperature for 48 h with rapid stirring, then filtered. The filtrate was evaporated at reduced pressure and the residue was partitioned between water and dichloromethane. The aqueous phase was then separated and extracted further (twice) with dichloromethane. The combined organic phase was dried with anhydrous sodium sulfate and the solution was then evaporated to dryness. The product (**2**) was purified by column chromatography on silica gel using 20% ethyl acetate/hexane as the eluent. The product was obtained as a pale yellow oil, yield: 4.1 g (35 %). ^{1}H NMR (500 MHz, CDCl3): δ = 1.47 (s, 9H *t*-Bu), 2.34 (s, 6H, $COCH_3$), 3.03(t, 4H, SCH_2), 3.37(t, 4H, NCH_2).

Synthesis of N- tert-butoxy carbonyl bis(2-thioethyl)amine [3]

This compound was obtained by hydrolysis of N-tert-butoxy carbonylbis(2-thioacetoxyethyl)amine (**2**). Sodium metal (1.5 g, 64 mmol) was treated with anhydrous MeOH (50 mL), the bis thioacetate **2** (4.1 g, 12.7 mmol) was then added into it. The reaction mixture was then allowed to stir under nitrogen atmosphere at room temperature for 20 min. Then conc. HCl was added dropwise until the pH of the solution became 2.0. The reaction mixture was then partitioned between water and dichloromethane. The aqueous phase was separated and extracted with two further portion of dichloromethane. The combined organic phase was dried with anhydrous sodium sulfate and evaporated to dryness. The product (**3**) was obtained as light yellow oil, yield: 4.8 g, (89 %). This product was immediately characterized and used for the next step for avoiding disulfide formation. ^{1}H NMR (500 MHz, $CDCl_3$): δ = 1.26 (br, 2 H, SH), 1.46(s, 9 H, *t*-Bu), 2.37 (t, 4 H, SCH_2), 3.39 (t, 4 H, NCH_2).

Synthesis of dichloro-tetraethylene glycol [4]

Di-chlorotetraethylene glycol was synthesized by the reaction of tetraethylene glycol with thionyl chloride as described in the literature.[18] A mixture of tetra ethylene glycol (4.3 g, 22 mmol) and pyridine (3.9 g, 46 mmol) in 20 mL benzene was heated to 86°C and then thionyl chloride (~ 6.0 g) was added into it. The reaction mixture was refluxed for 16 h, during which a white precipitate was formed. The solution was then

allowed to cool and then dilute HCl (5 mL in 20 mL of water) was added dropwise (~15 min). The benzene layer containing the product was removed and the solvent was evaporated by a rotary evaporator, which gave the product as light yellow oil, yield 4.6 g (90 %).

Synthesis of tert-butyl-1,4,16-trioxa-7,13-dithia-10-azacyclooctadecane-10-carboxylate [5]

Cesium carbonate (11.2 g, 34.5 mmol) and dichlorotetraethylene glycol (4.7 g, 20.2 mmol) were taken in a 1-liter round-bottom flask and 750 mL of acetonitrile was added into it. The N-Boc dithiol (**3**, 4.8 g, 20.2 mmol) dissolved in acetonitrile (30 mL) was then added into the reaction mixture very slowly (50 h) through a syringe under nitrogen atmosphere at 45–50 ^{0}C. The reaction mixture was kept for a further 10 h with rapid stirring, allowed to cool to room temperature and then filtered. The filtrate was evaporated and the residue was partitioned between water and dichloromethane. The aqueous phase was separated and extracted with two further portions of dichloromethane. The combined organic phases were dried with anhydrous sodium sulfate and evaporated to dryness. The crude product was purified by column chromatography on silica gel using 10% ethyl acetate/n-hexane as the eluent, which gave **5** as a pale yellow oil. Yield, 0.8 g, (10 %). ^{1}H NMR (500 MHz, $CDCl_3$): δ = 1.45(s, 9 H, *t*-Bu), 2.76 (m, 8 H, SCH_2), 3.44(t, 4 H, NCH_2), 3.66(m, 14 H, OCH_2), LC-MS: *m/z* = 418.72 (100%, calcd. for [**5**] + Na^+: 418.57), 434.69 (25%, calcd. for [**5**] + K^+: 434.68).

Synthesis of 1,4,7-trioxa-10,16-dithia-13-azacyclooctadecane [6]

To a stirred mixture of dichloromethane (30 ml) and trifluoro acetic acid (30 ml), N-Boc macrocycle (**5**, 0.8 g, 2.1 mmol) was added. The reaction mixture was then stirred at room temperature for 2 h. After evaporation of the solution by rotary evaporator, methanol was added and evaporated three times to remove the remaining trifluoro acetic acid. To the residue, 15% aqueous sodium carbonate (50 mL) was added and extracted with dichloromethane three times. The combined organic phases were dried with anhydrous sodium sulfate and evaporated to yield **6** as a pale yellow glassy solid. Yield, 0.45 g, (75 %). ^{1}H NMR (500 MHz, $CDCl_3$): δ = 2.73-2.87 (m, 12

H, NCH_2/SCH_2), 3.60-4.0 (m, 12 H, OCH_2), 2.14 (br, 1H, NH). LC-MS: *m/z* = 296.70 (100 %, calcd. for [**6**] + H^+: 296.46), 318.69 (50%, calcd. for [**6**] + K^+: 318.45).

Synthesis of 2,2'-bipyridine-4,4'-dicarbonyl dichloride [7]

The compound 2,2'-bipyridyl 4,4'-dicarbonyl chloride was synthesized as described in ***chapter-II*** *(section* ***2.2.3****).*

Synthesis of 4-(Bromomethyl)-4'-methyl-2, 2'-bipyridine [8]

This compound was prepared following a published procedure [15].

5.2.4 Synthesis of the Ligands L^1-L^3

Synthesis of L^1

To a stirred solution of **6** (0.3 g, 1 mmol) in dry THF (50 mL), triethylamine (2 mL) was added and then 2,2'-bipyridine-4,4'-dicarbonyl dichloride, dissolved in THF (20 mL), was added dropwise (30 min) into the reaction mixture cooled in a ice bath under nitrogen atmosphere. The solution was then allowed to stir at room temperature for 24 h. The solution was then filtered and the filtrate was evaporated, the residue thus obtained was partitioned between water and dichloromethane. The organic phase was dried with anhydrous sodium sulfate and evaporates to dryness to yield ligand $\mathbf{L^1}$ as a pale yellow glassy oil which is further purified by column chromatography on silica gel using 10% ethyl acetate/n-hexane as the eluent. Yield 0.40 g (54 %). ^{1}H NMR (500 MHz, $CDCl_3$): δ = 8.46 (d, *J* = 4.5 Hz, 2 H, 6-H and 6′-H of bpy), 8.14 (s, 2H, 3-H and 3′-H of bpy), 7.06 (d, *J* = 3.5 Hz, 2 H, 5-H and 5′-H of bpy), 3.66-3.58 (m, 20 H, -CH_2O of crown ether), 2.71-2.66 (m, 28 H, -CH_2O of crown ether), ppm. LC-MS: *m/z* = 799.68 (30%, calcd. for [$\mathbf{L^1}$ + H^+]: 799.33).

Synthesis of L^2

To a stirred solution of **6** (0.45 g, 1.5 mmol) and triethylamine (2 mL) in THF (60 mL) was dropwise added (30 min) **8** (0.4 g, 1.5 mmol) dissolved in 20 mL of

THF. The reaction mixture was refluxed for 24 hours under nitrogen atmosphere and then allowed to cool to room temperature. After filtration, the filtrate was evaporated and partitioned between water and dichloromethane. The aqueous phase was separated and extracted with two further portions of dichloromethane. The combined organic phases were dried with anhydrous sodium sulfate and then evaporated to dryness. The crude product was purified by column chromatography on silica gel using 10% ethyl acetate/n-hexane as the eluent, which gave $\mathbf{L^2}$ as a pale yellow glassy oil. Yield, 0.5 g (61 %). ^{1}H NMR (200 MHz, $CDCl_3$): δ = 8.54 (d, *J* = 5 Hz, 1 H, 6-H/6′-H of bpy), 8.46 (d, *J* = 5 Hz, 1 H, 6'-H/6-H of bpy), 8.23(s, 1 H, 3-H/3′-H of bpy), 8.16(s, 1 H, 3'-H/3-H of bpy), 7.37 (d, *J* = 4.4 Hz, 1 H, 5-H/5′-H of bpy), 7.06(d, *J* = 4.6 Hz, 1 H, 5'-H/5-H of bpy) 3.66-3.61 (m, 14 H, -CH_2O of crown ether, -CH_2-), 2.71-2.64 (m, 12 H, -CH_2O of crown ether), 2.37 (s, 3 H, -CH_3), ppm. LC-MS: *m/z* = 478.29 (100%, calcd. for [$\mathbf{L^2}$ + H^+]: 478.68).

Synthesis of L^3

This compound was synthesized following the similar procedure as described for $\mathbf{L^2}$, except 1-aza-18-crown-6 was added instead of **6**. Yield 0.23 g (51 %). ^{1}H NMR (500 MHz, $CDCl_3$): δ = 8.53 (d, *J* = 5 Hz, 1H, 6-H/6′-H of bpy), 8.45 (d, *J* = 5 Hz, 1H, 6'-H/6-H of bpy), 8.22(s, 1H, 3-H/3′-H of bpy), 8.14 (s, 1H, 3'-H/3-H of bpy), 7.38 (d, *J* = 4.5 Hz, 1H, 5-H/5′-H of bpy), 7.05 (d, *J* = 3.9 Hz, 1H, 5'-H/5-H of bpy) 3.75-3.56 (m, 22H, -CH_2O of crown ether, -CH_2-), 2.77(t, 4 H, -CH_2N of crown ether), 2.36 (s, 3H, -CH_3), ppm. LC-MS: *m/z* = 446.84 (85%, calcd. for [$\mathbf{L^3}$ + H^+]: 446.55, 468.77 (100%, calcd. for [$\mathbf{L^3}$ + Na^+]: 468.55, 484.83 (55%, calcd. for [$\mathbf{L^3}$ + K^+]: 484.55.

5.2.5 Synthesis of Metal Complexes

General Procedure for the synthesis of $[Ru(bpy)_2(L^1)][PF_6]_2$ (1), $[Ru(bpy)_2(L^2)][PF_6]_2$ (2) and $[Ru(phen)_2(L^2)]$ $[PF_6]_2$ (3)

A mixture of *cis*-$Ru(bpy)_2Cl_2{\cdot}2H_2O$ (0.2 mmol) and appropriate ligand $\mathbf{L^1}$/$\mathbf{L^2}$/$\mathbf{L^3}$ (0.2 mmol) in ethanol-water (1:1, 50 mL) was refluxed for 12 h. The volume of the

reaction mixture was reduced to ca 20 mL by rotary evaporation, filtered and to the filtrate an aqueous solution of NH_4PF_6 (0.20 g, 1.3 mmol) was added. The precipitate was filtered off and washed with water and diethyl ether. The compound was purified by column chromatography packed with neutral alumina, with acetonitrile-toluene (3:2) as eluent. The solvent of the desired fraction was removed by rotary evaporation and the compound was washed with diethyl ether and dried in vacuum. Yield: 0.135g (55 %) for **1**, 0.16 g (61 %) for **2** and 0.155 g (65 %) for **3**

Characterization data for 1: ^{1}H NMR (500 MHz, CD_3CN): δ = 8.52 (s, 2H, 3-H and 3′-H of bpy of $\mathbf{L^1}$), 8.50 (d, *J* = 8.0 Hz, 4H, 6-H and 6′-H of bpy), 8.10-8.05 (overlapped triplets, 4H, 5-H and 5′-H of bpy), 7.79 (d, *J* = 5.0 Hz, 2H, 3-H and 3′-H of bpy), 7.76 (d, *J* = 5.5 Hz, 2H, 6-H and 6′-H of bpy of $\mathbf{L^1}$), 7.71 (d, *J* = 5.0 Hz, 2H, 3-H and 3′-H of bpy), 7.37-7.44 (m, 6H, 5-H and 5′-H of bpy of $\mathbf{L^1}$, 4H, 4-H and 4′-H of bpy), 3.88 (s, 4H, -CH_2S of crown ether), 3.75 (s, 4H, -CH_2N of crown ether), 3.59-3.50 (m, 40H, -CH_2O of crown ether). LC-MS: *m/z* = 1397.49 (75%, calcd. for [**1**-PF_6^- +K^++H^+]: 1397.60, IR (KBr pellets): ν = 1636 cm^{-1} (C = O), 840 cm^{-1} (PF_6^-). UV-Vis (CH_3CN): λ = 454 nm (ε, 9.83 x 10^3 $M^{-1}cm^{-1}$), 288 nm (ε, 5.45 x 10^4 $M^{-1}cm^{-1}$). $C_{56}H_{70}F_{12}N_8O_8P_2RuS_4$ (1502.25): calcd. for C 44.77, H 4.70, N 7.46; found: C 44.34, H 4.56, N 7.32.

Characterization data for 2: ^{1}H NMR (500 MHz, CD_3CN): δ = 8.49 (s, 1H, 3-H/3′-H of bpy of $\mathbf{L^2}$), 8.48 (d, *J* = 5.0 Hz, 4H, 6-H and 6′-H of bpy), 8.35 (s, 1H, 3'-H/3-H of bpy of $\mathbf{L^2}$), 8.03-8.05 (t, 4H, 5-H and 5′-H of bpy), 7.72 (d, *J* = 4.5 Hz, 4H, 4-H and 4′-H of bpy), 7.52 (d, *J* = 5.5 Hz, 2H, 5-H and 5′-H of bpy of $\mathbf{L^2}$), 7.38 (t, 4H, 3-H and 3′-H of bpy), 7.22 (d, *J* = 4.5 Hz, 2H, 6-H and 6′-H of bpy of $\mathbf{L^2}$), 3.832(s, 2H, -CH_2-), 3.55-3.65 (m, 16H, -CH_2O of crown ether), 2.66-2.76 (m, 8H, -CH_2O of crown ether), 2.52(s, 3H, -CH_3). LC-MS: *m/z* = 1037.58 (100%, calcd. for [2-PF_6^- + H^+]: 1037.09). IR (KBr pellets): ν = 840 cm^{-1} (PF_6^-). UV-Vis (CH_3CN): λ = 454 nm (ε, 1.15 x 10^4 $M^{-1}cm^{-1}$), 288 nm (ε, 6.78 x 10^4 $M^{-1}cm^{-1}$). $C_{44}H_{51}F_{12}N_7O_3P_2RuS_2$ (1181.05): calcd. for C 44.75, H 4.35, N 8.30; found: C 43.95, H 4.31, N 8.25

Characterization data for 3: ^{1}H NMR (500 MHz, CD_3CN): δ = 8.50-8.48 (m, 4H, 6,6'-H bpy), 8.43 (s, 1H, 3-H/3′-H of bpy of $\mathbf{L^3}$), 8.35 (s, 1H, 3′-H/3-H of bpy of $\mathbf{L^3}$), 8.05-8.03 (overlapped triplets, 4H, 5-H and 5′-H of bpy), 7.72 (m, 4H, 4-H and 4′-H

of bpy), 7.64 (d, *J* = 5.5 Hz, 1H, 5-H/5′-H of bpy of $\mathbf{L^3}$), 7.52 (d, *J* = 5.5 Hz, 1H, 5′-H/5-H of $\mathbf{L^3}$), 7.39 (overlapped triplets, 4H, 3-H and 3′-H of bpy), 7.27-7.21 (m, 2H, 6-H and 6′-H of bpy of $\mathbf{L^3}$), 3.32-3.51 (m, 20H, -CH_2O of crown ether, -CH_2-), 2.53 (m, 4H, -CH_2O of crown ether), 2.32(s, 3H, -CH_3). LC-MS: *m/z* = 1003.55 (20%, calcd. for [**3**–PF_6^-]$^+$: 1003.95), 1171.05 (18%, calcd. for [**3** + Na^+]$^+$: 1171.91). IR (KBr pellets): ν = 840 cm^{-1} (PF_6^-). UV-Vis (CH_3CN): λ = 454 nm (ε, 1.64 x 10^4 $M^{-1}cm^{-1}$), 288 nm (ε, 9.04 x 10^4 $M^{-1}cm^{-1}$). $C_{44}H_{51}F_{12}N_7O_5P_2Ru$ (1148.92): calcd. for C 46.00, H 4.47, N 8.53; found: C 45.88, H 4.26, N 8.47.

Synthesis of [Re(L^1)$(CO)_3$Cl].THF (4)

A mixture of [$Re(CO)_5Cl$] (0.073g, 0.2 mmol) and ligand $\mathbf{L^1}$ (0.095g, 0.2 mmol) was refluxed in dry THF (30 mL) under nitrogen atmosphere for 15 h. The solution was then allowed to cool to room temperature and the solvent was removed by rotary evaporation. The residue thus obtained was dissolved in dichloromethane (10 mL) and was added dropwise into n-hexane (50 mL) with stirring. The precipitate thus obtained was isolated by filtration and purified by column chromatography packed with neutral alumina using acetonitrile-toluene (1:1) as eluent. The solvent from the desired fraction was removed by evaporation. Yield: 0.085 g (55 %). ^{1}H NMR (500 MHz, CD_3CN): ^{1}H NMR (500 MHz, CD_3CN): δ = 8.92 (d, *J* = 4.5 Hz 1H, 6-H/6′-H of bpy), 8.82 (d, *J* = 5.5 Hz 1H, 6′-H/6-H of bpy), 8.37 (s, 1H, 3-H/3′-H of bpy), 8.27 (s, 1H, 3′-H/3-H of bpy), 7.61 (d, *J* = 6.5 Hz 1H, 5-H/5′-H of bpy), 7.45 (d, *J* = 6.0 Hz 1H, 5′-H/5-H of bpy) 3.27-3.81 (m, 24H, -CH_2), 2.55 (s, 3H, -CH_3). LC-MS: *m/z* = 877.11 (25 %, calcd. for [**4** + Na^+]: 878.48), 899.05(50%, calcd. For [**4** + K^+]: 898.58. IR (KBr pellets): ν_{CO} = 2019 (A_1), 1900 and 1886 (E) cm^{-1}. UV-Vis (CH_3CN): λ = 366 nm (ε, 9.66 x 10^3 $M^{-1}cm^{-1}$), 287 nm (ε, 4.46 x 10^4 $M^{-1}cm^{-1}$). $C_{31}H_{43}ClN_3O_7ReS_2$ (855.49): calcd. for C 43.53, H 5.06, N 4.91; found C 43.07, H 5.26, N 5.16.

5.2.6 Ion-binding property

5.2.6.1 Luminescence method

Stock solutions of the complexes **1**-**4** (2 x 10^{-5} M) and that of the perchlorate salts (2 x 10^{-2} M) of various cations (Na^+, K^+, Li^+, Cs^+, Ag^+, Mn^{2+}, Ni^{2+}, Co^{2+}, Mg^{2+},

Ca^{2+}, Zn^{2+}, Ba^{2+}, Sr^{2+} Cd^{2+}, Hg^{2+}, Pb^{2+}, Fe^{3+} and Cu^{2+}) were prepared in freshly purified acetonitrile. Then 2 mL stock solution of the complex and 2 mL stock solution of each anion salt were taken in a 5 mL volumetric flask, so that the effective concentration of the complex is 1 x 10^{-5} M and that of the anions are 1 x 10^{-2} M (1000 fold). The luminescence spectra of the resulting solutions and that of the original complex (1 x 10^{-5} M) were recorded with excitation at the absorption maxima (λ_{max}) of the MLCT band, which is 454 for **1-3** and 360 for **4,** respectively. The spectra of the cation containing reaction mixtures were compared with that of the original solution to ascertain the interactions of the cations with the ionophore. Similar experiments were also carried out with tetrabutyl ammonium salts of various anions (F^-, Cl^-, Br^-, I^-, $H_2PO_4^-$, ClO_4^- , NO_3^-, BF_4^-, CH_3COO^-, and HSO_4^-) to ascertain the interactions of the anions with the ionophore. The UV/Vis spectra of all the solutions containing anions and cations (1000 equiv) were also recorded and the same were compared to that of the original solutions to examine the changes.

Anions and cations, which exhibited substantial changes in emission intensity, were considered for emission titration to evaluate association constant. For emission titration study, the same stock solutions of the complexes (**1**-**4**) were used and the solution of perchlorate salts of the selected cations (Pb^{2+}, Hg^{2+}, Cu^{2+} and Fe^{3+} for complex **1,** Cu^{2+} and Fe^{3+} for complex **2**, Cu^{2+} for complex **3,** and Hg^{2+}, Cu^{2+} and Fe^{3+} for complex **4**) and the tetrabutyl ammonium salts of the selected anions (I^-, F^- and $H_2PO_4^-$ for complex **1,** F^- for complex **2,** $H_2PO_4^-$ for complex **3** and F^-, CH_3COO^- and $H_2PO_4^-$ for complex **4**) of desired concentration (0.4 x 10^{-5} – 2 x 10^{-3} M) were prepared by proper dilution of the stock solution. Then 2 mL of each solution were mixed in a 5 mL volumetric flask to prepare reaction mixture with 0.1 to 1000 molar equivalent of the concentration of metal ion with respect to the concentration of complexes and the luminescence spectra of the resulting solutions were recorded. Binding constants were calculated following the literature procedure as described in the Results and Discussion Section.[19,20]

5.2.6.2 NMR method

^{1}H NMR technique is used to study the interaction between guest ions and fluoroionophore. The complexes of Ru(II) and Re(I) are highly soluble in acetonitrile.

Therefore all the spectra are recorded using 2 mg of complex in 0.5 mL of acetonitrile-d_3. The solutions of the guest ions were then added with increasing concentration to make it 1, 2, 3 and 5-equivalent of the concentration of complex and corresponding ^{1}H NMR spectra were recorded. The spectra in presence and in absence of guest ion were compared to assess the interaction between guest ions and the ionophores.

5.3 Results and discussion

5.3.1 Synthesis of Ligands L^1-L^3

The ligands **L^1, L^2** and **L^3** were synthesized by the procedure shown in Scheme 1. All the intermediates (**1**-**8**) were synthesized either by following the reported procedures or by the method described above and the characterization data are given in the experimental section. All the data are in agreement with the compositions/structures of the compounds.

The ligands **L^1- L^2** were synthesized from the intermediates **6** and **L^3** was synthesized from 1-aza-18-crown-6 by the reaction with appropriate bipyridine derivatives (**7** and **8**) in presence of triethyl amine in THF, as described in the Experimental Section.

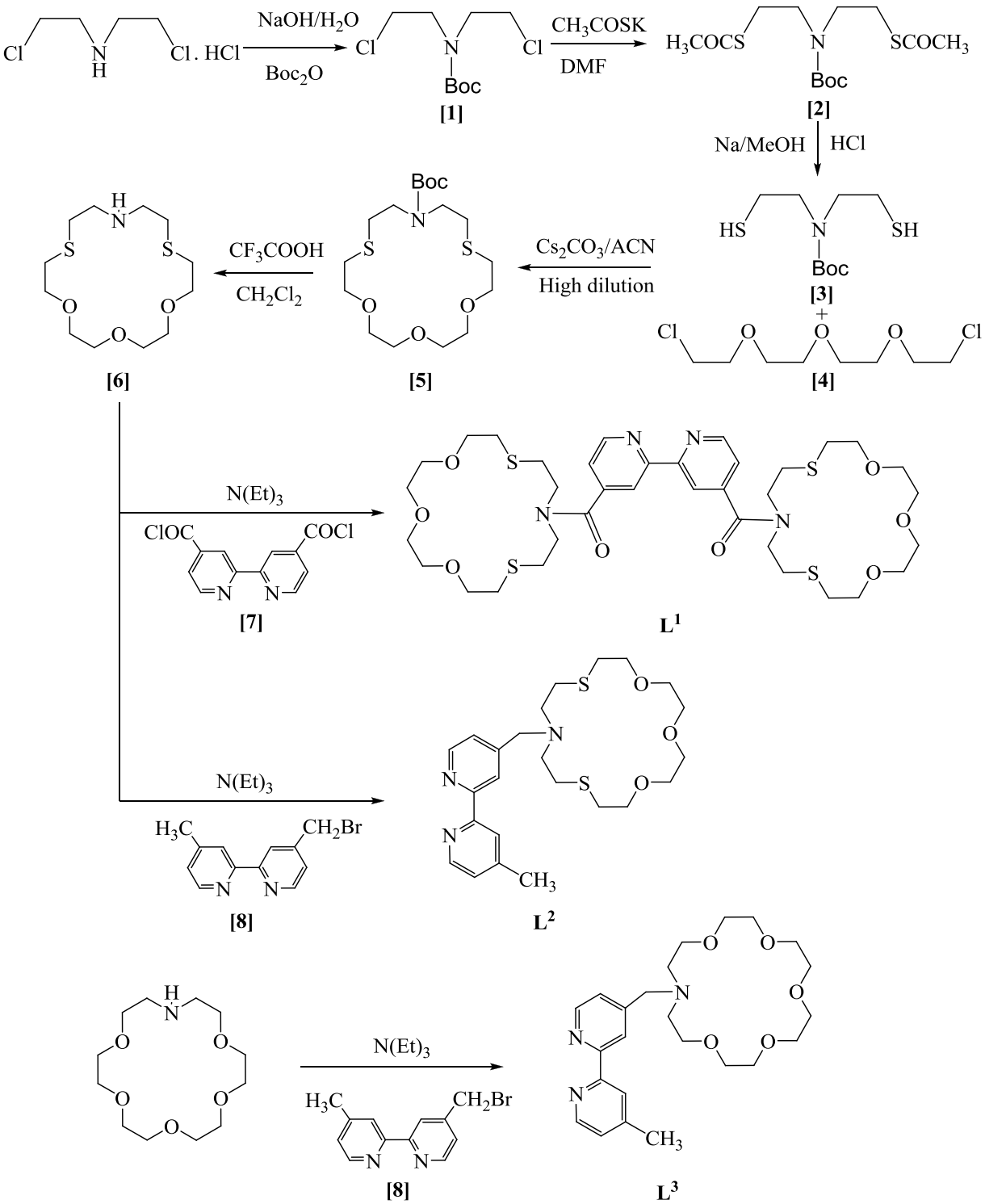

Scheme 1. Route followed for the synthesis of $\mathbf{L^1}$, $\mathbf{L^2}$ and $\mathbf{L^3}$.

All the ligands have been characterized by analytical and spectroscopic methods. The characterization data for $\mathbf{L^1}$-$\mathbf{L^3}$ are given in the Experimental Section. Microanalytical (C, H and N analysis) and mass spectrometric data are in excellent agreement with the calculated values of the respective proposed structure of the ligands. The mass and ^{1}H NMR spectra of $\mathbf{L^1}$, $\mathbf{L^2}$ and $\mathbf{L^3}$ are shown in Figures 5.1-5.5. The aromatic region of the ^{1}H NMR spectra of $\mathbf{L^1}$ exhibited two doublets at δ 8.46 and 7.06, and a singlet at δ 8.14 due to the 4,4'-disubstituted bipyridine units of the ligand. In the aliphatic region, it exhibited two multiplets (overlapped signals) in the ranges δ 3.58-3.66 and δ 2.66-2.71, which correspond to CH_2 protons associated to the CH_2O and CH_2N/S moieties, respectively of the macrocyclic units. The proton NMR spectra of $\mathbf{L^2}$ exhibited four doublets at δ 8.54, 8.46, 7.37 and 7.06 and two singlets at δ 8.23 and 8.16, which are due to unsymmetrically disubstituted bipyridine unit of the ligand. In the aliphatic region, like $\mathbf{L^1}$**,** it also showed two multiplets in the regions δ 3.66-3.61 and 2.71-2.64 for the CH_2 protons of the macrocyclic moiety. The CH_3 attached to the bipyridine unit, appeared as singlet at δ 2.37. The aromatic region of the ^{1}H NMR spectra of $\mathbf{L^3}$ is similar to that of $\mathbf{L^2}$, it exhibited four doublets at δ 8.53, 8.45, 7.38 and 7.05 and two singlets at δ 8.22 and 8.14 for unsymmetrically disubstituted bipyridine unit. In the aliphatic region, a multiplet in the range δ 3.56-3.75 appeared for the CH_2 protons of the aza crown moiety. A triplet at δ 2.77 is also observed which is assigned to the CH_2N protons of the azacrown ring. The CH_3 attached to the bipyridine unit appeared at δ 2.36. On the basis of analytical and spectroscopic data discussed above, the proposed structures of the ligands $\mathbf{L^1}$, $\mathbf{L^2}$ and $\mathbf{L^3}$ are shown in Scheme 1**.**

5.3.2 Synthesis of complexes 1-4

The Ru(II) complexes (**1**-**3**) were synthesized by the reaction of *cis*-$[(bpy)_2RuCl_2].2H_2O$ and $\mathbf{L^1}$/ $\mathbf{L^2}$/$\mathbf{L^3}$ in refluxing ethanol-water, isolated with PF_6^- counter ion and purified by column chromatography using deactivated alumina as packing material and acetonitrile-toluene (1:2) as eluent. The analytical and spectroscopic data of all complexes are given in the Experimental Section.

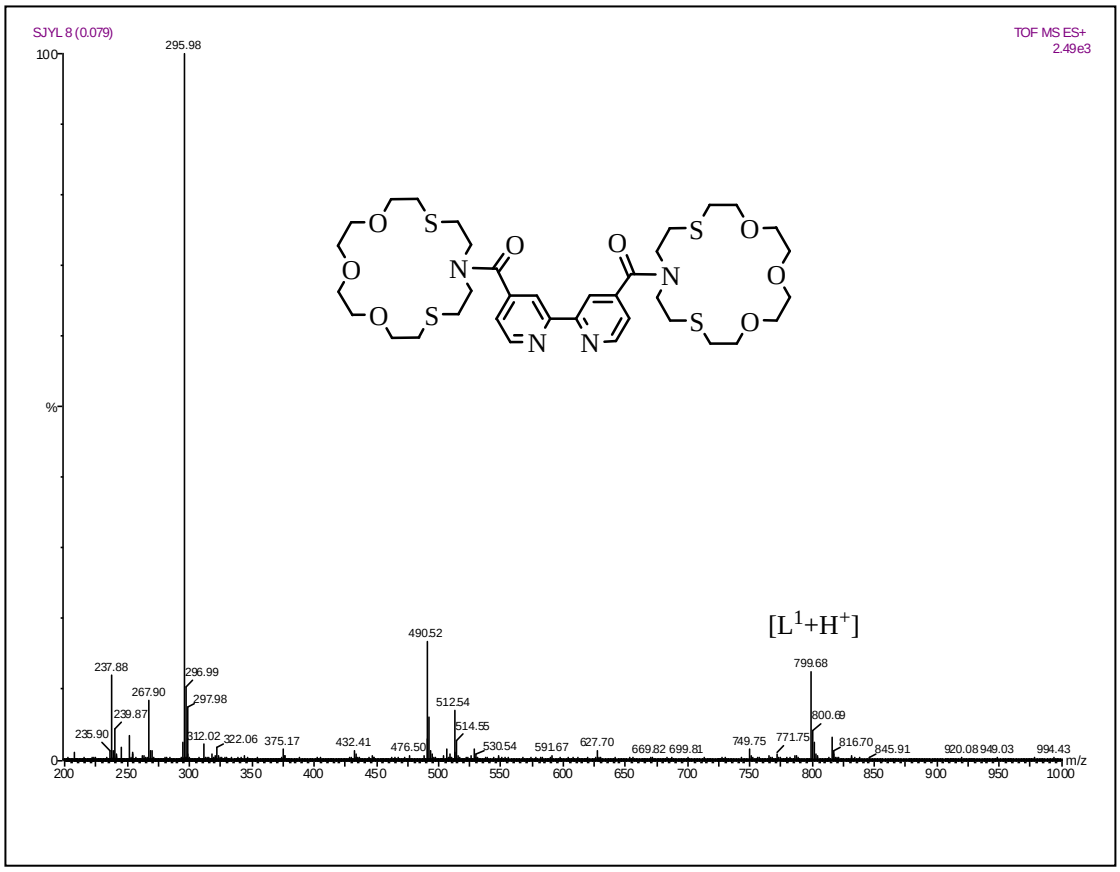

Figure 5.1 Mass spectrum of **L**^{1}

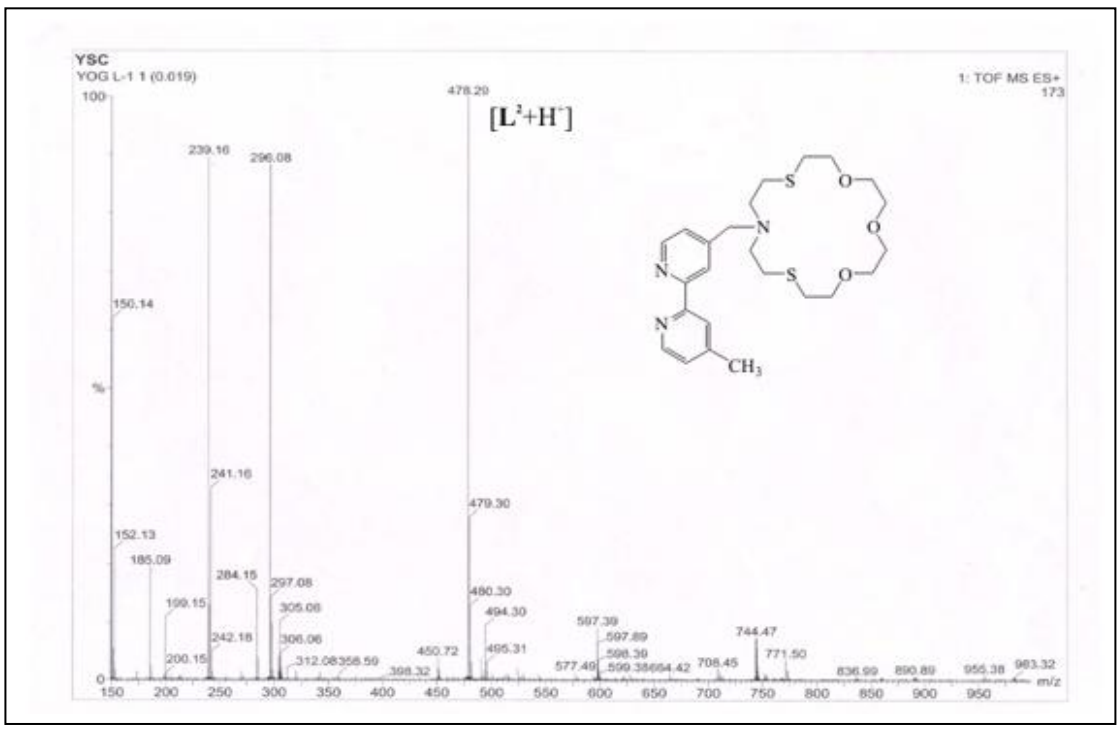

Figure 5.2 Mass spectrum of **L**^{2}

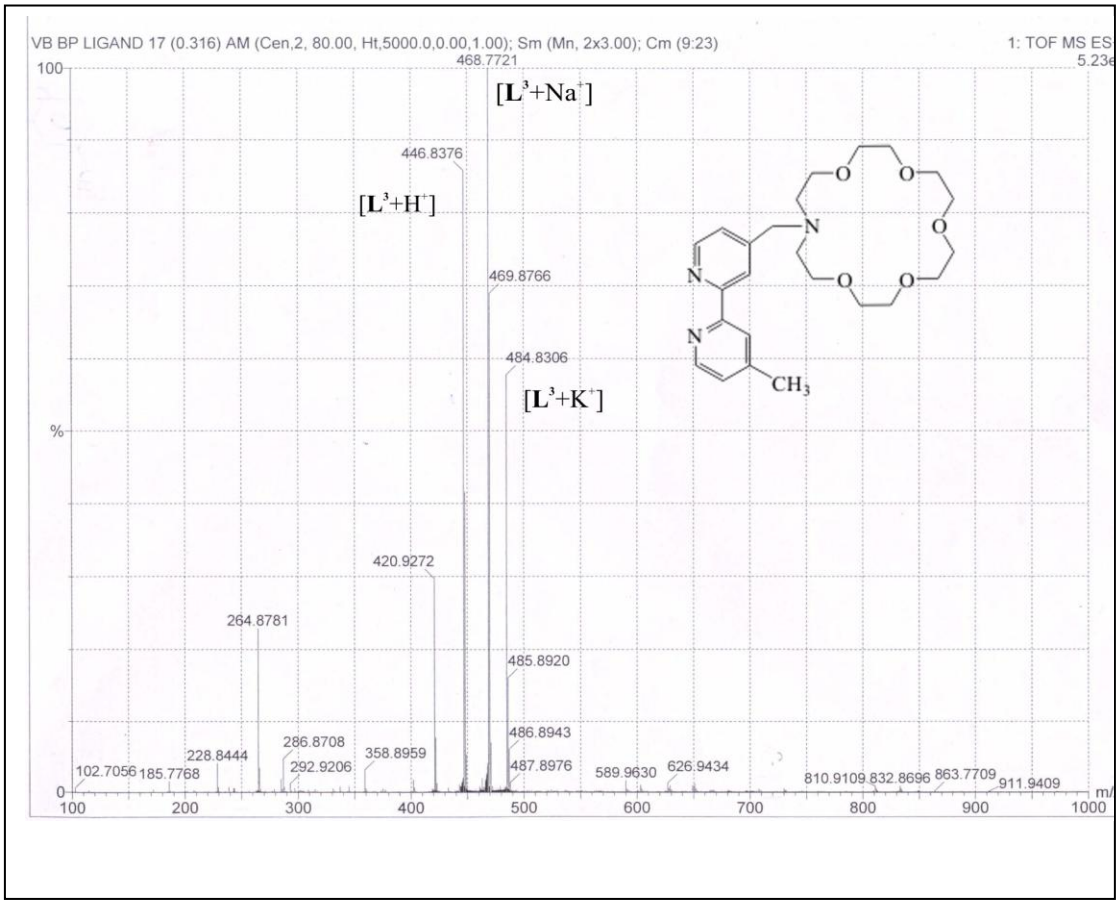

Figure 5.3 Mass spectrum of $\mathbf{L^3}$

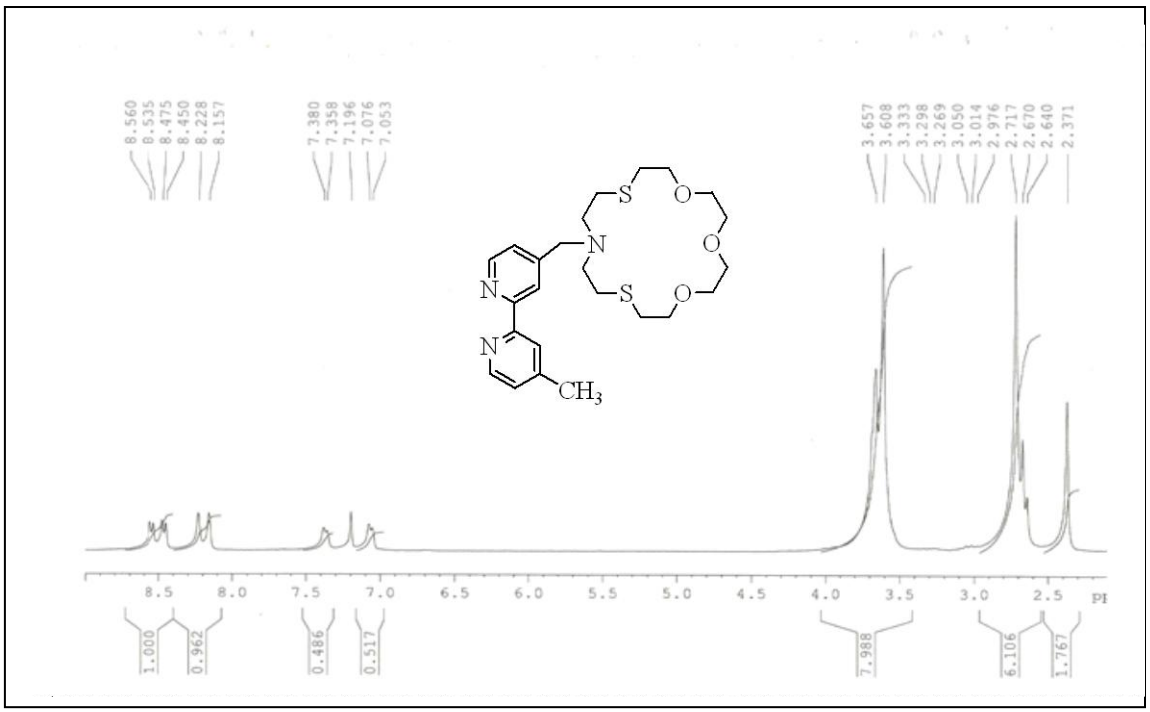

Figure 5.4 ^{1}H NMR spectrum of $\mathbf{L^2}$

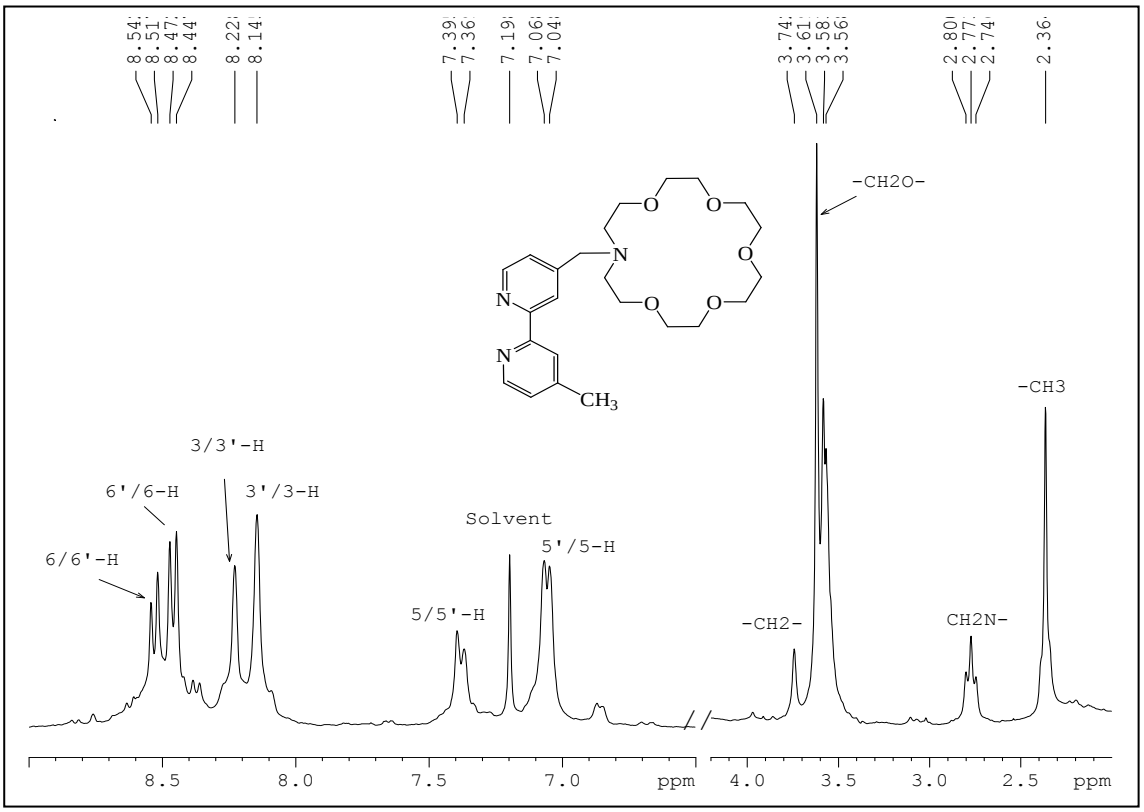

Figure 5.5 ^{1}H NMR spectrum of **L^{3}**

The experimental data of C, H, N and S analysis are in agreement with the proposed molecular formula of the complexes. The mass spectral data of the complexes **2** and **3** are shown in Figures 5.6 and 5.7, respectively. The e/m values, which are correspond to H^+, Na^+ and K^+ adduct with and without PF_6^-, are in excellent agreement with the calculated values. The ^{1}H NMR spectra of the complexes **1-3** were recorded in CD_3CN and the data with assignment of peaks are given in the Experimental Section. The ^{1}H NMR spectrum of complex **1** is shown in Figure 5.8. The most deshielded singlet at δ 8.52 is assigned to 3-H and 3′-H of the bpy moiety of **L^{1}**, this signal is partially overlapped with the doublet at δ 8.50, which is due to 6-H and 6′-H of the two bpy ligands. The overlapped triplets in the range δ 8.05-8.10 are assigned to the 5-H and 5′-H of the bpy ligand. The doublets at δ 7.79 and 7.71 are due to 3-H and 3′-H of the bpy units. The other doublet at δ 7.76 is due to 6-H and 6′-H of the bpy of L^{1}. The multiplet in the range δ 7.37-7.44 is due to 5-H and 5′-H of the bpy of **L^{1}** and 4-H and 4′-H of the bpy. The signals due to crown moiety appear as singlets at δ 3.88 and 3.75 and multiplets in the region δ 3.50-3.59. The ^{1}H NMR spectra of **2** and **3** are similar, the peak appeared at δ 8.49 in both the complexes are due to 6-H and 6′-H of

the bpy ligand. The singlet at δ 8.42 and 8.35 are due to 3-H and 3′-H of the bpy moiety of $\mathbf{L^3}$ for complex **3** but for complex **2**, a singlet at δ 8.49 is overlapped with the doublet. The overlapped triplets in the range δ 8.03-8.05 are due to 5-H and 5′-H of the bpy ligand. The triplet at δ 7.72 is due to 4-H and 4'-H bpy. The doublet at δ 7.52 is assigned to 5-H and 5'-H of the bpy of $\mathbf{L^2}$ and $\mathbf{L^3}$. The overlapped triplets at δ 7.38 are due to 3-H and 3′-H of the bpy units. The multiplet at δ 7.22 is due to 6-H, 6′-H of the bpy of $\mathbf{L^2}$ and $\mathbf{L^3}$. The signals due to crown moiety appear as multiplets in the region δ 3.50-3.65. The CH_3 protons appeared as singlet at δ 2.32 as singlet.

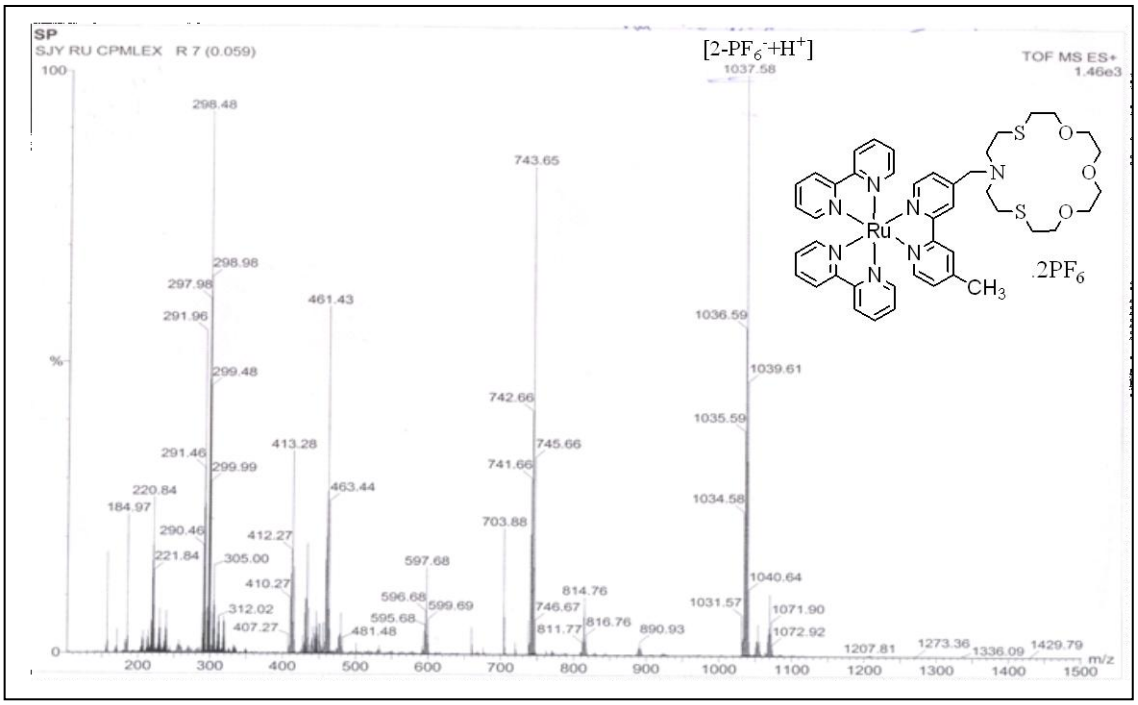

Figure 5.6 mass spectrum of complex **2**

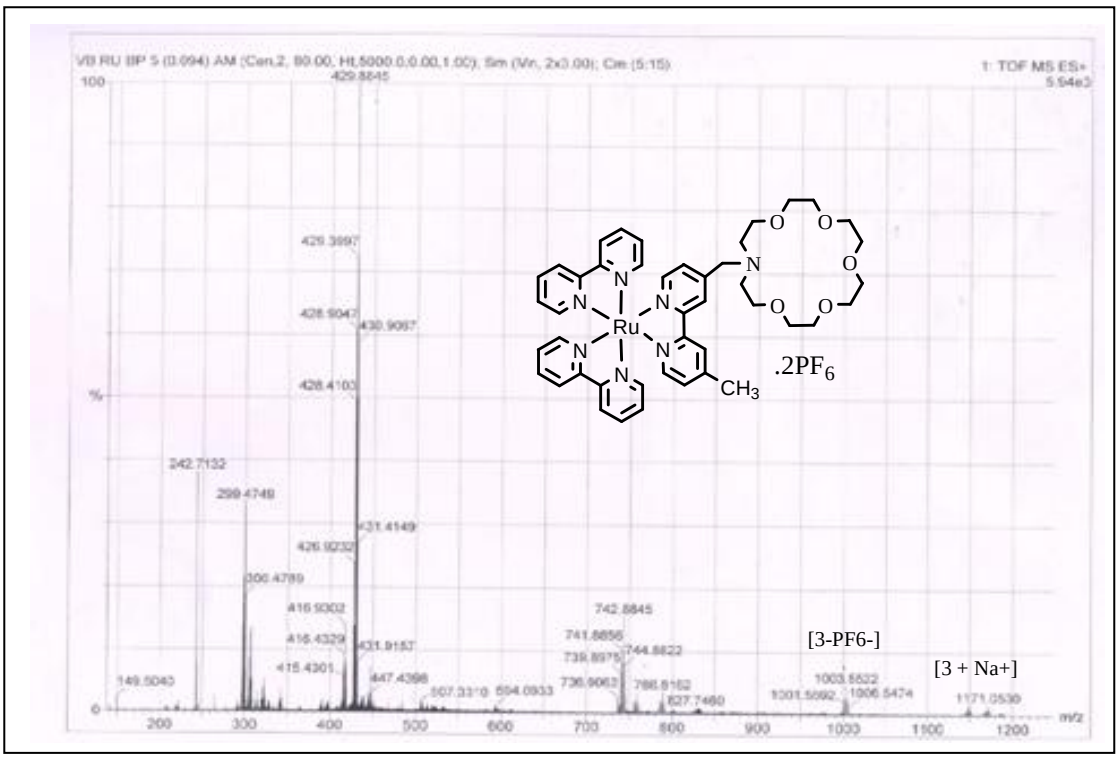

Figure 5.7 mass spectrum of complex **3**

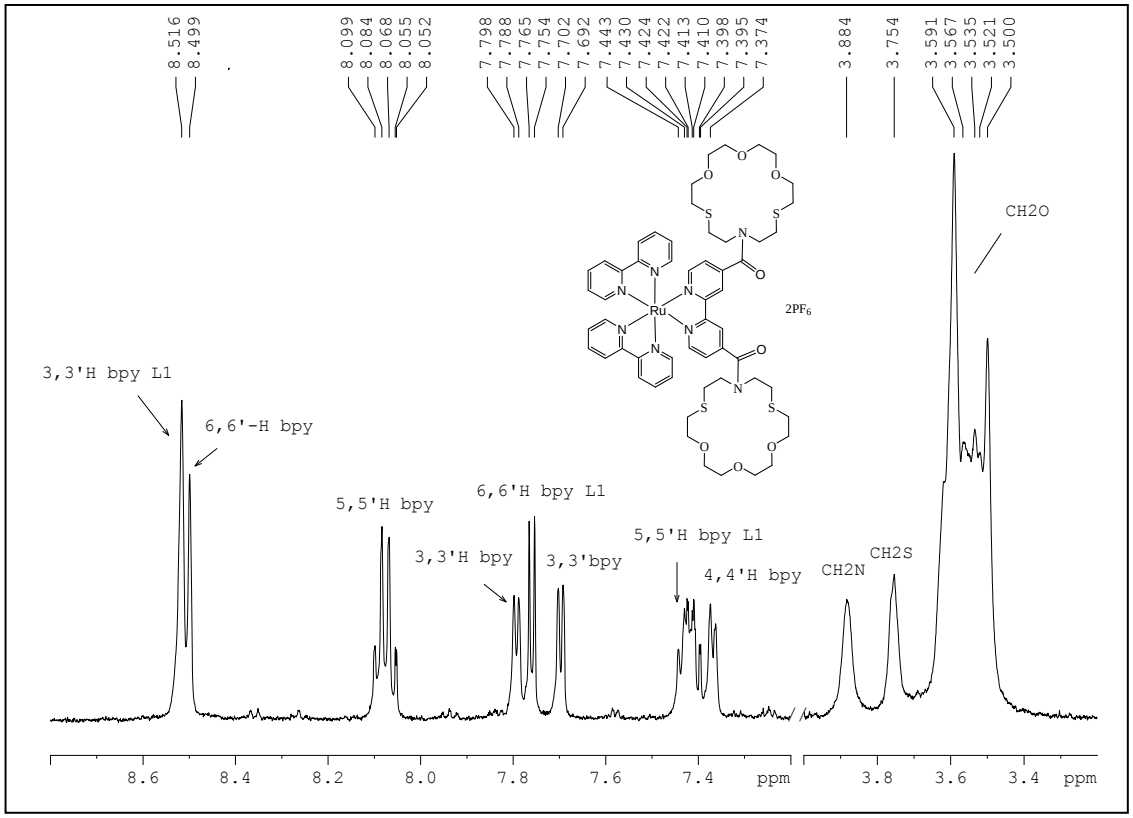

Figure 5.8 Relevant portion of the ^{1}H NMR spectrum for **1**.

The Re(I) complex (**4)** was synthesized by the reaction of [Re(CO)5Cl] and $\mathbf{L^1}$ in refluxing THF and the crude product was purified by column chromatography. Analytical and spectroscopic data are given in the Experimental Section. The mass spectrum of **4** is shown in Figure 5.9. The ^{1}H NMR spectrum of **4** is similar to that of the ligand $\mathbf{L^2}$, only difference is slight changes in chemical shifts of some of the signals. The IR spectra of **4** exhibits strong bands at 2019 and 1900 cm^{-1}, which are assigned to ν(CO) (A_1) and (E) of the metal bound CO.

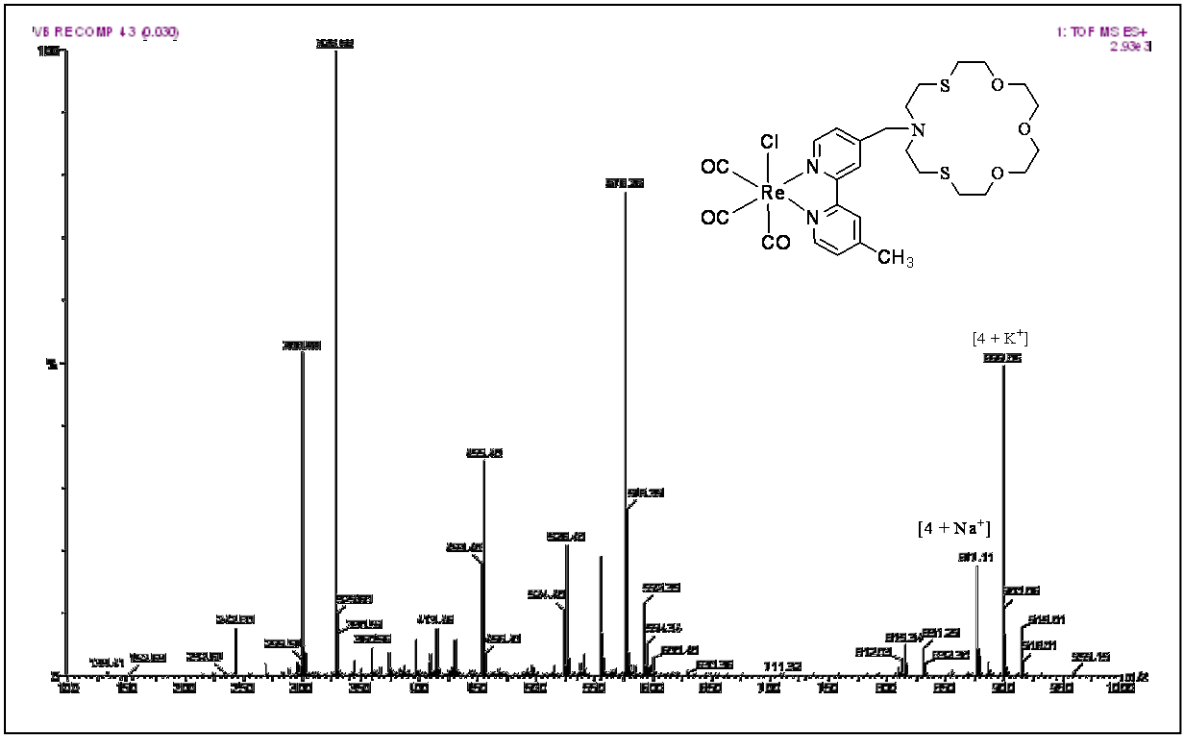

Figure 5.9 Mass spectrum of the complex **4**

On the basis of all analytical and spectroscopic data the proposed molecular structures of complexes **1-4** are shown in Figure 5.10.

5.3.3 Absorption and Luminescence

The absorption and luminescence spectra of all these complexes were recorded in acetonitrile and the data are given in the Experimental Section. The absorption and luminescence spectra of complexes **1-3** are similar. They exhibit a low energy band at 454 nm due to metal-to-ligand (bpy) charge-transfer (MLCT) transitions ($d\pi \rightarrow \pi^*$).[21,22] They also exhibit a high-energy band around 288 nm, which is a ligand-

centered charge transfer (CT) band due to $\pi \rightarrow \pi^*$ transitions.[23,24] The steady-state emission spectra of the Ru(II) complexes exhibit a strong band in the range 616-630 nm (^{3}MLCT) in acetonitrile at room temperature. As a representative one, the absorption and emission spectra of compound **1** is shown in Figure 5.11. The Re(I) complex (**4**) exhibits metal-to-ligand (bpy) charge-transfer (MLCT) band at 360 nm and emissions at 409 (weak) and 588 nm, as shown in the Figure 5.12.[25]

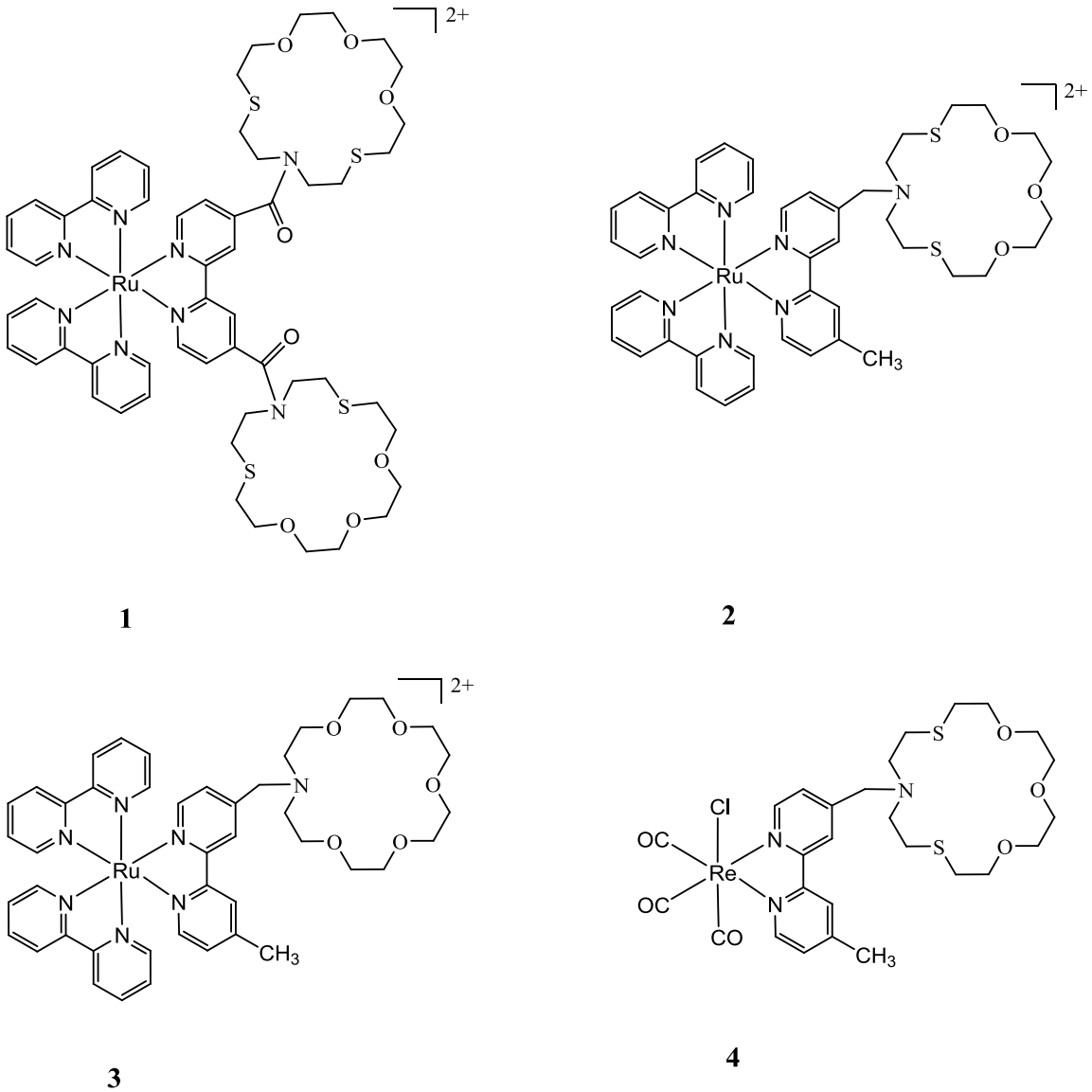

1 **2**

3 **4**

Figure 5.10 Structures of the complexes **1**-**4**

5.3.4 Ion-binding property

Ion-binding property of **1**-**4** have been investigated with a series of cations (Na^+, K^+, Mg^{2+}, Ca^{2+}, Zn^{2+}, Ba^{2+}, Sr^{2+}, Cd^{2+}, Hg^{2+}, Pb^{2+} and Cu^{2+}) and anions (F^-, Cl^-,

Br^-, I^-, $H_2PO_4^-$, ClO_4^- , NO_3^-, BF_4^-, CH_3COO^-, and HSO_4^-) and the host-guest interactions monitored by luminescence and ^1H NMR spectral changes.

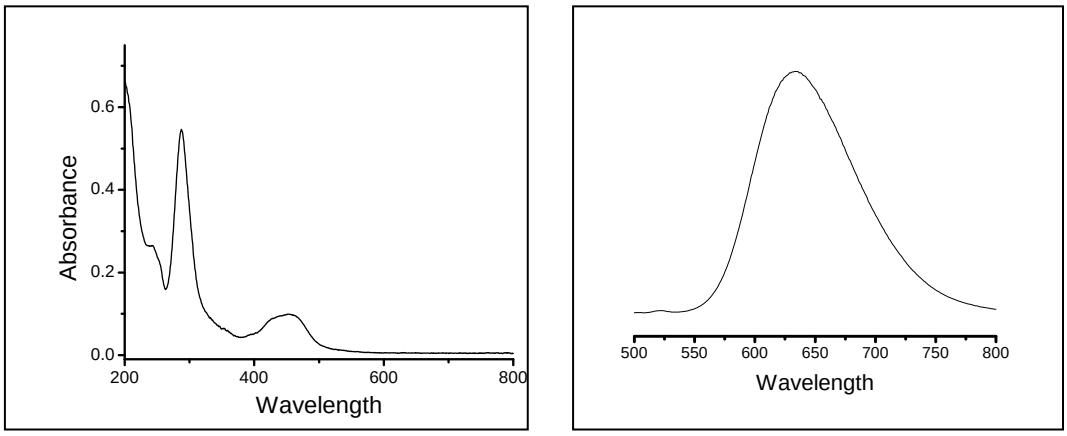

Figure 5.11. Absorption and luminescence spectra of complex **1,** recorded in acetonitrile at room temperature.

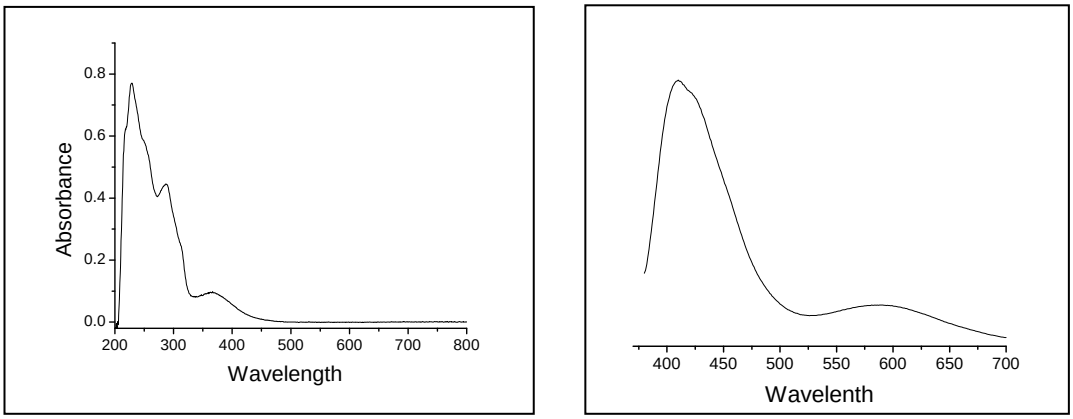

Figure 5.12 Absorption and luminescence spectra of complex **4,** recorded in acetonitrile at room temperature.

5.3.4.1 Luminescence study

The luminescence spectra of all the ionophores **1-4** were recorded in acetonitrile at room temperature. The same spectra were recorded again in presence of various cations (100 fold excess) and anions. The spectral changes for all the four compounds upon addition of metal ions are shown in Figures 5.13-5.16. For complex

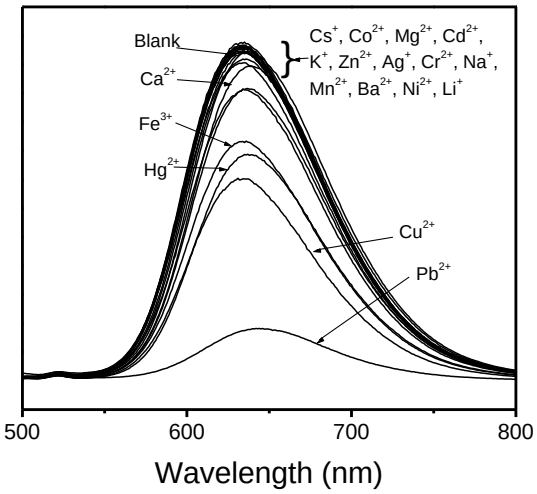

Figure 5.13 Luminescence spectral changes for **1** upon addition of various metal ions (100 fold excess).

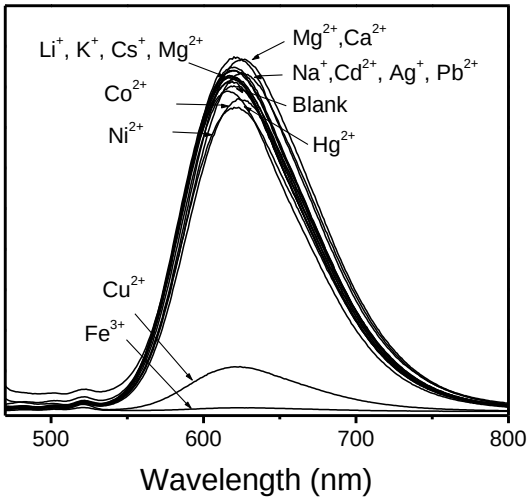

Figure 5.14. Luminescence spectral changes for **2** upon addition of various metal ions (100 fold excess).

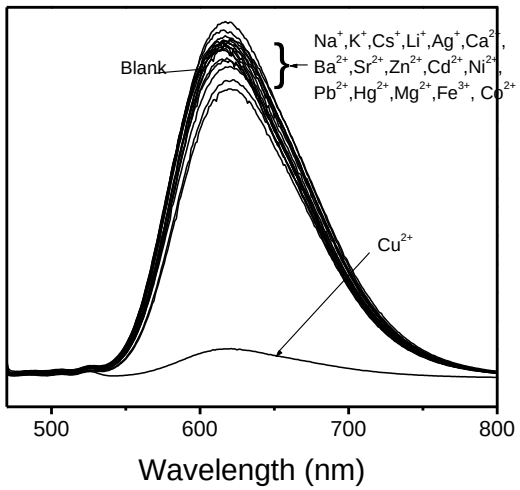

Figure 5.15. Luminescence spectral changes for **3** upon addition of various metal ions (100 fold excess).

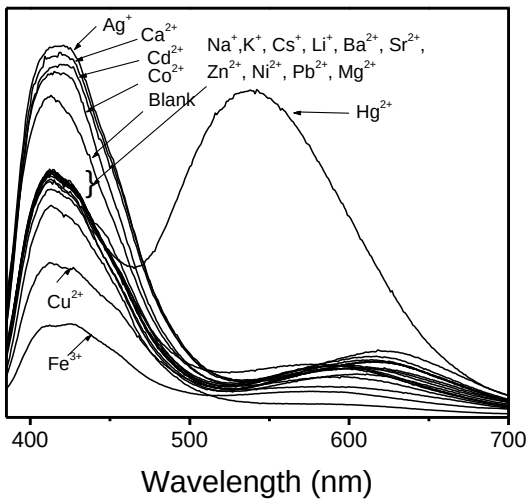

Figure 5.16 Luminescence spectral changes for **4** upon addition of various metal ions (100 fold excess).

1, the luminescence intensity is quenched by 85 % in presence of Pb^{2+}, 30-40 % in presence of Cu^{2+}, Fe^{3+} and Hg^{2+}, whereas other metal ions did not show any significant change. This observation suggests that these four metal ions form strong complex with the compound **1**. Compound **2** exhibited 87 and 96 % quenching in emission intensity (Figure 5.14) in presence of Cu^{2+} and Fe^{3+}, respectively indicating strong complexation of these two metal ions with the fluoroionophore. Complex **3** exhibited 92 % of quenching in presence of Cu^{2+}, whereas the Re(I) complex (**4**) showed 55-75 % enhancement in emission intensity upon addition of Cu^{2+}, Fe^{3+} and Hg^{2+}. In the case of **4** with Hg^{2+}, a strong new peak also appeared at 538 nm (Figure 5.16). The results indicate that incorporation of sulphur donor atoms in the ionophoric unit significantly enhanced complexation with Fe^{3+}, Hg^{2+} and Pb^{2+}, complex **3** did not show complexation with these metal ions as there is no sulphur donors. The quenching of emission intensity is ascribed to the metal-induced intramolecular charge transfer, it is observed when transition metal ions bind the host molecule strongly.[26] The complexation of metal ion with the crown moiety is also investigated by ^{1}H NMR study. The spectral changes for **1** upon addition of increasing concentration of Pb^{2+} and Hg^{2+} are shown in the Figures 5.17 and 5.18. It may be noted that the chemical shifts of the protons due to crown moiety in the aliphatic region is substantially changed whereas the signals in the aromatic region did not show any significant change. The change in chemical shifts of the crown moiety is due to the complexation of metal ion with the crown cavity. The result, therefore suggest that in addition to the size of the ionophore and cations, the donor atoms for the incoming ions is also play important role in ion-selectivity. The enhancement of emission intensity observed in **4** is probably due to blocking of the intramolecular electron-transfer quenching process because of coordination of metal ion into the crown cavity reduce the ability of the donor atoms of the crown moiety to quench emissive ^{3}MLCT state by photoinduced electron transfer.[27-30]

The fluoroionophores **1-4** are basically designed for cations, however the performance of these molecules towards anions has also been investigated. The spectral changes for all the four compounds upon addition of various anions are shown in Figures 5.19-5.22. From spectral changes it appears that $H_2PO_4^-$ has made significant interaction with all the four complexes. The F^- anion has also made

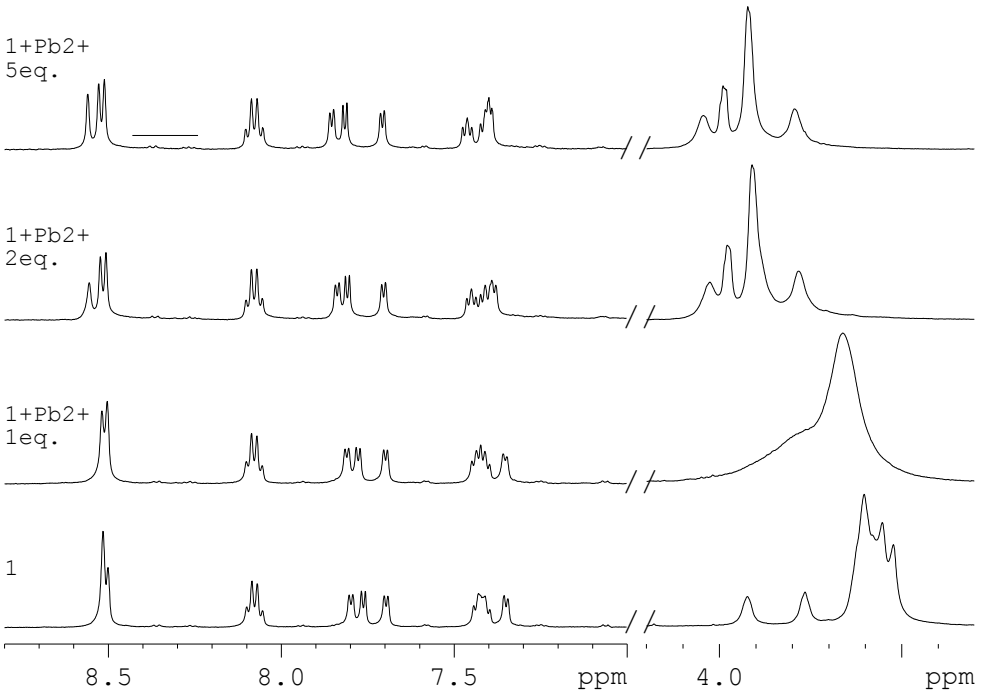

Figure 5.17 Selected portion of the ^{1}H NMR spectra of **1** recorded in CD_3CN with the addition of increasing concentration of Pb^{2+} at room temperature.

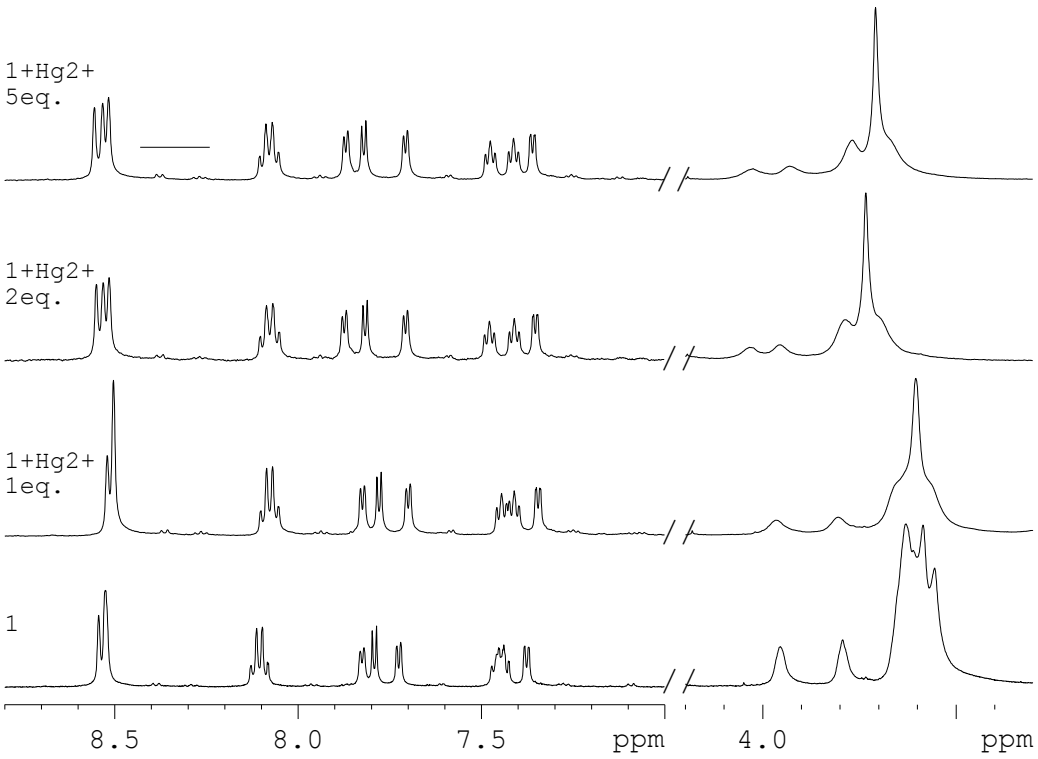

Figure 5.18 Selected portion of the ^{1}H NMR spectra of **1** recorded in CD_3CN with the addition of increasing concentration of Hg^{2+} at room temperature.

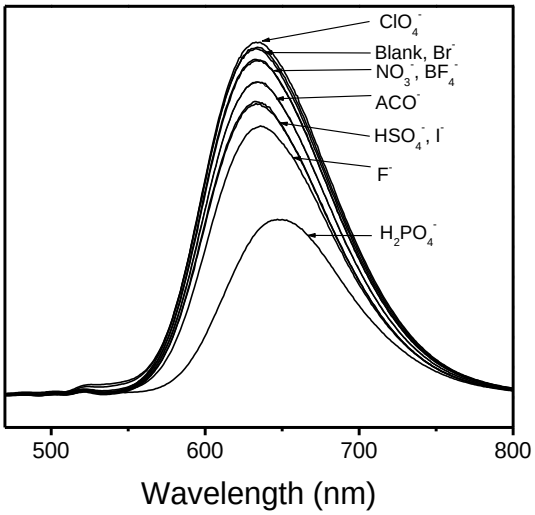

Figure 5.19 Luminescence spectral changes for **1** upon addition of various anions (100 fold excess).

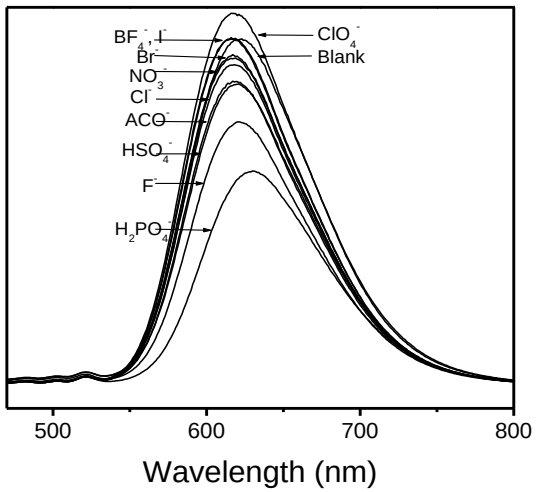

Figure 5.20 Luminescence spectral changes for **2** upon addition of various anions (100 fold excess).

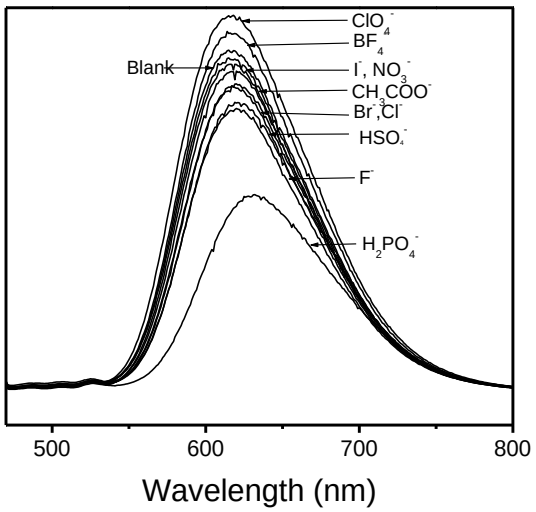

Figure 5.21 Luminescence spectral changes for **3** upon addition of various anions (100 fold excess).

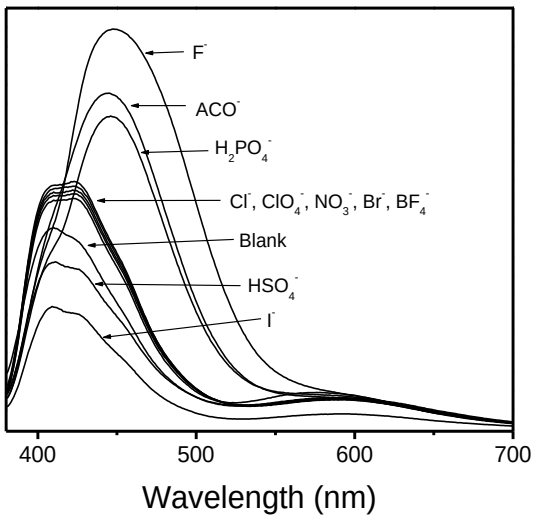

Figure 5.22 Luminescence spectral changes for **4** upon addition of various anions (100 fold excess).

significant interaction with **1**, **2** and **4,** and CH_3COO^- exhibited strong interaction with only **4**. For other anions, minor changes in fluorescence spectra are observed in few cases but they are not so significant to be considered for strong complex formation. The ionophores of these complexes were not designed for making interaction with anions but the spectral changes indicated formation of complex with certain anions. Therefore it was interesting to find out the possible sites, where anions can bind. For this purpose, ^{1}H NMR spectra of **1** with the addition of increasing concentration of $H_2PO_4^-$, F^- and I^- were recorded in CD_3CN and the spectral changes are shown in Figures 5. 23-5.25.

All of the four fluoroionophores contain positively charged metal ions, therefore electrostatic interaction brings the anions close to the metal ions. Figures 5.23-5.25 clearly show changes in chemical shifts both in aromatic and aliphatic regions. The 3,3'-protons of the metal bound bipyridine unit of the ligand is in adjacent to the amide group and because of the electron withdrawing ability of the latter the 3,3'-protons possess some positive charge (δ^+). These (partially) positively charged protons make interaction with the anions to form complex, as shown in the Figure 26. This interaction resulted in deshielding of the 3,3'-protons, as observed

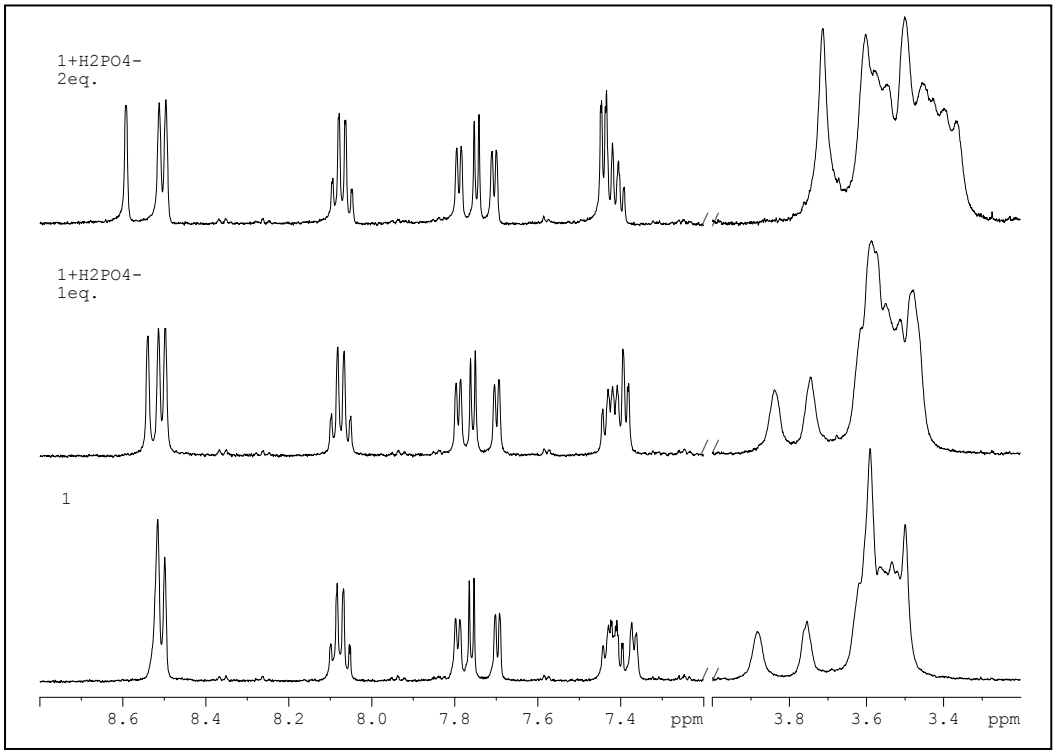

Figure 5.23 Selected portion of the ^{1}H NMR spectra of **1** recorded in CD_3CN with the addition of increasing concentration of $H_2PO_4^-$ at room temperature.

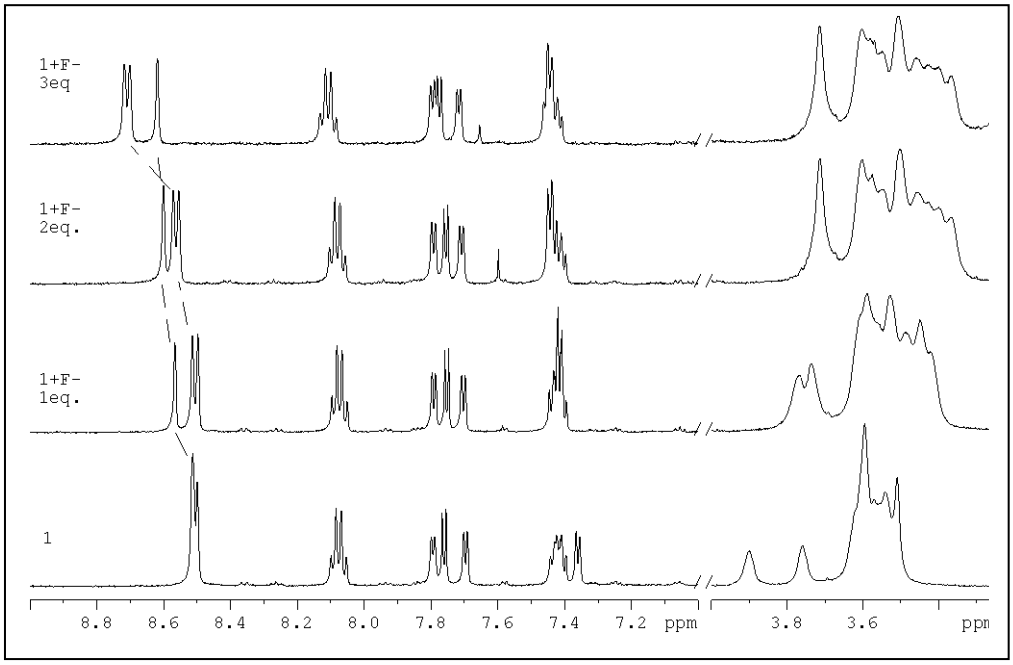

Figure 5.24 Selected portion of the ^{1}H NMR spectra of **1** recorded in CD_3CN with the addition of increasing concentration of F^- at room temperature.

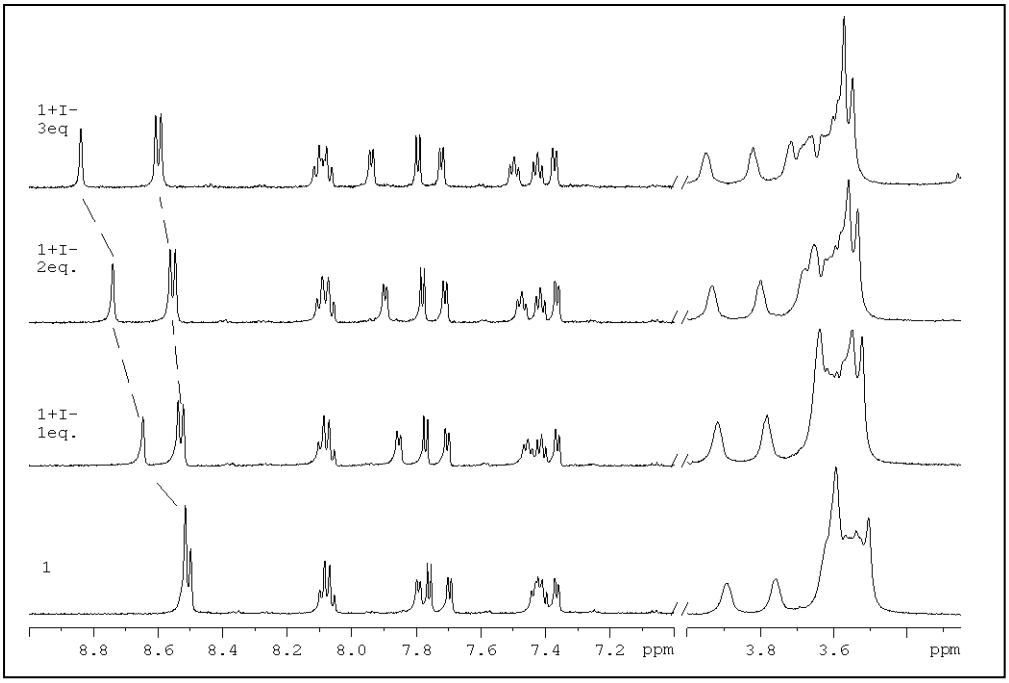

Figure 5.25 Selected portion of the ^{1}H NMR spectra of **1** recorded in CD_3CN with the addition of increasing concentration of I^- at room temperature.

experimentally. The minor change observed in the aliphatic region is probably due to change in orientation of the crown rings because of the complexation with anions. In the case of Re(I) complex (**4**), there is a possibility of replacement of CO by the anions, however solution study has not been done in detail to confirm it.

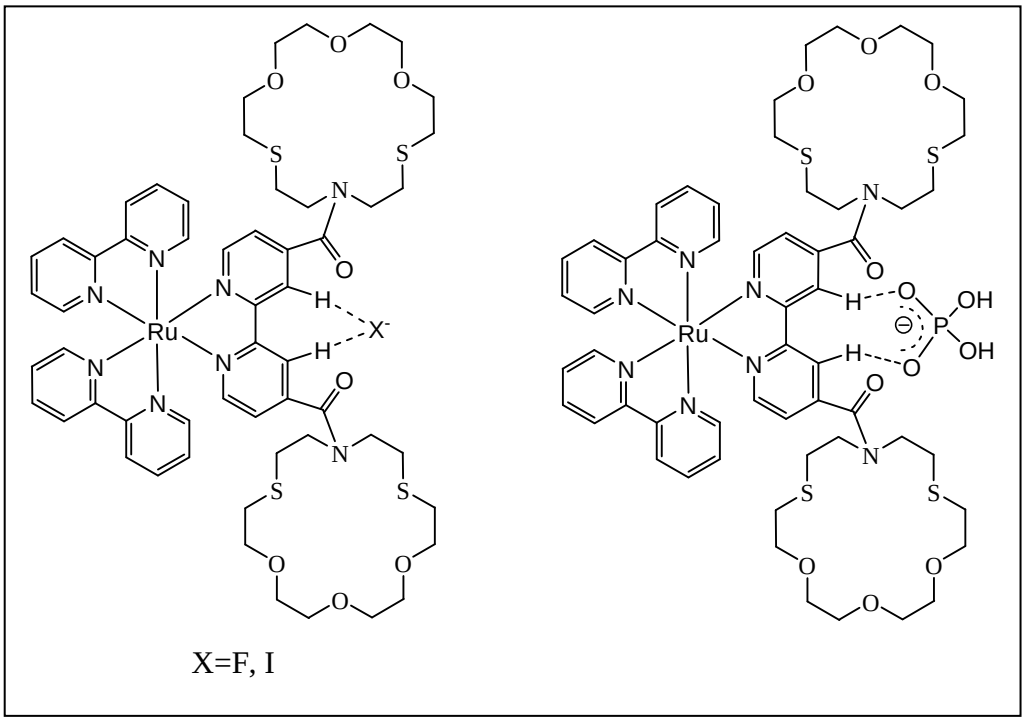

Figure 5.26 Structural drawing of complexes **1** showing interactions with the anions.

5.3.4.2 Binding constant

Binding constants for **1-4** with strongly interacting ions were calculated using emission titration data following the procedure as described in *chapter III* (Section **3.3.1**).[31-33] The spectral changes upon addition of increasing concentration of ions are shown in Figures 5.27-5.41 and the binding constants are summarized in Table 1. According to this procedure, the fluorescence intensity (F) scales with the metal ion concentration ([M])

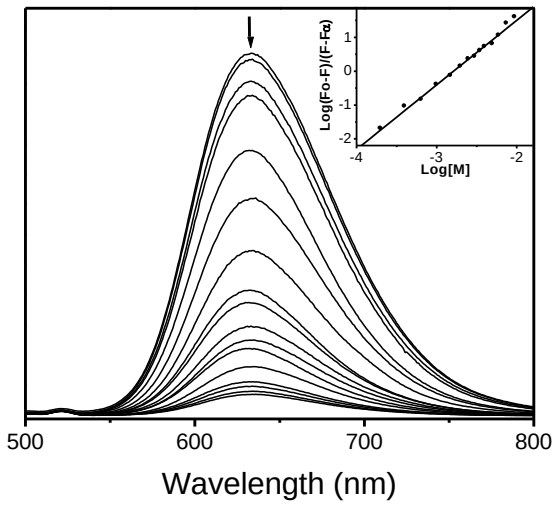

Figure 5.27 Emission spectral changes for **1** upon addition of increasing concentration of $Cu(ClO_4)_2$. Excitation wavelength: 454 nm. Inset: linear regression fit (double-logarithmic plot) of the titration data as a function of concentration of metal.

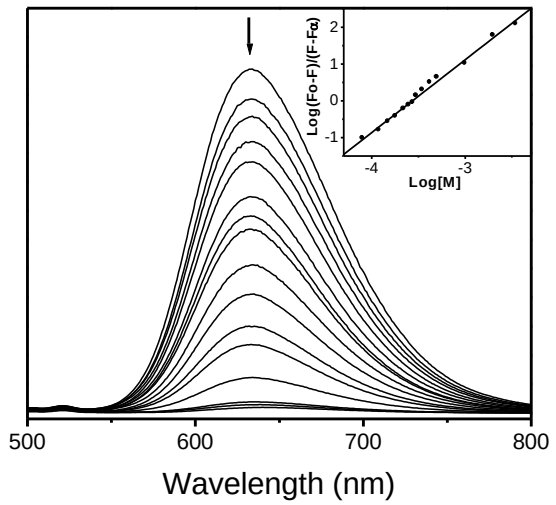

Figure 5.28 Emission spectral changes for **1** upon addition of increasing concentration of $Fe(ClO_4)_3$. Excitation wavelength: 454 nm. Inset: linear regression fit (double-logarithmic plot) of the titration data as a function of concentration of metal.

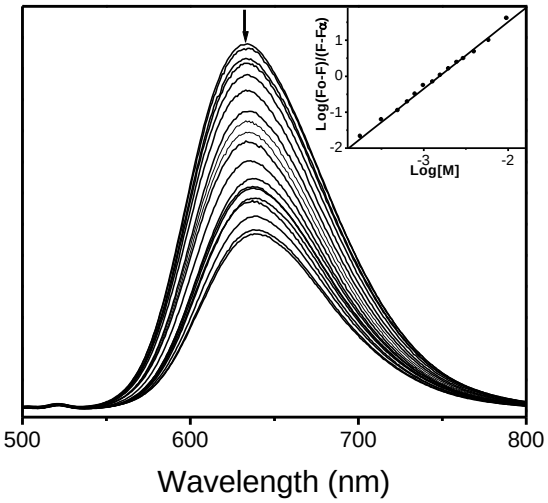

Figure 5.29 Emission spectral changes for **1** upon addition of increasing concentration of $Hg(ClO_4)_2$. Excitation wavelength: 454 nm. Inset: linear regression fit (double-logarithmic plot) of the titration data as a function of concentration of metal.

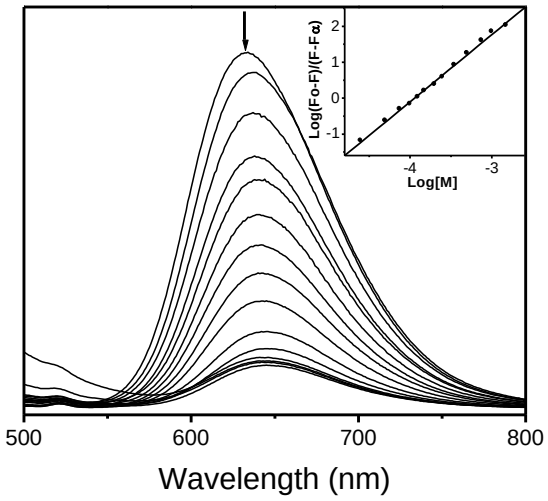

Figure 5.30 Emission spectral changes for **1** upon addition of increasing concentration of $Pb(ClO_4)_2$. Excitation wavelength: 454 nm. Inset: linear regression fit (double-logarithmic plot) of the titration data as a function of concentration of metal.

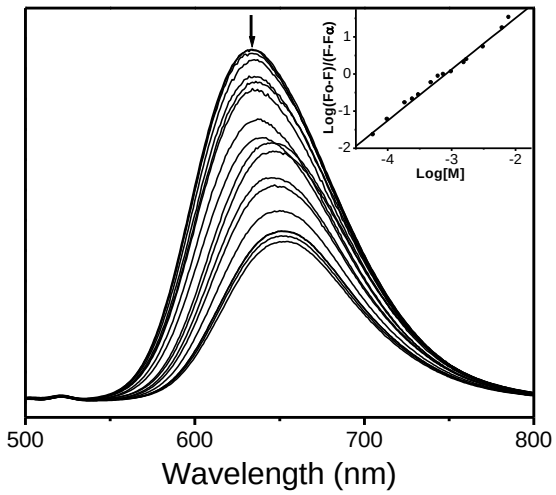

Figure 5.31 Emission spectral changes for **1** upon addition of increasing concentration of $H_2PO_4^-$. Excitation wavelength: 454 nm. Inset: linear regression fit (double-logarithmic plot) of the titration data as a function of concentration of metal.

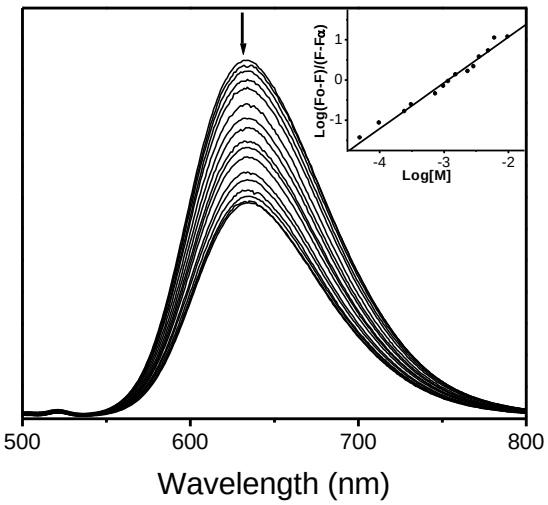

Figure 5.32 Emission spectral changes for **1** upon addition of increasing concentration of I^-. Excitation wavelength: 454 nm. Inset: linear regression fit (double-logarithmic plot) of the titration data as a function of concentration of metal.

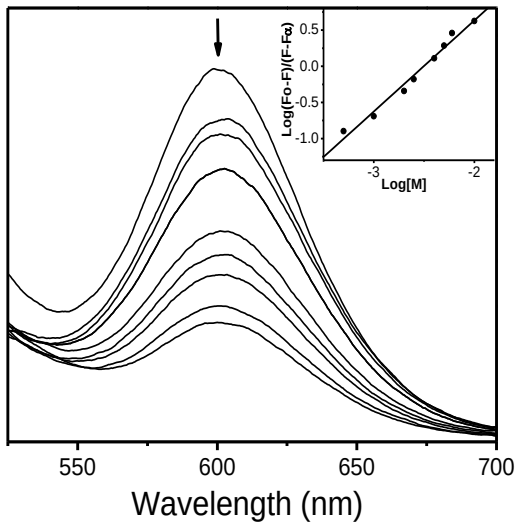

Figure 5.33 Emission spectral changes for **2** upon addition of increasing concentration of $Cu(ClO_4)_2$. Excitation wavelength: 454 nm. Inset: linear regression fit (double-logarithmic plot) of the titration data as a function of concentration of metal.

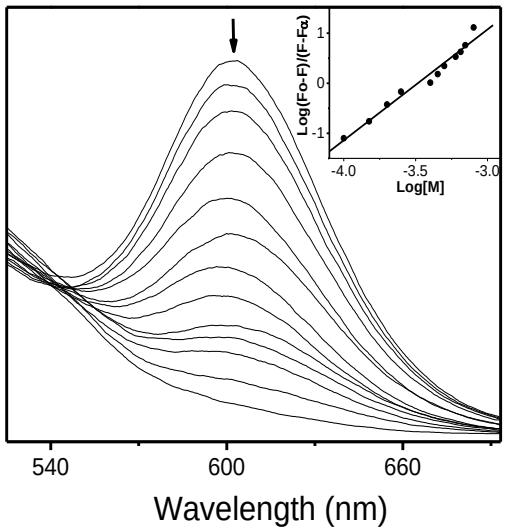

Figure 5.34 Emission spectral changes for **2** upon addition of increasing concentration of $Fe(ClO_4)_3$. Excitation wavelength: 454 nm. Inset: linear regression fit (double-logarithmic plot) of the titration data as a function of concentration of metal.

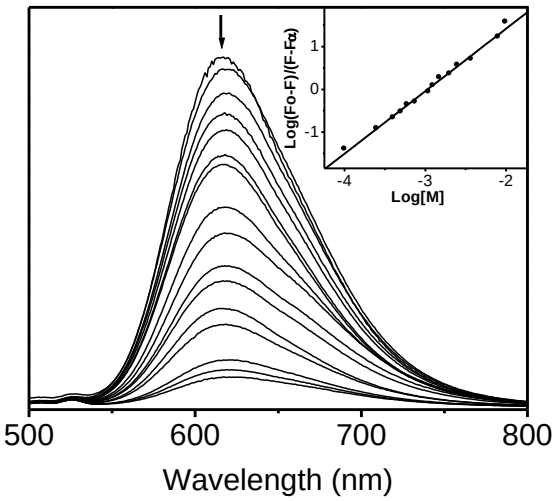

Figure 5.35 Emission spectral changes for **3** upon addition of increasing concentration of $Cu(ClO_4)_2$. Excitation wavelength: 454 nm. Inset: linear regression fit (double-logarithmic plot) of the titration data as a function of concentration of metal.

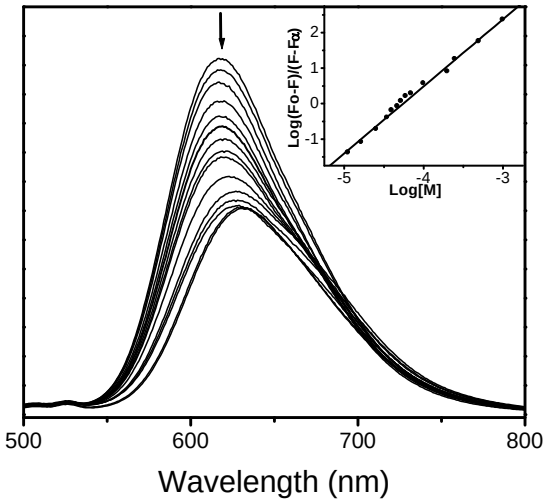

Figure 5.36 Emission spectral changes for **3** upon addition of increasing concentration of $H_2PO_4^-$. Excitation wavelength: 454 nm. Inset: linear regression fit (double-logarithmic plot) of the titration data as a function of concentration of metal.

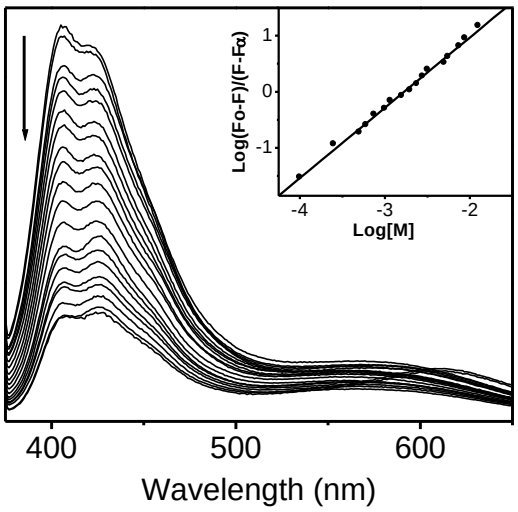

Figure 5.37 Emission spectral changes for **4** upon addition of increasing concentration of $Fe(ClO_4)_3$. Excitation wavelength: 360 nm. Inset: linear regression fit (double-logarithmic plot) of the titration data as a function of concentration of metal.

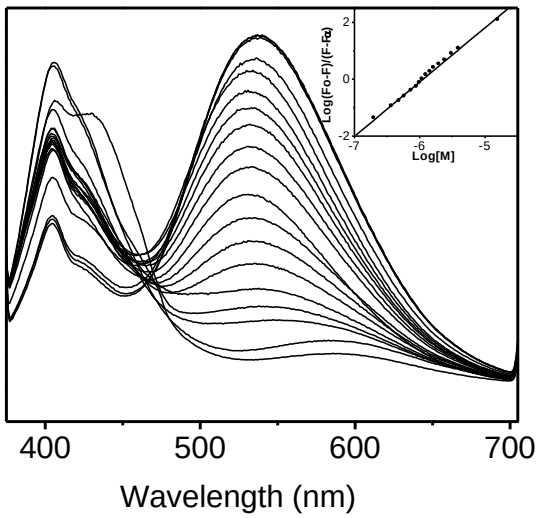

Figure 5.38 Emission spectral changes for **4** upon addition of increasing concentration of $Hg(ClO_4)_2$. Excitation wavelength: 360 nm. Inset: linear regression fit (double-logarithmic plot) of the titration data as a function of concentration of metal.

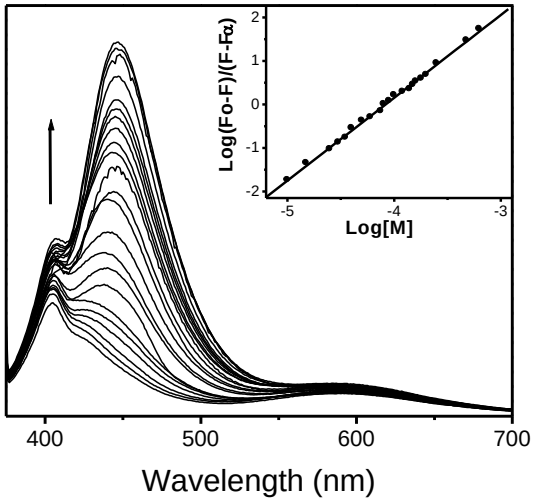

Figure 5.39 Emission spectral changes for **4** upon addition of increasing concentration of $H_2PO_4^-$. Excitation wavelength: 360 nm. Inset: linear regression fit (double-logarithmic plot) of the titration data as a function of concentration of metal.

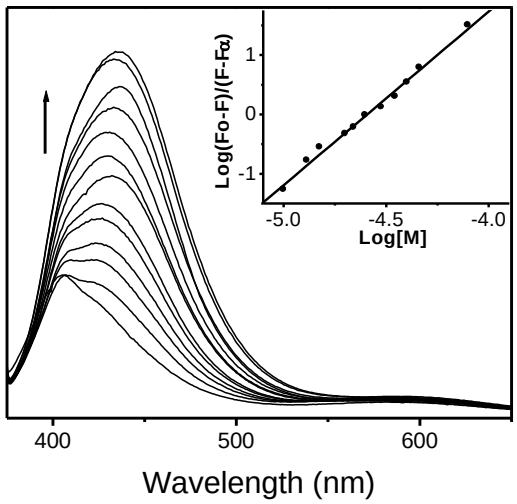

Figure 5.40 Emission spectral changes for **4** upon addition of increasing concentration of F. Excitation wavelength: 360 nm. Inset: linear regression fit (double-logarithmic plot) of the titration data as a function of concentration of metal.

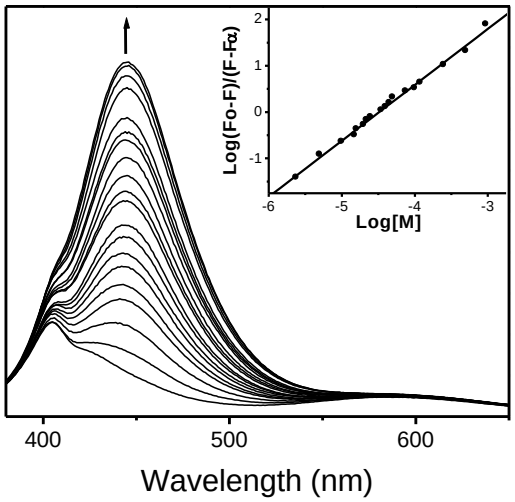

Figure 5.41 Emission spectral changes for **4** upon addition of increasing concentration of F. Excitation wavelength: 360 nm. Inset: linear regression fit (double-logarithmic plot) of the titration data as a function of concentration of metal.

through $(F_0 - F)/(F - F_\infty) = ([M]/K_{diss})^n$. The binding constant ($K_s$) is obtained by plotting $\log[(F_0 - F)/(F - F_\infty)]$ versus log[M]. The value of log[M] at $\log[(F_0 - F)/(F - F_\infty)] = 0$ gives the value of $\log(K_{diss})$, the reciprocal of which is the binding constant (K_s). The plots $\log[(F_0 - F)/(F - F_\infty)]$ versus log[M] are shown as insets of the Figure 5.25–5.41. The data in Table 1 indicate moderate to strong binding of all ions with the ionophores. For complex **1**, the binding constants for cations is in the order $Pb^{2+} > Hg^{2+} > Cu^{2+} > Fe^{3+}$, complex **4** also exhibits similar order, $Hg^{2+} > Cu^{2+} > Fe^{3+}$. The binding constant for Cu^{2+} for the complexes **2** and **3**, however significantly low compared to that of **1** and **2**. Binding constant for **2** with Fe^{3+}, however is comparable to that of complex **1**. The data indicates that inclusion of sulphur in the crown ring substantially increased the binding ability of the ionophores towards certain cations, particularly for Hg^{2+} and Fe^{3+}. The interaction with anions is interesting, the binding constant for F^- is higher than that of $H_2PO_4^-$. The cation-anion electrostatic interaction and electrophilicity of some of the protons are responsible for binding of anions. For **4**, replacement of CO by the anions can't be ruled out

Table 1. Luminescence data and binding constant (K_s) and stoichiometry of complex formation for the ionophores

Complex	λ_{em} (nm)	Metal ion	Binding constant (K_s) x 10^{-2} M^{-1}
1	632	Cu^{2+}	62.52
		Fe^{3+}	36.51
		Hg^{2+}	63.22
		Pb^{2+}	88.56
		F^-	53.29
		$H_2PO_4^-$	11.85
		I^-	8.89
2	620	Cu^{2+}	3.19
		Fe^{3+}	30.62
		F^-	9.89
3	617	Cu^{2+}	9.51
		$H_2PO_4^-$	173.78
4	616	Cu^{2+}	102.83
		Fe^{3+}	6.05
		Hg^{2+}	8709.63
		CH_3COO^-	306.19
		$H_2PO_4^-$	115.88
		F^-	386.99

5.4. Conclusion

Three new ligands containing macrocyclic unit having NS_2O_3 donor atoms as ionophores have been synthesized. New fluoroionophores incorporating Ru(II)/Re(I) bipyridine as fluorophore and newly synthesized ligand as ionophore have been synthesized and characterized on the basis of analytical and spectroscopic data. Ion-binding property of all these fluoroionophores has been investigated with a large number of cations and anions. The ion recognition event was monitored by luminescence and ^1H NMR spectroscopy. Out of large number of ions studied, Cu^{2+}

and $H_2PO_4^-$ forms strong complex with all fluoroionophores, in addition to that **1** forms complex with the cations Fe^{3+}, Hg^{2+}, Pb^{2+} and anions F^- and I^-. Complex **4** also forms complex with Fe^{3+}, Hg^{2+}, CH_3COO^-, and F^-. ^1H NMR study indicated involvement of crown cavity for complexation with metal ions, whereas 3,3'-protons of bipyridine unit of the ligand for **1** involves in interaction with anions. Binding constant for all strongly interacting ions has been evaluated by emission titration. The study clearly indicated that the spacer and donor atoms of the ionophore play important role in ion-selectivity.

5.5 Reference

1. K. A. Matis, A. I. Zouboulis and N. K. Lazaridis, *Water, Air, and Soil Pollution: Focus* 3, **2003,** 143.

2. A. V. AjayKumar,N. A. Darwish and N. Hilal, *World Applied Sciences Journal 5 (Special Issue for Environment)*, **2009**, 32.

3. H. Bedelean, A. Micneanu, S. Burc and M. Stanca, *Clay Minerals*, **2009**, *44*, 487.

4. K. Narasimhulu and P. Sreenivasa Rao, *ARPN Journal of Engineering and Applied Sciences*, **2009**, *4*, 7.

5. S. Manhan, *Toxicological Chemistry*, Lewis Publishers, Inc., Chelsea, MI, **1992**.

6. A. Krel, W. Leniak, M. Jeowska-Bojczuk, P. Mynarz, J. Brasun, H. Kozowski and W. Bal , *J. Inorg. Biochem.*, **2001**, *84*, 77.

7. M. Asmuss, L. H.F. Mullenders, A. Eker and A. Hartwig**,** *C**a**rcinogenesis*, **2000,** *21*, 2097.

8. A. T. Yordanov and D. M. Roundhill, *Coord. Chem. Rev*., **1998**, *170*, 93.

9 . S. T. Huang, H. S. Kuo, C. L. Hsiao and Y. L. Lin, *Bioorganic & Medicinal Chemistry*, **2002**, *10*, 1947.

10. G. W. Gokel, W. M. Leevy and M. E. Weber, *Chem. Rev.* **2004**, *104*, 2723.

11. F. Faridbod, M. R. Ganjali, R. Dinarvand, P. Norouzi and S. Riahi, *Sensors*, **2008**, *8*, 1645.

12. D.D. Perrin, W.L.F. Armarego, D.R. Perrin, *Purification of Laboratory Chemicals*, 2nd Ed, Pergamon, Press, Oxford, **1980**.

13. B.P. Sullivan, D.J. Salmon, T.J. Meyer, *Inorg. Chem,*. **1978**, *17*, 3334.

14. N. Garelli, P. Vierling, *J. Org. Chem*. **1992**, *57*, 3046.

15. S. Gould, G.F. Strouse, T. J. Meyer, and B. T. Sullivan, *Inorg. Chem.* **1978**, *30*, 3335.

16. L. G.A. van de Water, F. Hoonte, W. L. Driessen, J. Reedijk and D. C. Sherrington, *Inorganica Chimica Acta*, **2000**, *303*, 77.

17. Y. Jin, I. Yoon, J. Seo, J.-E. Lee, S.-T. Moon, J. Kim, S. W. Han, K.-M. Park, L. F. Lindoy and S. S. Lee, *Dalton Trans*, **2005**, 788.

18. C. J. Pedersen, *J. Am. Chem. Soc.*, **1967**, *89*, 26.

19. A.C. Tedesco, D.M. Oliveria, Z.J.M. Lacava, R.B. Azevedo, E.C.D. Lima, P.C. Morais, *J. Magn. Magn. Mater.*, **2004**, *272-276*, 2404.

20. S. Patra, P. Paul, *Dalton Trans.*, **2009**, 8683.

21. A. K. Bilakhiya, B. Tyagi, P. Paul, P. Natarajan, *Inorg. Chem*. **2002**, *41*, 3830.

22. J. Bolger, A. Gourdon, E. Ishow, J.-P. Launay, *Inorg. Chem.* **1996**, *35*, 2937.

23. A. K. Bilakhiya, B. Tyagi, P. Paul and P. Natarajan, *Inorg. Chem*. **2002**, *41*, 3830.

24. J. Bolger, A. Gourdon, E. Ishow and J.-P. Launay, *Inorg. Chem.* **1996**, *35*, 2937.

25. M. Busby, P. Matousek, M. Towrie, .I. P. Clark, M. Motevalli, F. Hartl and A. Vlcek, Jr, *Inorg. Chem*. **2004**, *43*, 4523.

26 R. Badugu, *Journal of Fluorescence*, **2005**, *15*,71.

27. P. D. Beer, S. W. Dent *J. Chem. Soc. Chem. Commun.* **1998**, 825.

28. M. Chiba, K. Ogawa, K. Tsuge, M. Abe, H. B. Kim, Y. Sasaki, N. Kitamura, *Chem. Lett*. **2001**, 692.

29. J. B. Cooper, M. G. B. Drew, P. D. Beer, *J. Chem. Soc. Dalton Trans.* **2001**, 392;

30. P. V. Bemhardt, E. G. Moore, *Aus. J. Chem.* **2003**, *56*, 239.

31. A. C. Tedesco, D. M. Oliveira, Z. G. M. Lacava, R. B. Azevedo, E. C. D. Lima, P. C. Morais, *J. Magnetism Magnetic Mater.* **2004**, *272-276*, 2404.

32. S. S. Lehrer, G. D. Fashman, *Biochem. Biophys. Res. Commun.* **1966**, *2*, 133.

33. D. M. Chipman, V. Grisaro, N. Shanon, *J. Biol. Chem.* **1967**, *242*, 4388.

PUBLICATIONS

1. Copper(II) diethylene tryamine perchlorato complexes bridged through varying length dicarboxylato spacers: synthesis, characterization and EPR studies, P. S. Subramanian, Paresh C. Dave, **Vinod P. Boricha** and D. Srinivas; Polyhedron, **1998,** 17, 443.
2. Synthesis, Characterization, Electrochemistry and Ion-binding Studies of Ruthenium(II) and Rhenium(I) Bipyridine Crown Ether Receptor Molecules; **Vinod P. Boricha,** Subrata Patra, Yogendra S. Chouhan, Pankaj Sanavada, E. Suresh and Parimal Paul, *Eur. J. Inorg. Chem.*, **2009**, 1256.
3. Luminescent metalloreceptors with pendant macrocyclic ionophore: Synthesis, characterization, electrochemistry and ion-binding study, Subrata Patra, **Vinod P. Boricha**, K.R. Sreenidhi, E. Suresh, Parimal Paul, ***In Press,*** *Inorg. Chim Acta***.,** **2010**.
4. Synthesis, characterization and ion-binding property of fluoroionophores containing Ru(II) and Re(I) bipyridine unit and appended crown having NS_2O_3 donors**, Vinod P. Boricha,** Sanjay Parihar, Yogendra S. Chouhan, and Parimal Paul (Manuscript under preparation)

Papers/Posters presented in Symposium:

1. Luminescent metalloreceptors of Ru(II) and Re(I): Synthesis, electrochemical behaviour and optical sensing towards cations and anions, Subrata Patra, Sreenidhi. K. R., **Vinod P. Boricha**, E. Suresh and Parimal Paul, *Poster presented in Modern Trends in Inorganic Chemistry*, MTIC-XII, IIT MADRAS, 6-8 DEC, **2007**.
2. Influence of steric factors on the equilibrium of coordination geometries in some nickel(II) and cobalt(II) complexes with heterocyclic amine, **Vinod Boricha**, Neha Mairh and Mohan Bhadbhade, published in XXVI National Seminar on crystallography, **1995**.
3. Synthesis, characterization, binding studies and molecular modeling of calixarene and crown dyes, S. K. Menon, Y. K. Agrawal, **Vinod P. Boricha** and Mohan Bhadbhade, paper presented in the National Seminar on

Challenges in calixarene chemistry on 25-26th Oct, **1996** held at Chemistry Department, School of Sciences, Gujarat University, Ahmedabad.

4. ^{13}C Quantitative Estimation. Application over small molecular system such as Mg(AA)2.xH2O Complexes, where AA=Gly, L-Phe, L-val. Synthesis and Characterization", P. S. Subramanian, **Vinod P. Boricha**. Poster presented in the Special Symposium on Current Trends in solid state NMR Methodology and Practice and 13th National Magnetic Resonance Society Meeting held during 5th to 8th February **2007** at National Chemical Laboratory, Pune

Participation in the workshop/Seminar:

1. "International conference on environmental sciences-96" at Regional Research Laboratory, Trivendrum on 8-9th Jan, 1996
2. "National seminar on "Reactive and functional polymers" on 2nd and 3rd March, 1996, held at Chemistry Department , School of Sciences, Gujarat University, Ahmedabad.
3. "National seminar on "Challenges in calixerene chemistry" on 25-26th Oct, 1996 held at Chemistry Department, School of Sciences, Gujarat University, Ahmedabad.
4. "Workshop on molecular structure determination by Spectroscopy and Defraction methods" organized by sophisticated analytical instruments laboratory, Central salt and marine chemicals research institute, Bhavnagar on 25th Feb, 1997.
5. "Recent Advancement in FT-IR Spectroscopy" organized by Anatech Services Private Limited and JASCO International company, Japan on 21-10-2002 held Chemistry Department, School of Sciences, Gujarat University, Ahmedabad.
6. "An approach to Analytical Instruments commenly Used in Chemical Industries" national workshop on 22-23 December, 2006 at Department of Chemistry, Bhavnagar Univesity, Bhavnagar.
7. "Special Symposium on Current Trends in solid state NMR Methodology and Practice and 13th National Magnetic Resonance Society Meeting" held during 5th to 8th February 2007 at National Chemical Laboratory, Pune.
8. 1st. Bruker Pre-NMRS Symposium 2009, held at IICT, Hyderabad on 2nd Feb, 2009.